Second Series *December 15, 1931* *Vol. 38, No. 12*

THE

PHYSICAL REVIEW

THE GRATING CONSTANT OF CALCITE CRYSTALS

By J. A. Bearden

Department of Physics, Johns Hopkins University

(Received November 7, 1931)

Abstract

The precise methods of measuring x-ray wave-lengths, now in use, raise two important questions concerning the crystal grating used. First, what variation in the grating constant is to be expected for crystals grown under different conditions? Second, what is the most accurate value of the grating constant? Since calcite crystals are the most used crystals in x-ray spectroscopy the present work was undertaken to answer as well as possible the above questions for this crystal. The variations in the grating constants of six calcite crystals from four sources (Iceland, Montana, Argentina, and Spain) have been determined by measuring the angle of diffraction for the molybdenum $K\alpha_1$ line in the fourth order. A high precision two-crystal spectrometer was used for measuring the diffraction angles. The results are given in the table below. The density of these crystals was then carefully determined. Six to nine independent determinations were made at a temperature of 20.00 ± 0.01°C. The averages of these values are given for a temperature of 20.00°C, in the fourth column of the table. The probable error determined by the method of least squares is given in the fifth column. The mass of the crystals used in determining the density is given in the sixth column. Considering the density measurements of DeFoe and Compton the writer gives the density ρ in g/cm^{-3} at 20°C as $\rho = 2.71030 \pm 0.00003$. The crystals were then chemically analyzed. The results showed that all samples contained about 0.01 percent ferrous oxide, 0.01 percent manganous oxide, and 99.98 percent calcium carbonate. The angle between the cleavage faces of the calcite crystals was determined by three methods. X-rays were used for determining the angle in the first two methods and an optical method for the third. The results for 20°C were $\alpha = 105° 3' 29''$ or $\beta = 101° 54' 4''$, where α is the interior obtuse dihedral angle, and β the angle between the edges of the crystal. The grating constant of the crystal can be calculated from the equation $d = (nM/\rho N\phi)^{1/3}$ $= 3.02816$A at 20°C, $= 3.002810$A at 18°C. The values of the constants used were, $n = 1/2$, $M = 100.078$, $\rho = 2.71030$, $N = 6.0669 \times 10^{23}$, $\phi = 1.09594$.

Origin	Diffraction angle θ	Difference from mean	Density g/cm^{-3}	Probable Error	Mass of crystals g
Iceland	37° 51′ 34.0″	−0.4″	2.7104	±0.000021	12.9764
Iceland	27° 51′ 34.0″	−0.4″	2.71035	±0.000015	15.5780
Montana	27° 51′ 34.6″	+0.2″	2.7102	±0.000081	7.1467
Montana	27° 51′ 34.7″	+0.3″	2.7102	±0.000024	14.8650
Argentina	27° 51′ 34.7″	+0.3″	2.7102	±0.000042	11.0769
Spain	27° 51′ 34.4″	0.0″	2.7102	±0.000036	13.0083
Mean	27° 51′ 34.4″		2.71026		

Introduction

IT IS now possible to measure the diffraction angles of certain x-ray lines to one part in 400,000, or better, by using a double crytal spectrometer[1,2] or a high precision photographic spectrometer.[3] Thus, it is essential to know more about the grating constant of the crystals used. This is especially true if the results obtained by different observers are to be compared. Since calcite crystals are the most used crystals in x-ray spectroscopy, the present work has been undertaken to remove as far as possible any existing uncertainty in the use of this crystal as an x-ray grating. This report may be divided into the following six divisions: (1) X-ray comparison of the grating constant of calcite. (II) Chemical analysis of samples used. (III) Density of calcite. (IV) A determination of the angle between the cleavage faces of calcite. (V) Calculation of the grating constant from chemical data. (VI) Discussion of results.

I. X-ray Comparison of the Grating Constant of Calcite

A comparison of the grating constant of different samples can be precisely made by measuring the diffraction angle of a given x-ray line for each sample.[2] In order to obtain the maximum precision in the comparison, several considerations are necessary. A large angle of diffraction is desired which could be secured by using either a long wave-length or a high order of diffraction. The latter was chosen because in using a high order of a shorter wave-length one has a much greater penetration of the rays into the crystal, and consequently a more reliable estimate of the variation in the grating constant. The method of measuring the diffraction angle must be such that a lack of perfect adjustment of each sample would make a minimum variation in the diffraction angle. A two crystal spectrometer has been used for the measurements because when properly adjusted it fulfills all the necessary conditions for a precise comparison.

The two crystal spectrometer used was a high precision type made by the Societe Genevoise.* The second crystal of this instrument is on the main axis of the spectrometer[1] thus permitting the angle through which this crystal is rotated to be measured very precisely. The graduated circle was calibrated by using a plane mirror on the axis of the spectrometer which reflected the images of two distant filaments into a telescope. As this calibration showed no error greater than 0.6″, which was the limit of resolution of the telescope used, another method was employed to obtain the absolute diffracting angle for one crystal.

A modified Michelson interferometer[4] was attached to the base of the in-

[1] A. H. Compton, Phys. Rev. **37**, 1694 (1931)A; Rev. Sci. Inst. **2**, 365 (1931).

[2] J. A. Bearden, Phys. Rev. **38**, 1389 (1931).

[3] The most precise photographic spectrometers in use are probably those used by Siegbahn and his collaborators.

* The author wishes to express his appreciation to Mr. Alfred L. Loomis of Tuxedo, New York, who so kindly furnished the necessary funds for the purchase of this instrument.

[4] J. A. Bearden, Phys. Rev. **37**, 1217 (1931).

strument and at the height of the crystal tables. This was used to adjust a three point support parallel to and on the axis of the spectrometer. A telescope with a Gauss eyepiece was placed perpendicular to the axis of the spectrometer. A crystal was then placed against the three points and held in place by three light springs. Thence by using the telescope, the cleavage plane of the crystal could be adjusted parallel to the axis of the spectrometer. The interferometer was used to place the part of the crystal which actually diffracted the x-rays on the axis of the spectrometer. The first crystal was then adjusted to diffract the molybdenum $K\alpha_1$ line over the axis of the spectrometer. It was then adjusted parallel to the second crystal by making the width of the rocking curve a minimum.

The slits, one near the x-ray tube and the other in front of the ionization chamber, were placed on a horizontal line perpendicular to the axis of the spectrometer to within 0.1 mm. As is well known, the height of these slits affects the width and angular position of a diffracted line. For a uniformly illuminated source and slits of equal height the correction may be written

$$d\theta''_{eff} = 0.204 \frac{a^2}{L^2} \tan\theta$$

where a is the height of the slit and L their separation. This equation was tested for four slit heights from 0.5 mm to 3.0 mm, and a separation of 52 cm.

The measured angles have been reduced to 18° C by using the equation[5]

$$d\theta = -1.04(t - 18°\text{C}) \tan\theta \times 10^{-5}$$

$$\text{or } d\theta'' = -2.15(t - 18°\text{C}) \tan\theta$$

where t is the temperature of the crystal at the time of the measurement of the diffracting angle θ.

The diffraction angle for one crystal was then very carefully measured in three different positions on the graduated circle (120° apart). The maximum variation observed was 0.4″ and an average variation slightly less than 0.2″. The average angle was accepted as the absolute diffraction angle for this crystal, and all other results have been obtained relative to this crystal. I do not believe the diffraction angle for this crystal is in error by more than 0.2″ and is probably less.

Some very clear and perfect samples of calcite crystals from Montana, Argentina, Spain, and Iceland have been obtained. (These samples will now be referred to by the first letter of each.) Slabs about 10 mm thick have been carefully cleaved from these samples. Some surfaces were obtained which were almost free from "steps," and the others showed only a few small "steps." Adjacent pairs were selected and the width of the rocking curves measured. The widths varied from 5.5″ to 7″. It was also found that pairs selected even from crystals of different origin gave the same rocking curve widths as adjacent pairs from the same crystal. Only one large I crystal (12×

[5] The value of the expansion coefficient α was misprinted as 1.09×10^{-5} in the Phys. Rev. **38**, 1390 (1931). The value actually used was $\alpha=1.04\times10^{-5}$.

8×3 cm) was available, so two samples were cleaved from it in order to see how well the various observations would check. Two M samples were cleaved from different crystals but from the same region.

The grating constants of these crystals were compared by using the molybdenum $K\alpha_1$ line and the fourth order of diffraction. That is, (1, +4), (1, −4) in Allison's notation. Fig. 1 shows typical data forming one set of measure-

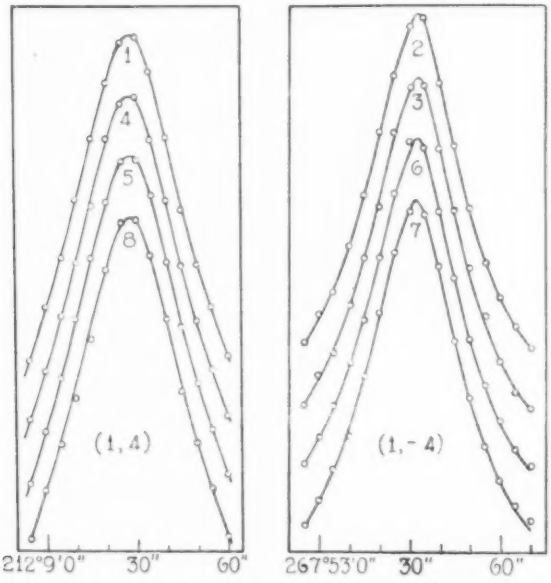

Fig. 1. One set of diffraction curves for (1, 4) and (1, −4) orders. The curves were taken in the order of the numerals.

ments. The curves were taken in the order of the small numerals so that any errors due to a slow change in the adjustment of the apparatus would be eliminated. Two such sets of measurements were made on each crystal in the order I_1, I_2, M_1, M_2, A, and S. Then two more sets in the order S, A, M_2, M_1, I_2, I_1. The results are given in Table I. The angles have been reduced to 18° C

TABLE I.

Origin	Diffraction angle	Difference from mean
Iceland	27° 51′ 34.0″	−0.4″
Iceland	27° 51′ 34.0″	−0.4″
Montana	27° 51′ 34.6″	+0.2″
Montana	27° 51′ 34.7″	+0.3″
Argentina	27° 51′ 34.7″	+0.3″
Spain	27° 51′ 34.4″	0.0″
Mean	27° 51′ 34.4″	0.26″

and corrected for the height of the slit. They have also been slightly corrected for the small error in the graduated circle. Since in each case the measurements have been made on the same part of the graduated circle, I believe the relative values are not in error by more than 0.1″. Thus, there is a real dif-

ference in the grating constant of the various crystals. However, the maximum difference is only one part in 145,000, and the maximum difference from the average is about 1 part in 250,000. If one only considers the M_1, M_2, A, and S crystals the maximum variation from the average is about one part in 500,000. These variations are so small that the differences in x-ray wavelengths reported by some observers must be due to the method used, and not to a variation in the grating constant of the crystals. A redetermination of a series of x-ray lines from 0.5A to 2.25A will be given in this Journal in a few weeks.

II. A Chemical Analysis of Crystals

After the above x-ray data had been secured, two samples were cut from each crystal near the point on the surface that had been used for diffracting the x-rays. Then samples, one from each crystal, were carefully analyzed for the writer by Dr. W. B. D. Penniman and Dr. A. L. Browne. The results are given in Table II. Thus, chemically there appears to be very little difference

Table II.

Origin	Silica	Alumina	Ferrous oxide	Manganous oxide	Magnesium oxide	Calcium carbonate
Iceland	absent	absent	0.007	0.008	absent	99.98%
Iceland	absent	absent	0.006	0.007	absent	99.98
Montana	absent	absent	0.005	0.011	absent	99.97
Montana	absent	absent	0.006	0.011	absent	99.97
Argentina	absent	absent	0.006	0.010	absent	99.98
Spain	0.004	absent	0.007	0.006	absent	99.98

between the various samples. These samples were selected because of their optical clearness and perfection, so that one might expect them to be almost chemically pure. It is well known that colored calcite may contain several percent of some impurity. However in x-ray work it is the general practice to select the best samples available, so that the above results are probably a fair estimate of the chemical purity of the crystals normally used.

III. Density of the Crystals

The other pieces of calcite which were cut from each crystal above, were prepared for determining the density. Five of the crystals were finely ground and all surface flaws due to cleaving the crystal were removed. The edges were rounded off so there would be no possibility of occlusion of air on the surface. Four of these crystals were used in this condition and the fifth was polished with rouge. The sixth crystal was left unground. The masses of the crystals were determined by weighing in air with calibrated weights and correcting for the buoyancy of the air. The crystals were then weighed in kerosene at a temperature of 20° $\pm$0.01° C. The density of the kerosene can be determined very accurately and thus the density of the crystals. Corrections were, of course, made for the weight of the rough gold plated copper supporting wire and surface tension. From 6 to 9 independent measurements have been made

on each crystal. In Table III the results, with the probable errors for each crystal, are given for a temperature of 20° C. The probable error was calculated according to least squares method as was used by Birge.[6] The best previous determinations of the density of calcite crystals were made by De Foe

TABLE III.

Origin	Density-g/cm 20°C	Probable error	Mass of crystal -g
Iceland	2.7104	±0.00002	12.9764
Iceland	2.71035	±0.00002	15.5780
Montana	2.7102	±0.00008	7.1467
Montana	2.7102	±0.00002	14.8650
Argentina	2.7102	±0.00004	11.0769
Spain	2.7102	±0.00004	13.0083
Mean	2.71026		

and Compton.[7] Their results are given in Table IV. They give as a probable error for each sample ± 0.0001 g/cm^{-3}. The variations in Table IV are much greater than those in Table III. This may be due to a fortuitous selection of crystals used in the present experiment. However if this were true, one would hardly expect the mean value for the two sets of crystals to agree so closely.

TABLE IV.

Origin	Density at 20°C g/cm^{-3}
Missouri	2.7106
U.S.A.	2.7102
Iceland	2.7103
Iceland	1/2 (2.7090)
Unknown	2.7101
Unknown	2.7103
Mean	2.7102

The second Iceland crystal in Table IV differs so much from the others that I believe the crystal must have been imperfect and should be given zero weight instead of 1/2. Thus, the mean would have been 2.71034. Taking this result into consideration with the present results of Table III, the writer believes that the most probable value of the density ρ is

$$\rho = 2.71030 \pm 0.00003 \text{ g/cm}^{-3} \text{ at } 20°\text{C}.$$

This probable error given assumes that the variations from this value were experimental errors. The maximum variation would be 0.0003 g/cm^{-3} for De Foe's and Compton's[7] results, and 0.0001 for the present results.

[6] R. T. Birge, Phys. Rev. Supplement **1**, 1 (1929).
[7] O. K. DeFoe and A. H. Compton, Phys. Rev. **25**, 618 (1925).

IV. A Determination of the Angle Between the Cleavage Faces of Calcite

Since the angle between the cleavage faces of a crystal enter into the calculation of the grating constant, it is important to know this angle as precisely as possible. This angle can be measured with high precision by using a two crystal spectrometer as described above. It has also been reported[8] that this angle varies slightly for different crystals.

In the first measurements crystals from 4 to 6 mm square and 10 to 20 mm long were used. The cleavage planes were aligned parallel to the spectrometer axis. The crystals were placed so that the molybdenum $K\alpha_1$ line could be reflected from two faces by simply rotating the crystal through the angle α where α is the angle between the planes of the crystal. Since the results obtained by this method differed from those of previous investigators two other methods were used.

In the second method, crystals about 1 mm$\times$1 mm$\times$10 mm were mounted parallel to and on the axis of the double crystal spectrometer. The first crystal was adjusted to diffract the silver $K\alpha_1$ line over the axis of the spectrometer. The small crystal was then rotated until it diffracted this line into the ionization chamber. Thus, when the crystal was rotated through an angle α or $180°-\alpha$ the same line was again diffracted into the ionization chamber.

In the last method, the crystals used in the first method were spluttered with gold and adjusted on the spectrometer as above. Optically the angles were determined by using the telescope with a Gauss eyepiece. The results of the three methods are given in Table V in terms of the interior obtuse dihe-

Table V.

Origin	1st method α	2nd method α	3rd method α
Iceland	105° 3′ 28″	105° 3′ 30″	105° 3′ 35″
Montana	105° 3′ 31″	105° 3′ 31″	105° 3′ 20″
Argentina	105° 3′ 29″	105° 3′ 27″	105° 3′ 25″
Spain	105° 3′ 30″	105° 3′ 28″	105° 3′ 25″

dral angle α. The angles were measured at 25° C to 26° C and reduced to 20° C by using the known expansion coefficients parallel to and perpendicular to the axis of the crystal. This correction can be calculated in terms of the angle β between the edges of the crystal β and α are connected by the trigonometric relation

$$\cos\frac{\beta}{2}=\left(2\sin\frac{\alpha}{2}\right)^{-1/2}.$$

The correction is then

$$\frac{d\beta}{dt}=2\tan\frac{\beta}{2}\left(1-\frac{3}{4}\sin^2\frac{\beta}{2}\right)(\alpha_1-\alpha_{11})$$

[8] H. N. Beets, Phys. Rev. **25**, 621 (1925).

by using the values $\alpha_\perp = -0.0000056$ deg.$^{-1}$C and $\alpha_\parallel = 0.000025$ deg.$^{-1}$C. one obtains $d\beta/dt = -3.1''$ per degree C.

The weighted mean of methods one and two gives

$$\alpha = 105^\circ\ 3'\ 29''$$
$$\beta = 101^\circ\ 54'\ 4''.$$

The value of α differs by about 90 seconds from the value obtained by Beets.[8] The present results also show very little, if any, variation in the angle α for different samples. The writer is unable to explain the difference but feels that the above experiments are conclusive.

V. Calculation of the Grating Constant d

From fundamental considerations of crystal structure it can be shown that the grating space of a rhombohedral crystal is given by

$$d = \left(\frac{nM}{N\phi}\right)^{1/3}$$

where n is the number of molecules in each elementary rhombohedron, M the molecular weight of the crystal, N is Avogadro's number, ρ the density of the crystal, and ϕ is the volume of a rhombohedron, the perpendicular distance between whose opposite faces is unity. It can also be shown that

$$\phi = \frac{(1 + \cos\beta)^2}{(1 + 2\cos\beta)\sin\beta}$$

where β is the same as in the last section. ϕ thus becomes

$$\phi = 1.09594 \pm 0.00001.$$

For a calcite crystal $n = \frac{1}{2}$.[9] Birge[6] gives for the molecular weight of calcite $M = 100.078 \pm 0.005$. The density as determined above is, $\rho = 2.71030 \pm 0.00003$. Avogadro's number can be most accurately determined from the relation

$$N = \frac{FC}{e}$$

where F is the Faraday constant, C the velocity of light, and e the charge on the electron. Birge[6] gives $FC = 2.8987 \pm 0.0002 \times 10^{14}$ Abs. e.s.u. and $e = 4.770 \pm 0.005 \times 10^{-10}$ e.s.u. From Millikan's experiments Birge obtained a value of $e = 4.768 \times 10^{-10}$ e.s.u. and in consideration of Wadlun's[10] grating wavelength measurements of x-ray spectra which gave $e = 4.774 \times 10^{-10}$ e.s.u. raised Millikan's value to 4.770×10^{-10} e.s.u. More recent grating measurements by the writer[11] have shown that e, from such experiments, is 4.806×10^{-10} e.s.u. It appears to the writer to be out of the question to average this

[9] W. H. Bragg and W. L. Bragg, X-rays and crystal structure.
[10] A. P. R. Wadlung, Phys. Rev. **32,** 841 (1928).
[11] J. A. Bearden, Phys. Rev. **37,** 1210 (1931).

result with that of Millikan's. The difference of such an average from the results of either experiment would be many times the experimental error of either. The writer thus believes it is preferable to retain Millikan's value

$$e = 4.768 \pm 0.005 \times 10^{-10} \text{ e.s.u.}$$

until the magnitude of the mosaic structure can be determined and the validity of the grating formula established for x-ray wave-lengths. From this value of e one obtains

$$N = 6.0669 \times 10^{23} \text{ molecules/mole.}$$

The value of d is then calculated to be

$$d = 3.02816\text{A at } 20°\text{C}$$
$$d = 3.02810\text{A at } 18°\text{C.}$$

The probable error is ± 0.001, which is almost entirely due to the probable error in e. This value is about one part in 3000 lower than the value adopted by Siegbahn.[12]

In order to calculate the true wave-length of an x-ray line with the true grating constant as determined above, the complete Bragg law

$$n\lambda = 2d\left(1 - \frac{1-\mu}{\sin^2\theta}\right)\sin\theta$$

must be used where λ is the true wave-length, d the true grating space, μ the index of refraction, and θ the diffraction angle for the n-th order. If we use the value $(1-\mu)/\lambda^2 = 3.69 \times 10^{-6}$ the above equation becomes

$$n\lambda = 2d\left(1 - \frac{135 \times 10^{-6}}{n^2}\right)\sin\theta$$
$$= 2d_n \sin\theta$$

where d_n is the effective grating constant for the n-th order. With the true grating constant $d = 3.02810$, the calculated values of d_n and $\log 2d_n$ are given in Table VI.

TABLE VI.

$d_1 = 3.02769$A	$\log 2d_1 = 0.7821415$
$d_2 = 3.02799$	$\log 2d_2 = 0.7821752$
$d_3 = 3.02805$	$\log 2d_3 = 0.7821937$
$d_4 = 3.02807$	$\log 2d_4 = 0.7821966$
$d_5 = 3.02808$	$\log 2d_5 = 0.7821980$
. . . . .	. . . . .
$d_\infty = 3.02810$	$\log 2d_\infty = 0.7822002$

VI. Discussion

Attention should be called to some of the results in the present experiment. Chemically all the samples seemed to be very similar and almost pure

[12] M. Siegbahn, Spectroskopie der Roentgenstrahlen.

calcium carbonate. In the calculation of the grating constant the effect of the slight impurities was neglected. In the x-ray comparison of the samples the variations in the diffraction angles were small, but the angles I_1 and I_2 were definitely smaller than the others. This would suggest a smaller crystal density. On the contrary the densities of I_1 and I_2 were the largest in the group. This indicates that a difference in density does not reflect itself as a corresponding change in the grating constant of the crystal. Consequently the measured density may not be the real density of the crystal lattice which is responsible for the diffraction of the x-rays.

It has been pointed out[2] that the absolute value of the diffraction angle for the molybdenum $K\alpha_1$ line, obtained by the writer, differs by about 1.4″ from the precision measurement reported by Compton.[1] This difference is about five times the apparent probable error of either experiment. However, the writer has recalculated the correction for the height of the slits in Compton's experiment and finds a value $d\theta_{eff} = -0.6''$ instead of $-2.2''$ as used by him. Thus his diffraction angle would be increased to 27° 51′ 34.6″ which agrees, within the experimental error, with the present results.

The difference between the writer's ruled grating wave-length measurements[11] and the corresponding crystal results now is 0.25 percent instead of 0.22 percent as previously given. Such a great difference must be due to a failure of the ruled grating diffraction equation to be valid for the x-ray region. The boundary conditions are probably not the same for optical wave-lengths and x-rays and might thus alter the position of the diffraction maxima. A careful analysis of the diffraction theory for x-ray wave-lengths and for the conditions under which x-ray spectra are obtained is badly needed in order to settle the questions raised by such experimental differences.

THE NORMAL STATE OF THE HYDROGEN MOLECULE

By N. Rosen
Massachusetts Institute of Technology

(Received October 30, 1931)

Abstract

The dissociation energy, moment of inertia, and fundamental vibration frequency are calculated for a normal hydrogen molecule by a variational method and are found to be 4.02 v, $4.66 \cdot 10^{-41}$ gm-cm^2, and 4260 cm^{-1} as compared to the experimental values 4.42, $4.67 \cdot 10^{-41}$, and 4380, respectively. The calculation is carried through with the simplest possible improvements in the wave functions. In the appendix a number of integrals are listed and two tables of functions are included that may be useful to calculators.

I. Introduction

THE problem of calculating some of the properties of the normal hydrogen molecule by wave-mechanical methods has been hitherto successful qualitatively but not quantitatively. Thus Sugiura[1] by completing the calculations of Heitler and London[2] based on a first-order perturbation method, obtained 3.2 volts for the dissociation potential as compared to the experimental value, 4.4 volts. Wang,[3] by using a variational method involving the introduction of a shielding constant, obtained 3.7 volts for this energy, which is a distinct improvement but still rather far from the goal. It is true that Condon[4] obtained an almost exact agreement with experiment, but it is questionable as to whether one can call his method of doing this a straight-forward calculation. Eisenschitz and London,[5] by carrying through a second order perturbation method, got 9.5 volts.

Similarly in the case of the two other quantities which are generally calculated at the same time as the energy, namely the equilibrium distance and the fundamental vibration frequency, the calculated results are not in very good agreement with the experimental values. If one surveys the available methods of calculating the quantities mentioned, it is at once evident that the only method for getting quantitative results is that based on the use of a variational principle, because the wave equation for this case cannot be solved exactly, and because solving it by the perturbation method is not to be trusted, as is shown by the fact that the second-order perturbation calculation gave a much worse result than the first-order calculation. In using the variational method one has the comforting assurance that one cannot go astray. If one starts with wave functions of sufficient complexity and having a large

[1] Sugiura, Zeits. f. Physik **45,** 484 (1927).
[2] Heitler and London, Zeits. f. Physik **44,** 455 (1927).
[3] Wang, Phys. Rev. **31,** 579 (1928).
[4] Condon, Proc. Nat. Acad. Sci. **13,** 466 (1927).
[5] Eisenschitz and London, Zeits. f. Physik **60,** 491 (1927).

enough number of parameters, and if one puts in enough labor one can generally approach the right answer, at least as far as the energy is concerned.

However, rather than to do this, it seems preferable to try to get an appreciable improvement in the calculated results with but a small increase in the complexity of the calculation. It is therefore the purpose of the present paper to try to improve the theoretical results for the normal hydrogen molecule, at the same time keeping the wave functions and the calculation as simple as possible.

II. Theory

To carry out this policy of simplicity, we begin with the understanding that we shall deal only with wave functions made up of products of individual electron wave functions. We than inquire as to what happens to the electron charge distribution in a hydrogen atom when it is brought up to another similar atom so as to combine with it. It is apparent that because of the various complicated interactions that occur, the charge distribution will be altered, this distortion becoming greater as the two atoms approach each other. The wave functions (from which the charge distributions are calculated) also become altered. The exact nature of the changes can be investigated only in a six-dimensional space, but for the purposes of the present problem one can try to consider the approximate distortion of an individual wave function in ordinary space. The simplest way to represent this distortion is to consider the radius of the atom to change with the distance to the other atom. This is effectively what Wang[3] did in his calculations, and it led to a definite improvement in the energy value.

However, since the perturbations involved are not spherically symmetrical this cannot be a very good approximation to the true state of affairs, and the next improvement that suggests itself is to introduce a change in the wave function that will depend on the direction with respect to the molecular axis and will be greatest in the direction of the latter. Since the interactions can be thought of roughly as being along this axis, it seems likely that the electron cloud tends to bulge out in the direction of the second atom.

Let us denote the nuclei by a and b, the electrons by 1 and 2, the internuclear distance by R, other distances by r with subscripts and the angle between a radius vector and the axis (the line joining the nuclei) by θ with subscripts. In accordance with the previous considerations we take as the simplest individual wave function

$$\psi = \psi^0 + \sigma\psi' \tag{1}$$

where ψ^0 is the hydrogenic wave function for the lowest state, but with a shielding constant, ψ' is a function symmetrical about the axis but not about a plane through the nucleus perpendicular to it, and σ is a parameter the magnitude of which is to be determined so as to minimize the variational integral.

The conditions imposed on the choice of ψ' are: (1) that it satisfy the boundary conditions for a wave function, (2) that it have reasonable direc-

tional properties, (3) that it be orthogonal to ψ^0, (4) that it satisfy a simple wave equation. Of these, (1) and (2) are necessary, but (3) and (4) are convenient in calculating. If we consider electron 1 on atom a and write the hydrogenic function in the form

$$\psi^0(a1) = N_0 e^{-\alpha r_{a1}} \tag{2}$$

then the simplest perturbation function satisfying these conditions seems to be

$$\psi'(a1) = N_1 e^{-\alpha r_{a1}} r_{a1} \cos\theta_{a1} \tag{3}$$

where N_0 and N_1 are the corresponding normalizing factors which, on integrating the squares of the wave functions over all space, one finds to have the values:

$$N_0 = (\alpha^3/\pi)^{1/2} \tag{4}$$

$$N_1 = (\alpha^5/\pi)^{1/2}. \tag{5}$$

In these expressions, we have used α to represent the quantity Z/a_0, where Z is the effective charge of the nucleus and a_0 the normal hydrogen radius. Accordingly, the wave equation satisfied by $\psi^0(a1)$ is

$$H_{a1}{}^0\psi^0(a1) = Z^2E_0\psi^0(a1) \tag{6}$$

where

$$H_{a1}{}^0 = -\frac{h^2}{8\pi^2 m}\nabla_1{}^2 - Ze^2/r_{a1} \tag{7}$$

and E_0 is the energy of a normal hydrogen atom.

Now ψ' can be seen to be identical with the wave function corresponding to the $2p$ state in a hydrogenic atom of nuclear charge $2Z$. Hence the equation which it satisfies is:

$$H_{a1}'\psi'(a1) = Z^2E_0\psi'(a1), \tag{8}$$

where

$$H_{a1}' = -\frac{h^2}{8\pi^2 m}\nabla_1{}^2 - 2Ze^2/r_{a1}. \tag{9}$$

Of course similar expressions can be written for the wave functions for the other electron or atom. Incidentally, it may be mentioned that for the atom b we take for the wave function

$$\psi'(b1) = -N_1 e^{-\alpha r_{b1}} r_{b1} \cos\theta_{b1} \tag{3a}$$

so as to keep all quantities symmetrical about the plane midway between the nuclei.

For the combined wave function of the normal state of the molecule we take

$$\Psi = \psi(a1)\psi(b2) + \psi(b1)\psi(a2). \tag{10}$$

The wave-mechanical Hamiltonian is given by

$$H = -\frac{h^2}{8\pi^2 m}(\nabla_1{}^2 + \nabla_2{}^2) + e^2[1/R - 1/r_{a1} - 1/r_{a2} - 1/r_{b1} - 1/r_{b2} + 1/r_{12}], \tag{11}$$

and according to the theory of the variational method it is necessary to minimize the quantity

$$W = \int \Psi H \Psi dv_1 dv_2 \Big/ \int \Psi^2 dv_1 dv_2, \tag{12}$$

which then gives the value of the energy.

Now by making use of Eqs. (6) and (8) we can write

$$\begin{aligned} H\psi^0(a1)\psi^0(b2) = \{ & 2Z^2E_0 + e^2[1/R + s/r_{a1} + s/r_{b2} - 1/r_{a2} \\ & - 1/r_{b1} + 1/r_{12}]\}\psi^0(a1)\psi^0/(b2), \end{aligned} \tag{13}$$

$$\begin{aligned} H\psi^0(a1)\psi'(b2) = \{ & 2Z^2E_0 + e^2[1/R + s/r_{a1} + (2s+1)/r_{b2} \\ & - 1/r_{a2} - 1/r_{b1} + 1/r_{12}]\}\psi^0(a1)\psi'(b2), \end{aligned} \tag{14}$$

$$\begin{aligned} H\psi'(a1)\psi'(b2) = \{ & 2Z^2E_0 + e^2[1/R + (2s+1)/r_{a1} + (2s+1)/r_{b2} \\ & - 1/r_{a2} - 1/r_{b1} + 1/r_{12}]\}\psi'(a_1)\psi'(b_2), \end{aligned} \tag{15}$$

where

$$s = Z - 1. \tag{15a}$$

By means of these relations and similar ones derived from them by replacing a by b or 1 by 2, W can be evaluated. If we adopt the following notation,

$$I_{00} = \int \psi^0(a1)\psi^0(b1)dv_1, \tag{16}$$

$$F_0 = \int \frac{[\psi^0(a1)]^2}{r_{a1}} dv_1, \tag{17}$$

$$G_{00} = \int \frac{[\psi^0(a1)]^2}{r_{b1}} dv_1, \tag{18}$$

$$K_{00,01} = \int \frac{[\psi^0(a1)]^2\psi^0(b2)\psi'(b2)}{r_{12}} dv_1 dv_2, \tag{19}$$

$$J_{01} = \int \frac{\psi^0(a1)\psi'(b1)}{r_{a1}} dv_1; \quad J_{10} = \int \frac{\psi'(a1)\psi^0(b1)}{r_{a1}} dv_1, \tag{20}$$

$$L_{01,10} = \int \frac{\psi^0(a1)\psi'(b1)\psi'(a2)\psi^0(b2)}{r_{12}} dv_1 dv_2, \tag{21}$$

with corresponding changes in the numbering when ψ^0 is replaced by ψ' or vice versa, we can then write W in the form:

$$W = \frac{e^2}{R} \sum_{i=0}^{4} \sigma^i(P_i + sQ_i) \Big/ \sum_{i=0}^{4} \sigma^i D_i + 2Z^2E_0, \tag{22}$$

where the quantities D_i, P_i, and Q_i are made up of the various integrals over wave functions and are defined as follows. In each case the "exchange" terms are grouped in brackets.

$$\left.\begin{aligned}
D_0 &= 1 + [I_{00}^2],\\
D_1 &= [4I_{00}I_{01}],\\
D_2 &= 2 + [4I_{01}^2 + 2I_{00}I_{11}],\\
D_3 &= [4I_{01}I_{11}],\\
D_4 &= 1 + [I_{11}^2].
\end{aligned}\right\} \tag{23}$$

$$\left.\begin{aligned}
P_0 &= 1 + R(K_{00,00} - 2G_{00}) + [I_{00}^2 + R(L_{00,00} - 2I_{00}J_{00})],\\
P_1 &= 4R(K_{00,01} - G_{01}) + [4I_{00}I_{01} + R(4L_{00,01} - 4I_{01}J_{00} - 2I_{00}J_{01})],\\
P_2 &= 2 + R(4K_{01,01} + 2F_1 + 2K_{00,11} - 2G_{00} - 2G_{11}),\\
&\quad + [4I_{01}^2 + 2I_{00}I_{11} + R(2L_{01,10} + 2L_{01,01} + 2L_{00,11}\\
&\quad - 2I_{11}J_{00} - 4I_{01}J_{01})],\\
P_3 &= 4R(K_{01,11} - G_{01}) + [4I_{01}I_{11} + R(4L_{01,11} - 2I_{11}J_{01})],\\
P_4 &= 1 + R(2F_1 + K_{11,11} - 2G_{11}) + [I_{11}^2 + RL_{11,11}].
\end{aligned}\right\} \tag{24}$$

$$\left.\begin{aligned}
Q_0 &= 2RF_0 + [2RI_{00}J_{00}],\\
Q_1 &= [R(4I_{00}J_{10} + 2I_{00}J_{01} + 4I_{01}J_{00})],\\
Q_2 &= R(2F_0 + 4F_1) + [R(4I_{00}J_{11} + 2I_{11}J_{00} + 4I_{01}(J_{01} + 2J_{10}))],\\
Q_3 &= [R(8I_{01}J_{11} + 2I_{11}(J_{01} + 2J_{10}))],\\
Q_4 &= 4RF_1 + [4RI_{11}J_{11}].
\end{aligned}\right\} \tag{25}$$

These integrals can be evaluated without great difficulty. The discussion of them is to be found in the appendix. It is easy to see that the various D_i, P_i, and Q_i are functions only of the quantity

$$\rho = \alpha R \tag{26}$$

and can be calculated for various values of ρ and plotted. If we let

$$\rho_0 = R/a_0, \tag{27}$$

then

$$Z = \rho/\rho_0, \tag{28}$$

$$s = (\rho - \rho_0)/\rho_0. \tag{29}$$

For a given value of R or ρ_0 one can then vary ρ and, by reading the values of the functions from the curves, minimize W. By repeating this for a number of values of ρ_0 one thus obtains a series of energy values which can be plotted as a function of ρ_0 and a smooth curve drawn. However, unless the points for which calculations are made are very close together it is not possible in general to determine the minimum of the energy curve very accurately in this way. If the points are fairly close together one can pass a parabola through the points in the vicinity of the minimum. But if, as was the case in the calculation carried out, the points are not sufficiently close together, one must resort to some other method.

What was done was to use instead of a parabola a curve of the type discussed by Morse[6] in connection with interatomic potentials:

$$\Delta E = De^{-2a(\rho_0-\rho_m)} - 2De^{-a(\rho_0-\rho_m)}. \tag{31}$$

A curve of this sort is known to fit molecular energy curves very well especially in the neighborhood of the minimum. By fitting this curve to three points near the minimum one can get the dissociation energy D and the equilibrium distance $\rho_m a_0$. (The details of the curve-fitting are given in the appendix.)

From the latter the moment of inertia follows:

$$J_0 = \tfrac{1}{2} M_H (\rho_m a_0)^2, \tag{31}$$

where M_H is the mass of a hydrogen atom.

Since at the minimum

$$\frac{d^2E}{d\rho_0^2} = 2a^2D \tag{32}$$

the fundamental vibration frequency is given by

$$\nu_0 = \frac{a}{\pi a_0 c} (D/M_H)^{1/2}. \tag{33}$$

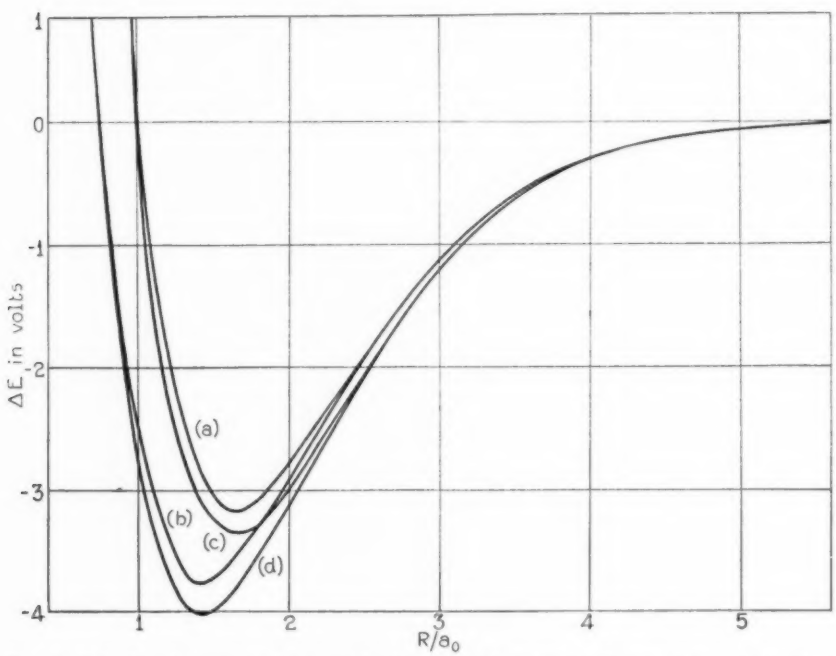

Fig. 1. Calculated energy of normal hydrogen molecule: (a) first order perturbation, (b) varying s, (c) varying σ, (d) varying σ and s.

[6]Morse, Phys. Rev. **34**, 57 (1929).

III. Results

The minimization was carried out first by keeping $\sigma=0$ and varying s. This is essentially what Wang[3] did except that his results were only for the equilibrium distance. The energy curve obtained is shown in Fig. 1 (b) and may be compared with the first-order perturbation energy 1 (a).

The value of s as function of the interatomic distance is shown in Fig. 2. For $R=0$ of course we have a helium atom and for this the effective nuclear charge (as given by a variational method calculation) is 1.6875 e, so that $s=0.6875$. For large distances s falls off rapidly. It is interesting to note that beyond a certain distance, s changes sign. This may be interpreted by saying that for large distances the second electron has more of an effect upon the atom than the second nucleus. Geometrically one may say that as the atoms

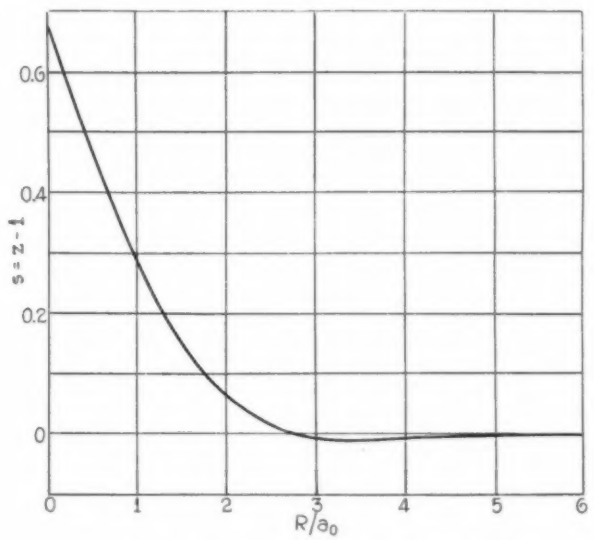

Fig. 2. Variation of s with interatomic distance.

approach each other, there is first an expansion of the charges and then, for smaller distances, a contraction.

The next step in the procedure was to set $s=0$, and minimize W with respect to σ. The energy resulting from this calculation is shown in Fig. 1 (c). Comparison with 1 (a) shows that the improvement in the energy near the equilibrium distance is rather small, but that there is a distinct improvement at somewhat larger distances. The curve of σ thus obtained, denoted by σ_0, is shown in Fig. 3 (a).

The quantity σ can be taken as a rough measure of the longitudinal distortion of the wave function. As the graph shows, for small distances there seems to be a sudden distortion of the wave function which disappears as the atoms merge to give helium. This apparent behavior at small distances is probably without significance, since the wave functions obtainable from a variational calculation need not approximate the true wave functions as closely as the calculated energy does the true value. In the present case, the

behavior of the true wave functions for small internuclear distance is exceedingly complex, and an attempt to fit this behavior into the narrow mold provided by a single parameter cannot be expected to be very successful.

To get a better approximation, the values of s obtained previously were put into W and then σ was varied once more. The energy obtained this time is given in Fig. 1 as curve (d). As is to be expected, it is below the other curves and merges with (b) for small distances and with (c) for large distances. The curve of the values of σ thus calculated, denoted by σ_1, is shown in Fig. 3 (b). It agrees with σ_0 down to about $\sigma_0 = 1.5$. For smaller distances the two differ widely, and this is probably the region in which they lose any physical significance they may have at larger distances.

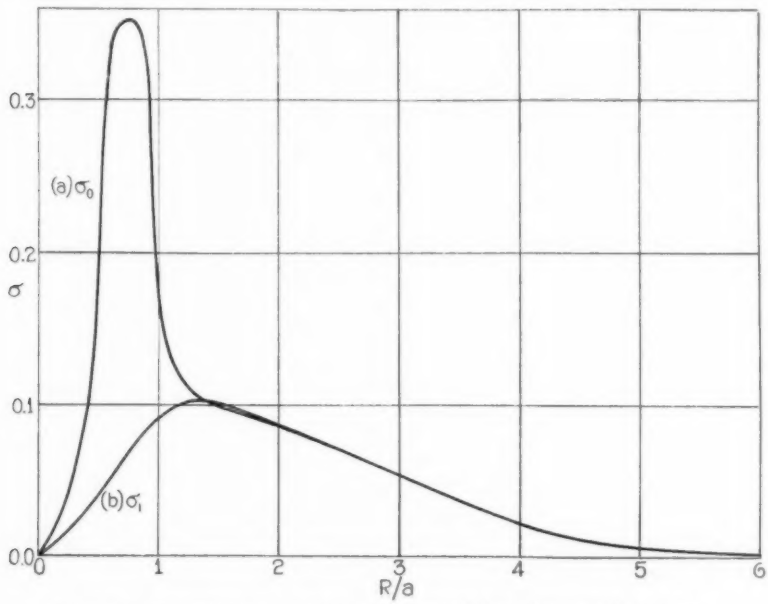

Fig. 3. Parameter σ to minimize energy: (a) without shielding constant, (b) with shielding constant.

The parameter was kept fixed at the set of values σ_1 and s was recalculated. It was found that within the accuracy available in reading graphs, s did not change appreciably—at least in the regions of any importance. Hence the energy curve 1 (d) represents the best result obtainable by the present method.

For this curve the dissociation energy was found to be 4.02 volts, the equilibrium distance between atoms 1.416 a_0 corresponding to a moment of inertia of 4.66×10^{-41} gm-cm^2 and a fundamental vibration frequency of 4260 cm^{-1}. In the following table[7] these results are compared with those obtained in previous calculations and with the experimental values.

[7] This table (except for obvious changes) is taken from the paper of Wang (reference 3). The experimental values given these are those of Witmer, Proc. Nat. Acad. Sci. **12,** 238 (1926), and Phys. Rev. **28,** 1223 (1926). Cf. Birge, Int. Crit. Table **V,** 409 (1929).

	E (Rh)	$\Delta E(v)$	J_0(gm−cm²)	ν_0(cm⁻¹)
Present paper	−2.297	−4.02	4.66×10^{-41}	4260
Wang[3]	−2.278	−3.76	4.59	4900
Condon[4]	−2.325	−4.40	4.26	5300
Sugiura[1]	−2.24	−3.2	5.2	4800
Observed[7]	−2.326	−4.42	4.67	4380

It is seen that the dissociation energy as calculated here is about 10 percent too small. However, if we consider the total energy of the molecule, the error is only about 1 percent. If we compare this to the helium problem—it is only fair that the total molecular energy be considered in this comparison—we note that the Hartree method[8] gives for the total energy of an He atom 5.75 Rh as compared to 5.81 Rh as observed, so that the error is also about 1 per cent. Now the Hartree method gives the greatest possible accuracy obtainable with wave functions made up of the products of individual wave functions, it being equivalent to a variational method with a function of complete flexibility. Since in the present case the wave function is likewise made up of products of individual wave functions, it is questionable whether one could hope to exceed this accuracy by very much, the situation in the hydrogen molecule being rather similar to that in the helium atom.

In concluding the main part of this paper, the writer wishes to acknowledge the advice and encouragement received from Drs. J. C. Slater and R. M. Langer and the assistance from Dr. S. Ikehara in checking parts of the calculation and in compiling the tables.

Note added in proof (December 4, 1931)—Shortly after the present article had been sent to the publisher, the writer learned of the paper of E. A. Hylleraas, Zeits. f. Phys **k 71,** 739 (1931) "Uber die Elektronenterme des Wasserstoffmolekuls," in which, among other things, he calculates the energy of the lowest state of H_2 in very close agreement with the experimental value. However, it ought to be pointed out that one should not compare the results of the present paper with his results, since he multiplies through his calculated value of the energy by a factor obtained by interpolating between values for $R=0$, and $R=\infty$, to get his final result.

Appendix

1. Integrals

Many of the integrals arising in the present calculations are not new. Thus a number are to be found in the papers of Heitler and London,[2] Sugiura,[1] and Bartlett.[9] However, for the sake of completeness they will all be given here (in perhaps a different form). All but a few of the integrals present no great difficulties in the evaluation. The ones which do give trouble are the exchange integrals and they can be handled in the following way:

On replacing $1/r_{12}$ by its Neumann expansion in terms of Legendre func-

[8] Gaunt, Proc. Camb. Phil. Soc. **24,** 328 (1928).
[9] Bartlett, Phys. Rev. **37,** 507 (1931).

tions of the elliptic coordinates any one of the exchange integrals arising here can be broken up into a sum of terms of the form $H(m, n, \alpha)$ and $S(m, n, \alpha)$ where

$$H(m, n, \alpha) = \int_1^\infty \lambda_1{}^m e^{-\alpha\lambda_1} Q_0(\lambda_1) d\lambda_1 \int_1^{\lambda_1} \lambda_2{}^n e^{-\alpha\lambda_2} d\lambda_2 \tag{A1}$$

$$+ \int_1^\infty \lambda_1{}^n e^{-\alpha\lambda_1} Q_0(\lambda_1) d\lambda_1 \int_1^{\lambda_1} \lambda_2{}^m e^{-\alpha\lambda_2} d\lambda_2, \tag{A2}$$

$$S(m, n, \alpha) = \int_1^\infty \lambda_1{}^m e^{-\alpha\lambda_1} d\lambda_1 \int_1^{\lambda_1} \lambda_2{}^n e^{-\alpha\lambda_2} d\lambda_2,$$

and

$$Q_0(\lambda) = \tfrac{1}{2} \ln \frac{\lambda + 1}{\lambda - 1}. \tag{A3}$$

To treat these quantities, use is made of the simpler functions[10]

$$A_n(\alpha) = \int_1^\infty \lambda^n e^{-\alpha\lambda} d\lambda, \tag{A4}$$

$$F_n(\alpha) = \int_1^\infty \lambda^n e^{-\alpha\lambda} Q_0(\lambda) d\lambda. \tag{A5}$$

These can be shown to satisfy the following recursion formulae[8,9]:

$$A_n(\alpha) = \frac{1}{\alpha}[e^{-\alpha} + nA_{n-1}(\alpha)], \tag{A6}$$

$$F_n(\alpha) = F_{n-2}(\alpha) + \frac{1}{\alpha}[nF_{n-1}(\alpha) - (n-2)F_{n-3}(\alpha) - A_{n-2}(\alpha)]. \tag{A7}$$

These, together with the "starting" formulae:

$$A_0(\alpha) = e^{-\alpha}/\alpha, \tag{A8}$$

$$F_0(\alpha) = \tfrac{1}{2}[(\ln 2 + C)e^{-\alpha}/\alpha - Ei(-2\alpha)e^{\alpha}/\alpha], \tag{A9}$$

$$F_1(\alpha) = \tfrac{1}{2}[(\ln 2 + C)e^{-\alpha}(1/\alpha + 1/\alpha^2) - Ei(-2\alpha)e^{\alpha}(-1/\alpha + 1/\alpha^2)] \tag{A9a}$$

$$C = 0.577216\cdots, \tag{A10}$$

are sufficient to compile tables of these functions. Such tables are included in the present paper[11] (Tables I and II).

By using these functions the integrations in (A1) and (A2) can be carried out. Thus on inverting the order of integration it follows readily that:

$$S(m, n, \alpha) = \int_1^\infty \lambda_1{}^n e^{-\alpha\lambda_1} d\lambda_1 \int_{\lambda_1}^\infty \lambda_2{}^m e^{-\alpha\lambda_2} d\lambda_2 \tag{A11}$$

[10] Zener and Guillemin, Phys. Rev. **34**, 999 (1929). See also Rosen, Phys. Rev. **38**, 255 (1931).

[11] Table I is essentially an enlargement of a table of $A_n(\alpha)$ given in the paper by the present writer mentioned in reference[8], but corrected for several errors mainly in the 5th and 6th figures. Cf. list of errata at the end of the present paper.

TABLE I. $A_n(\alpha)$.

α	n 0	1	2	3	4	5	6	7	8	9	10
0.5	1.21306	3.63918	1.57698·10	9.58318·10	7.67868·10²	7.67989·10²	9.21599·10⁴	1.29024·10⁶	2.06438·10⁷	3.71589·10⁸	7.43178·10⁹
1.0	3.67879·10⁻¹	7.35759·10⁻¹	1.83940·1	5.88607·1	2.39122·10	1.19929·10²	7.19940·10³	5.03995·10⁵	4.03200·10⁶	3.62880·10⁷	3.62880·10⁸
1.5	1.48753	2.47922	4.79317·10⁻¹	1.10739	3.10178·1	1.04880·10	4.21009·10	1.96620·10³	1.04879·10⁵	6.29287·10⁶	4.19526·10⁷
2.0	6.76676·10⁻²	1.01501	1.69169	3.21421·10⁻¹	7.10510·10⁻¹	1.84394·1	5.59950·1	1.96659·10	7.87313·10	3.54359·10³	1.77186·10⁵
2.5	3.28340	4.59676·10⁻²	6.96081·10⁻²	1.16364	2.19016	4.70866·10⁻¹	1.16291	3.28899·1	1.05576	3.80402·10	1.52193·10²
3.0	1.65957	2.21276	3.13474	4.79431·10⁻²	8.05198·10⁻²	1.50795	3.18186·10⁻¹	7.59031·10⁻¹	2.04068·1	6.13863·1	2.04787·10
3.5	8.62782·10⁻³	1.10929	1.49666	2.14364	3.31494	5.59841·10⁻²	1.04601	2.17829	5.06522·10⁻¹	1.31111	3.75467·1
4.0	4.57891	5.72364·10⁻³	7.44073·10⁻³	1.01595	1.47384	2.30019	3.90871·10⁻²	7.29719·10⁻²	1.50523	3.43255·10⁻¹	8.62716·10⁻¹
4.5	2.46867	3.01726	3.80967	5.00845·10⁻³	6.92062·10⁻³	1.01582	1.60130	2.73778	5.11402·10⁻²	1.04749	2.35245
5.0	1.34759	1.61711	1.99443	2.54425	3.38299	4.73058·10⁻³	7.02428·10⁻³	1.11816	1.92381	3.59762·10⁻²	7.33000·10⁻²
6.0	4.13125·10⁻⁴	4.81980·10⁻⁴	5.73785·10⁻⁴	7.00018·10⁻⁴	8.79804·10⁻⁴	1.14630	1.55942	2.23245·10⁻³	3.38972·10⁻³	5.49771·10⁻³	9.57598·10⁻³
7.0	1.30269	1.48879	1.72806	2.04328	2.47028	3.06717·10⁻⁴	3.93169·10⁻⁴	5.23438·10⁻⁴	7.28484·10⁻⁴	1.06689	1.65440
8.0	4.19328·10⁻⁵	4.71744·10⁻⁵	5.37264·10⁻⁵	6.20802·10⁻⁵	7.29729·10⁻⁵	8.75409·10⁻⁵	1.07589	1.36073	1.78006	2.42189·10⁻⁴	3.44669·10⁻⁴
9.0	1.37122	1.52358	1.70979	1.94115	2.23395	2.61231	3.11276·10⁻⁵	3.79225·10⁻⁵	4.74211·10⁻⁵	6.11333·10⁻⁵	8.16381·10⁻⁵
10	4.53999·10⁻⁶	4.99399·10⁻⁶	5.53879·10⁻⁶	6.20163·10⁻⁶	7.02065·10⁻⁶	8.05032·10⁻⁶	9.37018·10⁻⁶	1.10991	1.34193	1.66174	2.11573
12	5.12018·10⁻⁷	5.54686·10⁻⁷	6.04465·10⁻⁷	6.63134·10⁻⁷	7.33062·10⁻⁷	8.17460·10⁻⁷	9.20748·10⁻⁷	1.04912·10⁻⁶	1.21143·10⁻⁶	1.42059·10⁻⁶	1.69584·10⁻⁶
14	5.93949·10⁻⁸	6.36374·10⁻⁸	6.84860·10⁻⁸	7.40705·10⁻⁸	8.05579·10⁻⁸	8.81656·10⁻⁸	9.71802·10⁻⁸	1.07985·10⁻⁷	1.21101·10⁻⁷	1.37245·10⁻⁷	1.57427·10⁻⁷

TABLE I. $A_n(\alpha)$.(*Cont.*)

α	n 11	12	13	14	15	16	17	18	19	20
1.0	3.99168·10⁷	4.79002·10⁸	6.22702·10⁹	8.71783·10¹⁰	1.30767·10¹²	2.09228·10¹³	3.55687·10¹⁴	6.40237·10¹⁵	1.21645·10¹⁷	2.43290·10¹⁸
2.0	9.74530·10⁵	5.84719·10⁶	3.80067·10⁷	2.66047·10⁸	1.99539·10⁹	1.59628·10¹⁰	1.35684·10¹¹	1.22116·10¹²	1.16010·10¹³	1.16010·10¹⁴
3.0	7.51051·10	3.00437·10³	1.30191·10⁴	6.07560·10⁴	3.03780·10⁵	1.62016·10⁶	9.18091·10⁶	5.50855·10⁷	3.48875·10⁸	2.32583·10⁹
4.0	2.37705·1	7.13573·1	2.31957·10	8.11895·10	3.04465·10²	1.21787·10³	5.17593·10³	2.32917·10⁴	1.10636·10⁵	5.53178·10⁵
5.0	1.62608·10⁻¹	3.91606·10⁻¹	1.01952·1	2.85601·1	8.56938·1	2.74234·10	9.32408·10	3.35688·10²	1.27554·10³	5.10216·10³
6.0	1.79691·10⁻²	3.63513·10⁻²	7.91743·10⁻²	1.85153·10⁻¹	4.63296·10⁻¹	1.23587·1	3.50204·1	1.05065·10	3.32711·10	1.10904·10²
7.0	2.73004·10⁻³	4.81034·10⁻³	9.06375·10⁻³	1.82578·10⁻²	3.92541·10⁻²	8.98538·10⁻²	2.18347·10⁻¹	5.61593·10⁻¹	1.52445·1	4.35572·1
8.0	5.15853·10⁻⁴	8.15712·10⁻⁴	1.36747·10⁻³	2.43500·10⁻³	4.60755·10⁻³	9.25704·10⁻³	1.97131·10⁻²	4.43965·10⁻²	1.05484·10⁻¹	2.63751·10⁻¹
9.0	1.13492	1.65035	2.52096·10⁻⁴	4.05862·10⁻⁴	7.33062·10⁻⁴	1.24064	2.35715·10⁻³	4.72801·10⁻³	9.99506·10⁻³	2.22250·10⁻²
10	2.78131·10⁻⁵	3.79157·10⁻⁵	5.38304·10⁻⁵	7.99025·10⁻⁵	1.24394	2.03570·10⁻⁴	3.50609·10⁻⁴	6.35639·10⁻⁴	1.21225	2.42004·10⁻³
12	2.06654·10⁻⁶	2.57856·10⁻⁶	3.30546·10⁻⁶	4.36838·10⁻⁶	5.97250·10⁻⁶	8.47535·10⁻⁶	1.25188·10⁻⁵	1.92902·10⁻⁵	3.10548·10⁻⁵	5.22700·10⁻⁵
14	1.83088·10⁻⁷	2.16327·10⁻⁷	2.60270·10⁻⁷	3.19665·10⁻⁷	4.01893·10⁻⁷	5.18702·10⁻⁷	6.89247·10⁻⁷	9.45569·10⁻⁷	1.34267·10⁻⁶	1.97949·10⁻⁶

TABLE II. $F_n(\alpha)$.

α	n = 0	1	2	3	4	5	6	7	8	9	10
0.5	$7.11802 \cdot 10^{-1}$	1.41200	3.93368	$1.63121 \cdot 10$	$9.72429 \cdot 10$	$7.73476 \cdot 10^{2}$	$7.71272 \cdot 10^{3}$	$9.24193 \cdot 10^{4}$	$1.29282 \cdot 10^{6}$	$2.06747 \cdot 10^{7}$	$3.72021 \cdot 10^{8}$
1.0	3.00133	$4.67340 \cdot 10^{-1}$	$8.66934 \cdot 10^{-1}$	$2.03225 \cdot 1$	$6.22186 \cdot 1$	$2.46547 \cdot 10$	$1.22109 \cdot 10^{2}$	$7.28378 \cdot 10^{2}$	$5.08127 \cdot 10^{3}$	$4.05651 \cdot 10^{4}$	$3.64585 \cdot 10^{5}$
1.5	1.44136	2.01240	3.13287	$5.66441 \cdot 10^{-1}$	1.23593	3.32138 · 1	$1.09431 \cdot 10$	4.32774 · 10	$2.00403 \cdot 10^{2}$	$1.06355 \cdot 10^{3}$	$6.36072 \cdot 10^{3}$
2.0	$7.34145 \cdot 10^{-2}$	$9.61588 \cdot 10^{-2}$	1.35740	2.12310	$3.79616 \cdot 10^{-1}$	$7.97031 \cdot 10^{-1}$	1.99083 · 1	5.89394 · 1	2.03758 · 10	8.07840 · 10	$3.61354 \cdot 10^{2}$
2.5	3.86961	4.85789	$6.44256 \cdot 10^{-2}$	$9.20242 \cdot 10^{-2}$	1.44958	2.58084	$5.29515 \cdot 10^{-1}$	1.26246	3.48483 · 1	1.10096	3.92603 · 10
3.0	2.08628	2.54062	3.22684	4.33445	$6.26745 \cdot 10^{-2}$	$9.95525 \cdot 10^{-2}$	1.77147	$3.58173 \cdot 10^{-1}$	$8.27106 \cdot 10^{-1}$	2.17314 · 1	6.43555 · 1
3.5	1.14309	1.36042	1.67396	2.15170	2.92805	4.28677	$6.87058 \cdot 10^{-2}$	1.22455	2.45229	$5.53394 \cdot 10^{-1}$	1.40174
4.0	$6.33936 \cdot 10^{-3}$	$7.41008 \cdot 10^{-3}$	$8.89967 \cdot 10^{-3}$	1.10691	1.44035	1.98589	2.94382	$4.76208 \cdot 10^{-2}$	$8.51210 \cdot 10^{-2}$	1.69383	$3.75707 \cdot 10^{-1}$
4.5	3.54908	4.08877	4.81772	$5.84140 \cdot 10^{-3}$	$7.34625 \cdot 10^{-3}$	$9.67909 \cdot 10^{-3}$	1.35214	2.02926	3.31332	$5.94416 \cdot 10^{-2}$	1.17786
5.0	2.00209	2.27912	2.64422	3.14181	3.84713	4.89356	$6.52936 \cdot 10^{-3}$	$9.24142 \cdot 10^{-3}$	1.40385	2.31333	$4.16712 \cdot 10^{-2}$
6.0	$6.48493 \cdot 10^{-4}$	$7.24630 \cdot 10^{-4}$	$8.21182 \cdot 10^{-4}$	$9.46806 \cdot 10^{-4}$	1.11521	1.34889	1.68626	2.19580	$3.00521 \cdot 10^{-3}$	$4.36423 \cdot 10^{-3}$	$6.78624 \cdot 10^{-3}$
7.0	2.13850	2.35680	2.62577	2.96395	$3.39922 \cdot 10^{-4}$	$3.97474 \cdot 10^{-4}$	$4.75955 \cdot 10^{-4}$	$5.86811 \cdot 10^{-4}$	$7.49738 \cdot 10^{-4}$	1.00003	1.40364
8.0	$7.14706 \cdot 10^{-5}$	$7.79300 \cdot 10^{-5}$	$8.57115 \cdot 10^{-5}$	$9.52412 \cdot 10^{-5}$	1.07134	1.22298	1.42115	1.68747	2.05690	2.58789 · 10^{-4}	$3.38179 \cdot 10^{-4}$
9.0	2.41359	2.60941	2.84110	3.11898	$3.45747 \cdot 10^{-5}$	$3.87708 \cdot 10^{-5}$	$4.40776 \cdot 10^{-5}$	$5.09427 \cdot 10^{-5}$	$6.00541 \cdot 10^{-5}$	$7.25006 \cdot 10^{-5}$	$9.00590 \cdot 10^{-5}$
10	$8.21890 \cdot 10^{-6}$	$8.82415 \cdot 10^{-6}$	$9.52973 \cdot 10^{-6}$	1.03618	1.13557	1.25606	1.40453	1.59094	1.82994	2.14372	2.56673
12	$9.71638 \cdot 10^{-7}$	1.03210	1.10099	$1.18015 \cdot 10^{-6}$	$1.27198 \cdot 10^{-6}$	$1.37963 \cdot 10^{-6}$	$1.50733 \cdot 10^{-6}$	$1.66079 \cdot 10^{-6}$	$1.84798 \cdot 10^{-6}$	$2.08007 \cdot 10^{-6}$	$2.37322 \cdot 10^{-6}$
14	$1.17125 \cdot 10^{-7}$	$1.23441 \cdot 10^{-7}$	$1.30517 \cdot 10^{-7}$	$1.38497 \cdot 10^{-7}$	$1.47561 \cdot 10^{-7}$	$1.57939 \cdot 10^{-7}$	$1.69925 \cdot 10^{-7}$	$1.83903 \cdot 10^{-7}$	$2.00383 \cdot 10^{-7}$	$2.20045 \cdot 10^{-7}$	$2.43820 \cdot 10^{-7}$

TABLE II. $F_n(\alpha)$.(*Cont*.)

α	n = 11	12	13	14	15	16	17	18	19	20
1.0	$3.64239 \cdot 10^{6}$	$4.00388 \cdot 10^{7}$	$4.80219 \cdot 10^{8}$	$6.24040 \cdot 10^{9}$	$8.73387 \cdot 10^{10}$	$1.30976 \cdot 10^{12}$	$2.09519 \cdot 10^{13}$	$3.56125 \cdot 10^{14}$	$6.40936 \cdot 10^{15}$	$1.21764 \cdot 10^{17}$
2.0	$1.79936 \cdot 10^{3}$	$9.86767 \cdot 10^{3}$	$5.90791 \cdot 10^{4}$	$3.83389 \cdot 10^{5}$	$2.68033 \cdot 10^{6}$	$2.00822 \cdot 10^{7}$	$1.60527 \cdot 10^{8}$	$1.36357 \cdot 10^{9}$	$1.22653 \cdot 10^{10}$	$1.16466 \cdot 10^{11}$
3.0	2.12426 · 10	7.73360 · 10	$3.07733 \cdot 10^{2}$	$1.32831 \cdot 10^{3}$	$6.18018 \cdot 10^{3}$	$3.08280 \cdot 10^{4}$	$1.64105 \cdot 10^{5}$	$9.28490 \cdot 10^{5}$	$5.56382 \cdot 10^{6}$	$3.51998 \cdot 10^{7}$
4.0	9.25241 · 10^{-1}	2.51229 · 1	7.46274 · 1	2.40722 · 10	8.37697 · 10	$3.12734 \cdot 10^{2}$	$1.24650 \cdot 10^{3}$	$5.28245 \cdot 10^{3}$	$2.37150 \cdot 10^{4}$	$1.11425 \cdot 10^{5}$
5.0	8.23454 · 10^{-2}	1.78373 · 10^{-1}	4.21918 · 10^{-1}	1.08379 · 1	3.00563 · 1	8.94923 · 1	2.84677 · 10	9.63304 · 10	$3.45448 \cdot 10^{2}$	$1.30850 \cdot 10^{3}$
6.0	1.13816 · 10^{-2}	2.06797 · 10^{-2}	4.07512 · 10^{-2}	$8.69442 \cdot 10^{-2}$	2.00110 · 10^{-1}	4.94626 · 10^{-1}	1.30697 · 1	3.67594 · 1	1.09623 · 10	3.45451 · 10
7.0	2.08938 · 10^{-3}	3.32048 · 10^{-3}	$5.66027 \cdot 10^{-3}$	1.03720	2.04246 · 10^{-2}	4.31281 · 10^{-2}	9.73308 · 10^{-2}	1.30697 · 1	3.33886 · 10^{-1}	5.96233 · 10^{-1}	1.60690 · 1
8.0	4.62110 · 10^{-4}	6.64774 · 10^{-4}	1.01289	$1.64220 \cdot 10^{-3}$	2.84083 · 10^{-3}	5.24692 · 10^{-3}	1.03355	2.16629 · 10^{-2}	4.81711 · 10^{-2}	1.13286 · 10^{-1}
9.0	1.15726	1.54733	2.16547 · 10^{-4}	3.18946 · 10^{-4}	4.96609 · 10^{-4}	8.19859 · 10^{-4}	1.43697 · 10^{-3}	2.67310 · 10^{-3}	5.26965 · 10^{-3}	1.09841 · 10^{-2}
10	3.15400 · 10^{-5}	3.99623 · 10^{-5}	5.24757 · 10^{-5}	7.17886 · 10^{-5}	1.02825	1.54852	2.45950 · 10^{-4}	4.12686 · 10^{-4}	7.13745 · 10^{-4}	1.36990 · 10^{-3}
12	2.75117 · 10^{-6}	3.24967 · 10^{-6}	3.92398 · 10^{-6}	4.86160 · 10^{-6}	6.20504 · 10^{-6}	8.19299 · 10^{-6}	1.12371 · 10^{-5}	1.60689 · 10^{-5}	2.40296 · 10^{-5}	3.76551 · 10^{-5}
14	2.72997 · 10^{-7}	3.09398 · 10^{-7}	3.55645 · 10^{-7}	4.15593 · 10^{-7}	4.90034 · 10^{-7}	6.02868 · 10^{-7}	7.53104 · 10^{-7}	9.68341 · 10^{-7}	1.28599 · 10^{-6}	1.76966 · 10^{-6}

$$= \frac{m!}{\alpha^{m+1}} \sum_{\nu=0}^{m} \frac{\alpha^{\nu}}{\nu!} A_{n+\nu}(2\alpha). \tag{A12}$$

Rather than to calculate $S(m, n, \alpha)$ by this formula it is more convenient when compiling a table of values to use the recursion formula which the expression in A12) satisfies. This is:

$$S(m, n, \alpha) = \frac{1}{\alpha}[mS(m-1, n, \alpha) + A_{m+n}(2\alpha)] \tag{A13}$$

with

$$S(0, n, \alpha) = A_n(2\alpha)/\alpha. \tag{A14}$$

As a check in such calculation, one may use the following relation, easily derivable by the use of expressions of the form (A2) and (A11), namely:

$$S(m, n, \alpha) + S(n, m, \alpha) = A_m(\alpha)A_n(\alpha). \tag{A15}$$

By analogy with (A12) one can define the quantity

$$T(m, n, \alpha) = \frac{m!}{\alpha^{m+1}} \sum_{\nu=0}^{m} \frac{\alpha^{\nu}}{\nu!} F_{n+\nu}(2\alpha), \tag{A15}$$

which will have an analogous recursion formula,

$$T(m, n, \alpha) = \frac{1}{\alpha}[mT(m-1, n, \alpha) + F_{m+n}(2\alpha)] \tag{A17}$$

with

$$T(0, n, \alpha) = F_n(2\alpha)/\alpha. \tag{A18}$$

By means of this function, it is found that one can write

$$H(m, n, \alpha) = A_m(\alpha)F_n(\alpha) + A_n(\alpha)F_m(\alpha) - T(m, n, \alpha) - T(n, m, \alpha). \tag{A19}$$

Since the functions (A12), (A18), and (A19) are characterized by three parameters they are too bulky to be tabulated here; however, to calculate them from the tables of $A_n(\alpha)$ and $F_n(\alpha)$ is a simple matter.

By the help of these functions the "exchange" integrals can now be evaluated; the remaining integrals require no special comments. The integrals are as follows:

$$RF_0 = R\int \frac{[\psi^0(a1)]^2}{r_{a1}} dv_1 = \rho \tag{A20}$$

$$RF_1 = R\int \frac{[\psi'(a1)]^2}{r_{a1}} dv_1 = \rho/2 \tag{A21}$$

$$RG_{00} = R\int \frac{[\psi^0(a1)]^2}{r_{b1}} dv_1 = 1 - e^{-2\rho}(\rho + 1) \tag{A22}$$

$$RG_{01} = R\int \frac{\psi^0(a1)\psi'(a1)}{r_{b1}} dv_1 = 1/\rho - e^{-2\rho}(\rho^2 + 2\rho + 2 + 1/\rho) \tag{A23}$$

$$RG_{11} = R\int \frac{[\psi'(a1)]^2}{r_{b1}}\,dv_1 = 1 + 3/\rho^2 - e^{-2\rho}(\rho^3 + 3\rho^2 + 11\rho/2 + 7 + 6/\rho + 3/\rho^2) \tag{A24}$$

$$RK_{00,00} = R\int \frac{[\psi^0(a1)]^2[\psi^0(b2)]^2}{r_{12}}\,dv_1dv_1 = 1 - e^{-2\rho}(\rho^3/6 + 3\rho^2/4 + 11\rho/8 + 1) \tag{A25}$$

$$RK_{00,01} = R\int \frac{[\psi^0(a1)]^2\psi^0(b2)\psi'(b2)}{r_{12}}\,dv_1dv_2 = 1/\rho - e^{-2\rho}(\rho^4/12 + 11\rho^3/24 + 59\rho^2/48 + 2\rho + 2 + 1/\rho) \tag{A26}$$

$$RK_{00,11} = R\int \frac{[\psi^0(a1)]^2[\psi'(b2)]^2}{r_{12}}\,dv_1dv_2 = 1 + 3/\rho^2 - e^{-2\rho}(\rho^5/20 + 41\rho^4/120 + 301\rho^3/240 + 25\rho^2/8 + 89\rho/16 + 7 + 6/\rho + 3/\rho^2) \tag{A27}$$

$$RK_{01,01} = R\int \frac{\psi^0(a1)\psi'(a1)\psi^0(b2)\psi'(b2)}{r_{12}}\,dv_1dv_2 = 2/\rho^2 - e^{-2\rho}(\rho^5/30 + \rho^4/5 + 77\rho^3/120 + 71\rho^2/48 + 263\rho/96 + 4 + 4/\rho + 2/\rho^2) \tag{A28}$$

$$RK_{01,11} = R\int \frac{\psi^0(a1)\psi'(a1)[\psi'(b2)]^2}{r_{12}}\,dv_1dv_2 = 1/\rho + 9/\rho^3 - e^{-2\rho}(\rho^6/60 + 7\rho^5/60 + 113\rho^4/240 + 697\rho^3/480 + 3577\rho^2/960 + 8\rho + 14 + 19/\rho + 18/\rho^2 + 9/\rho^3) \tag{A29}$$

$$RK_{11,11} = R\int \frac{[\psi'(a1)]^2[\psi'(b2)]^2}{r_{12}}\,dv_1dv_2 = 1 + 6/\rho^2 + 54/\rho^4 - e^{-2\rho}(\rho^7/140 + 141\rho^6/2520 + 19\rho^5/70 + 893\rho^4/840 + 23809\rho^3/6720 + 6411\rho^2/640 + 30731\rho/1280 + 49 + 84/\rho + 114/\rho^2 + 108/\rho^3 + 54/\rho^4) \tag{A30}$$

$$I_{00} = \int \psi^0(a1)\psi^0(b1)dv_1 = e^{-\rho}(\rho^2/3 + \rho + 1) \tag{A31}$$

$$I_0 = \int \psi^0(a1)\psi'(b1)dv_1 = \rho I_{00}/2 = \tfrac{1}{2}e^{-\rho}(\rho^3/3 + \rho^2 + \rho) \tag{A32}$$

$$I_{11} = \int \psi'(a_1)\psi'(b1)dv_1 = e^{-\rho}(\rho^4/15 + 2\rho^3/15 - \rho^2/5 - \rho - 1) \tag{A33}$$

$$RJ_{00} = R\int \frac{\psi^0(a1(\psi^0(b1)}{r_{a1}}\,dv_1 = \rho e^{-\rho}(\rho + 1) \tag{A34}$$

$$RJ_{10} = R\int \frac{\psi'(a1)\psi^0(b1)}{r_{a1}}\,dv_1 = \tfrac{1}{3}\rho^2 e^{-\rho}(\rho+1) \tag{A35}$$

$$RJ_{01} = R\int \frac{\psi^0(a1)\psi'(b1)}{r_{a1}}\,dv_1 = \tfrac{2}{3}\rho^2 e^{-\rho}(\rho+1) = 2RJ_{10} \tag{A36}$$

$$RJ_{11} = R\int \frac{\psi'(a1)\psi'(b1)}{r_{a1}}\,dv_1 = \tfrac{1}{2}\rho e^{-\rho}(\rho^3/3-\rho-1) \tag{A37}$$

$$RL_{00,00} = R\int \frac{\psi^0(a1)\psi^0(b1)\psi^0(a2)\psi^0(b2)}{r_{12}} = (\rho^6/15)\,[9H(2,2,\rho) - 6H(2,0,\rho) + H(0,0,\rho) - 3S(1,2,\rho) + S(1,0,\rho)] \tag{A38}$$

$$RL_{00,01} = R\int \frac{\psi^0(a1)\psi^0(b1)\psi^0(a2)\psi'(b2)}{r_{12}} = (\rho/2)RL_{00,00} \tag{A39}$$

$$R(L_{01,01}+L_{01,10}) = R\int \frac{\psi^0(a1)\psi'(b1)\,[\psi^0(a2)\psi'(b2)+\psi'(a2)\psi^0(b2)]}{r_{12}}\,dv_1dv_2 = (\rho^2/2)RL_{00,00} \tag{A40}$$

$$RL_{00,11} = R\int \frac{\psi^0(a1)\psi^0(b1)\psi'(a2)\psi'(b2)}{r_{12}}\,dv_1dv_2 = R\left(\frac{\rho^2}{4}L_{00,00} - L'\right) \tag{A41}$$

$$RL_{01,11} = R\int \frac{\psi^0(a1)\psi'(b1)\psi'(a2)\psi'(b2)}{r_{12}}\,dv_1dv_2 = (\rho/2)RL_{00,11} \tag{A42}$$

$$RL_{11,11} = R\int \frac{\psi'(a1)\psi'(b1)\psi'(a2)\psi'(b2)}{r_{12}}\,dv_1dv_2 = R\left(\frac{\rho^4}{16}L_{00,00} - \frac{\rho^2}{2}L' + L''\right). \tag{A43}$$

The primed quantities are given by:

$$RL' = (\rho^8/840)\,[-21H(6,2) + 7H(6,0) + 60H(4,2) - 20H(4,0) - 27H(2,2) + 9H(2,0) + 21S(5,2) - 7S(5,0) - 18S(3,2) + 6S(3,0) + 21S(1,6) - 25S(1,4) + 6S(1,2)], \tag{A44}$$

$$RL'' = (\rho^{10}/15120)\,[147H(6,6) - 315H(4,6) + 225H(4,4) + 63H(2,6) - 135H(2,4) + 27H(2,2) - 294S(5,6) + 315S(5,4) - 63S(5,2) + 217S(3,6) - 240S(3,4) + 51S(3,2)]. \tag{A45}$$

The argument of these functions is ρ as before.

2. Curve Fitting

To fit a curve of the form

$$\Delta E = De^{-2a(\rho_0-\rho_m)} - 2De^{-a(\rho_0-\rho_m)} \tag{A46}$$

to the energy curve nears its minimum requires a knowledge of the energy at three points in that vicinity. In the calculation discussed the fitting was very easy because the minimum was near $\rho_0 = 1.5$, and values of ΔE had been calculated for $\rho_0 = 1, 1.5, 2$. Thus, if we denote these values of ΔE by E_1, E_2, E_3, and let

$$B = e^{-a/2}, \tag{A47}$$

$$C = e^{a\rho_m}, \tag{A48}$$

than the equations to be satisfied are:

$$E_1 = CD(CB^4 - 2B^2), \tag{A49}$$

$$E_2 = CD(CB^6 - 2B^3), \tag{A50}$$

$$E_3 = CD(CB^8 - 2B^4). \tag{A51}$$

The solutions are given by the appropriate root of:

$$E_1B^3 - E_2B^2 - E_2B + E_3 = 0, \tag{A52}$$

and by the relations:

$$C = \frac{2}{B^2}\left(\frac{E_1B - E_2}{E_1B^2 - E_2}\right), \tag{A53}$$

$$D = \frac{1}{2B^3C}\left(\frac{E_1B^2 - E_2}{1 - B}\right), \tag{A54}$$

$$a = 2\ln(1/B), \tag{A55}$$

$$\rho_m = \frac{1}{a}\ln C. \tag{A56}$$

Thus the constants required in (A46) have been evaluated.

Errata: In a recent paper by the author, Phys. Rev. **38**, 255, (1931), several errors appear which may cause inconvenience to anyone using it. The corrected portions should read as follows:

p. 254, Eq. (45): ${}_n{}^m(\alpha) = \sum_{\nu=0}^{m} \alpha^\nu F_{n+\nu}(\alpha)/2^\nu\nu!$

p. 266: $A_8(1, 3.5) = 5.06522$ instead of 5.06553

$A_{10}(1, 3.0) = 2.04787 \cdot 10$ instead of $2.04787 \cdot 1$

$A_{13}(1, 8.0) = 1.36747 \cdot 10^{-3}$ instead of $8.36747 \cdot 10^{-3}$

p. 267: $A_5(-1, 2.0) = 9.23632 \cdot 10^{-1}$ instead of $1.84726 \cdot 10^{-1}$

p. 274, line 5: $\alpha = 1.385\ A^{-1}$

p. 274, line 20: 0.87 instead of 1.11.

A NOTE ON THE GENERAL SOLUTION OF SCHRÖDINGER'S EQUATION AND THE UNCERTAINTY PRINCIPLE

By E. L. Hill
Department of Physics, University of Minnesota

(Received November 13, 1931)

Abstract

It is shown that the general solution of Schrödinger's equation in one dimension for a given energy can be written in a form representing two beams travelling in opposite directions with the classical velocity. This permits an interpretation of the uncertainty principle in which an electron in a conservative field, with a definite energy, has also a definite speed, but its direction of motion is indeterminate. In regions in which the classical velocity is imaginary this interpretation becomes indefinite. A brief consideration is given to the generalization to three dimensions.

Introduction

THE uncertainty principle is often characterized by the statement that "the position and velocity of an electron cannot be determined simultaneously." There are two general theoretical ways of explaining this result; (1) by saying that a localized electron can only be vizualized in terms of a wave packet, and (2) by appealing to the statistical interpretation of the function

$$e^{\pm i(2\pi/h)pq} \tag{1}$$

as the probability amplitude connecting a coordinate q and its conjugate momentum p. These two arguments are more or less equivalent since one can build up a wave packet by a superposition of functions of the type of Eq. (1); i.e., by a Fourier integral

$$\psi(q) = \int_{-\infty}^{+\infty} g(p)e^{i(2\pi/h)pq}dp. \tag{1'}$$

From this point of view it seems necessary to conclude that if an electron is considered to be at a given point, then its velocity can have any magnitude and any direction.

In a conversation with the writer some months ago, Professor Frenkel suggested that one might interpret the uncertainty principle in terms of an uncertainty in the *direction* of motion of the electron, and of a possible reflection coefficient for the electron at every point in a field of force. Due to the reflection the electron may change, and even reverse, its direction of motion at any point. This development will be made in the English edition of Frenkel's book on wave mechanics.

The purpose of the present note is to present some furthur ideas which have occurred to the present writer on this topic, principally for the purpose of making the above argument more precise and definite. It may be stated

here that the essential point about which our discussion turns is the possibility of expressing the general solution of Schrödinger's equation for a given value of the energy E by means of an integral of type somewhat different from (1′), but in a form in which the integration extends not over all values of the momentum, but over only those values which are consistent with the requirement that the absolute magnitude of the momentum of an electron at a given point with a given total energy shall be just the classical value. For one-dimensional motion the integral reduces to a sum since there are only two possible directions of motion. We discuss first motion in one dimension.

One Dimensional Case

Consider the "collision" of a group of electrons, all having energy E, with a field of force having a potential function $V(x)$, where we assume $E \geqq V(x)$. For simplicity in the later interpretation we assume that

$$\left.\begin{aligned} V(x) &= V_0 \text{ when } x \leqq \xi_0 \\ V(x) &= V_1 \text{ when } x \geqq \xi_1 \end{aligned}\right\} \tag{2}$$

where V_0 and V_1 are constants.

The wave equation to be solved is

$$d^2\psi/dx^2 + 4\pi^2\alpha^2(x, E)\psi = 0 \tag{3}$$

with

$$\alpha(x, E) = + \left[2m(E - V(x))\right]^{1/2}/h. \tag{4}$$

Let us try to solve Eq. (3) by replacing $V(x)$ by a "step-function," a portion of which is shown in Fig. (1). For such a step-function the solution can be obtained by elementary means, and one can then approach the actual case by

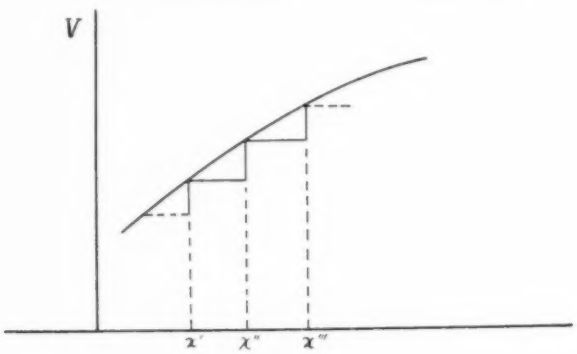

Fig. 1.

making the steps smaller, at the same time increasing their number. Let α' and α'' be the values of $\alpha(x)$ at x' and x'' respectively. For the step-function the solutions can be written as

$$x' \leqq x < x'' \quad \psi = c_1(x')e^{+i2\pi\alpha' x} + c_2(x')e^{-i2\pi\alpha' x} \tag{5}$$

$$x'' \leqq x < x''' \quad \psi = c_1(x'')e^{+i2\pi\alpha'' x} + c_2(x'')e^{-i2\pi\alpha'' x} \tag{6}$$

where $c_1(x')$, $c_2(x')$, $c_1(x'')$, and $c_2(x'')$ are constants.

Applying the usual boundary conditions of continuity for ψ and $d\psi/dx$ at x'', one obtains the expressions

$$\left.\begin{aligned} c_1(x'') &= \tfrac{1}{2}\{c_1(x')(1+\alpha'/\alpha'')e^{+i2\pi(\alpha'-\alpha'')x''} + c_2(x')(1-\alpha'/\alpha'')e^{-i2\pi(\alpha'+\alpha'')x''}\} \\ c_2(x'') &= \tfrac{1}{2}\{c_1(x')(1-\alpha'/\alpha'')e^{+i2\pi(\alpha'+\alpha'')x''} + c_2(x')(1+\alpha'/\alpha'')e^{-i2\pi(\alpha'-\alpha'')x''}\} \end{aligned}\right. \quad (7)$$

We now consider the interval $x''-x'=\Delta x$ to become an infinitesimal, and the c's as well as α to be functions of x which can be expanded in Taylor's serious about the point x':

$$\left.\begin{aligned} \alpha'' &= \alpha' + (d\alpha/dx)_{x=x'}\Delta x + \cdots \\ c_1(x'') &= c_1(x') + (dc_1/dx)_{x=x'}\Delta x + \cdots \text{ etc.} \end{aligned}\right. \quad (8)$$

Inserting these relations in Eq. (7) we get, after some elementary manipulations, in the limit $\Delta x \to 0$:

$$\left.\begin{aligned} (dc_1/dx) &= [d(\ln \alpha^{1/2})/dx][-(1+i4\pi\alpha x)c_1 + e^{-i4\pi\alpha x}c_2] \\ (dc_2/dx) &= [d(\ln \alpha^{1/2})/dx][e^{+i4\pi\alpha x}c_1 - (1-i4\pi\alpha x)c_2] \end{aligned}\right\}. \quad (9)$$

With the functions $c_1(x)$ and $c_2(x)$ as determined by these relations we can write for the general solution of Eq. (3):

$$\psi(x) = c_1(x)e^{+i2\pi a(x)x} + c_2(x)e^{-i2\pi a(x)x}. \quad (10)$$

It can easily be verified[1] directly that this function satisfies Eq. (3). In order completely to specify the solution (10) we must subject the functions $c_1(x)$ and $c_2(x)$ to some initial or boundary conditions. It is for this reason that we have introduced Eqs. (2). If we make $c_1(\xi_1)=1$, $c_2(\xi_1)=0$, then Eqs. (9) show that c_1 and c_2 retain these values[2] for all larger values of x, and also that c_1 and c_2 are both constant for $x \leqq \xi_0$, so that we can interpret the problem by saying that a beam of electrons of density $|c_1(\xi_0)|^2$ impinges on the force field from the left, a beam of density $|c_2(\xi_0)|^2$ is reflected, and a beam of unit density is transmitted. The reflection coefficient for the lattice is hence $|c_2(\xi_0)|^2/|c_1(\xi_0)|^2$.

Let us calculate the current at any point in the lattice. For $d\psi/dx$ we get, by using Eq. (9)

$$(d\psi/dx) = i2\pi\alpha(x)[c_1(x)e^{+i2\pi\alpha(x)x} - c_2(x)e^{-i2\pi\alpha(x)x}], \quad (11)$$

and for the current[2a]

$$\left.\begin{aligned} I &= (h/4\pi m i)(\psi^* d\psi/dx - \psi d\psi^*/dx) \\ &= [h\alpha(x)/m][\,|\,c_1(x)\,|^2 - |\,c_2(x)\,|^2] = \text{constant}. \end{aligned}\right. \quad (12)$$

Here $h\alpha(x)/m$ is just the classical velocity which an electron would have at the point x. Since this expression is in the form

$$\text{current} = \text{density} \times \text{velocity}$$

[1] Use of Eq. (11) will simplify the work.

[2] As by Eq. (2), $d\alpha/dx=0$ when $x>\xi_1$ or $x<\xi_0$. If $(d\alpha/dx)_{x=\xi_1}\neq 0$ we can choose a point just to the right of ξ_1 for which $d\alpha/dx$ will be zero. This point ξ_0 can be treated similarly.

[2a] These results were given in a previous note. E. L. Hill, Phys. Rev. **38**, 1258 (1931).

it seems very reasonable to conclude that the solution (10) can be interpreted as representing two beams of electrons, one of density $|c_1(x)|^2$ moving to the right, the other of density $|c_2(x)|^2$ moving to the left, each beam, however, having the *classical* velocity appropriate to that point.

This result is foreshadowed by Eq. (11) which shows that the application of the momentum operator

$$p_x = (h/2\pi i)d/dx$$

to ψ, makes $h\alpha(x)$ appear formally like a proper value of p_x, having the proper sign for each of the beams.

This argument makes it very plausible indeed that it is legitimate to think of an electron with a given energy as having a definite velocity at a given point; i.e., the classical velocity, but that the direction of motion is incompletely specified. The average drift of electrons is just sufficient to account for the correct current. The uncertainty in momentum becomes an uncertainty in direction, but not in absolute magnitude. This is all on condition, however, that one confine himself to electrons having one given energy; if one considers electrons in different energy regions, then the resultant solution would contain electrons having different velocities, but for the electrons in each energy state the magnitude of the momentum would have just the classical value.

These two beams, however, cannot be considered as representing *independent* or *alternative* states for the electrons, for in the first place neither of the two terms in Eq. (10) is a solution of Eq. (3) when taken separately, and further, Eqs. (11) and (12) are true only when both terms are included in (10); e.g.,

$$p_x[c_1e^{i2\pi\alpha x}] \neq h\alpha[c_1e^{i2\pi\alpha x}].$$

This simply means that the resolution into beams is not analogous to the resolution of a general ψ-function into a set of mutually orthogonal proper functions. The physical reason for this is obvious: under the influence of the force field the electron can, and in general must, transfer from one beam to the other. However, if one treats the force field as a small perturbation, the electrons being practically free, then in the zeroth order calculation the two directions of motion do represent independent states, between which transitions occur under the influence of the field. This type of treatment has been considered by Brillouin[3] in his theory of metallic conduction. In the general case the two states are so tightly coupled that the idea of a *rate* of transition between them becomes evanescent.

It is to be particularly emphasized here that there is no question of a "measurement" of the velocity or position of an electron involved in this reasoning, just as there is no real question of a physical measurement in any of the purely mathematical treatments of the uncertainty principle; e.g., as in Weyl, "Gruppentheorie und Quantenmechanik," 1st edition, p. 67. To the writer it seems fairly clear that derivations of this nature are logically not

[3] L. Brillouin, Jour. de Physique (7) **1**, 377 (1930).

related in any simple way, if indeed they are related at all, to arguments based on γ-ray microscopes and the like. The one is valid for isolated systems while the other depends upon interactions between systems, and although one may choose to say that an isolated system is a meaningless concept, yet there can be little question of the necessity of the concept for the purposes of general theoretical development.

We have explicitly limited ourselves to electron energies for which $E \geqq V(x)$. For regions in which $E < V(x)$ there is no reason to suppose that Eqs. (9) and (10) do not still hold formally. Since $\alpha(x)$ is a pure imaginary number, Eq (11) becomes

$$d\psi/dx = -2\pi |\alpha| [c_1(x)e^{-2\pi|\alpha|x} - c_2(x)e^{+2\pi|\alpha|x}] \tag{11'}$$

and Eq (12) changes to

$$I = i(h|\alpha|/m)[c_1c_2^* - c_1^*c_2]. \tag{12'}$$

Our interpretation is thus no longer valid unless we consider the imaginary part of $c_1c_2^*$ as a sort of density, but there seems to be no apparent meaning to this. Rojansky[4] has shown that one can formally still make the separation into two beams moving with the velocity $h|\alpha|/m$, but the densities of these beams are not governed by Eq. (9) through the whole range of the variable x.

This constitutes the essence of the physical argument of this note. In the remaining section we shall make some remarks about the generalization to three dimensions, but since the writer has not been able to give the complete solution of the problem for this more complicated case, these remarks must be regarded as being tentative. We shall restrict ourselves to energies for which the total energy is always greater than the potential energy.

Three Dimensional Case

The physical situation is here quite similar to the case of one dimension except that the degree of liberty for the direction of motion of the electron is infinitely greater, since an electron moving originally in a given direction can be reflected not only in the reverse direction, but also in any other direction.

On the basis of our physical idea that the velocity of an electron with definite energy has the classical value, we expect that at any point in coordinate space (x, y, z) designated by the position vector $\boldsymbol{r}$, we can write

$$\psi(\boldsymbol{r}) = \int_0^{2\pi} d\mu \int_0^{\pi} \sin\sigma d\sigma \{c(\sigma, \mu; \boldsymbol{r})e^{+i2\pi\alpha(\boldsymbol{r})\boldsymbol{n}\cdot\boldsymbol{r}}\} \tag{13}$$

where

$$h\alpha(\boldsymbol{r}) = [2m(E - V(\boldsymbol{r}))]^{1/2}$$

is the magnitude of the classical momentum, and $\boldsymbol{n}$ is an unit vector specifying the direction of the momentum, defined by the angles σ and μ in an ob-

[4] V. Rojansky and W. Wetzel, Phys. Rev. **38**, 1979 (1931).

vious manner. The quantity $|c(\sigma, \mu; \boldsymbol{r})|^2$ should then represent the number of electrons, at $\boldsymbol{r}$ moving in the direction of $\boldsymbol{n}$, per unit solid angle.

It is not easy to give a proof that the general solution of Schrödinger's equation (for a given energy E) can be put in the form (13), as we were able to do directly in one dimension. Assuming the correctness of the physical view of the problem it seems very plausible. A still stronger, although qualitative argument, can be made by examining Whittaker's proof[5] of the fact that the general solution of the equation

$$\nabla^2\Phi + \Phi = 0$$

can be represented by a superposition of plane waves of type similar to (13). If we imagine the function $\alpha(x, y, z)$ to be replaced by a three dimensional step-function in which α is constant over certain regions, then for each region Schrödinger's equation can be put in this form, and the general solution can be written in the form (13) with the appropriate value of α. On shrinking the size of the regions, just as we did in the one dimensional case we should expect to get a formula like (13). We are prevented from carrying out the process in detail because of the complexity of the boundary conditions in three dimensions.

We can make a reasonable guess at the equation for $c(\sigma, \mu; \boldsymbol{r})$ by writing down the three dimensional generalization of Eqs. (9); i.e.,[6]

$$\text{grad}\,[c(\sigma, \mu; \boldsymbol{r})e^{+i2\pi\alpha(\boldsymbol{r})\boldsymbol{n}\cdot\boldsymbol{r}}] = \boldsymbol{n}i2\pi\alpha(\boldsymbol{r})c(\sigma, \mu; \boldsymbol{r})e^{+i2\pi\alpha(\boldsymbol{r})\boldsymbol{n}\cdot\boldsymbol{r}}$$

$$- (3/4\pi\alpha)\,\text{grad}\,\alpha\left[\boldsymbol{n}\cdot\int_0^{2\pi}d\mu'\int_0^{\pi}\sin\sigma' d\sigma'\{\boldsymbol{n}'c(\sigma', \mu'; \boldsymbol{r})e^{+i2\pi\alpha(\boldsymbol{r})\boldsymbol{n}'\cdot\boldsymbol{r}}\}\right]. \quad (15)$$

It can readily be verified that

$$\text{grad}\,\psi(\boldsymbol{r}) = i2\pi\alpha(\boldsymbol{r})\int_0^{2\pi}d\mu\int_0^{\pi}\sin\sigma d\sigma\{\boldsymbol{n}c(\sigma, \mu; \boldsymbol{r})e^{i2\pi\alpha(\boldsymbol{r})\boldsymbol{n}\cdot\boldsymbol{r}}\} \quad (16)$$

which is the expected generalization of Eq. (11), and that ψ, as given by Eq. (13), formally satisfies Schrödinger's equation.

The writer has, however, not succeeded in giving a satisfactory proof that the current is given by the formula

$$I = (h\alpha(\boldsymbol{r})/m)\int_0^{2\pi}d\mu\int_0^{\pi}\sin\sigma d\sigma\,|\,c(\sigma, \mu; \boldsymbol{r})\,|^2\boldsymbol{n}$$

which is the generalization of Eq. (12), and is required by our physical interpretation. The trouble seems to lie in the continuity for the range of direc-

[5] E. T. Whittaker, Mathematische Annalen **57**, 333 (1903). Whittaker and Watson, "Modern Analysis,. Cambridge Univ. Press, Chapter 18.

[6] The factor $3/4\pi$ arises from the theorem that for any constant vector Γ

$$\int_0^{2\pi}d\mu\int_0^{\pi}\boldsymbol{n}\sin\sigma d\sigma\{\boldsymbol{n}\cdot\Gamma\} = \frac{4\pi}{3}\Gamma.$$

This is used in the proof that (13) satisfies Schrödinger's equation.

tions of the momentum which causes nearby directions to be related, in the sense of all continuous spectrum problems. One can make some progress towards the desired end by introducing delta functions for the sharp definition of a particular direction of motion, but the passage to the limit of a continuous distribution of directions then appears to be quite artificial. On the other hand, it may be that Eq. (15) is not the proper generalization of Eq. (9).

Added in Proof: Further consideration shows that while Eq. (10) yields a representation of the *momentum*, one must not attempt to apply it too generally to other quantities. One can correctly calculate the average value of p and the standard deviation of p by considering the two beams as independent. The first of these can be calculated from the current and the second by using Eqs. (10) and (11) for the calculation of c_1 and c_2

$$c_1 e^{i2\pi\alpha x} = \tfrac{1}{2}\left[\psi + (1/i2\pi\alpha)(d\psi/dx)\right];\ c_2 e^{-i2\pi\alpha x} = \tfrac{1}{2}\left[\psi - (1/i2\pi\alpha)(d\psi/dx)\right]$$

from which one obtains, for a closed system

$$(\Delta p)^2 = \int h^2\alpha^2\left[\,|c_1|^2 + |c_2|^2\right]dx.$$

This makes it clear that the existence of a mathematical uncertainty principle follows at once from the lack of knowledge of the phases of the motion, and not *primarily* because of any difficulty in the specification of the position or velocity of the electron. One must not, however, overlook the fact that the two "momentum beams" are really not independent: for some questions the interference between the two beams is of importance. The analogy with the classical motion in which the initial conditions are unspecified is thus incomplete; the wave equation contains more than an indeterminacy in the phases of motion.

ELECTRONIC TRANSITIONS BETWEEN AN INNER SHELL AND THE VIRTUAL OUTER SHELLS OF THE IONS OF THE RARE EARTHS IN CRYSTALS

By Simon Freed*
The Physical Laboratory of the University, Leyden, Holland

(Received September 18, 1931)

Abstract

In the rare earths, the inner $4f$ shell is incomplete and its electrons are much less stable than those in the outer complete $5s$ and $5p$ electronic shells. The rare earths possess sharp absorption lines which are ascribed to initial and final quantum states arising from different orientations of the spin and orbital moments of the electrons within the $4f$ shell. Ce^{+++} has only one electron in this shell giving rise to only one term ^2F, a doublet, with an interval of about 1000 cm^{-1}. Absorption in the ultraviolet must correspond, then, to a transition from the $4f$ shell to virtual outer shells such as $5d$ or $6s$, or to the lattice. The ultraviolet absorption spectra were taken of single crystals of hydrated cerium chloride and cerium ethylsulfate at room temperatures, at that of liquid nitrogen, and of liquid hydrogen. The crystals varied in thickness from about 0.2 mm to 3 mm, about the same thickness as has been employed in studying the line spectra of other rare earths. Aside from the very faint diffuse band at about 3020A found in one of the chloride crystals and which doubtless exists in the ethylsulfate also, the crystals were completely transparent from the visible to about 2700A and there, absorption set in and occupied the rest of the ultraviolet (to 2000A). To discover whether this continuum was caused by the overlapping of several regions of selective absorption, the cerium ions were diluted in the isomorphous lanthanum crystals which are transparent and possess practically the same electric fields as the cerium crystals. The ratio of Ce^{+++} to La^{+++} in the solution from which the crystals were grown varied from about 1 to 10 to about 1 to 5000. Three new diffuse bands were discovered which remained structureless even at great dilution and at the temperature of liquid hydrogen. The bands were recognized as transitions from a rather sharp inner quantum state ^2F (the electron in the $4f$ shell) to a diffuse outer quantum state ^2D (the electron in the virtual $5d$ shell). The electron of the activated Ce^{+++} is subject to enormous inhomogeneous electric fields because it is very close to the water molecules (and the negative ions) in the lattice. The ^2D term is decomposed by these fields into sublevels of wide separation which are extremely sensitive to all the variations in electric fields. The substitution of one negative ion for another or a change in the fields accompanying thermal contraction displaces the bands in some instances by a hundred times as much as the lines of Gd^{+++} are displaced under similar conditions. Whence, we return to the conclusion that the *lines* of the rare earths in general are associated with inner quantum states. It was predicated that transitions from the $4f$ electron to the outer shells would occur in other rare earths Pr^{+++}, Nd^{+++} etc., but the bands would begin further in the ultraviolet than they do in Ce^{+++}. A band extending from 2280A to 2100A was found in undiluted neodymium chloride which also remained without structure at the temperature of liquid hydrogen. Pr^{+++} exhibited no absorption band within the range of the spectrograph although the existence of one beginning at about 2100A would not have been determined. It is expected that the first band of Pr^{+++} begins somewhere in this region. The breadth of the bands has been discussed.

* Fellow of the John Simon Guggenheim Memorial Foundation.

IT HAS been proved[1] that the electronic configurations of the rare earths in crystals are the following:

Ionic number*	Ion	Basic term	$1s$, to $4d$	$4f$	$5s, 5p$
54	La^{+++}	^1S	full	0	full
55	Ce^{+++}	^2F	"	1	"
56	Pr^{+++}	^3H	"	2	"
57	Nd^{+++}	^4J	"	3	"
68	Lu^{+++}	^1S	"	14	"

* Ionic number is the atomic number less three.

The energy required to liberate an electron in the $5s$ shell from these ions is about 45 volts and to liberate an electron in the $5p$ shell about 34 volts.[2] However, an extrapolation is necessary to learn the ionizing energies for the electrons in the $4f$ shell. The $4f$ shell becomes less stable than the $5s$ shell at about atomic number 85 and less stable than the $5p$ shell at atomic number 79 and it remains so for all lower atomic numbers. It appears that the energy of the electron in the $4f$ shell of the rare earths may correspond to radiation in the ultraviolet. It would presumably be the least in Ce^{+++} because the effective nuclear charge is probably the least here.

The extraordinary sharpness of the absorption lines of the rare earths in crystals has been ascribed to stationary states arising from the electrons within the inner ($4f$) shell. The different states owe their origin to the different orientations of the orbital and spin moments of the electrons in this shell. Because of the enormous positive charge acting on these internal electrons, they are doubtless close to the nucleus and rather distant from the fluctuating perturbations of the oscillating molecules and ions. In addition the completely filled $5s$ and $5p$ shells serve as screens against these perturbations. Ce^{+++} has but one electron in the $4f$ shell and it can give rise to but one basic term.[3] Any absorption in the ultraviolet must imply a transition of the $4f$ electron to outer electronic shells such as $5d$,—, $6s$ etc. The possibility is open, of course, that the electron may end in the closely spaced quantum states which are equivalent to ionization in the lattice.

The absorption lines of most of the rare earths are diffuse at room temperature but they sharpen remarkably at lower temperatures. As a rule they are

[1] Hund, Linienspektren, Springer, Berlin (1927).

[2] The actual values differ little from one ion to another. Those given here apply to Nd^{+++} and were read from the Bohr-Coster diagram. See, for example, Ruark and Urey, Atoms, Molecules and Quanta, p. 253, McGraw-Hill, New York (1930).

[3] The basic term is ^2F, a doublet, with an interval of about 1000 cm^{-1} as calculated from Sommerfeld's formula for relativity doublets. These levels are further decomposed by the inhomogeneous electric fields of the surrounding molecules and ions. The magnitude of the electrical separation cannot be as much as several hundred cm^{-1} when the positive ions are surrounded with H_2O dipoles since the magnetic susceptibilities of these ions are almost the same as Hund calculated for the gaseous ions. If the separations reached any such order of magnitude, deviations from Curie's law would have been serious at room temperature. Kramers Proc. Acad. Amsterdam **32,** 1176 (1929).

fine at the temperature of liquid nitrogen. The total intensity of the diffuse lines seems to be concentrated within a very narrow range so that the lines are easy to observe. As a precaution, the temperature was reduced even further to that of liquid hydrogen where the intensification progresses still further.

The apparatus employed was a quartz Dewar tube furnished with four plane quartz windows. The single crystals were always immersed in the refrigerating liquid and were held in a metallic strip fastened to a tube of German silver which could be raised and lowered. In this way any one of several crystals could be placed in the path of the light. The source of continuous radiation in the ultraviolet was a hydrogen discharge tube similar to the type recommended by Bay and Steiner.[4] It was constructed of Pyrex glass and permitted the continuous use of more than 500 milliamperes. An E_2 spectrograph from Hilger was employed through the kindness of Professor Blanksma of the Organic Chemical Laboratory of this university. It contained one quartz prism and had a dispersion of about 5A per mm at 2500A.

Crystals of the following salts were investigated: cerium chloride, cerium ethylsulfate, cerium acetate, praseodymium chloride, neodymium chloride, lanthanum chloride. All contained water molecules of crystallization. The cerium salts were recrystallized many times; the chloride from absolute alcohol. The cerium chloride was obtained as the hydrated chloride "pur" from the Societé des Produits Chimiques des Terres Rares. The ethylsulfate of cerium and the acetate were made from a hydrated nitrate "reinst" of the Auer Gesellschaft. *All* the chemical operations and crystallizations were carried out at practically room temperatures to avoid oxidation. The oxidation of cerium, observed by the yellowing of the solution, sets in rapidly if the solution is boiled in air, but this reaction does not occur in alcohol. (It was later found reported that the oxidized cerium salt reverts easily in the presence of alcohol to the form desired for this work.)[5]

Thereafter, all crystallizations were performed at room temperature from solutions containing considerable concentration alcohol. The crystals were grown by the slow evaporation of a saturated solution in a dessicator containing calcium chloride.

The crystals of the three cerium salts varying in thickness from about 0.2 mm to 3 mm showed similar absorption spectra at all temperatures. They were completely transparent from the visible region of the spectrum to about 2700A and then absorption began rather abruptly and occupied the rest of the ultraviolet region (until about 2000A, the limit of transparency of the quartz spectrograph). The absorption edge moved toward the red with increasing thickness of crystal.

It was inferred at this stage of the work that the continuum corresponded to an ionization of the ion, a transition of the electron immediately to the lattice rather than to an outer shell such as $5d$, . . . , or $6s$ etc. Transition to the latter would presumably have resulted in broad lines or bands since the

[4] Bay and Steiner, Zeits. f. Physik **45**, 337 (1927).

[5] Treadwell-Hall, Analytical Chemistry, p. 471, Vol. I, New York (1916).

outer shells are susceptible to the oscillating electric fields of the water molecules. (Additional broadening influences will be discussed later.)

It was of course necessary to establish that the absorption was not due to the negative ions. For this purpose salts of other rare earths containing the same negative ions were examined so as to be entirely assured that the fields emanating from the positive ion, that is, the fields associated with the size and charge of Ce^{+++} could not displace the "natural" obsorption of the negative ions into the observed spectral region. (It is hardly necessary to remark that the ionic radii of the rare earths are almost identical, the well-known difficulty of separating them attests to the minutest differences.)

Lanthanum *chloride* was found to be completely transparent throughout the entire spectral range. This behaviour was expected since the chloride ion is known to be transparent here and lanthanum with no electrons in the 4*f* shell would require for the disruption of the completed shell many times the energy available in the shortest wave-lengths. Apart from a line spectrum, praseodymium *acetate* was also found to be transparent down to the shortest measurable wave-lengths. Dysprosium *ethyl sulfate* behaved similarly.

It was still possible that the unbroken continuum was really the superposition of several absorption bands either because of an interaction of neighboring cerium ions or because of an enormous intrinsic absorption of these ions. The consequences of both these influences could be obviated by separating the Ce^{+++} in the crystal lattice and by keeping the thickness of the resulting crystal about the same as in the previous experiments. The cerium ions were separated from each other by making mixed crystals of the cerium salts with the same lanthanum salts, the cerium comprising but a small fraction of the total. Mixed crytals of cerium and lanthanum chlorides and of cerium and lanthanum ethyl sulfates were investigated. La^{+++} was selected for the dilution because of its complete transparency. Mixed crystals of the La^{+++} and Ce^{+++} salts can be made in all proportions because the radii of these ions are almost identical. In the ethylsulfates and in the chlorides, both the Ce^{+++} ions and La^{+++} ions are immediately surrounded, with the same number of water molcules probably as $La(H_2O)_6^{+++}$, $Ce(H_2O)_6^{+++}$ and the fractional differences in the radii of these increased ions is even less than in the unhydrated ions. In addition the slight difference between the action of one cerium upon another and that of a lanthanum ion upon a cerium ion is lessened by the negative ions between them in the crystal lattice.[6]

Crystals prepared from a *solution containing* about ten times as much lanthanum chloride as cerium chloride exhibited a new faint diffuse absorption band with a maximum at about 3025A at room temperature and the continuum occurred in approximately the same region as before. This ab-

[6] The research of J. Becquerel (Gedenkboek H. Kammerling Onnes (1922)) shows that many absorption lines of the rare earths are sharp even in complicated mixtures such as minerals. The substitution of Br^- for Cl^- in $GdCl_3\,6H_2O$ (Freed and Spedding, Jour. Am. Chem. Soc. **52**, 3747 (1930)) shifted the absorption lines of Gd^{+++} on an average by about $4cm^{-1}$. The substitution of La $(H_2O)_6^{+++}$ for Gd $(H_2O)_6^{+++}$ would doubtless produce so small a displacement that it would be scarcely measurable with the quartz spectograph employed in this work.

sorption was never observed in crystals containing Ce^{+++} in smaller concentration such as are about to be discussed.[7] These crystals varied in thickness from about 0.3 mm to 2 mm. When the concentration of cerium in solution was about two percent of that of lanthanum, the continuum previously noted decomposed into three diffuse bands which remained as diffuse at the temperature of liquid hydrogen as at room temperature. The corresponding ethylsulfates showed similar absorption spectra. When the Ce^{+++} in solution was diluted further, about one hundred fold relative to the La^{+++}, the same absorption bands persisted, became fainter and narrower but showed no structure either to the eye or to a microphotometer. Lowering the temperature to that of liquid hydrogen did not perceptibly alter the diffuseness of the bands. (See Table I.)

TABLE I. *Data of mixed crystal of lanthanum and cerium ethylsulfate and mixed crystal of lanthanum and cerium chloide.*

Temperature	Number of band	$La^{+++}(Ce)^{+++}(C_2H_5SO_4)_3 \cdot 9H_2O$ Center of band	*Width of band A	$La^{+++}(Ce)^{+++}Cl_3 \cdot 6H_2O$ Center of band A	Width of band
	I			3020	
Room	II	2565	110	2575	50
	III	2380	100	2455	50
	IV	2200	50	2300	very wide
	II	2550	80		
Liquid nitrogen	III	2370	60		
	IV	2230	60		
Liquid nitrogen	II	2540	115	2540	80
	III	2365	90	2440	65
	IV	2245	very wide	2300	45

* The width of the band is only of qualitative significance since it varies with the time of exposure, especially in the wider bands.

Different crystals gave roughly the same maxima within 10A for the narrow bands and 15A for the wider ones. This is about the reproducibility with which the maxima of any single bands are known.

The same crystal of the ethylsulfate was employed at the three temperatures. It was grown from a solution containing about fifty times as much lanthanum as cerium.

The same crystal of the chloride was also employed at the two temperatures but it is possible that at room temperatures there was some moisture on the faces of the crystal. The chlorides differ from the ethylsulfates in being very hygroscopic.

The diffuseness of the bands, the magnitude of their separations the great displacement in their positions when one negative ion is substituted for another or when the temperature is reduced, confirm the expectations that the absorption represents a transition from the 4*f* shell to virtual outer shells of the ion. There is no escape from this interpretation if the final quantum

[7] After this research was finished, this band was recognized faintly in the spectrum of a crystal of cerium chloride undiluted with lanthanum.

states are to be identified with the positive ion. The diffuseness of the bands may be attributed to the outer quantum state or states. (I shall refer to an "outer quantum state" when I mean the quantum state of the ion if the electron is in an outer shell.) The latter is exposed to all the perturbations of the neighbors of the positive ion and to all the oscillations that the neighbors experience. In addition, the unordered electric fields resulting from the strains

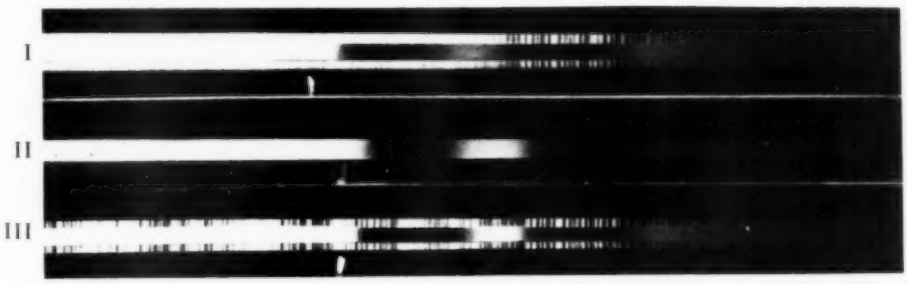

Fig. 1. Mixed crystal of lanthanum and cerium ethylsulfate. I. Room temperature, II. Temperature of liquid nitrogen, III. Temperature of liquid hydrogen.

in the crystal exercise a broadening on these sensitive levels. Even more important in this connection, the electronic levels probably couple with the oscillational levels of the water molecules of the crystal lattice in a way such as has already been anticipated.[8,9] On the other hand, the inner quantum state, the basic state, is relatively free from these oscillating perturbations. The coupling between the electronic motion in the $4f$ shell and the oscilla-

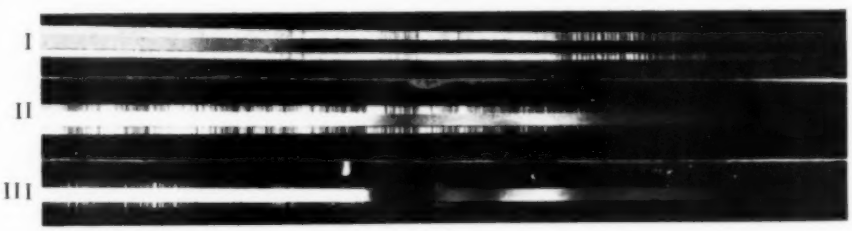

Fig. 2. Mixed crystal of lanthanum and cerium chloride. I. Room temperature: crystal grown from solution containing about ten times as much lanthanum as cerium. II. Room temperature: crystal grown from solution containing about 200 times as much lanthanum as cerium. III. Temperature of liquid hydrogen: crystal containing same concentration as II.

tional motion of the lattice is weak and judging by the sharpness of the absorption lines of the other rare earths such as Nd^{+++}, Gd^{+++}, Dy^{+++} etc., we would estimate the energy of the coupling to be less than the width of a rather sharp absorption line. The energy of this coupling must fall off rapidly with distance.

The H_2O molecules may be fairly well represented as dipoles in their action upon the relatively distant $4f$ electron. However, the proximity of the

[8] Ehrenfest, Gedenboek, H. Kammerling Onnes (1922).
[9] Frenkel, Phys. Rev. **37,** 17 and 1276 (1931).

H_2O groups to the outer electron of the activated Ce^{+++} brings into play their detailed electronic structures with their stupendous inhomogeneous electric fields. The influence of the negative ions also becomes more intense. We find that an alteration in the dipole attending the substitution of one negative ion for another displaces the bands of the Ce^{+++} by as much as 1000 cm^{-1} whereas a similar substitution displaces the lines of Gd^{+++} by less than 10 cm^{-1}. The contraction of the crystal, induced by lowering the temperature, with the resulting change in the electric fields, also effects a disproportionate readjustment of the inner and outer shells. In Gd^{+++} where both the basic and the activated states are in all probability inner states an absorption lines shifts about 6 cm^{-1} when the temperature is reduced from room temperature to that of liquid hydrogen.[10] Under like conditions we find a displacement in Ce^{+++} of from 200 cm^{-1} to 500 cm^{-1}. There is no reason for believing that transitions to outer shells are restricted entirely to Ce^{+++}. We should expect

Fig. 3. Absorption spectrum of Nd^{+++} in $NdCl_3 \cdot 6H_2O$ at 20°K. Band begins at about 2280A and ends at about 2100A, (very faint).

Pr^{+++}, Nd^{+++} etc. to have similar bands in their absorption spectra. Pr^{+++} and Nd^{+++} with higher nuclear charges than Ce^{+++} probably hold the $4f$ electrons more strongly and require more energy for analogous transitions. (Such is the ordinary progression in gases also.) Hence we should expect to find their bands further in the ultraviolet region of the spectrum. No bands were found in a hydrated crystal of praseodymium chloride which Professor Urbain had kindly purified for the Cryogenic Laboratory. Nd^{+++} ("Reinst" Auer Gesellschaft) definitely possessed such a band in our extreme ultraviolet. The band of the hydrated neodymium chloride extended from 2280A to 2100A and showed no structure even at the temperature of liquid hydrogen. It is probable that Pr^{+++} can be similarly activated but its first band lies just out of range of the quartz spectrograph. A faint band near 2100A would not have been detected for the general intensity of the radiation was feeble in this region.

It was surprising to observe so little contraction in the bands at the temperature of liquid hydrogen. The breadth of the bands which can be related to thermal oscillations (namely, the variation in the external electric fields and the coupling with the oscillations themselves) are doubtless greatly reduced. However, the low temperature would be accompanied by an in-

[10] Freed and Spedding, Phys. Rev. **34,** 945 (1929).

crease in the number and in the intensity of the strains and their "surface" fields would undo the normal effects of reduced temperatures.[11]

We have mentioned[3] that the separation between the levels of the basic doublet ^2F is expected to be about 1000 cm^{-1}. Corresponding to this difference in energy about 5 percent of the total Ce^{+++} ions would be activated and in the upper level at room temperature. At the temperature of liquid hydrogen, only one Ce^{+++} ion out of 10,000,000 would be activated. Transitions beginning at this activated level would produce faint bands at room temperature and they would disappear at the temperature of liquid hydrogen. Since there is little change in the relative intensities of the bands, we must accept that practically all the Ce^{+++} occupy the basic level or levels so close together that they behave as one relative to the width of the bands.[12] This statement, while almost certainly true, is not necessary for the conclusion that the electron occupies the 5*d* shell. It is sufficient and it makes the discussion more direct. The necessary condition is that the Ce^{+++} ions in these dilute crystals are not present in appreciable amounts at the temperature of liquid hydrogen in more than three levels 2500 cm^{-1} or more apart. There is no question but that this condition is rigorously fulfilled.

If we look at the electronic configurations of the metals of the rare earths, we observe that one 5*d* electron and two 6*s* electrons had been removed in the process of ionization. The 5*f* shell does not become a stable shell for an electron until the atomic number 90 (thorium) is reached and no atom has an electron in the 5*g* shell. We shall try to decide between the 5*d* shell and the 6*s* shell as the final state of the electron. The former would give rise to a ^2D term and the latter to a ^2S term. It is known[13,14] that *S* terms are not decomposed by electric fields (or as Kramers points out, only to a degree of several cm^{-1}) and since they are single, a transition to the 6*s* shell from the basic level could account for only one band. However at least four bands exist and hence we must conclude that the electrons of many cerium ions end in the 5*d* shell. The final state is then $^2D_{3/2,5/2}$ decomposed further by the electric fields of the lattice. On grounds of symmetry Bethe[13] has concluded that a $D_{3/2}$ term is decomposed into three terms in a hexagonal crystal (ethyl sulfate) and in tetragonal crystals and into at least as many in crystals of lower symmetry. (The chloride is probably monoclinic.) The $D_{5/2}$ term will be decomposed into more than three.

[11] These strains are only feebly effective in broadening the lines associated with inner quantum states. Er^{+++} with an ionic number of 66 exhibits very broad and diffuse bands at room temperature which undergo a striking refinement into sharp lines at lower temperatures such as that of liquid nitrogen (Freed and Spedding Nature, **123,** 525 (1929)).

[12] Possibly, the faint band observed at room temperature in some crystals of the chloride, originates at this activated level. The intensities referred to have been shown by the same crystal of the ethylsulfate at the three temperatures. Here we can see little difference in the relative intensities. In the chloride, band II has apparently gained somewhat in intensity at the expense of band III at the temperature of liquid hydrogen. The chlorides, however, are very hygroscopic. At room temperature, there was possibly a little moisture on the faces of the crystal which would influence the absorption and hence make comparison of the intensities, invalid.

[13] Bethe, Ann. d. Physik **3,** 133 (1929).

[14] Kramers, Proc. Acad. Amsterdam **32,** 1176 (1929).

Transitions from the $2F$ term to $D_{3/2}$ and $D_{5/2}$ states would conserve the selection rules of $\Delta j = \pm 1$ and 0 and $\Delta l = \pm 1$ and such transitions would be highly probable. Only very high probabilities of transitions can accord with such enormous intensities in the absorption as have been found. Transitions to the $6s$ shell would introduce $\Delta j = 2$ and $\Delta l = 3$ which would be of much lower probability.[15] The high positive charge on Ce^{+++} would probably make the $5d$ electron more stable than the $6s$, $6p$ etc. electrons. (The concept of many virtual orbits in the crystals becomes more and more vague.) There are numerous examples in gases where a high nuclear charge stabilizes an inner shell. The best known are the iso-electronic gases K and Sc^{++} and their electronic configurations are

	$1s$ to $3p$	$3d$	$4s$
K	full		1
Sc^{++}	"	1	

In a recent letter to this review[16] Spedding advanced the hypothesis that the sharp absorption lines of the rare earths are due quite generally to transitions from the inner $4f$ shell to the outer shells $5d$, $-6s$, etc. He was led to this supposition because the transitions between the states arising within the $4f$ shell in Gd^{+++} must result in intercombination lines, that is in transitions between ^8S and ^6P, for example, intercombination lines occur frequently in the heavier gases free from perturbations and hence there is no reason to dismiss such possibilities in ions imbedded in a lattice where many influences are still unknown. It was observed that the intensity of the absorption bands in Ce^{+++} was much greater than in Nd^{+++} or Pr^{+++} since upon diluting Ce^{+++} with La^{+++} and Nd^{+++} with La^{+++} the bands of Ce^{+++} persisted long after the lines of Nd^{+++} had disappeared. The greater intensity confirms the view that the bands of Ce^{+++} arise from permitted transitions while most of the lines of Nd^{+++} are transitions of less probability, such as intercombination lines. The extreme sensitivity of the bands of Ce^{+++} to external conditions shows clearly that electrons close to the sources of perturbation are responsible for the absorption. In Gd^{+++} the initial and final states are either insensitive to the surrounding molecules or are almost equally sensitive to them. They must then have almost identical electron distributions and hence both the initial and final states of the absorption lines are due to electrons in the $4f$ shell.

I should like to express here my gratitude to Professor W. J. de Haas and to all in his laboratory for their kind hospitability.

[15] As Bethe observes, the presence of the electric fields introduces different quantum numbers and a selection principle applies to them. Nevertheless, the above discussion on transition probabilities is qualitatively valid since in the limit of feeble fields, the above considerations are approximated.

[16] Spedding, Phys. Rev. **37**, 777 (1931).

THE ABSORPTION SPECTRUM OF CHLORINE DIOXIDE*

HAROLD C. UREY AND HELEN JOHNSTON[1]
COLUMBIA UNIVERSITY

(Received October 5, 1931)

ABSTRACT

The wave-lengths of 134 absorption bands of ClO_2 have been measured with the Hilger E-1 and E-185 quartz instruments. The bands have been arranged in progressions and the energy levels deduced. Five vibrational levels of the normal electronic state have been found; the vibrational levels of the excited electronic state can be described with the use of two vibrational quantum numbers. Formulae for these bands and their isotope separations are given. The shapes of the molecule in the normal and excited electronic states have been calculated from Bjerrum's formulae for the vibrations assuming valency forces and all but one solution for each electronic state is excluded by the isotope effect or the intensity distribution of the bands. The central force formulae give no possible solutions. The normal modes of vibration for the molecule have been calculated. The intensity distribution is consistent with the extension of the Franck-Condon principle to polyatomic molecules. The predissociation limit agrees with a very approximate extrapolated value for the energy of dissociation through one mode of vibration of the excited electronic state into a ClO molecule and an O atom. Dissociation through a second mode of vibration of the excited electronic state gives only a very rough value. A discontinuity in the $\Delta E{:}v_2'$ curve noted by Goodeve and Stein appears at about the energy required for an oscillation of the molecule through a straight line position and it is proposed that this is the cause of the discontinuity.

OF THE various triatomic molecules whose electronic bands lie in the more accessible wave-length regions, chlorine dioxide seems to be one of the most promising molecules. It has an intense absorption spectrum lying between $\lambda\lambda$ 5225 to 2600A and because chlorine has two isotopes of comparable abundance, it is possible to study the isotope effect, giving another way of attacking the assignment of vibrational quantum numbers to its energy levels. This research was undertaken on this molecular spectrum in order to make use of this particular advantage.

The first attempt to classify the bands of ClO_2 was made by Käbitz.[2] Mayer[3] succeeded in arranging them into progressions. In both of these researches only about forty nine bands were considered. Goodeve and Stein[4] investigated the spectrum of ClO_2 and measured 138 bands, and found that many of the observed bands were isotopic bands. These bands were arranged

* Contribution No. 683 from the Department of Chemistry, Columbia University.

[1] The material in this paper is taken from the dissertation submitted by Helen Johnston in partial fulfillment of the requirements of the degree of Doctor of Philosophy, Columbia University, 1931.

[2] B. Käbitz, Diss. Bonn, 1905.

[3] H. Mayer, Zeits. f. physik. Chem. **113**, 220 (1924).

[4] C. F. Goodeven and C. P. Stein, Trans. Faraday; Soc. **25**, 738 (1929).

into 4 principal and 5 sub-"series." They also observed the phenomenon of predissociation, which they located at λ3293A. Very recently Finkelnburg and Schumacher[5] have published a paper on ClO_2. These experimentors have photographed the band heads with a two meter grating, but have not arranged the bands into progressions. They have also determined the limit of predissociation λ3753.28A.

Experimental

The chlorine dioxide was prepared by the reaction of oxalic acid and potassium chlorate as described by Bray.[6] The gas evolved was collected in a trap cooled with dry ice. This trap was connected directly to the absorption cell.

Since chlorine dioxide is decomposed rather rapidly by light, it was necessary to keep a stream of the gas flowing through the absorption cell during the time of exposure. To do this we connected a glass needle valve to an outlet tube of the absorption cell to regulate the rate of flow of the ClO_2 and evacuated the system protecting the pump with a liquid air trap. When this procedure was used, the trap containing the chlorine dioxide was cooled in dry ice or dry ice-alcohol mixtures in order to regulate the pressure of ClO_2. In some cases a stream of nitrogen was passed through the chlorine dioxide trap and then through the absorption cell and thus the cell was kept filled with undecomposed chlorine dioxide. The dry ice-alcohol bath provided a range of temperatures from $-76°C$ to $10°C$. The bath was easily regulated to within $\pm 0.5°$ by the addition of dry ice about every 15 or 20 minutes.

Three absorption cells were used in these experiments. The first cell was made of Pyrex with plane Pyrex windows. There were three compartments in this cell, the two end ones ten cm long being evacuated and sealed off. The middle compartment was 30 cm long. This construction was used so that the middle compartment containing the ClO_2 gas could be cooled in dry ice in order to sharpen the band heads and simplify the general band structure. This could only be used for the stronger bands. The second cell consisted of a Pyrex tube 60 cm long with quartz windows sealed on which de Khotinsky cement. (ClO_2 is said to explode when brought in contact with organic matter, but we had no such difficulty.) The third cell was an all quartz one of the same general design as the first described above.

As sources of light in the visible and near ultraviolet we used a tungsten filament lamp or a point-o-lite lamp. A Pfund iron arc was used as a reference source. This was mounted directly in front of the slit with the lower electrode remaining in place during the exposure of the absorption spectrum to insure its correct alignment during the exposure of the reference spectrum.

The Hilger E–1 Quartz Spectrograph was used for nearly all our measurements, only a small number being made with the Hilger E–185 three meter instrument.

[5] W. Finkelnburg and H. J. Schumacher, Zeits. f. physik. Chemie, Bodenstein-Festband, 704 (1931).

[6] W. Bray, Zeits. f. physik. Chemie **54**, 575 (1906).

Experimental Results

We have measured 134 bands of ClO_2 between λλ5042 and 3226. The reproducibility of our measurements on different plates is about 0.7A or from 3 to 6 cm^{-1} depending on the wave-length range. Table I gives the wave numbers of all bands measured by us and the wave numbers given by Finkelnburg and Schumacher and by Goodeve and Stein. Goodeve and Stein say that their results could be duplicated to within a few wave numbers but that sometimes readings differed by as much as 10 cm^{-1}. In the far ultraviolet, they claimed not to be able to repeat within 15 cm^{-1}. Finkelnburg and Schumacher claim an accuracy of ± 0.05A in the visible and ± 0.5A in the far ultraviolet. We find that the measurements of the latter authors do not follow smooth formulae as well as ours and we do not feel certain that these band heads can be measured so precisely as they claim. The wave-lengths which we secured were reduced to vacuum by reducing the wave-lengths of the standard iron lines to vacuum and making the entire calculation with these standards. The wave-lengths were calculated by using the usual Hartmann formula.

Classification of Bands

Inspection of Goodeve and Stein's results immediately shows that it is impossible to derive a formula that will fit the isotope effect. A formula can be made to fit the isotope effect from the sixth member of their "sequence," but their classification up to this point must be incorrect or the isotope effect surprisingly irregular. Our arrangement of the bands into progressions differs in many details from that of Goodeve and Stein though the main features remain.

In discussing our arrangement, it is convenient to adopt the assignment of vibrational quantum numbers at this point and justify this selection later. We find it necessary to use three quantum numbers for the normal state, v_1'', v_2'' and v_3'', and two for the excited state, v_1' and v_2'. Transitions can be indicated by the symbol $(v_1', v_2') \leftarrow (v_1'', v_2'', v_3'')$, the arrow indicating the direction of the change in absorption.

Anticipating the final assignment of quantum numbers, the progression with the most intense bands is $(0, v_2') \leftarrow (0, 0, 0)$, $v_2' = 0$ to 30, the third most intense band system $(1, v_2') \leftarrow (0, 0, 0)$, $v_2' = 1$ to 17, the second $(0, v_2') \leftarrow (0, 0, 1)$, $v_2' = 4$ to 15, and the fourth $(1, v_2') \leftarrow (0, 0, 1)$, $v_2' = 0$ to 13. If the progression difference between progressions $(0, v_2') \leftarrow (0\ 0, 0)$ and $(0, v_2') \leftarrow (0, 0, 1)$ and between progressions $(1, v_2') \leftarrow (0, 0, 0)$ and $(1, v_2') \leftarrow (0, 0, 1)$ are taken it will be found that this difference is 528.8 cm^{-1}. It would thus appear that the first and third most intense progressions originate from the same unexcited level and go to different excited levels and the second and fourth in intensity come from a level with 528.8 cm^{-1} more energy and terminate on the same two sets of excited levels. If the differences between the bands having the same value of v_2' of the progressions $(0, v_2') \leftarrow (0, 0, 0)$ and $(1, v_2') \leftarrow (0, 0, 0)$ and of progressions $(0, v_2') \leftarrow (0, 0, 1)$ and $(1, v_2') \leftarrow (0. 0, 1)$ and of progressions $(1, v_2') \leftarrow (0, 0, 1)$ and $(2, v_2') \leftarrow (0, 0, 1)$ are taken it is found to be about 300

TABLE I.

U. & J. $\tilde{\nu}$ in cm^{-1} in vacuo	F. & S. $\tilde{\nu}$ in cm^{-1} in vacuo	G. & S. $\tilde{\nu}$ in cm^{-1} in air	U. & J. $\tilde{\nu}$ in cm^{-1} in vacuo	F. & S. $\tilde{\nu}$ in cm^{-1} in vacuo	G. & S. $\tilde{\nu}$ in cm^{-1} in air
	19134.1	19140	*23938.2		23944
	19424.4	19423	23959.1		23967
†	19625.4	19635	*24058.6		24062
19831.9	19841.7	19848	24078.2	24079.3	24084
†		19900	††24169.6		
20070.2		20079	24227.7	24228.3	24232
*20080.2	20081.5		†	24241.0	
20125.8	20130.4	20130	*24463.9		24471
†20185.3			24488.1	24488.4	24495
20332.7		20341	*24610.9		
20359.8		20368	24635.8	24636.8	24641
*20368.4	20369.9		24709.7		
20542.3		20548	*24732.2		24738
20569.4		20574	24757.2	24757.1	24763
*20574.2	20572.7		24899.1	24907.4	24904
20782.1	20778.8	20786			24986
*20785.9			25116.3		
20825.1		20835	*25132.8		25141
21014.2	21016.4	21023	25163.9	25164.2	25170
21064.6	21064.1	21070	25238.7		
21275.8	21276.2	21283	*25274.6		25284
21307.7	21305.4	21310	25307.0	25307.5	25313
21479.8	21480.4	21483	*25397.8		25397
*21716.8			25428.0	25428.0	25436
21724.8	21724.3	21733	*25536.9		25544
21760.6	21761.2	21769	25569.2	25571.4	25575
21842.2		21849			25656
21979.1		21980	25769.9		
22009.7	22010.3	22016	*25799.7		25810
22172.3	22173.7	22178	25834.2	25835.4	25843
†22369.4			25903.4		
22426.4	22425.4	22437	†25916.5		
22449.2	22450.2	22457	*25936.2		25948
22536.2	22537.0	22542	25972.1	25973.6	25979
22590.9	22598.7	22580	26029.9		
		22675	*26059.5		26065
*22703.2		22703	26094.4	26095.4	26107
22706.4	22706.3	22711	††26151.9		
*22860.6	22860.7	22856	26195.5		26208
22873.2	22875.0	22869	26230.7	26232.2	26242
†23029.2			26303.4	26310.6	26306
*23107.6		23116	*26459.4		
23120.5	23119.2	23124	26500.4	26504.9	26503
23140.5			26549.5		
23221.7		23225	*26591.4		
23280.5	23281.7	23277	26633.5	26635.8	26648
*23382.2		23391	26664.0		
23395.7	23395.8	23402	26686.5		
23548.6	23553.0	23556	*26715.5		
*23789.7		23796	26756.0	26757.4	26764
23806.3	23813.8	23812	*26843.5		26860
23902.0		23904	†26875.8		

* Isotopic bands.

† Unclassified bands.

‡ These are the two bands that agree approximately with the calculated values for transitions (2, 6)←(1, 0, 0) and (2, 9)←(1, 0, 0).

The Editors of the Physical Review suggest that the accuracy of our measurements probably does not justify the use of six significant figures. We fully agree with them but we retain the sixth significant figure because all of our tables and calculation would have to be revised if this figure were dropped. Also the precision of the isotopic separations probably warrants the retension of the fractional values.

TABLE I.—(*Continued*)

U. & J. $\bar{\nu}$ in cm^{-1} in vacuo	F. & S. $\bar{\nu}$ in cm^{-1} in vacuo	G. & S. $\bar{\nu}$ in cm^{-1} in air	U. & J. $\bar{\nu}$ in cm^{-1} in vacuo	F. & S. $\bar{\nu}$ in cm^{-1} in vacuo	G. & S. $\bar{\nu}$ in cm^{-1} in air
26887.0	26888.6	26900	†		29900
26963.8	26967.2	26971	*		29936
*27117.4			29980.9	29982.2	29996
27162.3		27163		30153	
*27240.2			*		30307
27288.6	27293.2	27302	30375.3	30380	30377
*27368.6		27377	*		30400
27412.9	27414.9	27424	30435.6		30477
*		27507	†		30529
†27525.0			†30570.9		
27536.6	27540.4	27550			30613
27625.2	27618.5	27623	*		30976
*27761.5		27772	30989.3	30996	31014
27815.7		27821	†		31142
†27829.7					31218
*27883.1			*		31539
27939.0	27946.7	27956		31601	31619
*		28021	†		31749
†28037.3					31847
28063.0	28065.1	28079		32190	32202
*		28148		32768	32779
28172.8	28186.0	28194		33330	33336
*28415.0		28424	*		33761
28470.7		28475		33848	33877
*28523.5			*		34238
28583.7	28590.2	28603		34346	34341
28704.5	28713.8	28724	*		34746
†28762.8				34841	34855
†28843.9		28840		35288	
29112.4		29114			35370
†29170.1				35805	35840
29223.8	29229.3	29236			36260
*		29304		36321	
29346.0	29351.8	29365			36700
*29685.1		29686			37106
29748.7		29745			37509
29843.0	29850.5	29858			37922

cm^{-1} if v_2' is small and that this difference decreases with increasing v_2'. With this procedure it was found necessary to postulate three upper sets of energy levels and two unexcited energy levels. This is essentially the scheme used by Goodeve and Stein.

The search for further vibration levels of the normal electronic state was then made by first plotting all bands not included in these progressions and then moving a scale having the differences of the $(0, v_2')$, $(1, v_2')$ and $(2, v_2')$ levels along this until agreement with the positions of the unclassified bands was secured. In this way evidence for five vibrational levels of the normal state was secured.

We have not been able to find convincing evidence for the third fundamental vibration frequency of the excited state. Those agreements we have found could be explained as due to chance coincidences.

The final arrangement of bands and combination differences are given in Tables II, III, and IV. The wave number differences are indicated by numbers placed between the columns and rows. The differences indicated by the

Δ's at the top of the columns are the differences between the column of wave numbers following a particular Δ and the first column of the table in each case. In this way the Δ's represent the wave number differences between the lowest lying level and the four higher vibrational levels of the normal state.

TABLE II.

(v_1', v_2')	(v_1'', v_2'', v_3'') (0, 0, 0)	Δ_1	(0, 0, 1)	Δ_2	(0, 1, 0)	Δ_3	(1, 0, 0)
0, 0	20332.7						
	681.5						
0, 1	21014.2						
	710.6						
0, 2	21724.8						
	701.6						
0, 3	22426.4						
	694.1						
0, 4	23120.5	529.6	22590.9				
	685.8		689.6				
0, 5	23806.3	525.8	23280.5				
	681.8		678.6				
0, 6	24488.1	529.0	23959.1				
	675.8		676.7				
0, 7	25163.9	528.1	24635.8				
	670.3		671.2				
0, 8	25834.2	527.2	25307.0	717.9	25116.3	855.2	24979.0*
	666.2		665.1		653.6		669.8
0, 9	26500.4	528.3	25972.1	730.5	25769.9	851.6	25648.8*
	661.9		661.4				654.6
0, 10	27162.3	528.8	26633.5			858.9	26303.4
	653.4		655.1				660.4
0, 11	27815.7	527.1	27288.6			841.9	26963.8
	655.0		650.4				661.4
0, 12	28470.7	531.7	27939.0			845.5	27625.2
	642.0		644.7				
0, 13	29112.7	529.0	28583.7				
	636.0		640.1				
0, 14	29748.7	524.9	29223.8				
	626.6		619.2				
0, 15	30375.3	532.3	29843.0				
	614.0						
0, 16	30989.3						
Ave.		528.5		724.2		850.6	

Some variation in these differences is present but no evidence of trends in values. The wave numbers marked with an asterisk are those of Goodeve and Stein corrected to vacuum.

The energy levels of the normal electronic state are spaced as follows above the lowest level:

(0, 0, 0)	0	cm^{-1}
(0, 0, 1)	528.8	"
(0, 1, 0)	727.0	"
(1, 0, 0)	857.7	"
(0, 2, 0)	1471.3	"

The last level is classified as the first harmonic of the 727.0 cm^{-1} level. It is greater than twice the value of the fundamental but this is quite common among polyatomic molecular levels. These values do not represent average

value of all the differences of Table II, III, and IV but only average values of our own measurements.

All but 21 bands have been assigned to progressions, of this number six were reported by Goodeve and Stein and one by Finkelnburg and Schu-

TABLE III.

(v_1'', v_2'', v_3'') (v_1', v_2')	(0, 0, 0)	Δ_1	(0, 0, 1)	Δ_2	(0, 1, 0)	Δ_3	(1, 0, 0)	Δ_4	(0, 2, 0)
1, 0			20070.2						19134.7*
			711.9						697.2
1, 1	21307.7	525.6	20782.1	738.3	20569.4			1475.8	19831.9
	702.0		697.7		706.4				710.4
1, 2	22009.7	529.9	21479.8	733.9	21275.8			1467.4	20542.9
	696.7		692.5		703.3				
1, 3	22706.4	534.1	22172.3	727.3	21979.1	864.2	21842.2		
	689.3		700.9		689.8		694.0		
1, 4	23395.7	522.5	22873.2	727.0	22688.7*	859.5	22536.2		
	682.5		675.4				685.5		
1, 5	24078.2	529.6	23548.6			856.5	23221.7		
	679.0		679.1				680.3		
1, 6	24757.2	529.5	24227.7			855.2	23902.0		
	670.8		671.4						
1, 7	25428.0	528.9	24899.1	718.3	24709.7				
	666.4		670.1						
1, 8	26094.4	525.2	25569.2			855.7	25238.7		
	661.6		661.5				664.7		
1, 9	26756.0	525.3	26230.7	726.1	26029.9	852.6	25903.4		
	656.9		656.3		656.5		646.1		
1, 10	27412.9	525.9	26887.0	726.4	26686.5	863.4	26549.5		
	650.1		649.6						
1, 11	28063.0	526.4	27536.6						
	641.5		636.2						
1, 12	28704.5	531.7	28172.8						
	638.5								
1, 13	29343.0								
	637.9								
1, 14	29980.9								
	Ave.	527.9		728.2		858.2		1471.6	

macher and have not been confirmed by the authors of this paper and fourteen were first reported by us. Two of the latter fourteen agree very approxi-

TABLE IV.

(v_1'', v_2'', v_3'') (v_1', v_2')	(0, 0, 1)	$\Delta_4 - \Delta_1$	(0, 2, 0)
2, 0	20359.8	942.2	19417.6*
	704.8		708.2
2, 1	21064.6	938.8	20125.8
	696.0		699.3
2, 2	21760.6	935.5	20825.1
	688.6		
2, 3	22449.2		
	691.3		
2, 4	23140.5		
Ave.		938.8	

mately with the calculated values using the formulae below for the transitions (2, 6)←(1, 0, 0) and (2, 9)←(1, 0, 0). These unclassified bands are denoted by a dagger in Table I.

TABLE V.

$(v_1'', v_2'', v_3'') \rightarrow$ v_2'	(0, 0, 0) $v_1'=0$	(0, 0, 1) $v_1'=0$	(0, 0, 0,) $v_1'=1$	(0, 0, 1) $v_1'=1$	(0, 0, 1) $v_1'=2$	(0, 1, 0) $v_1'=1$	(0, 1, 0) $v_1'=0$	(1, 0, 0) $v_1'=0$	(1, 0, 0) $v_1'=1$	(1, 0, 0) $v_1'=2$	(0, 2, 0) $v_1'=1$	(0, 2, 0) $v_1'=2$
0	+27.8			−3.3	+6.1						+3.7*	−5.8*
1	−2.0		−1.0	+2.4	−2.8	−12.3					−5.9	+0.9
2	+3.0		+0.3	−0.8	−1.7	−6.6					+3.6	+4.3
3	+4.6		+1.9	−3.4	−4.3	+1.6			−4.6			
4	+4.3	+3.4	+1.7	+8.0	+2.5	+1.7*			−0.1			
5	+1.4	+4.4	+0.4	−0.4					+1.6			
6	+0.1	−0.1	+1.2	+0.5					+3.7	+8.2		
7	−1.5	−0.6	−0.6	−0.7		+8.1						
8	−3.0	−1.4	−1.1	+2.5			+6.1	−0.6*	+0.9			
9	−3.0	−2.5	−0.8	+2.7		+0.1	−6.5	+3.1*	+4.3	+4.4		
10	−1.7	−1.7	+0.4	+3.3		+1.0		−2.9	−5.7			
11	−3.2	−1.5	+0.5	+2.9				+2.6				
12	+3.3	−0.4	−1.4	−5.3				+14.7				
13	+0.9	−5.3	−2.6									
14	−1.6	+2.3	+1.7									
15	−7.3	−10.1										
16	−20.1											

TABLE VI.

v_2'	$v_1''=0, v_2''=0, v_3''=0$ $v_1'=0$		$v_1''=0, v_2''=0, v_3''=1$ $v_1'=0$		$v_1''=0, v_2''=0, v_3''=0$ $v_1'=1$		$v_1''=0, v_2''=0, v_3''=1$ $v_1'=1$		$v_1''=0, v_2''=0, v_3''=1$ $v_1'=2$		$v_1''=0, v_{2,}=1, v_3,=0.$ $v_1'=1$	
	Obs.	Calc.	Obs.	Calc.	Obs.	Calc.	Obs.	Calc.	Obs.	Calc.	Obs.	Calc.
0		8.1		11.3		8.3	10.0	10.5	8.6	9.7		
1		2.7		6.0		2.9	5.0	5.2		4.4	4.8	6.5
2	−4.5	−2.7		0.6		−2.5		−0.2				0.1
3		−8.0		−4.8		−7.8		−5.6				
4	−12.9	−13.4		−10.2	−13.5	−13.2	−12.6	−11.0				
5	−16.6	−18.8		−15.2	−19.6	−18.6		−16.3				
6	−24.2	−24.2	−20.9	−20.9	−25.0	−24.0		−21.7				
7	−31.1	−29.5	−24.9	−26.3	−30.2	−29.3		−27.1				
8	−34.5	−34.9	−32.4	−31.6	−34.9	−34.7	−32.3	−32.4				
9	−41.0	−40.3	−35.9	−37.0	−40.5	−40.1	−35.2	−37.8				
10	−44.9	−45.6	−42.1	−42.4	−44.3	−45.4	−43.5	−43.2				
11	−54.2	−51.0	−48.4	−47.8		−50.8	−53.7	−48.6				
12	−55.7	−56.4	−55.9	−53.1				−53.9				
13		−61.7	−60.2	−58.4								
14	−63.6	−67.1		−63.8								
15												
16												

The wave numbers of these classified bands can be calculated by an equation of the type,

$$\tilde{\nu} = \tilde{\nu}_e + a(v_2' + \tfrac{1}{2}) - b(v_2' + \tfrac{1}{2})^2 + c(v_1' + \tfrac{1}{2}) - d(v_1' + \tfrac{1}{2})^2 - e(v_1' + \tfrac{1}{2})(v_2' + \tfrac{1}{2}) - \tilde{\nu}''$$

where $\tilde{\nu}_e$ is the wave number for the electronic transition and $\tilde{\nu}''$ is the wave number of the normal vibrational level and a, b, c, d, and e are constants. With the numerical values of the constants which we have secured this becomes,

$$\tilde{\nu} = 19795.38 + 719.34(v_2' + \tfrac{1}{2}) - 2.817(v_2' + \tfrac{1}{2})^2 + 304.82(v_1' + \tfrac{1}{2}) - 2.488(v_1' + \tfrac{1}{2})^2 - 4.892(v_1' + \tfrac{1}{2})(v_2' + \tfrac{1}{2}) - \tilde{\nu}''. \quad (1)$$

This formula applies to bands for which v_2' is equal to or less than 14. The precision with which the measurements in the far ultraviolet can be made is so low that it is impossible to derive a satisfactory formula for this region. In Table V we have given the results of the observed minus the calculated values for the band heads. In most cases there is very close agreement, and the agreement in the case of nearly all the bands is satisfactory and probably within the limits of error of the measurements.

Fig. 1 is the energy level diagram consisting of the levels required by our assignment of quantum numbers. The black circles indicate the observed bands.

The Isotope Effect

The isotope effect is very prominent in these bands. We have indicated the isotopic bands in Table I with an asterisk. This selection was made partly by inspection and partly by means of the formulae derived in this section. The $Cl^{37}O_2$ bands lie on the high frequency side of $Cl^{35}O_2$ bands in the case of bands involving transitions to the lowest excited vibrational levels, but otherwise on the low frequency side.

We have found it possible to fit the experimental differences, $(Cl^{37}O_2) - (Cl^{35}O_2)$, to the formula

$$\Delta\tilde{\nu} = -5.37(v_2' + \tfrac{1}{2}) - 0.80(v_1' + \tfrac{1}{2}) - \Delta\tilde{\nu}'', \quad (2)$$

where $\Delta\tilde{\nu}''$ is -11.16 cm^{-1}, -14.42 cm^{-1} and -15.75 cm^{-1} for the (0, 0, 0), (0, 0, 1) and (0, 1, 0) normal vibrational levels, respectively. The agreement between this formula and the observed values is shown in Table VI, which also shows which isotope bands have been observed. The isotopic bands in many cases could not be observed because of fine structure, superposition of the weaker $Cl^{37}O_2$ band on the strong $Cl^{35}O_2$ band, diffuseness of band heads in the predissociation region, and the general weakness of many of the bands, both $Cl^{35}O_2$ and $Cl^{37}O_2$.

The separations of the vibrational levels in either the excited or normal electronic state should follow a formula of the form,

$$\frac{\Delta E}{hc} = a(v_1 + \tfrac{1}{2}) + b(v_2 + \tfrac{1}{2}) + c(v_3 + \tfrac{1}{2})$$

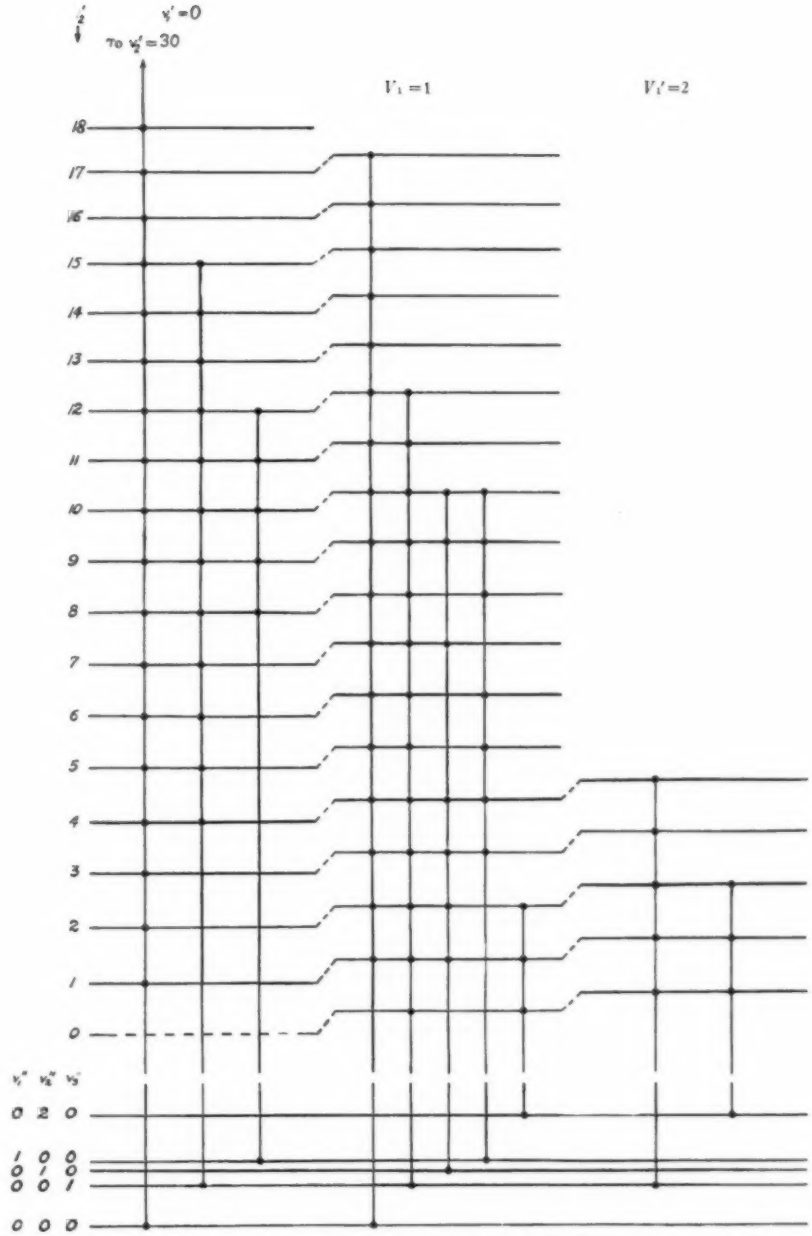

Fig. 1. Energy level diagram of the ClO_2 molecule. Bands that agree approximately with the calculated values for the transitions. (0, 8)←(0, 1, 0); (0, 9)←(0, 1, 0); (2, 6)←(1, 0, 0) and (2, 9) − (1, 0, 0) are omitted. These transitions are discussed in the text.

where the a, b, and c will be negative if ΔE is the energy of the $Cl^{37}O_2$ molecule minus that of the $Cl^{35}O_2$ molecule and higher power terms in the v's are neglected. If we assume that $v_3' = 0$ for all levels which we have observed the isotope separation is then,

$$\tilde{\nu}_{37} - \tilde{\nu}_{35} = \Delta\tilde{\nu} = a'(v_1' + \tfrac{1}{2}) + b'(v_2' + \tfrac{1}{2}) + c'/2 - a''(v_1'' + \tfrac{1}{2}) - b''(v_2'' + \tfrac{1}{2}) - c''(v_3'' + \tfrac{1}{2}). \quad (3)$$

With our assignment of quantum numbers we see from Eqs. (2) and (3) and the values of $\Delta\tilde{\nu}''$, that

$$a' = -0.80 \qquad \frac{c'}{2} - \frac{a''}{2} - \frac{b''}{2} - \frac{c''}{2} = -\Delta\tilde{\nu}''$$

$$b' = -5.37 \quad b'' = -15.76 + 11.16 = -4.60$$

$$c'' = -14.42 + 11.16 = -3.26$$

and thus

$$\frac{c'}{2} - \frac{a''}{2} = 7.23. \quad (4)$$

Our calculated value (see below) for this difference is 3.19 cm^{-1}. This difference would be diminished, if the 11.16, 14.42, and 15.76 cm^{-1} differences in our formula (2) were decreased. This would mean that our calculated differences for the bands having $v_2' = 0$ should be less than those given in Table VI by about 4 cm^{-1}. Examination of that table shows that a change of a few wave numbers in these values may be possible. We shall discuss this further after the theoretical formulae have been presented.

The Normal Modes of Vibration of the ClO_2 Molecule

Bjerrum[7] has considered the problem of the vibrations of molecules of this kind assuming two types of binding; (1) the potential energy is a function of the linear distances between the nuclei, that is the forces are central; (2) the restoring forces consist of harmonic forces along the chemical bond and perpendicular to this direction, that is, the forces are valency forces as he called them. The three frequencies of vibration in each case are functions of three constants, two force constants and the half angle at the apex of the isosceles triangle. All solutions for this angle using the formulae based on assumption (1) gave imaginary angles.

The equation for θ the half angle at the apex by using the formulae based on assumption (2) is a cubic in $\cos^2\theta$ and there are three possible ways of assigning the observed frequencies to the theoretical formulae for the frequencies. This gives nine possible solutions. The possible values of $\cos^2\theta$ must be real and lie between 0 and 1. We find that there are three possible values for θ in the normal electronic state and thus three possibilities for the two force constants k_1, and k_2 as well. In the case of the ClO_2 normal state, our experimental data give us the isotope effect constants as well and it must

[7] N. Bjerrum, Verh. d. D. phys. Ges. **16**, 737 (1914).

TABLE VII.

	Assumed assignment of frequencies			Normal electronic state									
	$\tilde{\nu}_1$	$\tilde{\nu}_2$	$\tilde{\nu}_3$	$k_1\times10^4$	$k_2\times10^4$	θ	2θ	$\Delta\tilde{\nu}_1$ Calc.	$\Delta\tilde{\nu}_1$ Obs.	$\Delta\tilde{\nu}_2$ Calc.	$\Delta\tilde{\nu}_2$ Obs.	$\Delta\tilde{\nu}_3$ Calc.	$\Delta\tilde{\nu}_3$ Obs.
	528.8	857.7	727.0	26.06	34.17	1°19′	2°38′	−0.0073	−3.20				−4.60
	727.0	857.7	528.8	38.71	11.61	31°55′	63°55′	−4.17	−4.60	−10.90	—	−0.39	−3.26
	857.7	727.0	528.8	38.59	8.41	65°10′	130°20′	−10.32	—	−5.88	−4.60	−2.80	−3.26
	Excited electronic state												
	661.1*	719.34	304.8	36.65	3.015	55°19′	110°38′			(−5.37)	−5.37	−1.88	−0.80
	226.1*	719.34	304.8	6.03	18.33	34°39′	69°18′			(−5.32)	−5.37	−1.90	−0.80
I	719.34	779.6*	304.8	35.86	3.62	38°28′	76°56′	(−5.37)	−5.37	−8.53	—	−0.83	−0.80
II	304.82	719.34	382.1*	7.96	21.81	18°47′	37°34′	(−0.80)	−0.80	−6.06	−5.37	−3.93	—

* These are calculated frequencies.

be possible to calculate these from the formulae by using the same set of values of k_1, k_2 and θ.

In the case of the excited electronic state we have observed two fundamental frequencies and the isotope effects for each of these. With three of these quantities we can solve for the constants k_1, k_2 and θ again and the fourth quantity must also agree with the calculated value. We find four possible values of θ of which two give sets of values for k_1, k_2 and θ from which the second isotope effect can be calculated. The formulae for ν_1, ν_2 and ν_3 and for the isotope effects for each of these are given below. Table VII gives the results of the calculations for the normal and excited states. Columns 1, 2, 3 give the possible assignments of the observed frequencies to the three theoretical formulae, columns 4, 5, 6, 7 the calculated constants, and columns 8, 9, 10 the calculated and observed isotope effects.

$$\nu_1 = \frac{1}{2\pi} k_1^{1/2} \left(\frac{1}{m} + \frac{2 \sin^2 \theta}{M} \right)^{1/2} \tag{5}$$

$$\nu_{2,3} = \frac{1}{2\pi} \left\{ \frac{k_1 + 2k_2}{2m} + \frac{k_1 \cos^2 \theta + 2k_2 \sin^2 \theta}{M} \pm \left[\left(\frac{k_1 + 2k_2}{2m} + \frac{k_1 \cos^2 \theta + 2k_2 \sin^2 \theta}{M} \right)^2 - 2k_1 k_2 \frac{2m + M}{m^2 M} \right]^{1/2} \right\}^{1/2} \tag{6}$$

$$\Delta\nu_1 = \frac{\partial \nu_1}{\partial M} \Delta M = - \frac{\Delta M k_1 \sin^2 \theta}{4\pi^2 \nu M^2} \tag{7}$$

$$\Delta\nu_{2,3} = \frac{\partial \nu_{2,3}}{\partial M} \Delta M = \frac{\Delta M}{8\pi^2 \nu_{2,3} M} \left\{ - \frac{k_1 \cos^2 \theta + 2k_2 \sin^2 \theta}{M} \pm \frac{1}{2\left[\left(\frac{k_1 + 2k_2}{2m} + \frac{k_1 \cos^2 \theta + 2k_2 \sin^2 \theta}{M} \right)^2 - 2k_1 k_2 \frac{2m + M}{m^2 M} \right]^{1/2}} \cdot \left[- \left(\frac{k_1 + 2k_2}{m} \right) \left(\frac{k_1 \cos^2 \theta + 2k_2 \sin^2 \theta}{M} \right) - 2 \left(\frac{k_1 \cos^2 \theta + 2k_2 \sin^2 \theta}{M} \right)^2 + \frac{4 k_1 k_2}{mM} \right] \right\} \tag{8}$$

We have calculated the one possible set of normal coordinates for the normal state and the two possible sets of coordinates for the excited state. The results are shown in Fig. 2.[8] Since the calculations for the excited state make

[8] The normal coordinates for these modes of vibration in terms of Cartesian coordinates with origin at the center of mass and x-axis parallel to the line joining the like atoms in the equilibrium position, are

$$q_1 = 2(x_1 + x_2) + y_1 - y_2$$
$$q_2 = B(x_1 - x_2) - 2(y_1 + y_2)$$
$$q_3 = A(x_1 - x_2) + 2(y_1 + y_2)$$

use of the small and inaccurate isotope effects, the shape, normal coordinates and force constants for this state are very approximate. These quantities in the case of the normal state should be much more reliable. Of course, the assumption of valency forces may be only approximate.

Intensities and the Application of the Franck-Condon Principle

Intensities have not been given in the tables for we have been unable to get consistent relative intensities for the bands by comparing spectra with different times of exposure and different pressures of ClO_2 gas in the absorption cell. We can see no evidence of irregularities in intensities of the bands in any progression and therefore we have constructed curves giving the approximate intensity distributions for the four most intense progressions as shown in Fig. 3 in the following way. The strongest bands are found to be suitable for measurement when the partial pressure of ClO_2 in the cell is about 0.2 mm. This was secured by cooling the trap containing the ClO_2 in

---

where x_1, x_2, y_1 and y_2 are the displacements of the like atoms from the equilibrium position and A and B are constants. The conservation of momentum and angular momentum (both taken equal to zero) give the relations

$$y_2 = y_1 + \cot\theta(x_1 + x_2),\quad x_3 = -\frac{m}{M}(x_1 + x_2) \text{ and } y_3 = -\frac{m}{M}(y_1 + y_2),$$

x_3 and y_3 being the displacements of the unlike atom from the equilibrium position. From these equations it is a simple matter to secure the values of the Cartesian coordinates of each atom for each mode of vibration.

The values of A and B were secured by making the transformation of coordinates from the x, y, $\cdots$ etc. to q_1, q_2, q_3 and expressing the potential and kinetic energies in these coordinates. The determinental equation for the frequencies is diagonal then, if,

$$AB = \frac{4M}{M + 2m} \equiv \frac{4}{\mu}$$

and

$$A - B = -\frac{M}{M + 2m}\,\frac{2k_1\tan\theta + 4k_2\cot\theta}{k_1 - 2k_2} + \frac{2k_1\cot\theta + 4k_2\tan\theta}{k_1 - 2k_2}.$$

Setting the quantity on the right equal to X and solving for A and B,

$$A = \frac{X}{2} + \left[\frac{X^2}{4} + \frac{4}{\mu}\right]^{1/2}$$

$$B = -\frac{X}{2} + \left[\frac{X^2}{4} + \frac{4}{\mu}\right]^{1/2}.$$

(Other values for A and B are secured by using the minus sign before the radical, but this gives nothing new for q_2 only becomes q_3 and q_3 becomes q_2.) The frequencies associated with the coordinates q_2 and q_3 are then,

$$\nu_2 = \frac{1}{2\pi}\left[\frac{\frac{1}{2}k_1(\sin\theta - \frac{1}{2}\cos\theta\mu B)^2 + k_2(\cos\theta + \frac{1}{2}\sin\theta\mu B)^2}{\frac{1}{2}m + \frac{1}{8}B^2m/\mu}\right]^{1/2}$$

and

$$\nu_3 = \frac{1}{2\pi}\left[\frac{\frac{1}{2}k_1(\sin\theta + \frac{1}{2}\cos\theta\mu A)^2 + k_2(\cos\theta - \frac{1}{2}\sin\theta\mu A)^2}{\frac{1}{2}m + \frac{1}{8}B^2m/\mu}\right]^{1/2}.$$

These expressions are equivalent to those given above except that either ν_2 or ν_3 may be the greater of the two depending on the values of the constants k_1, k_2 and θ.

dry ice so that the vapor pressure of ClO_2 was about 2 mm[9] and passing 1/10 of a stream of air through the trap and cell and the remainder past the trap and through the cell, the gas stream being divided by using capillary tubes of different lengths. The weakest bands were photographed with the trap containing the ClO_2 at about 5°C at which temperature the vapor pressure of ClO_2 is about 600 mm. Thus the ratio of most intense to least intense bands is considerably more than 3000 probably, for the strongest bands were yet easily measureable and the weakest difficult to observe. From our plates we can determine the most intense bands of each progression and also the bands

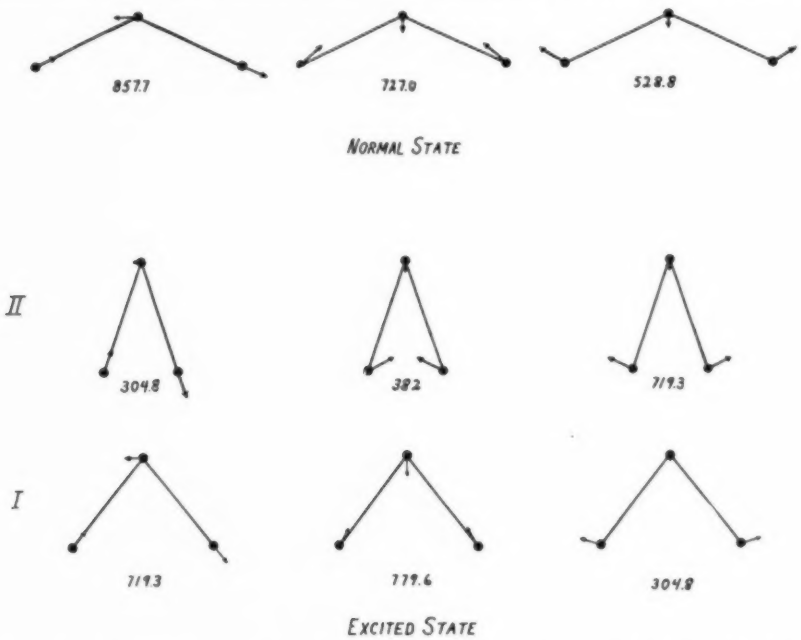

Fig. 2. Normal coordinates of the ClO_2 molecule. The acute angles between the direction of vibration of the oxygen atoms and a horizontal line are:
Normal state: $\tilde{\nu}_1=857.7$, $\alpha=24°50'$; $\nu_2=727.0$, $\alpha=41°39'$; $\nu_3=528.8$, $\alpha=30°25'$;
Excited state: Configuration I; $\tilde{\nu}_1=719.3$, $\alpha=51°32'$; $\tilde{\nu}_2=779.6$, $\alpha=60°23'$; $\tilde{\ }_3=304.8$, $\alpha=16°33'$.
Configuration II; $\tilde{\nu}_1=304.8$, $\alpha=71°13'$; $\tilde{\nu}_2=719.3$, $\alpha=22°30'$; $\tilde{\nu}_3=382$, $\alpha=51°34'$.

at which two progressions have the same intensity. We have determined the bands of greatest intensity from plates taken with a hydrogen discharge tube as source since it gives a more uniform intensity in this region. No correction has been attempted for the changing dispersion of the instrument, which, of course, changes the blackening on the plate at different wave-lengths even if the intensity of the source were uniform.

[9] This was determined by passing a slow stream of N_2 gas through the trap, catching the ClO_2 with liquid air, measuring the volume of gas passed through and determining the amount of ClO_2 vaporized by the method described by Bray (W. Bray, Zeits. f. physik. Chemie **54,** 569 (1906)).

The most intense band of the system is in the progression $(0, v_2')\leftarrow(0, 0, 0)$ and has been assigned the intensity 3000, while the first observed band of each progression has been given the intensity 1. The most intense band of the $(0, v_2')\leftarrow(0, 0, 1)$ progression has been assigned an intensity of 300. This appears to be about right and would be the intensity, if the Boltzmann factor, $e^{-h\nu/kT}$, giving the relative abundance of molecules in the two normal levels were the only factor determining the relative intensities. The maximum intensity of the strongest band of the $(1, v_2')\leftarrow(0, 0, 0)$ comes at $v_2' = 11$ which has the same intensity as the $v_2' = 6$ band of the $(0, v_2')\leftarrow(0, 0, 0)$ progression. The maximum of the $(1, v_2')\leftarrow(0, 0, 1)$ progression is taken as 1/10 that of the $(1, v_2')\leftarrow(0, 0, 0)$ progression agreeing again with the Boltzmann factor

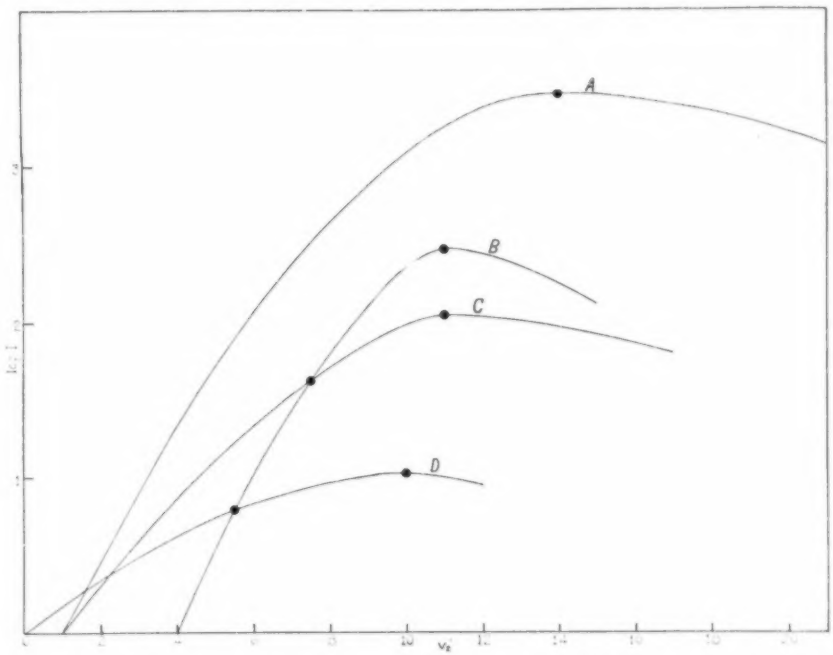

Fig. 3. Log I plotted against v_2'. A. Progression $(0, v_2')\leftarrow(0, 0, 0)$; B. Progression $(0, v_2')\leftarrow(0, 0, 1)$; C. Progression $(1, v_2')\leftarrow(0, 0, 0)$; D. Progression $(1, v_2')\leftarrow(0, 0, 1)$.

as mentioned above. The intersections marked by the dots have been determined by comparing the intensities of the bands of the two progressions. The The curves are terminated at the last observed band. The intensities are probably not small in this region but observation of the bands is difficult because of the diffuseness due to predissociation. The figure is somewhat more than a qualitative representation of the intensities, and does represent the general trend of intensities in the bands.

Large changes in the vibrational quantum number associated with the 719.34 cm^{-1} vibration have been observed and only small changes in that associated with the 304.8 cm^{-1} vibration while the third frequency has not been observed. The most intense bands of the $(0, v_2')\leftarrow(0, 0, 0)$ and $(1, v_2')\leftarrow(0, 0, 0)$ progressions are those to the levels with $v_2' = 14$ and 11. (This is using the

final assignment of quantum numbers which has been done throughout this paper.) The Franck-Condon[10] principle should be applicable to polyatomic molecular spectra and enables us to make a choice between the two possible assignment of frequencies to the normal modes of vibrations of the excited state.

We consider the configuration I of Table VIII and Fig. 2 first. In the electronic transition from the normal state to the excited state, we assume with Condon that the dimensions of the molecule do not change. (The velocities are small in the normal state and thus need not be considered.) Superimposing the normal molecule (Fig. 2) on the excited molecule assuming configuration I, we see that the molecule should vibrate strongly with frequency 304.8 cm^{-1} thus leading us to expect large changes in the associated vibrational quantum number, in contradiction to observation. A large change in the equilibrium distance between Cl and O should cause large changes in the quantum number associated with the calculated 779.6 cm^{-1} frequency. Failure to observe this would be consistent with no change in this distance. The large change in the angle at the apex should not cause a large amplitude of oscillation of the 719.34 cm^{-1} frequency and thus small changes in the quantum number associated with this frequency should be observed again in contradiction to observation. Thus configuration I for the excited state appears to be impossible.

The configuration II for the excited state is consistent with the intensity distribution. Superposition of the normal molecule on this configuration II, shows that the frequency 719.34 should be strongly excited in agreement with observation. The frequency 382.1 (calc.) should be strongly excited if the equilibrium distance Cl-O changed markedly. That it is not observed indicates that this distance is not changed. The asymmetric vibration 304.8^{-1} should not be strongly excited again in agreement with observation. This qualitative agreement enables us to decide between configurations I and II and is, we believe, the first application of the Franck-Condon principle to polyatomic molecular spectra.

The Assignment of Quantum Numbers

Thus far we have anticipated our final assignment of quantum numbers and we shall justify it at this point. The calculated structure of ClO_2 in the normal state requires that $\tilde{\nu}_1 = 857.7$ cm^{-1}, $\tilde{\nu}_2 = 727.0$ cm^{-1} and $\tilde{\nu} = 528.8^{-1}$. From these calculations the assignment of quantum numbers in the normal state is $v_1'' = 1$ for the 857.7 cm^{-1} level, $v_2'' = 1$ for the 727.0 cm^{-1} level and $v_3'' = 1$ for the 528.8 cm^{-1} level. Since the 1471.3 cm^{-1} level is assumed to be a harmonic of the 727.0 cm^{-1} level it is designated by $v_2'' = 2$. Thus the assignment of quantum numbers in the normal state becomes

Level	v_1'', v_2'', v_3''
0. cm^{-1}	0, 0, 0
528.8 cm^{-1}	0, 0, 1

[10] J. Franck, Trans. Faraday Soc. **21,** Part 3 (1925); E. U. Condon, Phys. Rev. **28,** 1182 (1926).

727.0 cm^{-1}	0,	1, 0
857.7 cm^{-1}	1,	0, 0
1471.3 cm^{-1}	0,	2, 0.

For the reasons given above v_1' is the quantum number associated with the 304.8 cm^{-1} frequency, v_2' with the 719.3 cm^{-1} frequency and v_3' with the calculated 382.1 cm^{-1} frequency. No transitions have been observed in which the 382.1 cm^{-1} frequency is involved and therefore we assume that v_3' is zero for all observed bands. We believe that the most intense progression has for its higher levels a set with $v_1'=0$ because we have been unable to find any evidence for levels with a smaller value of v_1', though we have found levels with v_1' one and two units larger.

In Eq. (4) we give the relation between the constants c' and a'' required by our experimental data. Our calculated values of c' and a'' taken from Table VII are -3.93 and -10.32 which make $c/2'-a/2''=+3.19$ instead of 7.23 required by our data, a difference of about 4 cm^{-1}. This may be partially accounted for on the assumption that the $\Delta\tilde{\nu}''$ of Eq. (2) may be too large as pointed out above. The isotope effects of the $\tilde{\nu}_1'$ and $\tilde{\nu}_2'$ frequencies have been estimated from the energy levels having large values of v_2'. Thus, we have calculated the configuration and frequencies of vibration and their isotope effects by using two frequencies for infinitesimal amplitudes of vibration and two isotope effects for large amplitudes of vibration. Thus even if the model were exact, some discrepancy between calculated and observed might be expected.

The difference between the calculated and observed values of $c/2'-a/2''$ could be eliminated by assuming that all bands having $v_2'=0$, as we have assigned the quantum numbers, do not belong to this band system and that the bands having $v_2'=1$ (our numbering) should be numbered as $v_2'=0$. However, we see no experimental reason for doing this and believe that the reason for the discrepancy lies in the approximate character of our calculations.

The Dissociation of the Molecule and Predissociation

From our assignment of frequencies to the normal modes of vibration, it is evident that the unsymmetric vibration of the excited state with $\tilde{\nu}_1'=$ 304.8 cm^{-1}, if the amplitude is large, will lead to dissociation into the ClO molecule and the O atom, either or both with energy of excitation. The formula (1) permits an extrapolation to dissociation though the value for the dissociation energy will probably be very approximate. This extrapolation gives 28968 cm^{-1} above the normal level of the molecule for this energy.

Goodeve and Stein observed predissociation from λ3293A, toward the ultraviolet. Our own plates indicate that the limit is about λ3595A, while Finkelnburg and Schumacher using highest dispersion have observed this limit as λ3753A. We believe their observation to be most reliable because of their higher resolving power.[11] Interpreting this in terms of our energy level

[11] Dr. G. M. Murphy working in our laboratories has attempted to observe the resonance radiation of ClO_2 excited by the λ3660 lines of mercury with negative results as would be expected on the basis of Finkelnburg and Schumacher's value for the predissociation limit but not on the basis of either of the other values.

diagram we place the predissociation at 27162 cm^{-1} above the lowest level, which is as close to our value of 28968 cm^{-1} for dissociation as can be expected considering the likely errors in this extrapolation. The agreement shows that the predissociation limit *does* correspond to dissociation into ClO and O as has been assumed by the previous observers.

Goodeve and Stein[4] showed that there is a distinct break in the curve when the first differences of the progression $(0, v_2')\leftarrow(0, 0, 0)$ are plotted as ordinates against v_2' as abscissa. This is shown in Fig. 4 where we have plotted

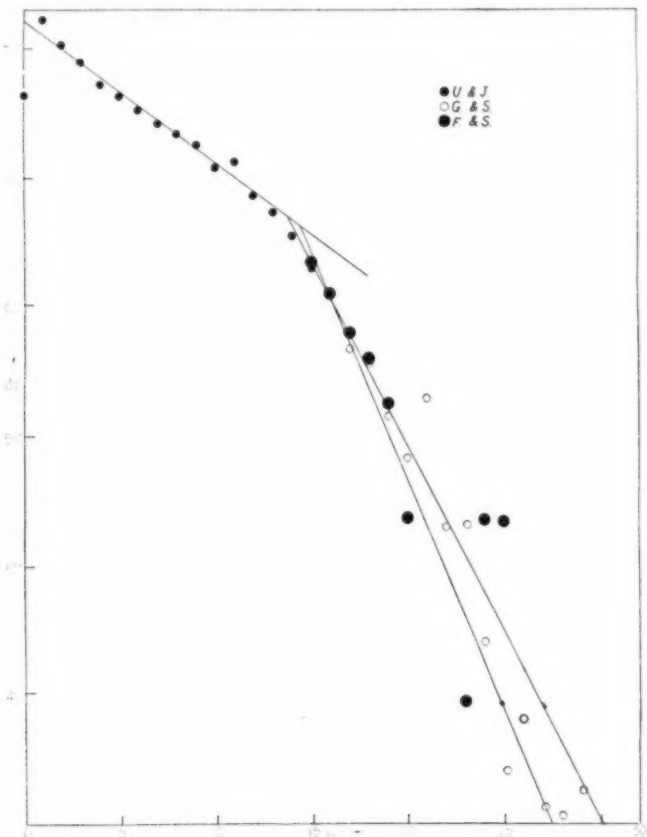

Fig. 4. Values of $E(v_2'+1)-E(v_2')$ plotted against v_2'.

our values up to $(v_2'=15)-(v_2'=14)$ difference and both Goodeve and Stein's and Finkelnburg and Schumacher's from that point on. The discontinuities in these differences is evident and the scattered character of the points from $v_2'=15$ on shows that any formula fitting this part of the energy level diagram would be very doubtful and that any extrapolation to $\Delta E=0$ would be doubtful using either set of data in this region of large values of v_2'. The extrapolated value of v_2' at dissociation might lie anywhere between about $v_2'=59.11$ and $v_2'=67.98$ and the energy of dissociation, assuming a straight line for the $\Delta E:v_2'$ curve from $v_2'=15$ on and these two values of v_2', should lie be-

tween 48268.3 cm^{-1} and 51300.7 cm^{-1}. These wave numbers correspond to 137.1 and 145.7 cal. per mol., respectively. The scattered nature of the points, see Fig. 4, and the very doubtful extrapolation makes us feel that any energy of dissociation derived from such data and calculations is very doubtful except between very wide limits, perhaps even wider than those assumed in the above calculations.

Fig. 5 shows a plot of $\Delta E:v_2'$ in the region of small values of v_2' on a larger scale and including the points of all three sets of data. The straight line drawn

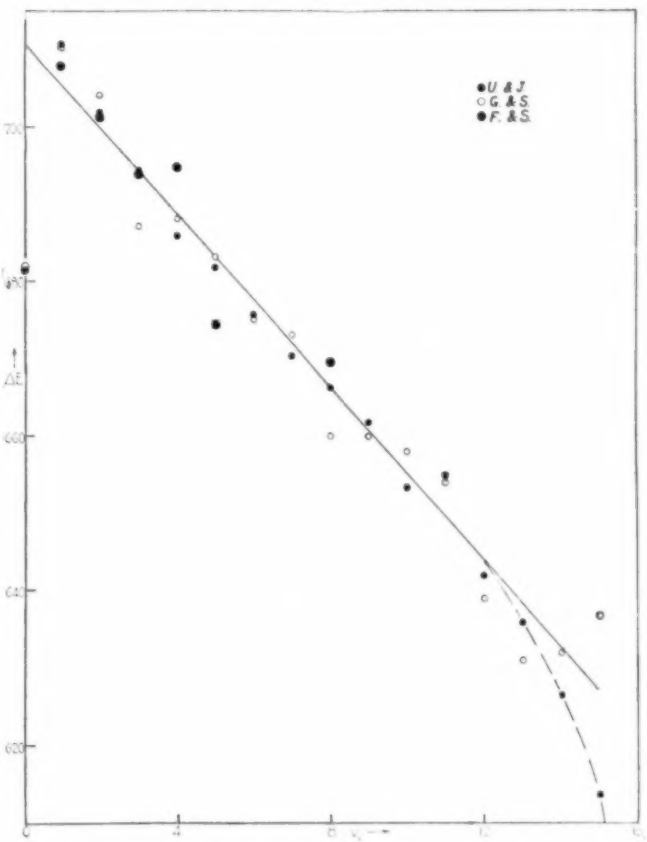

Fig. 5. Values of $E(v_2'+1)-E(v_2')$ plotted against v_2'.

through the data is that required by Eq. (1). It will be seen that our values follow a smoother curve than either of the other sets of data. Finkelnburg and Schumacher claim a higher precision for their work than we do and thus the greater irregularities which their data show may be real. Our values indicate that this curve is not a straight line but the precision of the data does not warrant a definite conclusion.

The broken curve at the lower end of the figure shows the marked way in which the break in the curve occurs. The break in the curve at the left is very similar to the discontinuities in the SO_2, $\Delta E:v'$ curve as observed by Watson

and Parker.[12] The curve with positive slope in the case of SO_2 extended over 3 or 4 differences whereas in ClO_2 it is apparent for only one difference, and therefore the discontinuity in this case may not be real.

The Character of the High Amplitude Vibrations

The half angle at the apex of the isoceles triangle in the excited state is nearly a normal coordinate of the molecule as can be seen from Fig. 2. The application of the Franck-Condon principle for the intensity distribution indicates that the oscillation using the classical model for the most intense band of any progression having the v_2' levels as higher levels, is between $\theta = 65°$, its value for the normal state, and something less than 18.5°. This most intense band appears to be that with $v_2' = 12$ approximately. It should not require much more energy in this mode of vibration to make the molecule oscillate between $\theta = 90°$ and some small angle. Such an oscillation would be an oscillation through the straight line position and would be similar to that of a straight line molecule.

The discontinuity in the plot ΔE against v_2 discovered by Goodeve and Stein and discussed above appears at $v_2' = 15$, just a few levels above the value of v_2' for the most intense band. Therefore it seems that the discontinuity in the $\Delta E : v_2'$ curve at $v_2' = 15$ may occur when the molecule first acquires sufficient energy to vibrate through the straight line position.

We wish to thank the Physics department and particularly Professor H. W. Webb for the privilege of using the Hilger E−1 instrument and the comparator in this work.

[12] W. W. Watson and A. E. Parker, Phys. Rev. **37**, 1484 (1931).

ROTATIONAL STRUCTURE OF THE RED BANDS OF POTASSIUM

By F. W. Loomis[1]
The Alfred Loomis Laboratory, Tuxedo Park, New York

(Received November 6, 1931)

Abstract

A rotational analysis has been made of four bands of the red system of K_2 which had been photographed under high dispersion. The principal molecular constants of the ground state ($^1\Sigma_g^+$) and of the upper state ($^1\Pi_u$) are as follows:

$B_0''=0.05611$	$r_e''=3.91\times10^{-8}$	$\alpha''=0.000219$
$B_0'=0.04812$	$r_e'=4.22\times10^{-8}$	$\alpha'=0.000235$

The magnitude of the Λ type doublings of the $^1\Pi$ state agrees with Van Vleck's formula for it. The relationships between the molecular constants show that all rotational levels, with both even and odd values of J, are present. Alternating intensities are observed, the lines with odd J'' being stronger. It is concluded that the nuclear spin of K^{39} is definitely not zero, and that the nucleus obeys the Fermi-Dirac statistics.

THE red absorption bands of diatomic potassium were photographed, with the cooperation of Professor R. W. Wood, primarily with the object of determining whether or not the nuclear spin of the principal isotope, K^{39}, was zero, as had been concluded by two independent observers[2,3] of the hyperfine structure of arc and spark lines respectively. We were able to report immediately[4] that an inspection of our plates showed conclusively that this could not be true, for alternating intensities were clearly apparent in the well resolved branches; and moreover the spacing of the lines was such as to preclude the possibility that alternate ones were missing, as they must be if the spin were zero. This latter statement was based on a comparison of the observed spacing with that estimated by extrapolating the known spacings of the corresponding bands of Li_2 and Na_2.

A rotational analysis of four bands of this spectrum has now been completed and thoroughly checked by the combination relations, with the result that our earlier conclusions are verified, independently of the extrapolation from Li_2 and Na_2.

As stated in the joint paper,[4] the spectrum was photographed in absorption in the fourth order of the Tuxedo forty foot spectrograph with a particularly fine seven inch plane grating with 15,000 lines per inch. Sunlight was used as a background and the solar lines as a comparison, their wavelengths being obtained from the revised Rowland's Table.[5]

The red band system of potassium is expected to be, like the green ones of

[1] The University of Illinois.

[2] Schüler and Brück, Zeits. f. Physik **58**, 735 (1929).

[3] Frisch and Kronig, Naturwiss. **19**, 444 (1931).

[4] Loomis and Wood, Phys. Rev. **38**, 854 (1931).

[5] Revision of Rowland's Preliminary Table of Solar Wave-lengths, St. John, Moore, Ware, Adams and Babcock. Published by Carnegie Inst. of Washington (1928).

lithium and sodium, a $^1\Pi - ^1\Sigma$ transition and this is confirmed by the analysis, since each band is found to consist of one P, one Q and one R branch.

The analysis was carried out in much the same way as that[6] of the green bands of Na_2. The lines belonging to the branches were found, where possible, by picking out series of regularly spaced lines by inspection and the assignments were checked and completed by the construction of graphs similar to Figs. 2 of the paper on sodium.[6] In this way three series were found in each band, though there were some regions where two or even three series coalesced. The Q branches could be identified by inspection because of their greater intensity. The P and R branches were identified and triples of lines with common values of J'' were picked out from them and the Q branches by application of the PQR combination relation

$$R(J'') - Q(J'') \cong Q(J''+1) - P(J''+1). \qquad (1)$$

It is true, of course, that this relation is theoretically not exact, since there is Λ type doubling in the upper state and hence the initial levels for the Q lines differ from those of the P and R lines and there is a "combination defect". In the case of potassium, however, this combination defect is so small that it is barely detectable and the PQR combination relation is quite sufficient for the identification of the lines in the three branches which have common J''.

The measured frequencies of the lines of the (1, 0) (1, 1) (0, 1) and (0, 2) bands, with the quantum numbers assigned to them, as described below, are given in Table I.

TABLE I. *Measured frequencies of band lines.*

(1, 0) band				(1, 1) band		
P	Q	R	J''	P	Q	R
	15438.82		21	15345.08		
	38.45		22	44.63		
	38.08		23	44.14		
15435.34	—		24	43.69		
34.88	37.27		25	43.20		
34.35	36.83		26	42.66		
33.80	36.38		27	42.14		
33.25	35.94		28	41.61		
32.68	35.44		29	—		
32.12	34.95		30	40.47		
31.48	34.45	15437.39	31	39.91		
30.89	33.92	37.09	32	39.28		
30.24	33.39	36.63	33	38.67	15341.84	15345.08
29.59	32.82	36.17	34	38.00	—	44.63
28.90	32.25	35.71	35	37.37	40.75	44.14
28.23	31.66	35.22	36	36.70	40.14	43.69
27.50	31.05	34.68	37	36.00	39.57	43.20
26.80	30.43	34.13	38	—	38.96	42.66
26.07	29.78	33.61	39	34.63	38.34	42.14
25.32	29.14	33.05	40	33.86	37.71	41.61
24.58	28.45	32.46	41	33.13	—	—
23.77	—	31.86	42	—	36.36	40.47
22.97	27.04	31.26	43	31.60	35.69	39.91
22.17	26.34	30.70	44	30.82	34.98	39.28
21.32	25.60	30.00	45	30.00	34.26	38.67

[6] Loomis and Wood, Phys. Rev. **32**, 223 (1928).

TABLE I. (*Continued*).

(1, 0) band				(1, 1) band		
P	*Q*	*R*	*J''*	*P*	*Q*	*R*
15420.43	15424.85	15429.36	46	15329.16	15333.54	15338.00
19.60	24.09	28.65	47	28.33	32.80	37.37
18.62	23.30	27.97	48	27.49	32.04	36.70
17.83	22.47	27.23	49	26.60	31.24	36.00
16.90	21.67	26.51	50	25.72	30.45	35.27
15.98	20.80	25.76	51	24.80	29.62	34.55
14.97	19.96	25.04	52	—	28.78	33.86
14.07	19.09	24.23	53	22.94	27.94	33.08
13.09	18.22	23.45	54	22.02	27.10	32.33
12.08	17.29	22.64	55	21.03	26.21	31.49
11.09	16.38	21.82	56	20.08	25.34	30.73
10.06	15.44	20.98	57	19.04	—	29.90
09.01	14.48	20.11	58	18.05	23.48	29.08
07.99	13.52	19.24	59	16.95	22.55	28.23
06.91	12.56	18.35	60	15.94	21.59	27.35
05.80	11.53	17.41	61	14.86	20.60	26.50
04.65	10.53	16.49	62	13.75	—	25.60
03.58	09.51	15.55	63	12.68	18.64	24.67
02.39	08.47	14.59	64	11.57	17.62	23.75
01.21	07.42	13.60	65	10.44	16.57	22.82
00.11	06.32	12.56	66	09.30	15.51	21.81
15398.92	05.22	11.63	67	08.14	14.45	20.88
97.70	04.12	10.62	68	07.01	13.37	—
96.49	02.97	09.51	69	05.80	12.28	18.86
—	01.82	08.47	70	04.57	11.18	17.82
94.00	00.66	07.42	71	03.36	10.03	16.81
92.74	15399.46	06.32	72	—	08.86	15.76
91.44	98.28	05.22	73	00.88	07.71	14.66
—	97.06	04.12	74	15299.60	06.54	13.60
88.82	95.86	02.97	75	98.31	05.34	12.47
—	94.60	01.82	76	96.98	—	11.36
86.14	93.33	00.66	77	95.72	02.92	10.22
84.77	—	15399.46	78	94.37	01.67	09.07
83.40	90.76	98.28	79	93.04	—	07.91
81.99	89.47	97.06	80	91.64	15299.14	06.79
80.58	88.15	95.86	81	90.28	97.86	05.54
79.15	86.82	94.60	82	88.87	96.55	—
77.68	85.45	93.33	83	87.50	95.22	03.07
76.25	84.09	—	84	86.06	—	01.82
74.75	82.71	90.76	85	84.62	92.52	—
73.25	—	89.41	86	83.17	91.15	15299.31
71.74	—	88.10	87	81 68	89.78	—
—	78.42	86.76	88	80.18	88.40	96.71
68.68	—	85.39	89	78.70	86.98	95.37
67.12	75.47	83.98	90	—	85.54	—
—	73.99	82.55	91	75.59	84.09	—
63.95	72.50	—	92	74.07	82.63	91.29
62.31	70.95	79.72	93		81.12	89.90
60.71	69.43	78.20	94		79.64	88.48
59.05	67.86	76.83	95		78.15	87.06
57.40	—	75.34	96		76.64	—
55.70	64.69	73.85	97		75.09	84.17
54.02	—	72.29	98		73.54	82.71
52.32	—	70.74	99			81.24
50.58		69.23	100			
48.86	58.19	67.63	101			
47.12	56.54	66.28	102			
	54.84	64.49	103			
	53.14	62.85	104			
	51.42	61.24	105			
	49.69	—	106			
		57.94	107			

TABLE I. (*Continued*).

(1, 0) band				(1, 1) band		
P	*Q*	*R*	*J''*	*P*	*Q*	*R*
		15356.22	108			
		54.56	109			
		52.86	110			
			10		15184.77	
			11		84.60	
			12		84.42	
			13		84.17	
			14		83.98	
			15		83.75	
			16		83.51	
			17		83.23	
			18		82.94	
			19		82.71	
			20		82.39	
			21	15180.08	82.07	
			22	79.66	81.75	
	15272.34		23	79.18	81.42	
	71.97		24	78.78	81.02	
	—		25	78.28	80.69	
	71.18		26	77.82	80.33	
15268.17	70.75		27	77.28	79.88	15182.59
67.64	70.32		28	76.76	79.48	—
67.09	69.86		29	76.23	79.01	81.91
—	69.38		30	75.72	78.58	81.53
65.95	68.91		31	75.14	78.10	81.15
65.35	68.43		32	74.57	77.61	80.69
64.76	67.91		33	73.93	77.12	80.33
64.14	67.39		34	73.36	76.61	79.88
63.51	66.86		35	72.74	76.07	79.48
62.84	66.28		36	—	75.52	79.01
62.18	65.71		37	71.45	74.97	78.58
61.50	65.13		38	—	74.39	78.10
60.79	64.52		39	—	73.79	77.61
60.06	63.88		40	—	73.19	77.12
59.34	63.27		41	68.63	72.58	76.61
58.58	62.62		42	67.89	71.98	76.07
57.84	61.94		43	67.16	71.28	75.52
57.07	61.27	15265.49	44	66.35	70.61	74.97
56.27	60.54	64.97	45	65.63	69.95	74.39
55.47	59.84	64.34	46	64.86	69.26	73.79
54.64	59.12	63.71	47	64.05	68.63	73.19
53.80	58.39	63.07	48	63.23	67.89	72.58
52.97	57.63	62.39	49	62.40	67.16	71.98
52.09	—	61.71	50	61.54	66.35	71.28
51.20	56.05	61.01	51	60.73	65.63	70.61
50.29	55.24	60.34	52	59.84	64.86	69.95
49.36	54.43	59.59	53	58.96	64.05	69.26
48.48	53.60	58.81	54	58.05	63.23	68.43
47.52	52.75	58.10	55	57.14	62.40	67.72
46.55	51.86	57.33	56	56.20	61.54	66.88
45.59	50.99	56.53	57	55.27	60.73	66.20
44.62	50.11	55.71	58	54.30	59.84	65.46
43.60	49.19	54.92	59	53.32	58.96	64.67
42.57	48.26	54.06	60	52.32	58.05	63.81
41.53	47.32	53.20	61	51.30	57.14	63.04
40.47	—	52.35	62	50.30	56.20	62.18
39.43	45.38	51.46	63	49.27	55.27	—
38.32	44.37	50.57	64	48.20	54.30	60.42
37.20	43.40	49.65	65	47.13	53.32	59.54
36.10	42.36	48.76	66	46.07	52.32	58.68
35.01	41.33	47.74	67	44.97	51.30	57.76
—	40.26	46.82	68	43.86	50.30	56.82

TABLE I. (*Continued*).

(0, 1) band				(0, 2) band		
P	*Q*	*R*	*J''*	*P*	*Q*	*R*
—	15239.23	15245.84	69	15142.72	15149.27	15155.87
15231.50	38.16	44.86	70	41.59	48.20	54.92
30.33	37.01	43.84	71	40.43	47.13	53.95
29.12	35.92	42.81	72	39.26	46.07	52.98
27.92	34.80	41.80	73	38.08	44.97	51.96
26.72	—	40.74	74	36.88	43.86	50.94
25.47	—	39.67	75	35.66	42.72	49.89
24.16	31.32	38.57	76	34.44	41.59	48.90
22.89	30.14	37.53	77	33.21	40.43	47.82
21.60	28.94	36.37	78	31.94	39.26	46.73
20.32	27.72	35.26	79	30.67	38.08	45.63
18.95	26.47	—	80	29.40	36.88	44.51
17.65	25.27	—	81	28.10	35.66	43.40
16.26	23.97	—	82	26.76	34.44	42.26
14.92	22.69	30.61	83	25.44	33.21	41.11
13.51	21.41	29.43	84	24.11	31.94	39.91
12.15	20.08	28.17	85	22.73	30.67	38.78
10.72	18.76	26.96	86	21.37	29.40	37.58
09.30	17.45	25.68	87	19.97	28.10	36.35
07.83	16.07	24.40	88	18.56	26.76	35.09
06.39	14.70	23.13	89	17.14	25.44	33.88
04.92	13.33	21.84	90	15.71	24.11	32.65
03.43	11.92	20.55	91	14.25	22.73	31.38
01.94	10.51	19.21	92	12.79	21.37	30.07
00.42	09.08	17.87	93	11.32	19.97	28.75
15198.88	07.64	16.52	94	09.82	18.56	27.45
97.34	06.16	15.15	95	08.30	17.14	26.15
95.78	—	13.74	96	06.79	15.71	24.76
—	03.16	12.33	97	05.25	14.25	23.42
92.53	01.70	10.87	98	03.72	12.79	22.06
91.04	00.20	09.50	99	02.12	11.32	20.66
89.40	15198.61	08.02	100	00.55	09.82	19.24
87.77	97.10	06.59	101	15098.96	08.30	17.84
	95.53	05.14	102	97.33	06.79	16.41
	—	03.62	103			
	—	02.08	104			
	90.72	00.56	105			
	89.06	15199.04	106			
	87.44	97.47	107			
		95.88	108			
		94.32	109			
		92.69	110			
		91.04	111			
		89.40	112			
		87.77	113			

After the lines of the branches had been sorted out, the Δ_2F's were obtained and used to determine the absolute values of the quantum numbers and the magnitude of the constants B' and B'' according to the equations:

$$\Delta_2F'(J') = R(J'') - P(J'') = 4B'(J' + \tfrac{1}{2}) + 8D'(J' + \tfrac{1}{2})^3 \quad (2)$$

$$\Delta_2F''(J'') = R(J'' - 1) - P(J'' + 1) = 4B''(J'' + \tfrac{1}{2}) + 8D''(J'' + \tfrac{1}{2})^3 \quad (3)$$

The higher power terms, $12F(J+\frac{1}{2})^5$ etc., have been omitted from these equations because calculation shows them to be negligible in the case of potassium. The calculation of the B's was made by successive approximations and least squares, the D's being determined by the equations

$$D_v = D_e + \beta(v + \tfrac{1}{2}) \quad (4)$$

$$D_e = \frac{-4B_e^3}{\omega_e^2} \tag{5}$$

$$\beta = \frac{\alpha^2}{6\omega_e} + \frac{20\alpha B_e^2 - 32x_e B_e^3}{\omega_e^2}. \tag{6}$$

The values of ω_e and x_e in Eqs. (5) and (6) were taken from a paper by Crane and Christy[7] which gives the vibrational constants of the red system of K_2 as follows:

$$\begin{aligned}\nu &= \nu_0 + \omega_e'(v' + \tfrac{1}{2}) - \omega_e' x_e'(v' + \tfrac{1}{2})^2 - \omega_e''(v'' + \tfrac{1}{2}) + \omega_e'' x_e''(v'' + \tfrac{1}{2})^2 \\ &= 15377.73 + 74.73(v' + \tfrac{1}{2}) - 0.327(v' + \tfrac{1}{2})^2 - 92.64(v'' + \tfrac{1}{2}) \\ &\quad + 0.354(v'' + \tfrac{1}{2})^2\end{aligned} \tag{7}$$

The constants α' and α'' of the equation

$$B_v = B_e - \alpha(v + \tfrac{1}{2}) \tag{8}$$

were calculated, after the true J's had been assigned as just described, but before the final adjustment of the B's was made, from the variation of the differences of the Q lines of different bands, according to the equations

$$Q(1, 0) - Q(1, 1) = Q_0(1, 0) - Q_0(1, 1) - \alpha''(J + \tfrac{1}{2})^2 + \beta''(J + \tfrac{1}{2})^4 \tag{9}$$

$$Q(1, 1) - Q(0, 1) = Q_0(1, 1) - Q_0(1, 0) - \alpha'(J + \tfrac{1}{2})^2 + \beta'(J + \tfrac{1}{2})^4 \tag{10}$$

Finally, the combination defects in the (1, 0), (1, 1) and (0, 1) bands were expressed by the theoretical relations

$$\begin{aligned}R(J'') - Q(J'') - Q(J'' + 1) + P(J'' + 1) &= (B_{PR}' - B_Q')((J'' + 3/2)^2 + (J'' + \tfrac{1}{2})^2) \\ &\cong 2(B_{PR}' - B_Q')(J + 1)^2\end{aligned} \tag{11}$$

and the coefficient $(B'_{PR} - B'_Q)$ determined by least squares to be 2.02×10^{-6}. This is in adequate agreement with the theoretical expression for this quantity.

$$B_{PR}' - B_Q' = 4B^2/\nu(^1\Pi_u\,^1\Sigma_u^+) = 2.52 \times 10^{-6} \tag{12}$$

which has been found by Mulliken and Christy[8] to hold well for the corresponding $^1\Pi$ states of the similar molecules H_2, Li_2 and Na_2. The combination

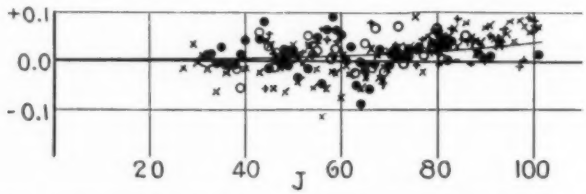

Fig. 1. *PQR* combination defect. Full circles, hollow circles, ×'s and +'s represent data from bands (1, 0), (1, 1), (0, 1) and (0,2) respectively.

defects of Eq. (11) are plotted in Fig. 1. The curve represents the function $4.04 \times 10^{-6}(J+1)^2$.

[7] Crane and Christy, Phys. Rev. **36,** 421 (1930).

[8] Mulliken and Christy, Phys. Rev. **38,** 87 (1931).

The rotational constants as above determined are summarized in Table II.

TABLE II. *Rotational constants of K_2^{39} molecule.*

	Ground state ($^1\Sigma_g^+$)				Upper state ($^1\Pi_u$)		
v	equil.	0	1	2	equil.	0	1
B	0.05622	0.05611	0.05589	0.05567	0.04824	0.04812	0.04788
$D\times10^8$	−8.28	−8.32	−8.41	−8.49	−8.06	−8.09	−8.17
α	0.000219				0.000235		
β	-0.083×10^{-8}				-0.074×10^{-8}		
I_e	492.0×10^{-40}				573.4×10^{-40}		
r_e	3.91×10^{-8}				4.22×10^{-8}		
$B_{PR}-B_Q$					2.0×10^{-6}		

The accuracy with which the values of B and D in Table II represent the Δ_2F's, as well as the precision with which the combination relations hold, is

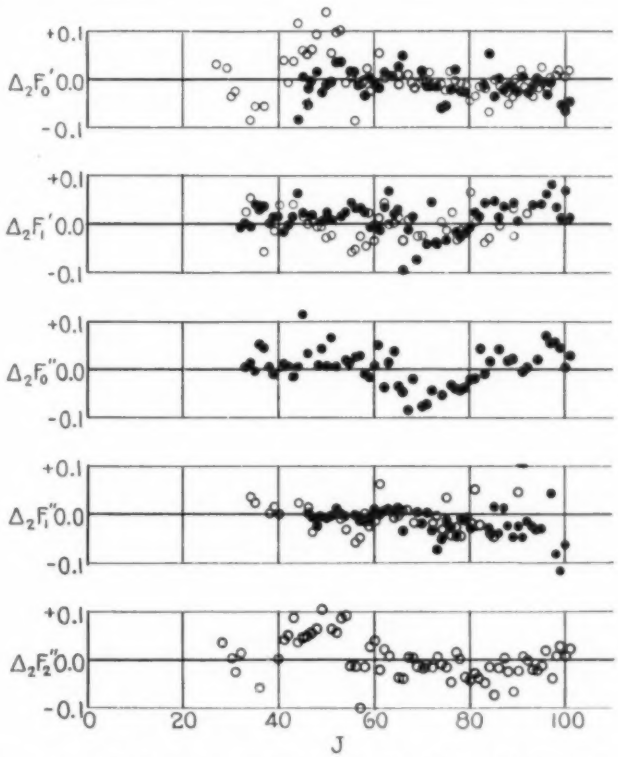

Fig. 2. Residuals of Δ_2F's from those calculated by Eqs. (2) and (3) with constants in Table II. Full circles represent data from bands (0, 1) and (1, 0), hollow circles data from bands (1, 1) and (0, 2).

shown in Fig. 2, wherein the residuals of the observed Δ_2F's from those calculated by Eqs. (2) and (3) are plotted against J. The fact that these representations are within the experimental error of observation (which is far from true of the representations with the quadrupled value of D/B which would have been called for by Eq. (5) had it been assumed that alternate

TABLE III. *Comparison of constants of similar molecules*[9]

	Ground state: $^1\Sigma_g^+$				Upper state: $^1\Pi_u$				Upper state: $^1\Sigma_u^+$			
	H_2	Li_2	Na_2	K_2	H_2	Li_2	Na_2	K_2	H_2	Li_2	Na_2	K_2
F_0	0	0	0	0	99086	20398	20302	15369	90083	14022	15007	11672
B_0	59.19	0.6691	0.1543	0.05611	29.4	0.5532	0.1254	0.04812	19.45	0.495	0.1085	(0.042)
$r_e \times 10^8$	0.74	2.67	3.07	3.91	1.05	2.93	3.41	4.22	1.30	3.11	3.67	(4.5)
α	2.79	0.00744	0.00082	0.000219	1.2	0.00804	0.00094	0.000235	(0.4)	0.005	0.0004	(0.00010)
$-D_0 \times 10^5$	33596	9.952	0.5860	0.0832	18051	9.531	4.076	0.0809	16470	7.7	0.38	(0.063)
ω_e	4371	349.9	159.2	92.64	2446	270.4	125.0	74.73	1354	253.2	115.6	69.09
$\omega_e x_e$	113.5	2.5	0.73	0.354	66.5	3.1	0.84	0.327	16	1.5	0.38	0.153
B_e/ω_e	0.0139	0.00192	0.00097	0.000607	0.0123	.00206	0.00101	0.000646	0.0145	0.00196	0.00094	(0.00061)
$R=2x_eB_e/\alpha$	1.13	1.29	1.73	1.96	1.36	1.59	1.81	1.80	(1.25)	1.2	1.8	(1.9)
D (volts)	4.34	1.14	0.76	0.51	2.25	0.46	0.35	0.22	3.37	1.25	1.01	0.68

[9] The data in Table III have been taken from the following sources: for hydrogen, Hyman, Phys. Rev. **36,** 187 (1930) and Birge, Proc. Nat. Acad. **14,** 12 (1928); for lithium, Harvey and Jenkins, Phys. Rev. **35,** 789 (1930), Wurm, Zeits. f. Physik **58,** 562 (1929) and **59,** 35 (1929), Loomis and Nusbaum, Phys. Rev. **38,** 147 (1931); for sodium, Loomis, Phys. Rev. **31,** 323 (1928), Loomis and Nile Phys. Rev. **32,** 873 (1928), Loomis and Wood, reference 6; for potassium, Crane and Christy, Phys. Rev. **36,** 421 (1930), and as yet unpublished information from Loomis and Nusbaum as to the heats of dissociation for potassium and sodium.

lines of the bands were missing) is additional definite proof that the latter hypothesis is wrong and that the spin of the K^{39} nucleus is not zero. A further and independent proof of this is that the frequencies of the band lines can be represented by the formulae

$$R,\ P(J'') = \nu_0 + B' \pm 2B'(J'' + \tfrac{1}{2}) + (B' - B'')(J'' + \tfrac{1}{2})^2 \pm 4D'(J'' + \tfrac{1}{2})^3 + (D' - D'')(J'' + \tfrac{1}{2})^4 \quad (13)$$

$$Q(J'') = \nu_0 + (B' - B'')(J'' + \tfrac{1}{2})^2 + (D' - D')(J'' + \tfrac{1}{2})^4 \quad (14)$$

in which the constants are those, given in Table II, which were determined from the $\Delta_2 F$'s. Had alternate lines been missing the quadratic coefficients in Eqs. (13) and (14), for instance, would have been twice the difference of the B's determined as above. It has not been thought worthwhile to include graphs showing the agreement between measured and calculated frequencies, but it is within about 0.3 cm^{-1} and systematic deviations could be practically eliminated by adjusting the coefficients, within the limits of error with which they can be determined from the $\Delta_2 F$'s. The result would not, however, be an increase in the precision of our knowledge of these coefficients, but only of certain differences between them which are not particularly significant, so it has not been done.

In Table III a comparison is made between some of the constants of these two states of the K_2 molecule and those of the corresponding states of the similar molecules H_2, Li_2 and Na_2. Data for the upper ($^1\Sigma_u^+$) states have been added for completeness. Since the rotational constants of this state of potassium have not been determined (it would necessitate an analysis of the infrared K_2 system) they have been estimated by extrapolating values for B_e/ω_e and for $R = 2x_e B_e/\alpha$ and by using these to calculate the others. Values based on these extrapolations are given in parentheses. The data in Table III have been compiled from various sources, as indicated in the footnotes. Particularly in the case of hydrogen, difficulties have been encountered owing to contradictions and incompleteness with which the data have been reported, but the data are more than good enough for the purpose of Table III, which is to show the nature of the variations of the various constants along the series of homologous molecules.

The alternation of intensities is most obvious in the 0, 2 band and especially so in the region where for a long interval the lines $Q(M)$ fortuitously coincide closely with $P(M-6)$. It is the lines with odd values of J'' which are stronger, just as has been found to be the case with H_2, Li_2 and Na_2.[10] This signifies that the K^{39} nuclei also obey the Fermi-Dirac statistics. The present observations were made under conditions that do not permit the determination of nuclear spin from the ratio of alternating intensities, but it is hoped to make this determination at a later time.

It is probable that lines due to the molecule $K^{39}K^{41}$ would be sufficiently intense to be found if they were sought for, but as no particular interest attaches to them this has not been done. The lines of the molecule $K^{41}K^{41}$, which would be interesting, are probably too faint to be found.

[10] Urey, Phys. Rev. **38**, 1074 (1931).

HIGH RESOLUTION IN THE INFRARED

By J. D. Hardy*
Physics Laboratory, University of Michigan

(Received November 6, 1931)

Abstract

An instrument is described which is capable of giving an experimental resolving power of ten thousand in the near infrared region. With this instrument several of the infrared lines of helium I have been examined and their components resolved. The exceedingly faint lines of the neon I spectrum lying between 1μ and 2μ have been discovered and their wave-lengths measured.

THE following paper is the result of the work done during the winter of 1930–31 in an attempt to increase the resolution of infrared spectrometers. The work to be done in the near infrared region now consists almost entirely of the examination of fine structures; a work which is constantly demanding higher resolving powers. With the help of the resonance radiometer[1] and a carefully constructed spectrometer it is believed than an instrument has been developed which partially fulfills the requirements of high resolution and of wavelength accuracy. The resonance radiometer has been used only in those cases where the more easily manipulated direct deflection amplifier has proved not sensitive enough.[2]

Resolving power in the infrared has already been carried as high as ten thousand by Ignatief[3] when he resolved the helium line at 1.0830μ. The method he employed to obtain such high resolution was that of using a Fabry and Perot interferometer arrangement. However, the difficulty of interpreting the results and the minuteness of the spectral range of such an instrument render it unsuitable for most purposes. Therefore the work described here was devoted entirely to the grating spectrometer with the hope of increasing its efficiency to that obtained by Ignatief. This would mean that it would be possible to resolve lines as close together as one frequency unit throughout the near infrared range. The two factors tending to increase the sensitivity of the spectrometer which have been most carefully considered in this paper are the optical perfection of the spectrometer and increased bolometric sensitivity. It is recognized that the matter of suitable sources for infrared use is a most important factor, and although some work has been done along that line nothing very definite has been accomplished.

Pfund and later Barnes[4] have described methods for obtaining very sharp

* National Research Fellow.

[1] J. D. Hardy, Rev. Sci. Inst. **1,** 429–448 (1930).

[2] The instrument referred to here is not the "Moll thermo-relay," but is the Pfund grid amplifier which is used to amplify the deflections of galvanometers. See reference 6.

[3] Ignatief, Ann. d. Physik **43,** 1117–1136 (1914).

[4] R. B. Barnes, Phys. Rev. **36,** 296–304 (1930).

lines by using the mirrors of a spectrometer exactly upon their optic axes. Barnes has discussed the futillity of using very narrow slits, in order to increase the resolving power of an instrument, beyond the point where the defects in the optical images formed by the mirrors become noticeable. The test for this lower value of slit width can be easily made by placing the eye behind the exit slit and observing the illumination of the grating as the slits are narrowed. As soon as it becomes evident that further narrowing of the slits results in rather large unilluminated areas in the grating the narrow limit of useful slit widths has been reached. A further narrowing will not only not increase the available detail in the spectrum but will result in a great loss of energy. Several tests were made by the author on spectrometers whose mirrors were used but ten degrees off their optic axes, and when the slits had been narrowed to 0.1 mm only about sixty percent of the grating was illuminated. It was thus evident that where high resolution is desired more carefully constructed optical systems must be employed. Is is obvious that with more perfect optical systems a saving in energy will be had.

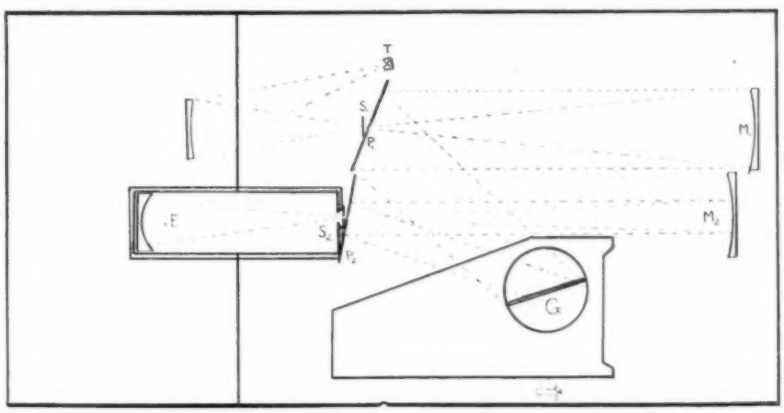

Fig. 1. Diagram of spectrometer.

In accord with this idea a spectrometer was constructed on the plan suggested by Barnes with the difference that the mirrors were of one meter focus and that the last focusing mirror could be replaced by a mirror of four meters focus when high dispersion was desired. A diagram of the spectrometer is shown in Fig. 1. The light from the source T is received by a convex mirror and brought to a focus upon the entrance slit of the spectrometer. (While investigating emission spectra between 1μ and 2μ no fore-prism was used to separate the orders, but an infrared filter was placed in the path when wavelengths longer than 1.2μ were to be examined.) The light on passing through the first slit passes through a hole in the center of the plane mirror P_1. It is then received by the parabolic mirror M_1 and returned directly back to the plane mirror P_1 which reflects the parallel beam onto the grating. The diffracted beam is received by a second plane mirror and sent to the focusing mirror M_2 which focuses the light through a hole in P_2 onto the exit slit. The image thus formed is very sharp and well defined on both sides even when

examined under considerable magnification. The light is finally received by a short focus mirror and brought to a focus upon the thermocouple.

The mirrors M_1 and M_2 are parabolic mirrors with their optic axes through the centers; they are eight inches in diameter and of one meter focus. They were tested and found to be acceptable, although no by and means perfect, as were also the plane mirrors. The last mirror M_2 could be removed and a spherical mirror of four meters focus substituted for it. The reason for substituting such a long focus mirror is simply to spread out the spectrum and allow the use of slightly wider slits, because after the width of the slits has been reduced to a certain point the dust lines, slit imperfections, and diffraction become very important. The introduction of this mirror causes a decrease in energy of six fold, due to the increased size of the image formed; the increase in dispersion is four fold. The grating used in this experiment was a five inch Rowland grating with 15,000 lines to the inch, which gives very sharp lines and a good intensity in the first order. The position of the grating was determined by means of a graduated circle provided with a reading microscope, and any position could be determined with an accuracy of one second of arc, which corresponds to 0.2A.

The thermocouple is of Pfund's design and was constructed by the author. It is exceedingly sensitive and was so constructed that its action in a vacuum is rapid enough to permit its being used with the resonance radiometer without appreciable loss of sensitivity. Direct comparisons, under identical conditions, were made between the thermopiles (three junctions) constructed by Firestone[5] and the single junction element in use in the spectrometer. It was found that in vacuum the single junction thermocouple would give more than three times the deflection produced by the three junction thermopile and its action more than twice as rapid. More recent experiments with thermocouples of this type have lead to the conclusion that an additional increase in sensitivity of five fold can be expected when the elements are used at the temperature of liquid air.

The thermocouple, by a switching arrangement, could be connected to either the resonance radiometer or to a Leeds and Northrup galvanometer. The Pfund thermoelectric amplifier[6] served equally well for both instruments. The amplifier, set upon a small table, could be set up in front of the first resonance galvanometer, and with the second thermocouple connected to the second resonance galvanometer the spectrometer was ready to be used with the resonance radiometer. By moving the table with the amplifier over in front of another shelf, upon which were mounted two Leeds and Northrup high sensitivity galvanometers, with one galvanometer connected to the thermocouple in the spectrometer and the other connected to the thermocouple in the amplifier, a very efficient steady-deflection amplifier could be obtained. (This arrangement, which is more rapid in its response, was used for all survey work and was replaced by the resonance radiometer only in those cases where the highest possible sensitivity was needed.) The amplifi-

[5] F. A. Firestone, Rev. Sci. Inst. **1**, 630–649 (1930).

[6] A. H. Pfund, Science **69**, 71 (1929).

cation could be varied both by changing the intensity of the amplifier lamp and by changing the spacing of the grids. Two sets of grids were used with this amplifier; one set, with a spacing of 1 mm, to give amplifications ranging from 2500 to 15,000 was used entirely with the resonance radiometer; the other set, with 2 mm spacing, to give a range from 50 to 2500, was used with both instruments. The advantage of this type of amplifier is obviously the large range of amplifications and its steadiness even while being pushed to the highest amplification possible. When working with the Leeds and Northrup galvanometers an amplification of six hundred was used, and the steadiness was such that readings could be made in the daytime as well as at night. The principal source of unsteadiness was found to be of an electrical nature and

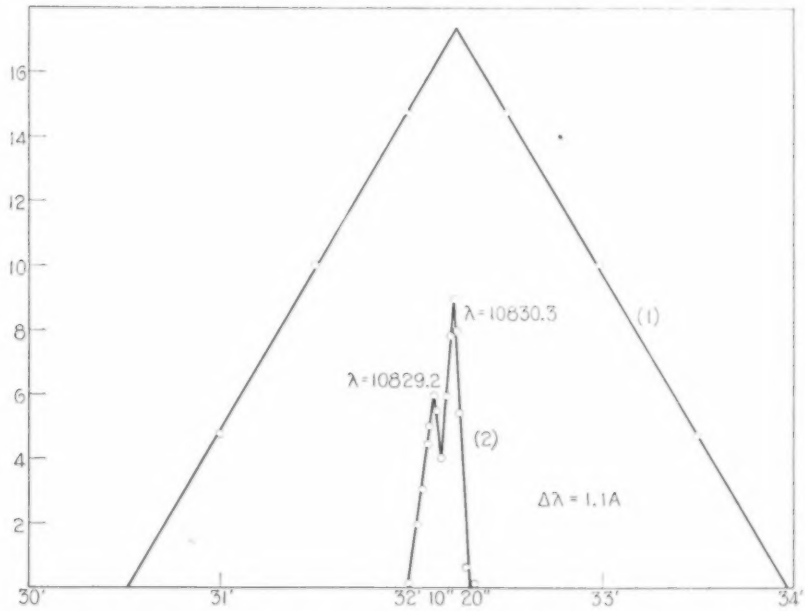

Fig. 2. Helium line at 10,830A. (1) Energy curve with astigmatic spectrometer (unamplified deflections). (2) Energy curve under high dispersion with new type spectrometer (resonance radiometer).

this was reduced, although not eliminated, by carefully shielding every part of the galvanometer circuit. When working with the resonance radiometer an amplification of 6000 was generally used.

After the spectrometer had been set up and focused, tests similar to the ones described above were made to determine the advantage to be gained in line sharpness with narrow slits. It was found that the grating was completely illuminated even with slits so narrow that diffraction prevented further examination. The instrument was calibrated by means of the visual and infrared lines of helium, and the calibration was checked along with the position of the central image at frequent intervals, although they appeared to change very little. The temperature in the basement room in which the spectrometer is located did not vary more than one degree centigrade over long periods of time, and therefore the grating error due to temperature was found to be negligible.

In order to test for the highest resolution that could be realized with the instrument by using ordinarily strong and constant sources, it was decided to examine the 1.0830μ line of helium and see if it were possible to resolve it into its components. The source of radiation was a small glass Geissler tube provided with a capillary 1 mm in diameter. The tube was used 'side on,' and was connected to a neon-sign transformer which was operated from the 110 volt a.c. circuit. The intensity of this source was such that with the spectrometer set on the line and with slits 0.1 mm wide, a deflection of 4 cm was produced by a L and N galvanometer with scale at three meters. The amplifying system was set up and the slits narrowed until no deflection could be detected. However, the helium line could not be resolved. The long focus mirror was then substituted for the parabolic mirror and the slits opened up until the entrance slit was 0.01 mm and the exit slit 0.03 mm. Then with the

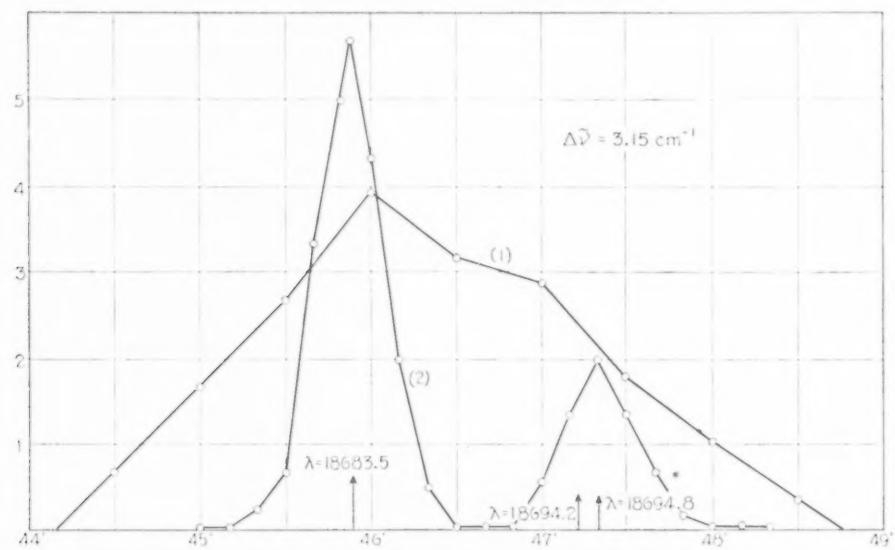

Fig. 3. Helium line at 1.868μ. (1) Curve by Paschen 1908. (λ' position of companion line as deduced by Paschen). (2) Curve with new spectrometer.

help of the resonance radiometer the line could be very nicely resolved. During later experiments a much more powerful source was developed so that it was possible to resolve the line even with the amplified deflections of a L and N galvanometer.

It will be noticed that the "effective slit width" used above is about 0.3A. while the separation between the lines is narly four times that amount. The author has found repeatedly that the "slit-width" must be from a third to a half the amount to be resolved.

Several other lines of the helium spectrum were observed and the line at 1.868μ is shown in Fig. 3, with the line as first observed by Paschen[7] in 1908. This line was observed with wider slits and without the use of the long focus mirror.

The efficiency of the spectrometer was next tested in the matter of energy

[7] F. Paschen, Ann. d. Physik **27**, 537–564 (1908).

conservation. The infrared spectrum of neon, which is very faint, was examined between 1μ and 2μ. The slits of the spectrometer had to be opened to a width of 0.8 mm, with the result that the wave-lengths of the lines could not be determined with as great an accuracy as might be desired. The spectrum of neon had been extended photographically by Gremmer[8] out to a wave-length of 9665.0A, and beginning with this line the region out to 2μ was examined. Most of the lines found gave deflections about one hundredth that produced by the visible yellow line at 5852A.

TABLE I.

Wave-length (vacuum)	Intensity	Frequency		Combination
9667.6	8	10343.8	0.5	$(^2P_{1\frac{1}{2}})3p1_1-(^2P_{1\frac{1}{2}})4s1_2$
10564.3	10	9466.1	0.7	$(^2P_{\frac{1}{2}})3p10_0-(^2P_{\frac{1}{2}})3d12_1$
10624.8	1	9411.8	0.3	$(^2P_{1\frac{1}{2}})3p4_1-(^2P_{\frac{1}{2}})4s4_1$
10800.6	3	9258.7	0.3	$(^2P_{1\frac{1}{2}})3p4_1-(^2P_{\frac{1}{2}})4s3_0$
10849.5	7	9217.5	0.5	$(^2P_{1\frac{1}{2}})3p5_2-(^2P_{\frac{1}{2}})4s4_1$
11142.5	13	8974.9	0.1	$(^2P_{1\frac{1}{2}})3p3_2-(^2P_{1\frac{1}{2}})4s2_1$
11178.8	14	8945.6	0.9	$(^2P_{1\frac{1}{2}})3p2_2-(^2P_{1\frac{1}{2}})4s1_2$
11391.6	4	8778.5	0.7	$(^2P_{1\frac{1}{2}})3p3_2-(^2P_{1\frac{1}{2}})4s1_2$
11410.6	3	8764.0	1.3	$(^2P_{\frac{1}{2}})3p7_1-(^2P_{\frac{1}{2}})4s4_1$
11527.7	25	8674.5	0.1	$(^2P_{1\frac{1}{2}})3p4_1-(^2P_{1\frac{1}{2}})4s2_1$
11540.0	5	8665.5	0.4	$(^2P_{\frac{1}{2}})3p10_0-(^2P_{1\frac{1}{2}})3d6_1$
11616.8	3	8608.0	0.1	$(^2P_{\frac{1}{2}})3p7_1-(^2P_{\frac{1}{2}})4s3_0$
11771.1	4	8495.0	0.3	$(^2P_{\frac{1}{2}})3p9_1-(^2P_{\frac{1}{2}})4s4_1$
11789.4	4	8482.4	0.1	$(^2P_{\frac{1}{2}})3p4_1-(^2P_{1\frac{1}{2}})4s2_1$
11989.5	2	8341.0	0.5	$(^2P_{\frac{1}{2}})3p9_1-(^2P_{\frac{1}{2}})4s3_0$
12069.2	10	8285.7	0.4	$(^2P_{1\frac{1}{2}})3p5_2-(^2P_{1\frac{1}{2}})4s1_2$
12461.0	1	8024.8	0.8	$(^2P_{1\frac{1}{2}})3p7_1-(^2P_{1\frac{1}{2}})4s1_2$
12597.4	1	7938.4	0.2	$(^2P_{\frac{1}{2}})3p8_2-(^2P_{1\frac{1}{2}})4s2_1$
12692.7	2	7878.4	0.6	$(^2P_{1\frac{1}{2}})3p6_0-(^2P_{1\frac{1}{2}})4s2_1$
12770.0	0.3	7830.8	1.8	$(^2P_{\frac{1}{2}})3p7_1-(^2P_{1\frac{1}{2}})4s1_2$
12915.0	2	7742.8	0.1	$(^2P_{\frac{1}{2}})3p8_2-(^2P_{1\frac{1}{2}})4s1_2$
13222.0	1	7563.1	0.2	$(^2P_{\frac{1}{2}})3p9_1-(^2P_{1\frac{1}{2}})4s1_2$
15237.0	2	6562.9	0.1	$(^2P_{\frac{1}{2}})3p10_0-(^2P_{\frac{1}{2}})4s4_1$
17168.0	1	5824.8	0.2	$(^2P_{\frac{1}{2}})3p10_0-(^2P_{1\frac{1}{2}})4s2_1$
18081.0	1	5530.7	2.2	$X-(^2P_{1\frac{1}{2}})3d2_1$
18274.0	3	5472.3	5.0?	$Y-(^2P_{1\frac{1}{2}})3d4_2$
18309.0	1	5462.0	0.2	$X-(^2P_{1\frac{1}{2}})3d3_4$
18389.0	2	5438.0	5.0?	$Y-(^2P_{1\frac{1}{2}})3d6_1$?
18433	1	5425		
18552	1	5390		

In Table 1 are given the wave-lengths, the intensities, and the probable classification of these lines. The intensities given are proportional to the deflections produced and are therefore purely arbitrary. The lines in the region around 1.8μ are apparently due to combinations between the $3d$ levels and the X and Y groups, and although the wave-lengths have been checked as well as possible the agreement with the calculated frequencies from the known terms does not check very well with the experimental values.

The usefulness of the spectrometer in the matter of band spectra has been demonstrated in the examination of the 3μ absorption band of ammonia; the results of which will appear shortly. The infrared emission spectra of krypton and xenon are now under investigation.

The author wishes to express his appreciation to Professor H. M. Randall for his advice and many helpful suggestions.

[8] W. Gremmer, Zeits. f. Physik **50**, 716 (1928).

RAMAN EFFECT FOR BENZENE SUBSTITUTION PRODUCTS BY IMPROVED TECHNIQUE

By R. W. Wood
Johns Hopkins University

(Received November 2, 1931)

DURING the past summer a book entitled "The Smekal-Raman effect" by K. W. F. Kohlrausch has been published. It contains tables of the Raman lines, expressed in frequency differences for some three or four hundred organic compounds and a vast number of inorganic salts.

So much discussion has occurred in the past as to the reality of certain faint lines recorded in various publications, that it seems worth while to publish results obtained during the past winter on the spectra of some of the substances which have been studied by many observers. The object of the investigation was to improve the technique of mercury arc excitation to the highest possible degree, as this is the most generally available source of light. Few observers are equipped to work with a helium lamp, which as I showed some years ago, was superior in some respects to the mercury lamp.

My feeling was that many of the published tables contain errors. Some observers work with unfiltered radiation, measuring all the lines, and taking frequency differences of the various combinations, and finally selecting the true lines due to a monochromatic excitation. This is a very laborious and risky proceeding.

Filters should always be used. Quinine sulphate dissolved in dilute sulphuric acid is the most efficient for removing 4046, but it turns yellow under the action of the light and must be renewed every half hour or so.

After trying to stabilize it chemically, I finally found that the photochemical change is due chiefly to the 3650 group of lines, and these are absorbed by noviol glass, which however transmits 4046.

If noviol is used of sufficient density to cut off 4046, the 4358 line is also much reduced in intensity. This is the trouble with the Zeiss glass filter recommended for 4358 excitation. It appears to be the same as noviol, showing a red fluorescence when under mercury arc illumination. A thin sheet of pale noviol combined with quinine is the most efficient filter, for complete absorption of 4046 and perfect transmission for 4358. The most suitable thickness is noviol "O", 2.5 mm obtainable ground and polished from the Corning Glass Company, Corning, N.Y. A plate six inches square should be ordered, cut into strips 2×6. I now use a Hanovia 220-volt quartz arc in the metal housing turning on trunnions as supplied by the manufacturers. The burner is operated in a horizontal position just below a narrow aperture in the roof of the iron box. The noviol plate is supported about 1 cm above the aperture as shown in Fig. 1, and a bent sheet of thin aluminum directs the air blast of an electric fan across the aperture under the noviol plate. The fluid filter is

contained in a glass tube 5 cm in diameter and 25 cm in length mounted just above the aperture. This acts as a cylindrical lens as well, forming an image of the arc along the axis of the tube containing the liquid under investigation, constructed as described in my earlier papers. Over this is placed a reflector of thin highly polished sheet aluminum now obtainable in the market. This disposition has proved the most satisfactory of any I have tried. It should be mounted about two meters from the spectrograph, and an image of the end of the tube focussed on the slit with a lens of about 25 cm focus. I made this adjustment by mounting a small disk of white paper against the front window of the tube, and illuminating this strongly with a lamp. Its image can then be seen on the slit. This arrangement gives maximum illumination with a minimum of parasitic light. For excitation by 4046 I employ a tube filled with a solution of iodine in carbon tetrachloride, a saturated solution should first be made, and diluted for use. A 1:10 dilution will reduce 4358 by about the right amount. It can be abolished entirely with a 1:5 dilution, but 4046 will then be considerably reduced as well. With a dilution of 1:35 the excitation is by both 4046 and 4358 but the continuous background is considerably reduced

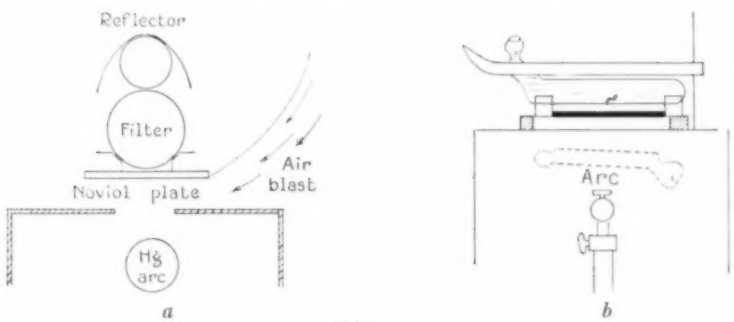

Fig. 1.

between these two lines and faint Raman lines come out which cannot be well seen without the iodine filter. I believe that the best method to follow, and the one most likely to give results free from error is to take two photographs of each substance, one with the noviol quinine filter, and one with noviol iodine, the noviol suppressing 3650, and the iodine 4358.

It is very helpful to make enlargements of each, on such scales that the Raman lines can be brought into coincidence, as shown by Plate I, Figs. *a* and *b*. In other words enlarge the 4358 excitation more than the 4046, which is more dispersed by the prism spectrograph, mark on the 4046 plate or enlargement all lines excited by 4077. This can be done by simply making two marks on a plate or slip of paper separated by the distance between 4066 and 4077 and then fitting the left-hand mark to all of the strongest lines; if the right-hand mark coincides with a much fainter line the chances are that this was excited by 4077. The distance between the two marks must be slightly reduced as we move up the spectrum, of course. Examining spectrum *a*, we see at once that line 177 obtained with 4358 excitation would not be found with 4046 excitation as it is in coincidence with 4077. In general we can be fairly

sure that lines which appear in both spectra are real. For example, in spectrum *a* one might easily come to the conclusion that lines 1161 and 997 were

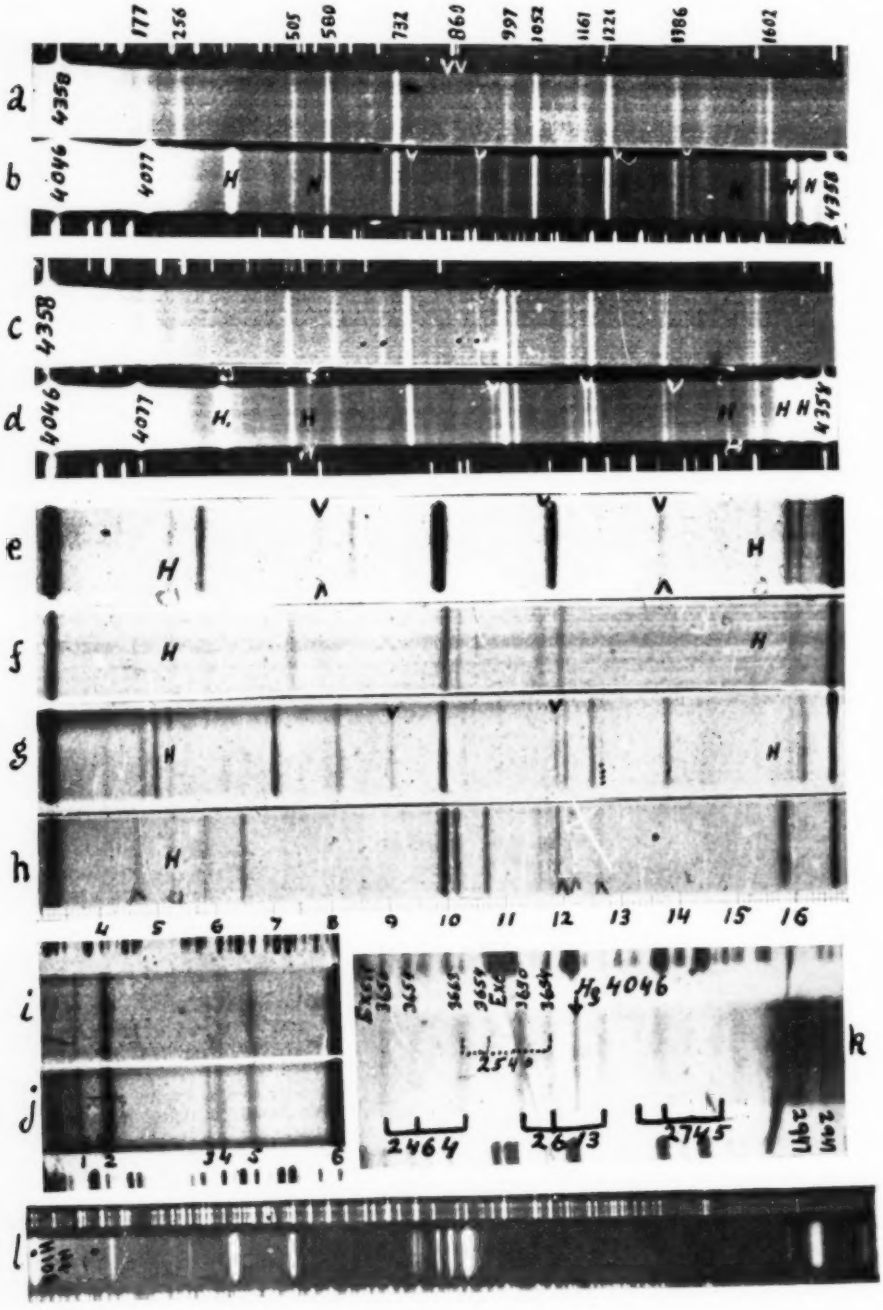

Plate 1.

merely the 4348 excitation of lines 1221 and 1052 (exicted by 4358) but they are found also in the lower spectrum, though much narrower, as in spectrum *a* they are fused with the lines excited by 4348.

In general the spurious lines are more readily picked out by mere inspection in the case of 4358 excitation than with 4046, as they form triplets with the real lines which can usually be recognized at a glance shown by dots in Fig. *c*. The greater separation of 4046 and 4077, makes it difficult or impossible to pick out the lines due to 4077 without measuring their distance from the 4046 lines as described. For study of the fine structure of the complicated Raman band at 3050, excitation by 4046 is all that is necessary, as the band then occurs in a region free from mercury lines and of high photographic sensitivity. With 4358 excitation, however, the band falls at a point of very low sensitivity just above the two mercury lines at 4915.

We will now examine in detail some of the results obtained by this method.

Benzene

The lines given in the table in Kohlrausch's book are the only ones which are real. Bhagavantam reported some new lines not recorded by others. I have investigated these with great care. 4163.8 does not exist. 4494.2 was wrongly assigned to 4358; it is excited by 4046 and gives $\Delta\nu = 2455$, one of the faint lines in the group which I reported in an earlier paper and which will be more fully discussed presently. 4438 assigned by Bhagavantam to 4046 excitation is probably in reality excited by 3906 giving $\Delta\nu = 3068$. Line 4397 was not found. It may have the band of reflected light from the back of the plate, which often resembles a broad line.

4513 unassigned by Bhagavantam (he suggests 4358) is in reality excited by 4046 giving $\Delta\nu = 2543$ which belongs to the group mentioned above.

The spectrum excited by 4046 with a filter of noviol glass and iodine in carbon tetrachloride is reproduced on Plate I Figs. *e* and *l*. In the former lines excited by 4077 are marked with a *v*. In the latter the entire spectrum up $\Delta\nu = 3050$ is reproduced in coincidence with the iron spectrum. Hg 4339–4358 appears at the center greatly reduced in intensity and giving rise to no Raman lines. Line 2947 is very distinct, and 3162–3185 show in the print. The line at the extreme right is due to 4077 excitation.

Toluene

In previous tables a single line only is given $\Delta\nu = 1604$. There are really two lines here as with benzene, the one of shorter wave-length being less intense. The double line was obtained both with 4046 and 4358 excitation as is shown by Figs. *c* and *d* of Plate I. With 4046 excitation they fall just to the left of 4339 Hg. $\Delta\nu = 1604$ and 1583. The other lines of the table in Kohlrausch's book are correct but there seems to be in addition, a faint line to the left of the single bright line at the center of the spectra. In spectrum *c*, the two lines marked with dots are evidently due to 4339–4348 excitation, but in spectrum *d* a faint doublet appears, the left hand member of which may be due to 4077 excitation, and corresponds to the line to the left of the faint mercury line *H*. The right-hand member must be regarded as a real line $\Delta\nu = 720$ and possibly both are. This point can be settled by helium excitation. Lines excited by 4077 are marked with a *v*.

Ortho-xylene

Plate I Figs. *a* and *b* gives a doublet $\Delta\nu = 1602–1580$ instead of the single line 1599 given in Kohlrausch. I cannot understand why other observers have reported only one line here for toluene and the xylenes, as the doublet is almost as conspicuous as in the case of benzene for which all report a doublet. It lies just to the left of the Hg 4358 group in spectrum *b*. The faint line near the center of each spectrum marked *w* is not given in Kohlrausch. Its $\Delta\nu$ is 860. Line 1023 given by Kohlrausch does not appear on either spectrogram. His other lines are correct. The $\Delta\nu$ values are given above the lines of spectrum *a*.

Meta-xylene

Plate I Fig *g*. We find a doublet as with ortho-xylene, $\Delta\nu = 1612–1593$, instead of a single line as given in Kohlrausch. A new line not recorded previously, and marked by a vertical row of dots, $\Delta\nu = 1265$. For the next two lines to the left, I obtain 1250 and 1205. Kohlrausch gives 1245 and 1180, the latter is obviously incorrect as it gives too great a separation of the lines. This can be seen at once if the $\Delta\nu$ values given in Kohlrausch's table are plotted on millimeter cross-section paper and the map thus obtained fitted to Fig. *g*. This scale is the same for both except for a slight variation due to prismatic dispersion. It is thus seen that Kohlrausch's 1180 line is the line marked with a *v* and excited by 4077. It can be seen also that the relative intensities recorded in Kohlrausch's table are far from correct, as he gives 1030 and 1180 at the same intensity one while the spectrogram shows the latter many times brighter. A millimeter scale graduated to $\Delta\nu$ values is given below spectrum *h*. This is only approximately correct, but serves for the identification of the lines.

Para-xylene

The lines 959 and 1012 given in the table in Kohlrausch were not found with 4358 excitation. With 4046 excitation a line was found giving a $\Delta\nu$ of about 1012 but it was due to 4077 excitation of the 826 line, and is therefore to be rejected. $\Delta\nu = 540$ was not found. The short wave-length component of the doublet at 1600 was very faint in this case. 1460 is diffuse and faint and a new line $\Delta\nu = 1325$ narrow and moderately strong was recorded.

Brom-benzene

The lines checked well with Kohlrausch's values, but 1369 failed to appear. It is recorded as very faint however.

Diphenyl oxide

This substance has not been previously investigated. Its spectrum was photographed when in the fluid state, the following lines being found.

$\Delta\nu = 1600$ (2) broad, 1195 (4), 1160 (2), 1020 (3), 1000 (3), 750 (2), 565 (0)? and about a dozen of smaller values not yet measured.

Diphenyl

Previously reported by the author shows the double line 994–1022, as well as lines 1191 and 1146. The strong line 1283 of diphenyl does not appear with the oxide.

Diphenyl-disulphide

In liquid state: 1600 broad (2), 1060 (2), 1020 (2), 1000 (2). These have about the same intensity while, in the case of the oxide 1000 is about three times stronger than 1020.

Anti-Stokes lines of benzene, toluene, and xylene

The existence of anti-Stokes lines in the case of benzene has been so vigorously denied by some investigators, working under conditions which were claimed to be superior to those previously employed, that it seems worthwhile to publish a spectrogram proving conclusively that such lines exist. Traces of them were shown in one of my earlier publications, but I now have plates which really bear reproduction and from which intensity ratios can be determined. Two spectrograms are shown on Plate I Figs. *i* and *j*, the upper made by Hg 4046–4077 excitation, the lower with 4046 and 4358. Line No. 3 appears only in the latter. It is the anti-Stokes line excited by 4358, its wavelength being 4178 and the frequency difference -990. The upper spectrogram was taken with the dense iodine filter combined with noviol glass, which absorbs 3650 and 4358. The lines in the spectrogram are as follows:

1. Mercury
2. $\Delta\nu =$ 606 excited by 4046
3. $\Delta\nu = -990$ excited by 4358
4. $\Delta\nu =$ 606 excited by 4077
5. $\Delta\nu =$ 845 excited by 4046
6. $\Delta\nu =$ 990 excited by 4046.

We see from the photograph that the anti-Stokes line has very nearly the same intensity as the 606 line excited by 4077. The superior contrast in this spectrogram was due to the suppression of the continuous background. A filter of noviol glass was employed combined with a very dilute iodine solution, not sufficiently dense to reduce greatly 4358. (saturated solution diluted 1:35.) This combination gives much cleaner spectra than those obtained with no filter. On a plate taken with a quinine filter combined with noviol glass only line No. 3 appeared, together with the other anti-Stokes line $\lambda = 4246.7$, $\Delta\nu = -606$. Two anti-Stokes lines came out very clearly in the case of toluene excited by 4358, also with para-xylene. In the latter case, the lines were measured giving $\Delta\nu$ values -458 and -314, in good agreement with the values 461 and 315.

In a previous communication on the Raman effect, I recorded the presence of a number of faint lines in the spectrum of benzene in the region lying on the short wave-length side of the strong double band with $\Delta\nu = 3060$. One of these ($\Delta\nu = 2947$) has been noted by other observers. These lines appear only when

the continuous background has been suppressed to the highest possible degree. Further investigation, with improved technique has confirmed the suspicion that the actual presence of certain of these lines depended on the wave-length of the exciting light, lines obtained with excitation by helium 3888 not being found with mercury 4046.

The Δv frequencies for these lines are given in the following table:

New lines of benzene

2465	2745
2545	2765
2596 (obtained only with helium excitation.)	2930
2615	2947.

Their presence has been verified with the following excitation wave-lengths; 5461, 4358, 4046, 3888, 3663, 3654, and 3650. Their relative intensities with these different types of excitation is roughly shown in Fig. 2.

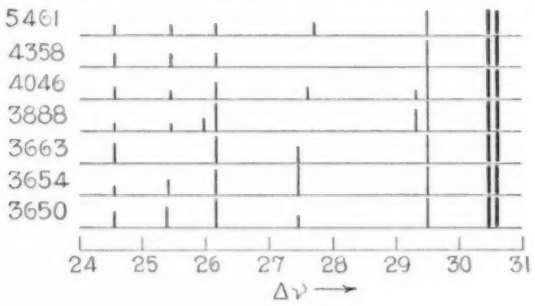

Fig. 2.

It was at first thought that the intensity differences found at different times with different excitations might result from a change in the benzene, due to continued illumination or impurities. But this seems not to be the case, for a marked difference in the intensity ratios was found when the lines were excited simultaneously by the three lines making up the mercury group at wave-length 3650–3663, in which case each Raman line appears in triplicate. A filter of nickel oxide glass was used in this case. A portion of the spectrogram is reproduced much enlarged on Plate I, Fig. *k*. In the interpretation of this spectrum we must remember that the intensities of the exciting lines are very different. 3650 is much brighter than 3663, which in turn is brighter than 3654.

I have bracketed the lines which I believe belong together, the Δv values being written below the brackets. It appears that two superpositions occur, which complicates the interpretation. There seems, however, to be strong evidence of a change in the intensity ration of the Raman lines for the three different excitations. The most conspicuous effect is obtained with helium 3888 excitation. Here we have a very distinct doublet at $\Delta v = 2596$–2615. No trace of the former line being found with any other excitation. Helium excitation also seems to be peculiar in that it gives benzene lines $\Delta v = 1178$, 1584,

and 1603 of the same intensity, while with 4046 and 4358 excitation the 1178 line is very much brighter than the other two. This matter will be more fully investigated shortly.

Explanation of plate

a. Raman spectrum of ortho-xylene excited by Hg 4358. Filter of noviol glass and sulphate of quinine. Line $\Delta v = 860$ not previously recorded marked with white *w*.

b. Ortho-xylene spectrum excited by 4046–4077. Filter of noviol glass and iodine in carbon tetrachloride. Lines excited by 4077 marked with a white *v*. Line $\Delta v = 860$ appears here also. The 4358 mercury group is at extreme right. Lines marked *H* are mercury.

c. Spectrum of toluene excited by 4358. Note doublet at right recorded as single line by previous observers. This doublet also appears in *a* and *b*. Quinine and noviol filter.

d. Toluene spectrum excited by 4046–4077. Lines due to 4077 marked *v*, mercury lines marked *H*. Iodine and noviol filter.

4046 *Excitations*

e. Benzene spectrum, reproduced as a negative. Iodine in carbon tetrachloride plus noviol glass as filter. Lines due to 4077 marked *v*. Mercury lines marked *H*. The strong line at the left is mercury 4108, that at the right 4339. The doublet at the left of 4339, ($\Delta v = 1584$–1606) is found with toluene and all three xylenes, contrary to observations by others. It is absent in brom-benzene. Fig. *h*. One 4077 excitation coincides with one by 4046.

f. Diphenyl-oxide. The doublet has fused. No lines excited by 4077 appear.

g. Meta-xylene. Lines excited by 4077 marked *v*.

h. Brom-benzene. The doublet at right shown by other substitution products replaced by a single broad line shifted towards shorter wave-length.

i. j. Anti-Stokes line (No. 3) of benzene. Spectrum *i* taken with iodine filter, which absorbs 4358, and the anti-Stokes line is absent. The lines are as follows: 1. Mercury, 2. $\Delta v606$, excited by 4046. 3. $\Delta v = -990$, excited by 4358. 4. $\Delta v606$, excited by 4077. 5. $\Delta v = 845$. 6. $\Delta v = 990$.

k. New faint lines of benzene in region $\Delta v = 2465$–2947 excited by 3650–54–63. The strong lines at right are $\Delta v = 2947$.

l. Complete spectrum of benzene excited by 4046 with iodine filter the line at right being $\Delta v = 3050$.

THE PASCHEN-BACK EFFECT OF HYPERFINE STRUCTURE I. THALLIUM II AND III

By J. B. Green* and John Wulff*
Mendenhall Laboratory of Physics and Massachusetts Institute of Technology.

(Received September 10, 1931)

Abstract

The Zeeman effect of several characteristic lines of Tl II and Tl III has been studied at field strengths of 14700, 32500 and 43350 gauss. The transition from weak to strong fields shows exceedingly good agreement with the theory of Goudsmit and Bacher. Careful measurements of the magnetic patterns of certain lines indicate that McLennan and Allin's results are inaccurate.

THE magnetic analysis of hyperfine structure permits a more definite determination of nuclear moment than the value interpreted from the interval separations of the hyperfine structure pattern of the fieldless line. The work of Heisenberg and Jordan,[1] Darwin,[2] and Mensing[3] on the Zeeman effect of multiplets for all field strengths has been extended by Goudsmit and Bacher[4] for hyperfine structure. The formulae in both cases are quite similar, yet in the latter the quantum vectors for electron spin and angular momentum, s and l respectively are replaced by the nuclear moment and the total momentum of the remainder of the atom, i and j respectively.

The additional quantum vector i, attributable to the nucleus, causes each line to separate into a tiny multiplet (hyperfine structure) and complicates the Zeeman pattern of the line, analogous to the way in which the electron spin produces an ordinary multiplet and alters the simple Lorentz triplet. The line λ4722 Bi I is no doubt the best example of the objectivity of determination of nuclear moment from the Zeeman effect. Each of the components of this line splits up in a strong magnetic field into ten lines which can be attributed to the presence of a nuclear moment $i=9/2$ having $2i+1=10$ orientations in the magnetic field.

Detailed magnetic analyses have been carried out for the arc spectra of Bi I and Tl I by Goudsmit and Bacher as well as Back and Wulff.[5] McLennan and Durnford[6] have investigated the Zeeman effect of Tl spark lines, yet the lack of resolving power of the spectroscopic instrument as well as the weak

* John Simon Guggenheim Memorial Fellow.

† International Education Board Fellow.

[1] Heisenberg and Jordan, Zeits. f. Physik **37,** 263 (1926).

[2] C. G. Darwin, Proc. Roy. Soc. **A115,** 1 (1927); K. Darwin, Proc. Roy. Soc. **A118,** 264 (1928).

[3] Mensing, Zeits. f. Physik **39,** 24 (1926).

[4] Goudsmit and Bacher, Zeits. f. Physik **66,** 13 (1930).

[5] Back and Wulff, Zeits. f. Physik **66,** 31 (1930).

[6] McLennan and Durnford, Proc. Roy. Soc. **A129,** 48 (1930).

field employed does not permit a complete interpretation. The instruments used in the present work have enabled us to give a more careful analysis of the problem.

Experimental Procedure

The quality of the large concave grating of the Physical Institute in Tübingen permitted the photography of 3rd and 4th order patterns in the visible and 5th order patterns in the ultraviolet. The multicomponent patterns present in the Zeeman effect of hyperfine structure and the small separations involved necessitated the maximum obtainable resolving power. For this purpose the focus of the grating was redetermined with the aid of a series of especially sharp tin lines. The plates rested at an angle, the middle of the plate being on the Rowland circle, the lower half toward the grating and the upper half away from the grating. The spectrograms showed a systematic deviation of the focal curve from a true circle. The final curve determined was found to be slightly elliptical with the minor axes approximately in the position of the normal to the grating. On the empirically determined curve it was possible to adjust the plate holders to insure maximum resolution.

The light source used is described in detail elsewhere. Briefly is consisted of a negative tungsten electrode and a positive electrode of rilled manganin upon which 0.5 mm thickness of Tl was melted. The latter electrode is stationary and isolated from the pole-shoe by a thin strip of mica. The tungsten electrode which is given an intermittent action by a spring eccentric on a constant speed motor makes some 300 contacts per minute. The vacuum chamber was kept at an average argon or hydrogen pressure of 5 mm Hg during the entire exposure. Current was applied at 110 volts and adjusted to 3–5 amperes with suitable rheostats. An inductance of about 100 turns of heavy wire around an iron core in series with the rheostats and a capacity of 5000 cm across the arc served to reduce fluctuations to a minimum. Under these conditions a new positive electrode was inserted about every half hour, and three hours net exposure usually sufficed for proper intensity.

The Weiss magnet had a interferricum of 3.8 mm and the special ferrocobalt pole-tips a diameter of 7 mm. A current of 73 amperes through the water-cooled coils of the magnet gave a field of 43350 gauss. Variations of 1 ampere have no effect on the sharpness of the lines at this field strength and are not detectable with a flip coil. This is to be expected from the calibration curve which shows that saturation is reached in this neighborhood. This was not the case with the two other field strengths employed, namely 32500 and 14700 gauss. Especially with the latter a variation in current of 0.05 amp. affects the sharpness of the lines. Easily controllable rheostats and continual observation were necessary to keep the current constant. During and after the exposure typical cadmium and zinc lines were flashed on the plates to serve as standards for field strength determinations. In many of the patterns studied the separations are at the limit of the resolving power of the grating, an great care had to be exercised in the choice and development of the photographic plate. The special Flieger plates of Perutz in Munich fulfilled all our re-

quirements, of speed, fineness of grain, and sensitivity (2200–5800A). The photometer curves were made with the photoelectric recording photometer at the University of Munich. (Magnification 13 ×) and show fringes which though often attributed to large grain size are here the direct result of the fine photometer slit employed. A wider slit alleviated this disturbance but also failed to bring out some of the fine structure. In any case, it is quite easy to distinguish the real from the apparent maxima.

Theory

The theory of the Paschen-Back effect of hyperfine structure has been admirably discussed by Goudsmit and Bacher[4] and the reader is referred to this paper for a complete discussion of the problem. We shall repeat here only those conclusions necessary for a clearer understanding of the present work.

The hyperfine structure of spectrum lines is caused by the interaction of the total momentum of the rest of the atom with the nuclear momentum, i, (which may have any half or full integral value, including zero). Up to the present, it has not been possible to predict the value of this nuclear moment, and we have had to rely entirely upon experimental data. Further, the different isotopes of the same element may have different nuclear moments. Thus, the progress in this field has not been so rapid as was the case some years ago with complex spectra, when Hund proposed his theory of the coupling of electron spin and angular momentum. Also, the experimental technique involved in the resolution of the very close patterns is very much more difficult than for gross multiplet structure.

In zero field, i and j interact to give a new quantum number f of hyperfine structure, which has either $2i+1$ or $2j+1$ values depending on whether i or j is the smaller of the two interacting vectors. On the basis of the old model theory of the atom, this vector precesses regularly about the field direction H, if H is small, and in the same way as we calculate a g-formula for the vector j, we find for f, a g-formula.

$$g(f) = g(j)\frac{f(f+1) + j(j+1) - i(i+1)}{2j(j+1)}. \tag{1}$$

Thus, in a weak field, each hyperfine energy level is split up into $2f+1$ levels symmetrically situated about the zero field level.

In a strong field the coupling between the i and j vectors is destroyed, and each of the vectors interact independently with the magnetic field. The effect is to introduce a new type of symmetry in which there are associated $2i+1$ equally spaced levels with each of the $2j+1$ orientations of j, m_j, in the magnetic field, the spacings of the $2i+1$ levels being proportional to the value of m_j with which they are associated. Here is seen the origin of the patterns found by Back and Goudsmit[7] in the spectrum of bismuth.

For medium field strengths all symmetry is lost and for the calculation of the positions of the energy levels, we must use the following formula of Goudsmit and Bacher.

[7] Back and Goudsmit, Zeits. f. Physik **47**, 174 (1928).

$$X_{m_i+1,m_j-1}(A/2)(i+m_i+1)(j-m_j+1)+X_{m_i,m_j}$$
$$(E-Am_im_j-m_jg\omega)-X_{m_i-1,m_j+1}(A/2)(i-m_i+1)(j+m_j+1)=0 \qquad (2)$$

where A is the hyperfine structure separation factor, ω the Lorentz separation factor corresponding to the field strength used, E the position of the magnetic level with reference to the center of gravity of the fieldless pattern, and X represents a transition probability.

For a given value of $m_i+m_j=m_f$, the above equation is written for all possible values of m_i and m_j. The determinant of this set of homogeneous equations is set equal to zero and its roots are the values of E for the given m_f. The order of the determinant will be $2j+1$ or $2i+1$ depending on whether j or i has the smaller value.

Thus, in the case of thallium the problem of determining the positions and intensities of the lines from a theoretical standpoint becomes exceedingly simple, since it has been definitely established that the nuclear moment of the Tl atom is 1/2. The equations are, then, all quadratic or linear.

The above theory has been applied very successfully to the spectrum of thallium I and so far has been checked in all details. Spark spectra have much greater hyperfine structure intervals and are therefore easier to resolve. In the spectrum of Tl II and Tl III the visible lines were studied in the magnetic field by McLennan and Durnford[6] but the apparatus used had not a sufficiently high resolving power to give a complete analysis of the lines. Schüler and Keyston[8] have studied the hyperfine structure of Tl II in zero field and we have used their values of the separations in our calculations of the magnetic patterns.

In particular, the lines 3092, 2530 and 2298 of Tl II have been studied at three different field strengths, and 5949 of Tl II and 4110 of Tl III at the maximum field strength, 43350 gauss. The line 3092 has been discussed by us in complete detail elsewhere, and is included here for the sake of completeness, as the simplest example of the Paschen-Back effect of hyperfine structure.

For the line 2298 ($6p^3P_2-7s^3S_1$) as an example, the positions of the levels of $6p^3P_2$ are found from equation (2) as

$$\begin{aligned}
m_f &= 5/2 \qquad & E &= A+2\omega g \\
m_f &= 3/2 \qquad & E^2&+E(A/2-3\omega g)+(2\omega^2g^2-3A^2/2)=0 \\
m_f &= 1/2 \qquad & E^2&+E(A/2-\omega g)-3A^2/2=0 \\
m_f &= -1/2 \qquad & E^2&+E(A/2+\omega g)-3A^2/2=0 \\
m_f &= -3/2 \qquad & E^2&+E(A/2+3\omega g)+(2\omega^2g^2-3A^2/2)=0 \\
m_f &= -5/2 \qquad & E &= A-2\omega g
\end{aligned} \qquad (3)$$

while for the levels of $7s^3S_1$ we get

$$\begin{aligned}
m_f &= 3/2 \qquad & E &= A/2+\omega g \\
m_f &= 1/2 \qquad & E^2&+E(A/2-\omega g)-A^2/2=0 \\
m_f &= -1/2 \qquad & E^2&+E(A/2+\omega g)-A^2/2=0 \\
m_f &= -3/2 \qquad & E &= A/2-\omega g.
\end{aligned} \qquad (4)$$

[8] Schüler and Keyston, Zeits. f. Physik **70**, 1 (1931).

The intensities of the components are given by

$m_f \rightarrow m_f$	Parallel polarization
$3/2 \rightarrow 3/2$	$12[X_{1/2,1}X'_{1/2,1}]^2$
$1/2 \rightarrow 1/2$	$8[2X_{1/2,0}X'_{1/2,0} + 3X_{-1/2,1}X'_{-1/2,1}]^2$
$-1/2 \rightarrow -1/2$	$8[3X_{1/2,-1}X'_{1/2,-1} + 2X_{-1/2,0}X'_{-1/2,0}]^2$
$-3/2 \rightarrow -3/2$	$12[X_{-1/2,-1}X'_{-1/2,-1}]^2$
$m_f \rightarrow m_f - 1$	Perpendicular polarization
$3/2 \rightarrow 1/2$	$4[X_{1/2,1}X'_{1/2,0}]^2$
$1/2 \rightarrow -1/2$	$2[3X_{1/2,0}X'_{1/2,-1} + 2X_{-1/2,1}X'_{-1/2,0}]^2$
$-1/2 \rightarrow -3/2$	$6[4X_{1/2,-1}X'_{1/2,-2} + X_{-1/2,0}X'_{-1/2,-1}]^2$
$-3/2 \rightarrow -5/2$	$12[X_{-1/2,-1}X'_{-1/2,-2}]^2$
$m_f \rightarrow m_f + 1$	Perpendicular polarization
$3/2 \rightarrow 5/2$	$12[X_{1/2,1}X'_{1/2,2}]^2$
$1/2 \rightarrow 3/2$	$6[X_{1/2,0}X'_{1/2,1} + 4X_{-1/2,1}X'_{-1/2,2}]^2$
$-1/2 \rightarrow 1/2$	$2[2X_{1/2,-1}X'_{1/2,0} + 3X_{-1/2,0}X'_{-1/2,1}]^2$
$-3/2 \rightarrow -1/2$	$4[X_{-1/2,-1}X'_{-1/2,0}]^2$

The X's are found by substituting the values of E, found by Eqs. (3) and (4), in the original determinantal equations. The umprimed terms refer to the level $^3S_1$, and the primed terms to $^3P_2$.

For the complete details of the calculations the reader is referred to Goudsmit and Backer.

Results

The results are shown in graphical form in Figs. 1–5; below are the theoretical patterns calculated from the theory of Goudsmit and Bacher and above the photometer curves made from the original plates. In comparing the theoretical and experimental curves several facts should be noted: (1) the photometer at best gives integrated results which seldom show the resolution detectable by the human eye; (2) lines just resolvable by the grating may be too close together for the resolving power of the plate which results in a broad diffuse line for a group of adjacent components; (3) lines not resolved by the grating will integrate their intensities in such a fashion that a strong line takes the place of a number of extremely close weak lines.

λ3092. Fig. 1, a, b, c show the parallel and perpendicular polarizations of 3092 Tl II ($6s6p\,^1P_1, -6s7s\,^1S_0$) in the fifth order at field strengths of 14700, 32500 and 43350 gauss. The transition from weak to strong fields is quite evident from the photometer curves. It need only be noted that the separation of the strong doublets in the perpendicular polarization approaches the same value with increasing field, while the two middle parallel components at 14700 gauss merge at 43350 gauss. The magnetic analysis in this case is an excellent check of the theory of the Paschen-Back effect of hyperfine struc-

ture and the value of the fieldless separation deduced therefrom is 0.092 $\pm$0.002A or 0.96$\pm$0.02 cm^{-1} a value slightly different from that found by McLennan and Crawford.

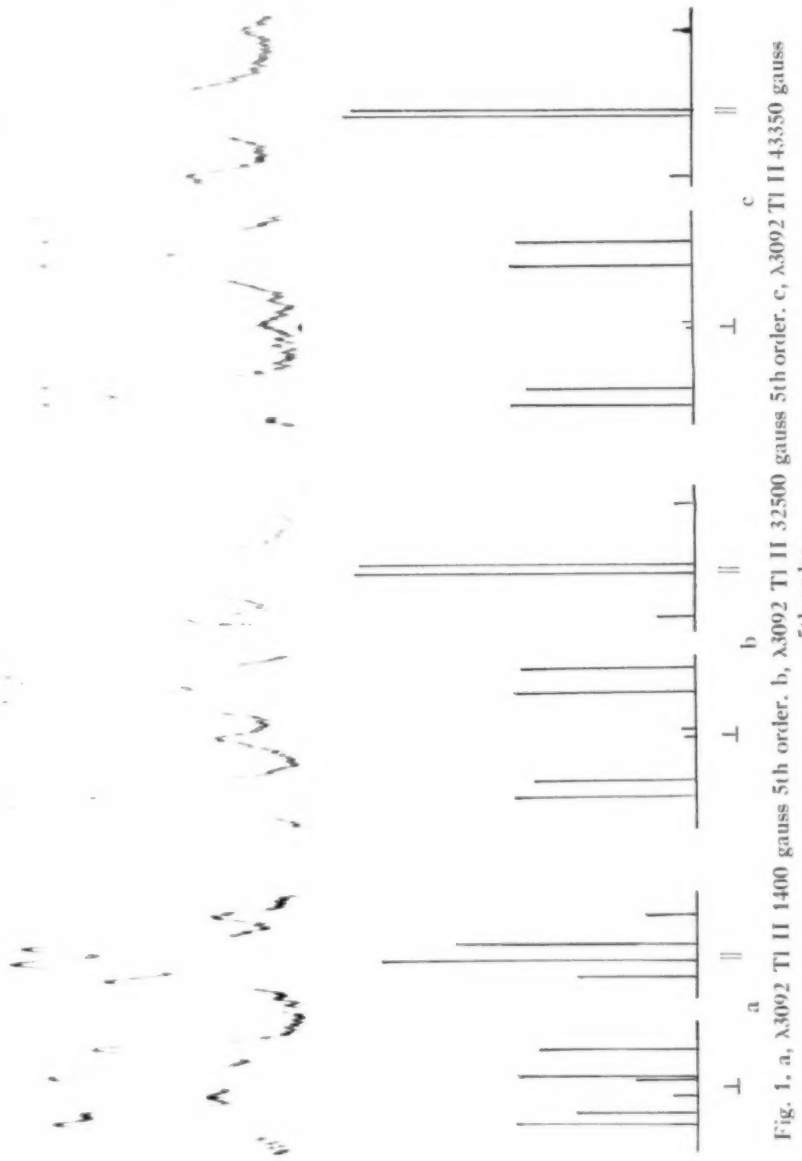

Fig. 1. a, λ3092 Tl II 1400 gauss 5th order. b, λ3092 Tl II 32500 gauss 5th order. c, λ3092 Tl II 43350 gauss 5th order.

λ2298. Figs. 2 a, b, c are taken from the 4th order spectograms of 2298 Tl II ($6s6p^3P_2-6s7s^3S_1$). The magnetic analyses of this line is not so complete as in the previous case (λ3092) yet it may be noted that the unresolved components of the weak fields become more apparent with increasing field strength. The faint side component (so called "forbidden components" of the Paschen-

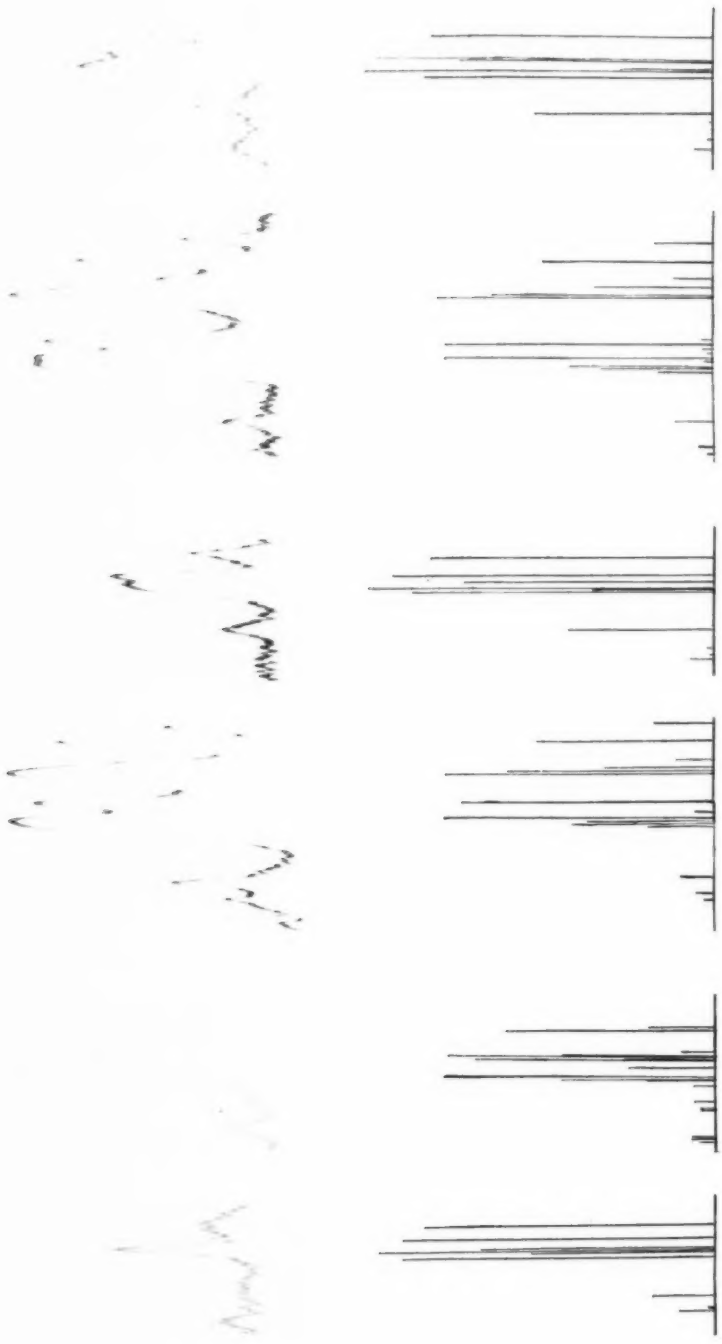

Fig. 2. a, λ2298 Tl II 14700 gauss 4th order. b, λ2298 Tl II 32500 gauss 4th order. c, λ2298 Tl II 43350 gauss 4th order.

Back effect) seem to decrease in intensity with increasing field strength in accordance with the theory.

λ2530. Figs. 3 a, b, c represent 5th order patterns of λ2530, Tl II (6*s*

$6p^1P_1-6s6d^1D_2$) at the above field strengths. Though the perpendicular polarization is in good agreement with the theory, there are discrepancies in the faint side components which have not as yet been accounted for. Here

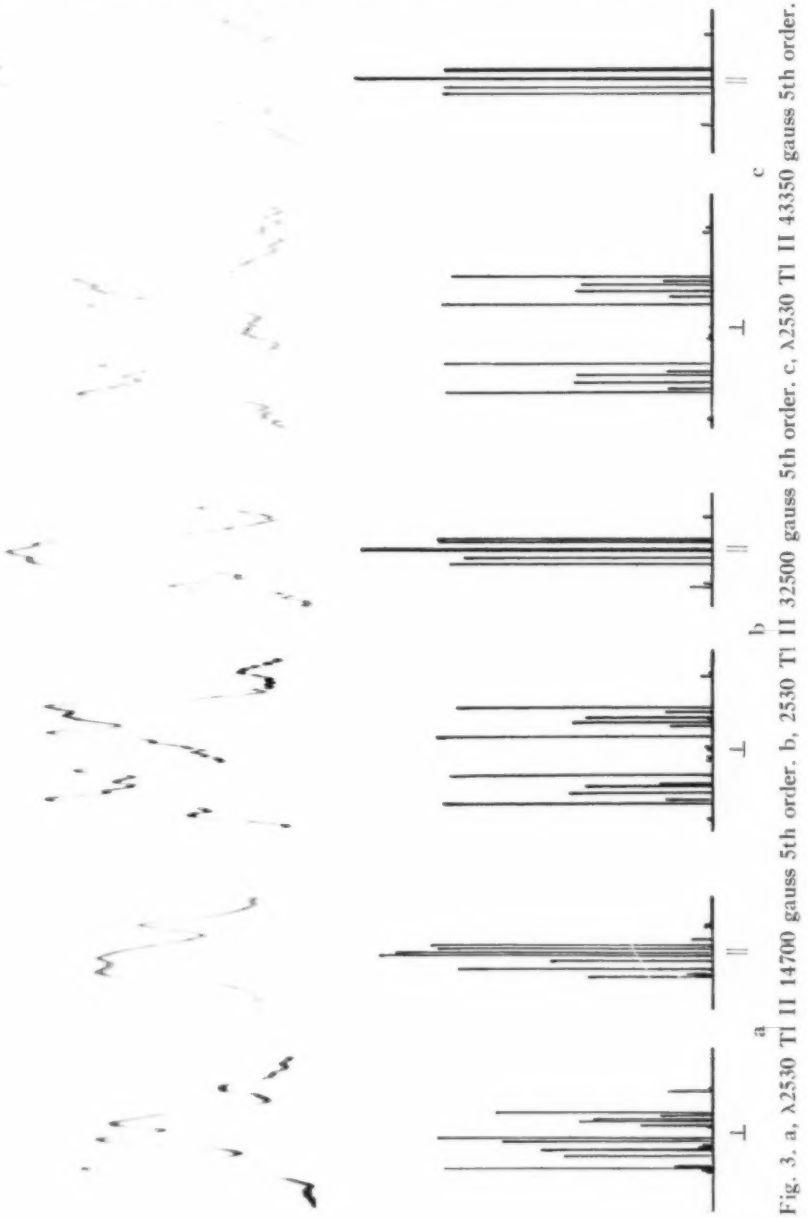

Fig. 3. a, λ2530 Tl II 14700 gauss 5th order. b, 2530 Tl II 32500 gauss 5th order. c, λ2530 Tl II 43350 gauss 5th order.

again it may be noted that the forbidden components decrease in intensity with increasing field.

λ5950. Fig. 4 a and b show both polarizations in the first order of λ5950 Tl II ($6s7s^3S_1-6s7p^2P_2$) at 43350 gauss. From its transition it is evident that

this line is the inverted counterpart of λ2298, which is also evident from the photograph. The increased scale of wave numbers brings out some of the very fine components not apparent in λ2298. The weak component in the center of the perpendicular polarization (on Fig. 4a) belongs to a neighboring line of argon.

λ4110. Fig. 5a, b gives the perpendicular and parallel polarizations of 4110 Tl III ($7s^2S_{1/2}-7p^2P_{3/2}$) in the second order at the high field strength. This line is the counterpart of Tl I 5350 and shows the same general charac-

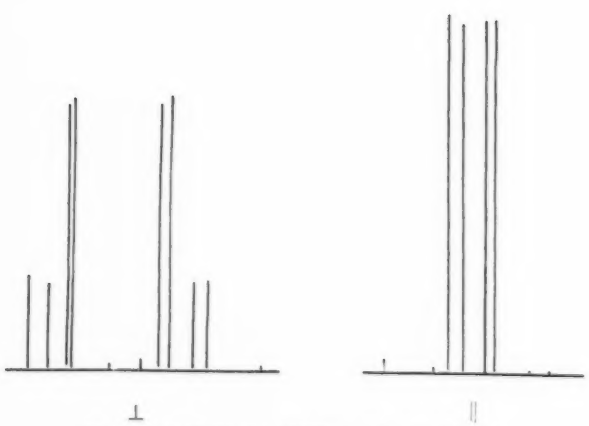

Fig. 4. λ4110 Tl III 43350 gauss second order.

teristics except that the $^2P_{3/2}$ is sufficiently large to influence the separations of the doubling resulting from the nuclear moment $i=1/2$. McLennan and Allin[9] report the separations of $7s^2S_{1/2}$ and $7p^2P_{3/2}$ as 1.37 and 0.44 cm^{-1} respectively. Our measurements on this line are not consistent with these results and indicate that the separation of $7s^2S_{1/2}$ is somewhat smaller, namely 1.24 cm^{-1}. (The faint middle component does not belong to the line; it is the O line 4111).

Conclusion

In the experimental material discussed we have again a very good argument in support of the present status of the theory of the Paschen-Back effect

[9] McLennan and Allin, Proc. Roy. Soc. **A129,** 43 (1930).

of hyperfine structure. The work of Goudsmit and Bacher as well as Back and Wulff has now been definitely applied to spark spectra, such discrepancies which occur are in most cases of a negligible order.

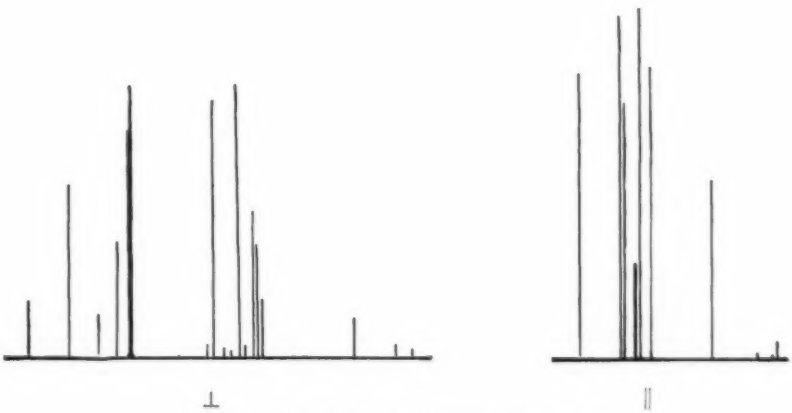

Fig. 5. λ5950 Tl II 43350 gauss first order.

The success of the work can be attributed largely to the excellent apparatus available in Tübingen. To Professors Geiger and Back we extend our thanks for the privilege of working in Tübingen as well as to Professor Gerlach for permitting us the use of the large recording photometer in Munich.

THE PASCHEN-BACK EFFECT OF HYPERFINE STRUCTURE II. Bi II AND Bi III

By J. B. Green* and John Wulff†
Mendenhall Laboratory of Physics and Massachusetts Institute of Technology.
(Received September 10, 1931)

Abstract

Goudsmit and Bacher's theory is successfully applied to the spectra of Bi II and Bi III. The lines λλ5719 of Bi II and 4561 and 3695 of Bi III are used as typical examples of these spectra. λ5719, like 3092 of Ti II, serves as an excellent check on the theory, because of its especially simple transition.

IN A previous paper, the authors showed that Goudsmit and Bacher's[1] theory is quite adequate to explain the complicated Zeeman patterns observed for the hyperfine structure components of the spectra of Tl II and Tl III. The present paper is a continuation of the work and treats the spectra of Bi II and Bi III.

The experimental arrangement was exactly the same as in the previous

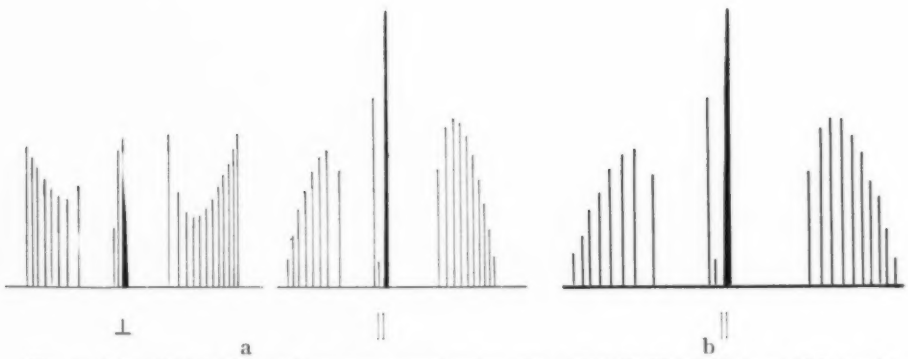

Fig. 1. (a). λ5719 Bi II 14700 gauss second order. (b). λ5719 Bi II 14700 gauss third order

* John Simon Guggenheim Memorial Fellow.
† International Education Board Fellow.
[1] Goudsmit and Bacher, Zeits. f. Physik **66,** 13 (1930).

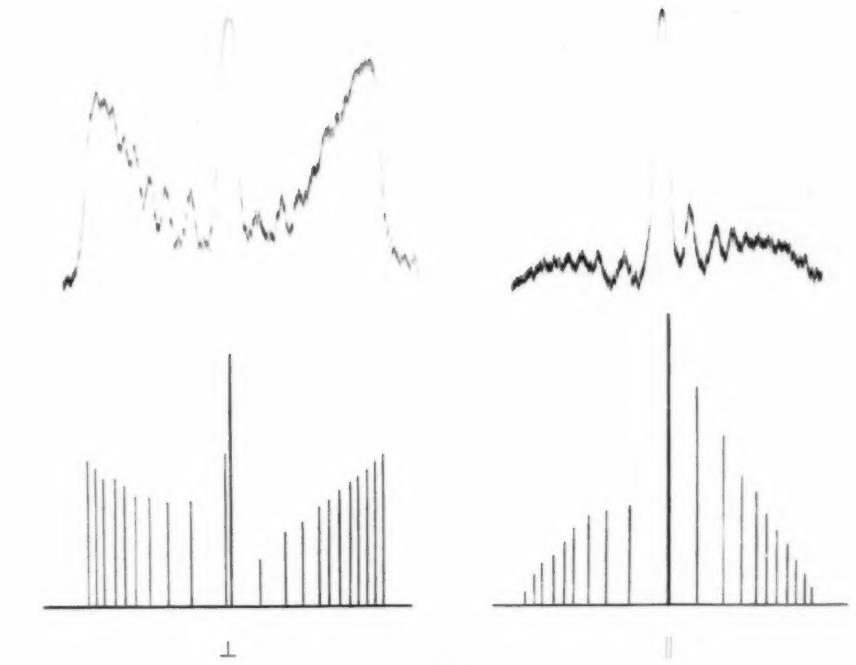

c

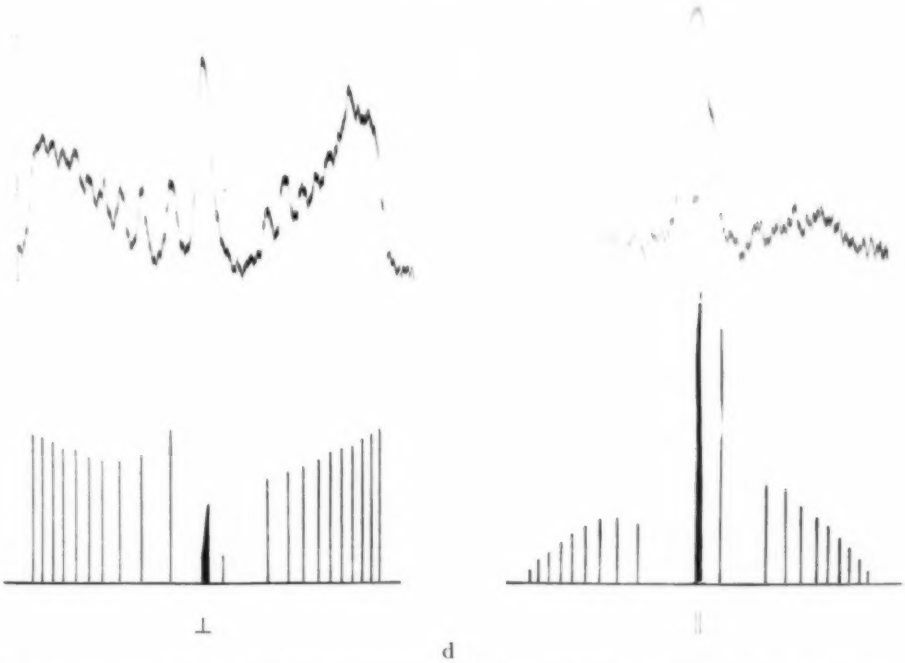

d

Fig. 1. (c). λ5719 Bi II 32500 gauss second order. (d). λ5719 Bi II 43350 gauss second order.

work, except that the thallium metal used on the positive electrode was replaced by pure bismuth metal. For the excitation of spark spectra, alloys of the metal did not prove at all satisfactory. It seems that large quantities of the metallic vapor must be present in order to bring out the spark lines; a condition that must be avoided in the study of arc lines, for it leads almost certainly to self-reversal of some of the components of the lines.

In all other respects too, it was necessary to pay strict attention to all the details. As may be seen from the microphotometer reproductions, the magnetic patterns of the lines are extremely complicated, and in order to prevent the groups of lines from becoming mere smears, the pressure on the vacuum chamber, the current in the arc, and the speed of the motor, had to be kept constant.

Flieger plates of the Perutz Company in Munich were again used, and long tank development with Perutz fine-grain developer served to bring out to the best advantage the really fine work that the grating is capable of doing.

The results of Back and Goudsmit,[2] and Back and Wulff[3] have shown conclusively that the nuclear moment of the bismuth atom is 9/2. Consequently, the Zeeman patterns of the bismuth lines are considerably more complicated than the thallium lines, for in the latter cases, the tendency of each Zeeman component was break up into two in strong magnetic fields, while in the latter, the tendency is to break up into ten!

In the theoretical calculations it would also be possible for the determinantal equation to be of the tenth order and the tedium of the solution of the problem would be enormous, unless one used approximate methods as suggested by Goudsmit and Back. We have therefore chosen a particularly simple type of transition in Bi II to illustrate the theory. The line λ5719 has been classified as $2_1{}^0-7_0$ (possibly $6p\ 7s^3P_1-6p\ 7p^3P_0$). We are thus dealing with a transition $j=1$ to $j=0$, exactly similar to λ3092 of Tl II. A glance at Eq. (2) of the previous paper shows that the determinantal equation will be of the third order. There is one further complication in the calculations for Bi II. This is a two-electron spectrum, and the coupling between the electrons is practically *jj* in type. Hence we cannot use the Landé *g*-value in our equations. Applying Houston's[4] theory to the case, we are able to calculate the *g*-values from the interval separations and for $6p\ 7s\ ^3P_1$ we find the value $g=1.35$ instead of 1.50, the Landé *g*-value. With this value, the agreement between theory and experient was excellent.

The results of the calculations are shown graphically in Figs. 1a,b,c,d. Fig. 1a is taken at a field strength of 14700 gauss in the second order. Above is the microphotometric reproduction of the original plate (13×enlarged), and below the calculated positions and intensities of the lines. Fig. 1b is a reproduction of the third order, parallel polarization. Figs. 1c and 1d were taken from second order plates with magnetic fields of 32500 and 43350 gauss respectively. The wide black lines indicate a large number of very close com-

[2] Back and Goudsmit, Zeits. f. Physik **47,** 174 (1928).
[3] Back and Wulff, Zeits. f. Physik **66,** 31 (1930).
[4] Houston, Phys. Rev. **33,** 297 (1929).

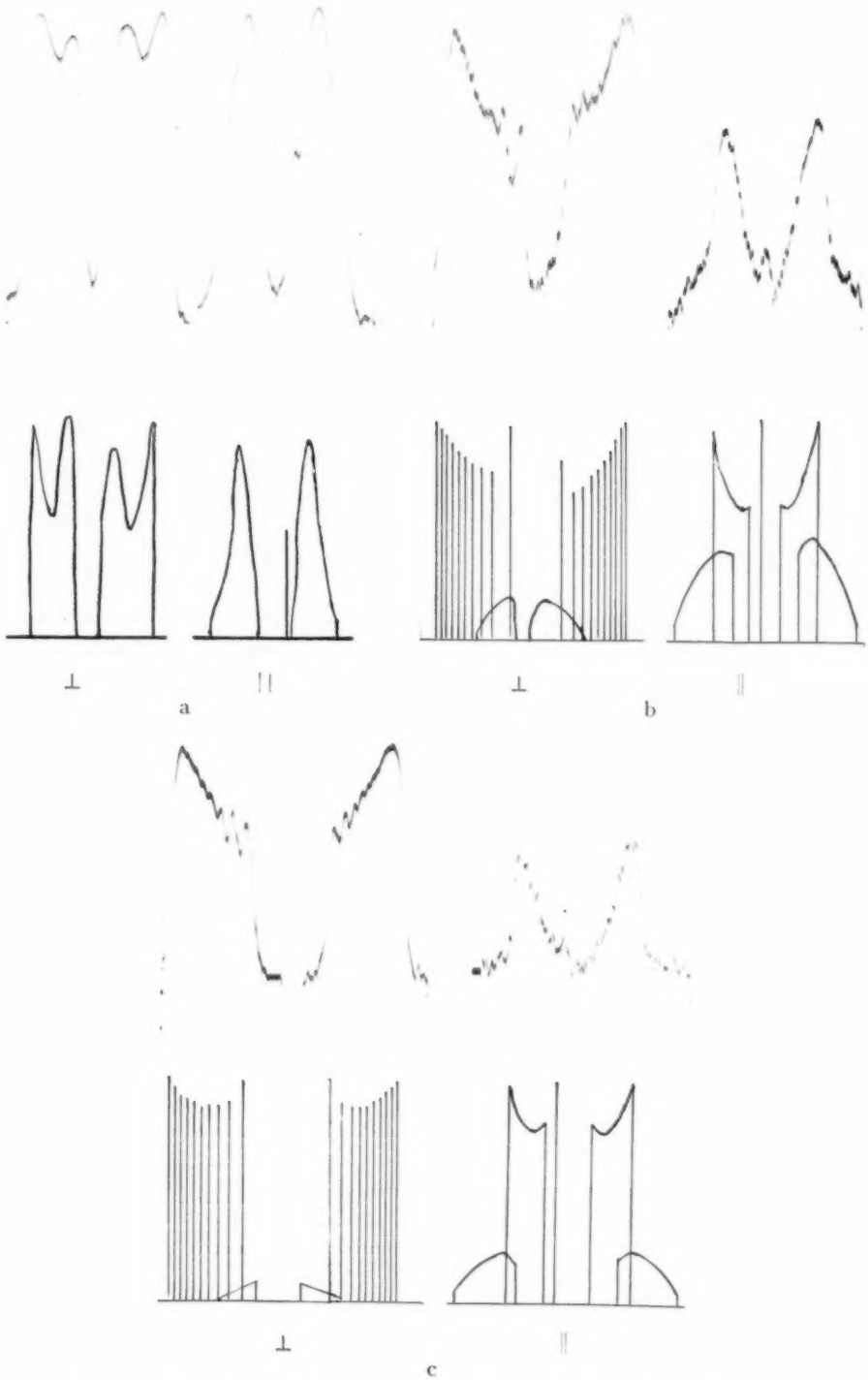

Fig. 2. (a). λ4561 Bi III 14700 gauss second order. (b). λ4561 Bi III 32500 gauss second order. (c). λ4561 Bi III 43350 gauss second order.

ponents and in Fig. 1d, parallel polarization, although these are relatively weak, the grating has integrated their intensities and shows them as one strong line. It is to be noted that the side components in the parallel polarization de-

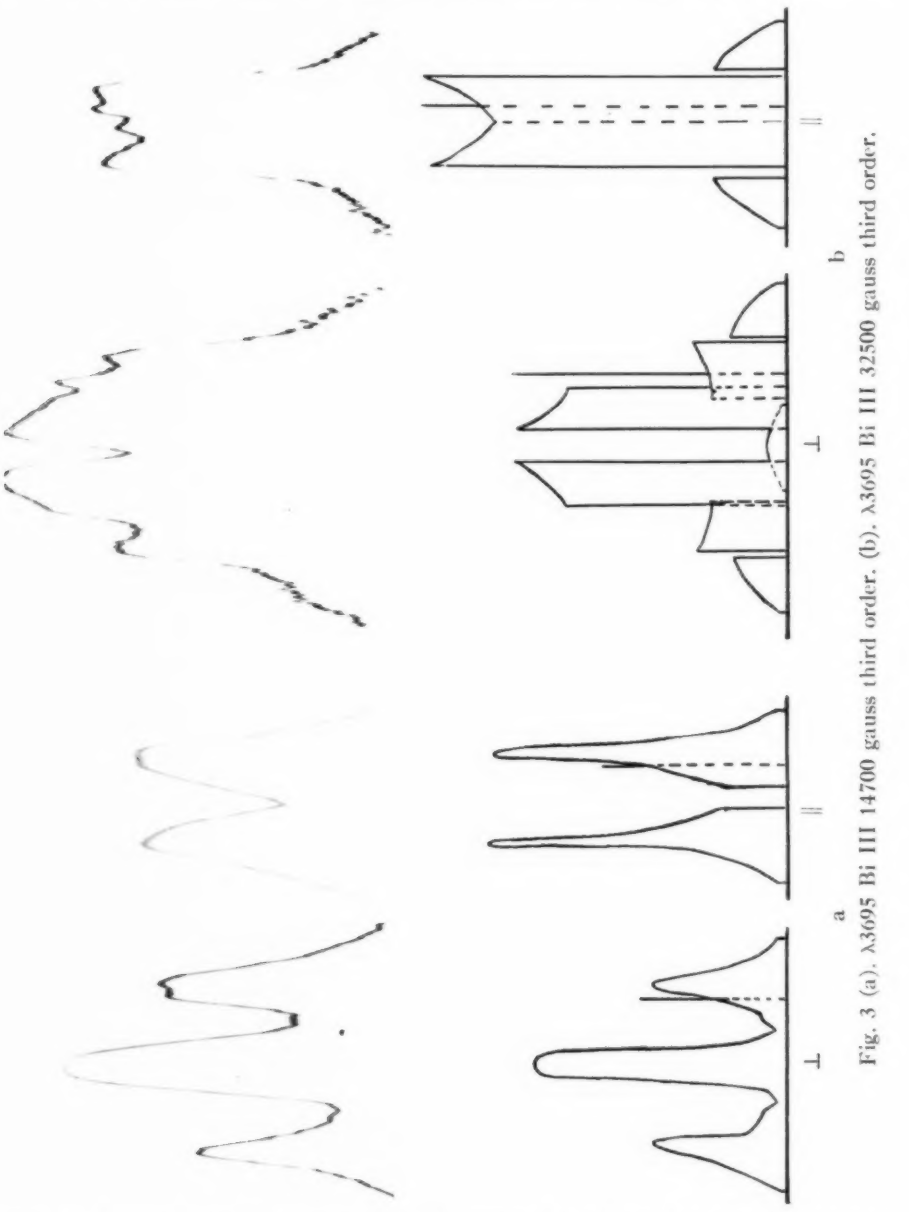

Fig. 3 (a). λ3695 Bi III 14700 gauss third order. (b). λ3695 Bi III 32500 gauss third order.

crease in intensity with increasing field strength, while the outside perpendicular components increase in intensity with increasing field strength. The side parallel components at 43350 gauss are barely perceptible on the photographic plate and their positions are very difficult to determine on the microphotometer record.

As representative lines in the spectrum of Bi III, we chose λλ4561 and 3695. These lines represent the transitions $7s^2S_{1/2}-7p^2P_{1/2}$ and $7s^2S_{1/2}-7p^2P_{3/2}$. These lines were also observed at the three field strengths used in the previous work, namely 14700, 32500 and 43350 gauss, and are represented in Figs. 2a, b,c and 3a b,c respectively.

λ 4561 in strong fields was completely resolved in the perpendicular polarization in the second order, as can be seen on the microphotometer record.

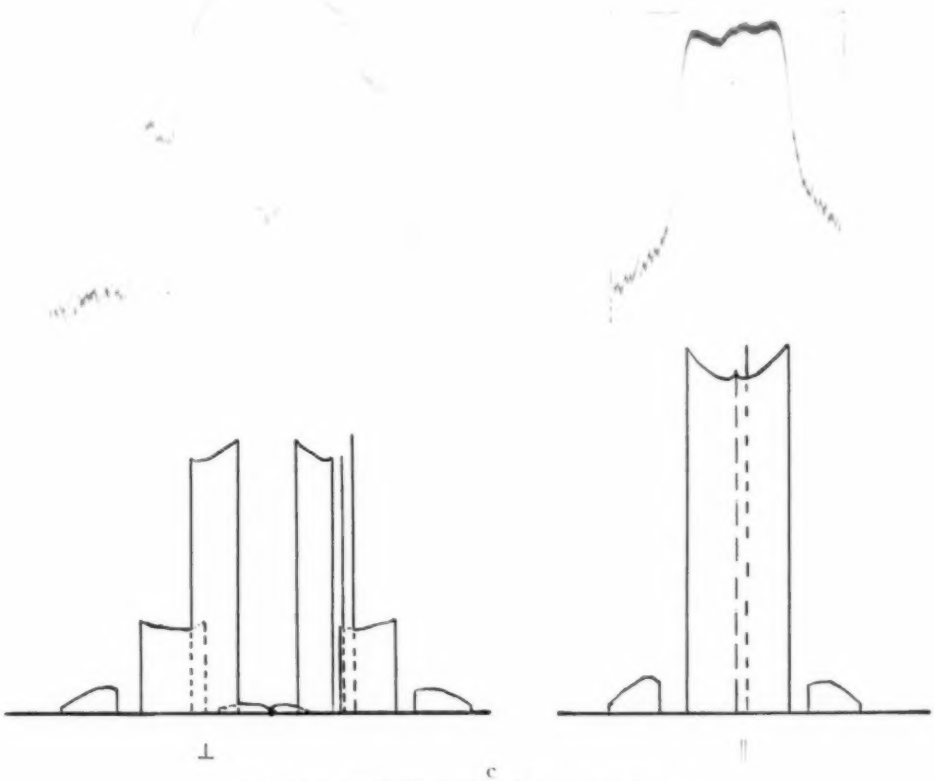

c

Fig. 3 (c). λ3695 Bi III 43350 gauss third order.

In the parallel components, the thing of interest to be noted is that the component marked with an arrow, the only resolvable component in this polarization, moves from the long wave-length group to the short wave-length group as the field strength increases, in complete accordance with the theory. The broad blocks on the computed patterns indicate groups of lines possibly resolvable by the grating but not by the phtographic plate. Fig. 2c shows the result of broadening the photometer slit. The parallel components were recorded with a very fine slit and show plate grain very noticably, while the perpendicular components were recorded with a wider slit, and the plate grain is hardly apparent, but the real breaks in the curve are also reduced so that in some cases they are barely perceptible.

Figs. 3a, b, c represent the results for λ3695 in the third order. The hyperfine separation of the $^2P_{3/2}$ term as given by Fisher and Goudsmit is very small, so that for this term, the approximate formula

$$E = m_j g\omega + A m_i m_j$$

sufficed to determine the energy levels. Here again, in the computed patterns, the blocks represent unresolved groups of lines. When a line sufficiently strong and separated from a group can be seen on the photometer curve, its position is also shown on the theoretical pattern. Unfortunately, the photometer curves are not nearly so rich as the patterns that could be observed with the eye. For example, in the perpendicular polarization for the strong field four sharp lines could easily be distinguished on the long wave-length side of the pattern, while only two show on the photometer curve; and three lines of the corresponding group on the short wave-length side could be separated from the pattern, while none appear on the photometer records. For the low field strength, the blocks on the theoretical pictures overlapped so badly that a sum curve was built and that is the one represented in the figure. This was also done for λ4561. The transition of one line in the parallel polarization from one side of the figure to the other is also noted here.

Here again, then, as in the case of Tl II and Tl III the present status of the theory of the Paschen-Back effect for hyperfine structure is verified in all of its details.

In concluding this work, it gives us great pleasure to acknowledge our thanks to Professors Geiger and Back for the privilege of working at Tübingen, and to the Rockfeller and Guggenheim Foundations for their financial assistance.

PHENOMENA IN OXIDE COATED FILAMENTS II. ORIGIN OF ENHANCED EMISSION

By J. A. Becker and R. W. Sears
Bell Telephone Laboratories, New York, N. Y.
(Received November 6, 1931)

Abstract

Various theories have been advanced regarding the mechanism of emission of electrons from oxide coated filaments. These theories postulate that; (1) the active layer is (a) at the outer oxide surface, (b) at the core-oxide interface; (2) the thermionic electrons come from (a) the adsorbed barium, (b) the oxide just underneath the adsorbed layer; (3) the current is carried through the oxide coating by (a) an entirely electrolytic process, (b) thermionic electrons which come from the core, diffuse through the pores of the coating and form a space charge therein, (c) electrolytic conduction through the oxide crystals and thermionic conduction between crystals, (d) electronic conduction, a small portion being carried by ions. A number of experiments were designed to test these various hypotheses. These experiments show that; (1) When barium is brought to the outer surface of the oxide, either by electrolysis or evaporation from an external source, the emission increases at first, passes through a maximum and then decreases. This change in activity is similar to that for barium on tungsten. (2) When oxygen is brought to the surface of the oxide of an activated filament, the activity decreases rapidly at first and then more slowly. (3) In these two respects, a filament with a core made of an alloy called "Konel" and consisting of nickel, cobalt, iron and titanium acts just like filaments with other cores. (4) When the oxide was stripped from a Konel core filament, the activity decreased by a factor of 6000. (5) The emission-limited current is independent of the area of the core provided that the area of the outer oxide surface remains constant. (6) The conductivity of the oxide varies with the time of sending current through the oxide. (7) The conduction current in the oxide obeys Ohm's law and does not saturate even though its value is hundreds of times larger than the saturated emission. (8) The oxide acquires a positive potential with respect to the core regardless of whether the space current is limited by space charge or by emission. This potential varies linearly with the space current drawn to the plate and is of the order of a few tenths of a volt. (9) The emission for the optimum amount of barium on the oxide surface depends upon the previous treatment of the oxide. From these results we conclude that; (1) The active layer is at the outer oxide surface. The activity depends on the concentration of barium and oxygen on this surface and also upon the amount of metallic barium dispersed through the oxide. The core material does not directly affect the emission but it does greatly affect the ease with which free barium is produced by heat treatment or electrolysis. (2) The thermionic electrons originate in the oxide just underneath the adsorbed barium. (3) Most of the current through the oxide is conducted by electrons, a small portion being carried by barium and oxygen ions.

Introduction

In 1929 one of us proposed a comprehensive theory to account for the complex phenomena observed in oxide coated filaments.[1] The essential points of this theory were: The activity depends upon the concentration of barium[2]

[1] Becker, Phys. Rev. **34,** 1323–1351 (1929).

[2] Throughout this article the word "barium" will be used for barium and / or strontium and / or calcium.

and oxygen on the surface of the oxide and on the composition of the coating. Both barium and oxygen diffuse quite readily from the surface into the oxide and vice versa. When current passes through the oxide most of it is carried by electrons, but a small portion is carried by oxygen and barium ions.

Since that time we have enlarged or extended the theory or made it more explicit. Others too have proposed theories which, in some respects, conflict with ours. Insofar as these extensions or conflicts deal with the production of the barium or the conduction of current through the oxide, they have been dealt with elsewhere.[3] The present article will deal with the question: Where do the thermionic electrons originate?

It has been quite generally held that these electrons come from the region near the outer oxide surface. Recently, however, in two important papers it has been proposed that the electron space current is or may be limited by the emission from the metallic core surface of the filament. Lowry[4] states that, "the source of emission is assumed to be a layer of metallic barium occluded on the surface of the base metal or alloyed with it". He further postulates that "the electrons emitted from this composite surface must diffuse through the pores of the coating". Reimann and Murgoci[5] believe that electrons are thermionically emitted from the core to an adjoining oxide crystal and from one oxide crystal to the next. In each crystal the current is carried exclusively by barium ions. The barium atoms adsorbed on the surface of the outermost oxide crystals emit the electrons which pass to the plate. They conclude that the observed current may be limited by "whichever of the two systems (core or oxide surface) has the lesser emissivity".

Koller,[6] Rothe,[7] Detels,[8] Espe,[9] Becker,[1] Schottky,[10] Gehrts,[11] Huxford[12] and others believe that the emission depends upon the concentration of barium on or very near the surface of the oxide and that the core surface does not determine or limit the emission. There are differences of opinion, however, concerning the origin of the thermions near the oxide surface. Some believe that the thermions come from barium atoms adsorbed on the oxide; that the activity is proportional to the concentration of this adsorbed barium; and that the work function is the same for all appreciable concentrations of barium. Others believe that the thermions originate in the oxide just beneath the surface and that the absorbed barium makes it easier for them to escape from the surface. On this view the work function depends on the concentration of barium and the activity is not directly proportional to this concentration.

In order to decide between these various theories we have designed and

[3] Becker, Trans. Amer. Electrochem. Soc. **59,** 207–220 (1931).
[4] Lowry, Phys. Rev. **35,** 1367–1378 (1930).
[5] Reimann and Murgoci, Phil. Mag. **9,** 440–464 (1930).
[6] Koller, Phys. Rev. **25,** 671–676 (1925).
[7] Rothe, Zeits. f. Physik **36,** 737–758 (1926).
[8] Detels, Jahrb. d. drahtl. Telegr. u. Teleph. **30,** 10–14 and 52–60 (1927).
[9] Espe. Zeits. f. techn. Physik **10,** 489–495 (1929).
[10] Schottky, See Wien-Harms Handbuch der Physik, Vol. XIII, part 2.
[11] Gehrts, Zeits. f. techn. Physik **11,** 246–253 (1930).
[12] Huxford, Phys. Rev. **38,** 379–395 (1931).

performed a number of crucial tests. These were so chosen that the predictions based on one theory were distinctly different from those predicted by some other theory. The first group of tests was designed to decide between the core-surface or the oxide-surface theory; the second group was intended to decide whether the electrons come from the adsorbed atoms or the underlying oxide. We shall describe these tests and discuss the deductions based on them and on tests described by others.

The experiments were conducted in radically different types of tubes. A description of each tube will be given in connection with the particular tests performed with it.

All of the tubes were evacuated on a four-stage mercury diffusion pump. During the pumping, which usually consumed two or three days, a tube was baked, the metal parts were outgassed and the tube was rebaked. The filaments were glowed at suitable temperatures until they were completely outgassed. The tubes were sealed from the pumps with the metal parts quite hot while the pressure was about 1×10^{-6} mm of Hg. All of the tubes contained auxiliary thoriated tungsten filaments which were used as "clean-up filaments" for several days or weeks after seal-off, until the pressure was about 3×10^{-8} mm of Hg or less, even when the oxide coated filaments were glowing.

The oxide coated filaments consisted of a mixture of barium and strontium carbonates, in a suitable suspension, coated on a metallic core. The carbonates were decomposed to the oxides by glowing while the tubes were on the pumps.

The Effect of Barium on the Emission

In a previous article[1] it was shown that the activity of an oxide coated filament changes as barium is put onto the outer oxide surface either by evaporation from an external source or by electrolysis of the oxide itself. From such results the conclusion was drawn that the source of the enhanced emission was at the outer oxide surface or within the oxide very close to the surface. The experiments were conducted with filaments having platinum and nickel cores. It has been reported[4] that oxide coated filaments having cores made of an alloy called "Konel" and consisting of nickel, cobalt, iron and titanium behave differently from filaments with other cores. It was therefore deemed advisable to repeat these experiments with a Konel core filament.

These experiments were conducted in a tube containing an oxide coated Konel filament and an auxiliary filament which could be used either as a source of electrons or as a source from which barium would evaporate under the proper conditions. A cross section of the tube showing the relative arrangement of filaments and plates is shown in Fig. 1. F_1 and F_2 are ribbon filaments mounted parallel to the plates P. F_1 is an oxide coated Konel filament and F_2 a barium-platinum alloy filament. The filaments F_3 were of thoriated tungsten. S is a shield between F_1 and F_2 extending along their entire length. When it was desired to evaporate barium from F_2 onto F_1, the shield could be removed into position S' by tilting the tube.

In these experiments, tests of the activity of the coated filament were made after subjecting the filament to various treatments. These treatments

consisted in: (1) Sending various amounts of current into the coated filament from the auxiliary filament F_2, (2) subsequent glowing of filament F_1 at various temperatures, (3) evaporating various amounts of barium onto F_1 from F_2, (4) subsequently glowing F_1 at various temperatures.

The results are shown in Fig. 2 which is a plot of the emission current in amperes on log scale at a filament temperature of 500°K versus the time of subjecting the filament to the various treatments. The coated Konel filament was conditioned initially by glowing at a temperature of 1100°K until the emission reached an equilibrium value. Then a current of 450 microamperes was sent into the cold coated filament from the auxiliary filament F_2. After various intervals the current was stopped and the activity of the coated filament determined at a temperature of 500°K. The activities at these intervals are shown on the curve by the black dots. The activity increased at first until

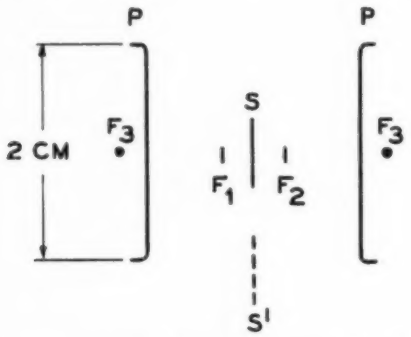

Fig. 1. Arrangement of plates and filaments in tube-152-S.

it reached an optimum value after which it decreased but at a slower and slower rate. A total of 7200 microampere minutes was sent into the coated filament.

The second treatment consisted in glowing the coated filament at 1040°K and later at 1100°K. The activity was again determined periodically at the testing temperature. The values of the activity thus obtained are shown on the curve by the first set of circles. The activity increased back to the optimum value and then decreased. The glowing at 1100°K caused the activity to fall rapidly to its equilibrium value.

The third treatment consisted in evaporating barium onto the surface of the cold coated filament. This was accomplished by removing the shield and glowing the auxiliary filament F_2 at a suitable temperature. During this evaporation no current passed between the two filaments. At intervals the evaporation was stopped and the activity determined as in the previous experiments. The activities at the various times of evaporation are shown on the curve by the crosses. The activity increased initially until it reached an optimum value after which it decreased. An increase in the rate of evaporation from the auxiliary filament increased the rate at which the activity decreased.

The last treatment consisted in glowing the coated filament at 1040 and 1100°K as before. The activities at the various intervals of glowing are shown

by the second set of circles. The activity again increased to an optimum and then decreased to an equilibrium value.

Several auxiliary tests were made on this filament to show that the phenomena observed in Fig. 2 were caused directly by the treatment. The testing temperature of 500°K was sufficiently low that glowing or drawing testing currents at this temperature did not change the emission, regardless of the state of activation.

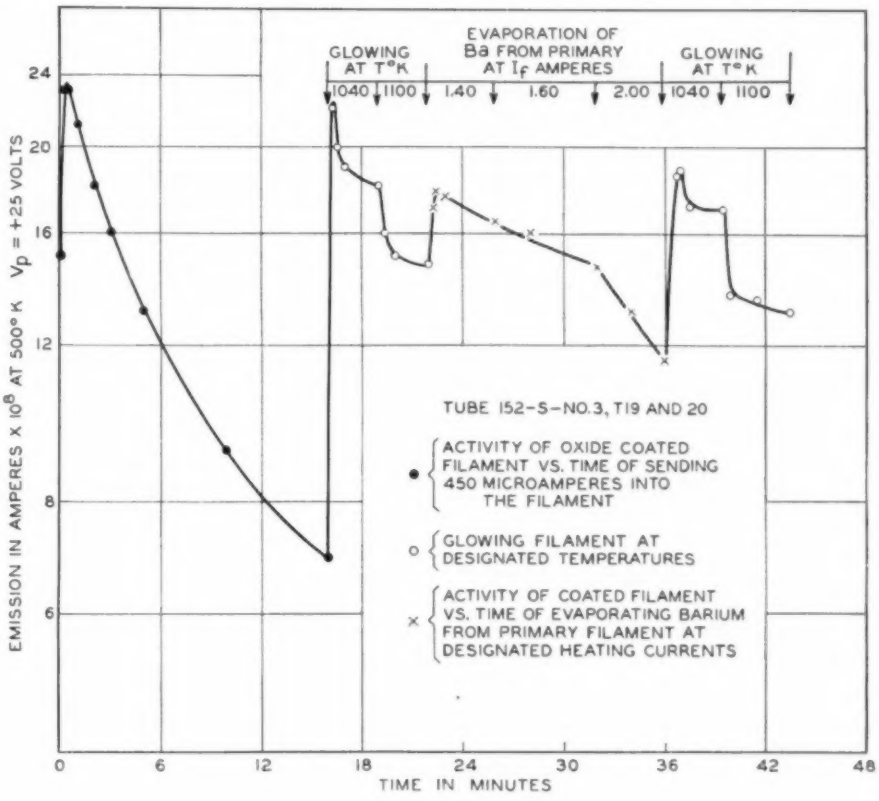

Fig. 2.

That the changes in emission, when electrons were sent into F_1, were due only to the action of the current entering the filament, was demonstrated in two ways. If the potentials of the various electrodes in the tube were arranged so that no electrons reached F_1 even though electrons left F_2, the activity of F_1 was not altered. In the second place, the change in activity of F_1 was the same whether the shield was between F_1 and F_2 or not, provided only that the current into F_1 was the same in the two cases. The insertion of the shield would prevent barium from reaching F_1, even if it did evaporate from F_2.

This last fact was demonstrated by inserting the shield when the temperature of F_2 was such that barium did evaporate from it. In that case the activity of F_1 was not affected until the shield was removed.

It should be noted that in order to obtain reproducible results when barium was evaporated onto the coated filament, it was necessary to have the pressure less than 5×10^{-8} mm of Hg. This is due to the fact that at higher pressures the rate of adsorption of gas atoms and molecules is appreciable. Such adsorbed gas will, of course, alter the activity. It was also necessary to have the platinum-barium alloy filament well conditioned in order that barium and only barium evaporated.

The results of the experiment shown in Fig. 2 can readily be interpreted on the view that the emission is dependent upon the amount of barium on barium oxide. When electrons are sent into an oxide coated filament, the direction of the electrolysis of the oxide is such that the barium ions travel toward the outer surface. Since the changes in emission noted in this experiment were caused by electrons entering the filament, we conclude that the emission changed as various amounts of barium were deposited on the oxide surface. As more and more barium was deposited on the surface the emission increased until it reached an optimum value, after which it decreased. Glowing the filament at 1040°K caused this excess of surface barium to diffuse into the interior of the oxide or to evaporate. The emission, therefore, increased back through the optimum value. Glowing at 1100°K caused the emission to decrease to its equilibrium activity on glowing at that temperature.

This interpretation is confirmed by the second part of this experiment in which barium was evaporated directly onto the oxide surface. The emission changed as the surface concentration of barium changed. As the amount of barium on the surface increased, the emission increased to the optimum value and then decreased just as in the previous case where barium was put on the surface by electrolysis. Subsequent glowing at 1040 and 1100°K again caused this barium to diffuse into the oxide or to evaporate. This in turn caused the emission to increase back to the optimum and then decrease to an equilibrium value.

The first two optima in Fig. 2 have the same value. From this we may conclude that the entire oxide surface was uniformly covered with barium. Presumably the electrons entered the coating from all directions and deposited barium uniformly over the entire surface. The optimum obtained by evaporation of barium onto the surface was less than these optima. The reason is that barium was evaporated onto only one side of the filament. Consequently, the emission from the back side of the ribbon remained constant while that from the front side increased to the optimum. The ratio of the first and third optima in Fig. 2 is of the proper magnitude to agree with this interpretation.

The last optimum emission on glowing at 1040°K was slightly higher than the optimum which just preceded it. After barium had been evaporated onto the ribbon, the front side was covered beyond the optimum while the back side was covered with less than the optimum amount of barium. The fourth optimum in Fig. 2 was slightly higher than the third because during the initial stages of glowing at 1040°K some of the barium from the front side migrated to the back side of the ribbon and increased the barium concentration there.

Thus far we have interpreted the changes in activity when current was

sent into the oxide coated filament in terms of the barium deposited at the outer oxide surface by electrolysis. The oxygen deposited near the core was assumed to have no effect on the activity. This assumption can be verified by comparing the results when the oxide was electrolized with those obtained when barium was evaporated onto the oxide surface. The third optimum in Fig. 2, when corrected for the fact that barium was evaporated onto only one side of the ribbon, is equal to the first optimum. Since oxygen was deposited near the core face in one case and not in the other we conclude that oxygen on the core face does not affect the activity.

Our observed changes in activity when barium was made to appear or to leave the surface of the oxide are qualitatively similar to those observed for barium on tungsten. They are strikingly different, however, in one respect. For barium on tungsten, the optimum activity is thousands of times greater than that for clean tungsten, while for the cases of barium on the oxide discussed above, the optimum activity is less than twice the initial activity. This dissimilarity is due to the fact that when an activated oxide filament is glowed at moderate temperatures, its surface is not freed from adsorbed barium. In fact, the surface in some cases may be nearly completely covered, as was shown in a previous paper.[1]

These results do not seem to be readily interpretable on the view that the emission is determined by the amount of barium on the core face. The testing temperature was so low that the barium could not have diffused into the oxide and increased the barium concentration at or near the core. The observed changes in emission were, therefore, not due to any change in the system at or near the core surface but must have been due to changes in barium concentration on the surface of the oxide.

The Effect of Oxygen on the Emission

Whether the emission is determined by the core surface or oxide surface can also be tested by observing the effects of oxygen on the emission. It has been shown[1] that if oxygen is brought to the surface of an active oxide coated platinum-nickel core filament, the activity decreases. The effect is the same whether the oxygen is deposited by evaporation from an external source or whether it is produced by electrolysis of the oxide. From these experiments it follows that in active filaments with a platinum nickel core, the emission is determined by the outer oxide surface. We have used a Konel core filament in repeating the experiments in which oxygen is brought to the surface by electrolysis.

These experiments were performed in a tube of the same type as that used in studying the effect of barium on the emission and shown in Fig. 1. As emission-limited current was drawn from the coated filament to the plates, the activity decreased rapidly and then more and more slowly. This is illustrated in Fig. 3. Curve 1 shows how the emission current decreased as current was drawn to the plates at a temperature of 660°K and a plate potential of 100 volts. At intervals, during this drawing of current, the activity was tested at a lower temperature, 500°K. Curve 2 shows how the activity under the nor-

mal testing conditions decreased with the time that current was drawn at a temperature of 660°K. The activity at the testing temperature decreased by a factor of ten. The filament was then glowed at 770°K and the emission increased rapidly at first and then more and more slowly as shown by curve 3. The glowing temperature was finally raised to 900°K and the activity increased back to its normal value as shown by curve 4.

These results are very similar to those previously found with a platinum-nickel core filament as can be seen by comparing Fig. 3 of this paper with Fig. 10 of the previous paper.[1] From this it seems clear that the behavior of coated filaments with Konel cores is not essentially different from that in filaments with platinum-nickel or platinum-iridium core. In both cases the decrease in activity is due to oxygen on the surface. This means that the thermionic emission is determined by the condition of the outer oxide surface.

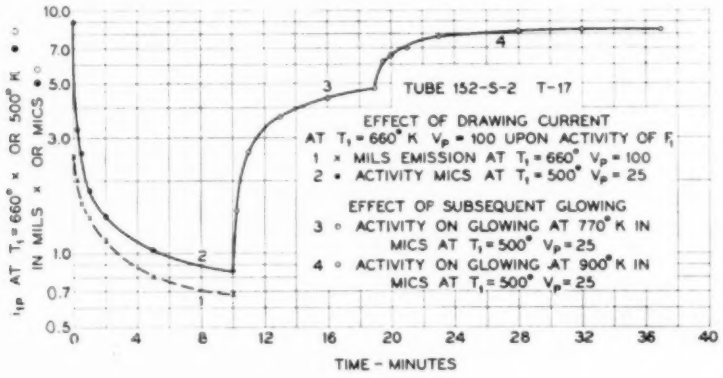

Fig. 3.

These time changes caused by the electrolytic deposition of oxygen are obtained most readily at moderate plate currents and moderate temperatures. However, in vacuum tubes operating normally, heavy currents are usually drawn from the filament to the plate at temperatures around 1050°K. Under these conditions the activity usually remains quite constant with the time of drawing current. There are two reasons for this: (1) The currents are usually limited by space charge and the proportion of current in the oxide carried by ions is very small.[1] (2) At this temperature the rates of diffusion of barium and oxygen in the oxide are high so that the oxygen and barium ions upon becoming neutralized at or near the outer oxide and core surfaces respectively diffuse quite rapidly back into the oxide.

Effect of Removing Oxide Coating

The next type of experiment was designed to make a test of the hypothesis that the enhanced emission is due to barium adsorbed on the core surface. On this view, if the oxide were removed from the core, the emission should be at least as great as before. The tube used for this test consisted of two parallel plates, in the center of which was placed an oxide coated filament with a

Konel core. The filament was in the from of a ribbon approximately 0.125 cm (50 mils) wide. The adherence of the coating to the core of this particular filament was exceptionally poor so that if the filament was subjected to a mechanical vibration or strain, the coating would completely peel off.

The experiment consisted in observing the activity before and after the coating was removed. The filament was activated initially by glowing. The activity of the coated filament on glowing for a number of hours at approximately 1050°K is shown by power-emission line *A* in Fig. 4. After this activity was observed, the filament was cooled to room temperature and the tube

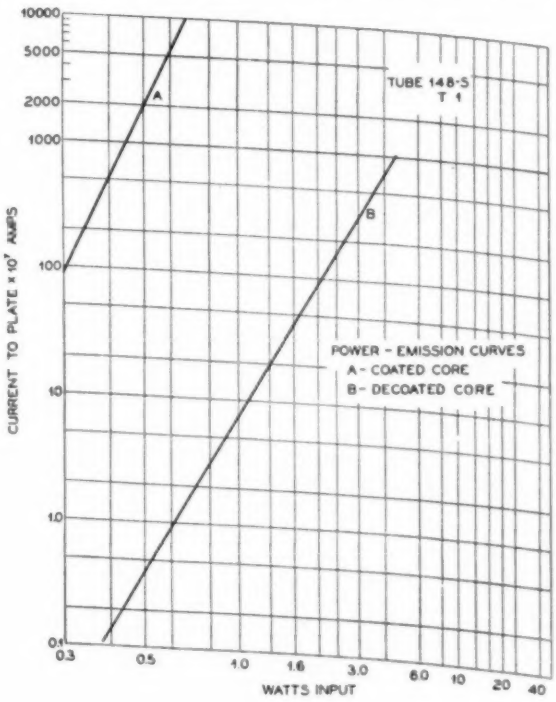

Fig. 4.

jarred. This caused all of the coating to fall off. The activity was again measured at low temperatures and is shown by power-emission line *B*. The activity decreased by a factor of about 6000. Subsequent glowing of the decoated core failed to change the emission appreciably. The decoated core was of a greyish appearance due to the usual oxidation of the core metal during the treatment of the filament.

Power-emission line *B* was taken at temperatures sufficiently low that barium could not have evaporated from the decoated core surface had it been there directly after the removal of the oxide. It is known that barium will not evaporate from a tungsten surface even at much higher temperatures than those used in determining line *B*.[13]

The results of this experiment can readily be interpreted on the view that

[13] Eglin, Phys. Rev. **31**, 1127 (1928).

the emission is dependent upon the amount of barium on barium oxide. The large decrease in emission was due to the loss of the oxide coating which carried the outer oxide surface of low work function with it.

The large decrease in emission is not in accord with the view that the emission is determined by the amount of barium adsorbed on the core face unless the assumption is made that the barium adsorbed on the core adheres more tenaciously to the oxide than to the core and that when the oxide and core are parted, the barium chooses to remain with the oxide. We know of no way of testing such an assumption. We do know that barium sticks tenaciously to both metallic and oxide surfaces. It seems quite probable, therefore, that some of the barium should have remained on the core. If the core had been

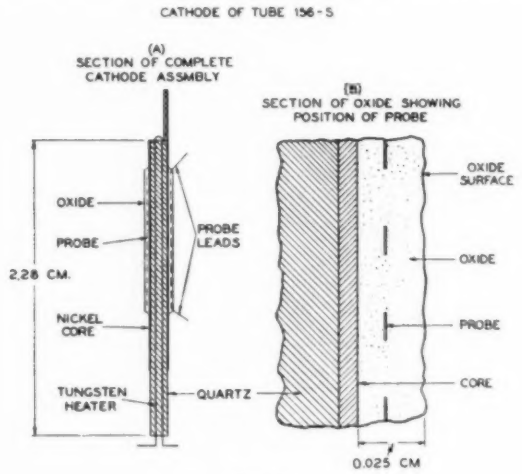

Fig. 5.

"active" when the coating was present it should have been partially "active" when the coating was removed and subsequent glowing at high temperatures should have changed the activity.

Effect of Changing the Area of Supposed Emitter

On the view that the electrons are emitted thermionically between core and coating, the current that reaches the plate may be limited by the number of electrons that are able to leave the core. If the area of the metallic core surface, from which the electrons are supposed to escape, could be reduced, the emission should be reduced proportionately. On the other hand, if the emission is limited by the external oxide surface, it should not change when the area of the core surface is changed.

Such an experiment was conducted in a tube containing an equipotential cathode cylinder coated with a mixture of barium and strontium oxide in which was embedded a metallic ribbon or probe completely insulated from the core. An enlarged cross-section of the cathode is shown in Fig. 5A. An indirectly heated cathode was employed, consisting of a tubular nickel core covering a quartz rod in which was a tungsten heater wire. The nickel core

was coated with a layer of oxide; then a 0.0025×0.0127 cm (1×5 mil) nickel ribbon, which had previously been coated with a layer of oxide, was wound helically about the coated core and the whole coated over with a second coat of oxide. A much enlarged cross-section of the oxide showing the relative positions of core, nickel ribbon or probe and oxide, is shown in Fig. 5B. The area of one side of the probe is equal to about one-third of the area of the core. The cathode assembly shown in Fig. 5A was placed in the axis of three cylindrical anodes, 1.5 cm in diameter. The outside two cylinders are 0.8 cm and the central collector 0.6 cm long. Six thoriated tungsten filaments were placed outside of these collectors for use as clean-up filaments.

The experiments consisted in measuring the emission from the cathode to the plate when the negative terminal of the battery was connected to: (1) the core with the probe floating, (2) the probe with the core floating and, (3) both core and probe. The metallic surface areas are as 1, 2/3 and 5/3.

The results of this test are shown in Table I. The emission currents, when the negative terminal of the battery was connected to the core, probe, and core and probe together are given for several different temperatures. At any temperature, the emission currents in all three cases are practically equal.

TABLE I.

Temp. °K	Emission current in amps. with 40 volts applied between plate and		
	Core (Probe floating)	Probe (Core floating)	Core and probe
545	4.85×10^{-8}	4.78×10^{-8}	4.80×10^{-8}
643	3.06×10^{-6}	2.84×10^{-6}	2.98×10^{-6}
711	2.42×10^{-5}	2.14×10^{-5}	2.31×10^{-5}

These results cannot be interpreted on the view that the electron current is limited by emission from the core. Since the current "emitted" from the core alone was equal to the current "emitted" from the probe alone, one would certainly expect the resultant emission, when the plate battery was connected to both core and probe, to be appreciably larger than the emission from either one alone. This was not verified as can readily be seen from the table.

On the other hand the results are to be expected on the view that the electrons are emitted thermionically from the external oxide surface. The emission was the same in all three cases simply because the area of the outer oxide surface was unchanged.

OXIDE CONDUCTIVITY

Reimann and Murgoci[5] have investigated the variation of the conduction current between two coated filaments, twisted together, with the potential. They found that the current varied linearly with the voltage at low current densities but sometimes showed incipient saturation at potentials of a few volts. They state that, "at current densities comparable with those in the coatings of oxide cathodes from which saturated thermionic space current is being taken, the current conducted through an oxide powder between two electrodes, embedded therein, also saturates". From this they conclude that

the conduction current in any individual oxide crystal obeys Ohm's law and that the current is carried by thermionic electrons between the various crystals and between core and oxide. At low current densities, the currents across the gaps are limited by space charge and most of the potential drop is across the oxide crystals. This accounts for the linear portion of their curves. At high current densities, the current is limited by thermionic emission in one or more gaps. This interpretation is the basis of their conclusion that there is a limitation of thermionic space current, "between the core metal and coating or within the coating itself".

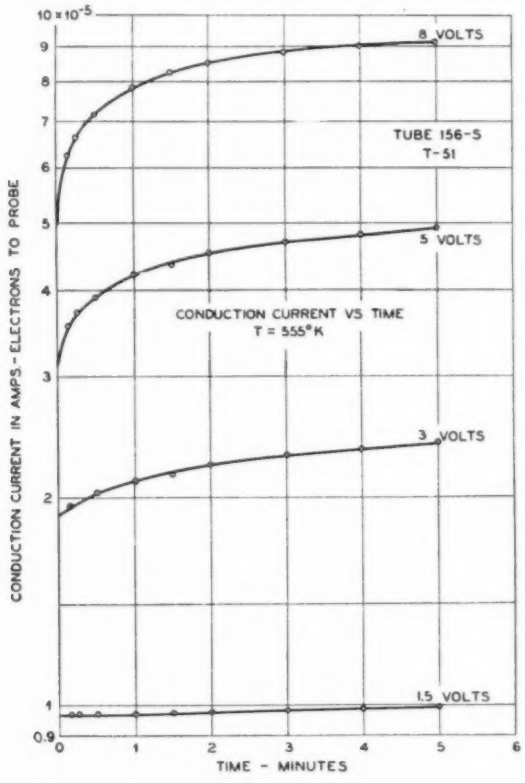

Fig. 6.

Due to the importance of this experiment, we have repeated their measurements with an improved design of tube. The tube contained the special equipotential cathode shown in Fig. 5. and was described in the preceding section.

The measurements consisted in noting the value of the conduction current when various potentials were applied between core and probe. It was found that as long as the currents and voltages were small, Ohm's law was obeyed, but if the applied potential was more than about one volt, the conduction current sometimes varied with the time. When the conduction current varied with the time, it always increased at a fast rate initially and then more and more slowly. In some cases it increased to an optimum value and

then decreased but did not fall below its initial value. The increase of conduction current with time is illustrated in Fig. 6. The conduction current on a logarithmic scale is plotted against the time that electrons were flowing from the core to probe at a temperature of 555°K. Four curves are shown for potentials between the core and probe of 1.5, 3, 5 and 8 volts. After each of these curves, the cathode was glowed for ten minutes at 555°K with no potentials applied. The curves were reproducible, showing that this glowing was sufficient to bring the oxide back to its initial condition. The conduction current always increased with time until at the end of five minutes it had reached an almost constant value. The phenomenon is attributed to an increase in oxide conductivity due to an accumulation of the products of electrolysis in the oxide. A more detailed study of this phenomenon is now in progress.

A current voltage curve can be obtained from the data of Fig. 6. Such a curve is shown in Fig. 7. Curve *A* was obtained by plotting the initial values of

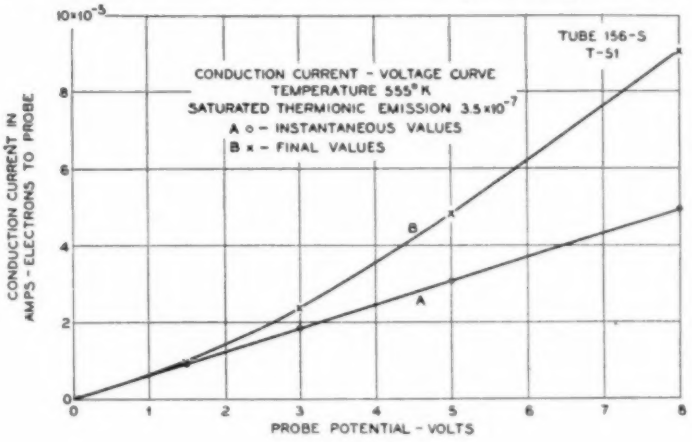

Fig. 7.

the conduction current against the applied potential. The points form a good straight line indicating that the oxide obeys Ohm's law. The final values of conduction current gave curve *B* which is concave toward the current axis. There is no indication of current saturation as reported by Reimann and Murgoci even though the current density at the highest potential is 300 times larger than the total saturated thermionic emission at this temperature. For these cathodes there can be no limitation of thermionic space current at the core face or in the oxide.

This particular test has been made on three cathodes with the same result. Furthermore we have never found a case in a large number of different types of coated filaments in which the behavior indicated such a limitation of thermionic current at the core surface. We therefore believe that the reported deviations from linearity may be attributed to changes in conductivity with time or to polarization since we have found the shape of our current voltage curves to be affected by these factors. It may also be that two filaments twisted together actually do form a gap in the oxide and that the current is limited at this gap.

Potential Distribution in the Oxide

By means of the probe it is possible to test whether the electrons are emitted thermionically from the core and then drift through the pores of the oxide where they form a pseudo space charge. On this view the probe should sometimes be negative with respect to the core and the probe potential should not vary linearly with the current emitted to the plate. On the other hand, if the electrons are emitted thermionically from the outer oxide surface and if they

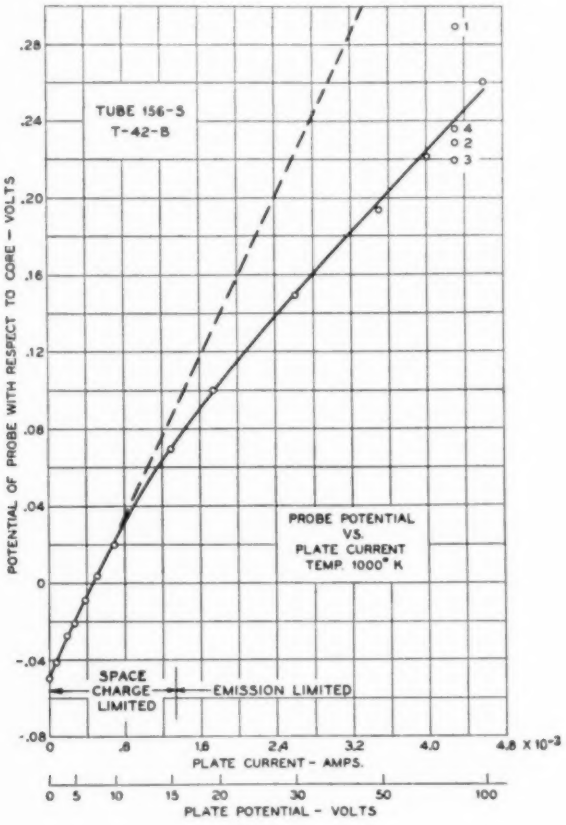

Fig. 8.

pass through the oxide as they would through a metal of high resistivity, the probe should always be positive with respect to the core and the probe potential should be directly proportional to the current through the oxide. Furthermore the ratio of the probe potential to the plate current should give the resistance of the oxide between the core and probe. The value of this resistance should agree with that determined in the conductivity measurements described above.

In the experiments to differentiate between these views, the potential of the probe in the oxide was measured as current was drawn from the core to the plate. A null method was used in measuring the probe potential. The results are illustrated in Fig. 8, which is a plot of the potential of the probe with re-

spect to the core versus the current to the plate in amperes at a temperature of 1000°K. The current to the plate was varied by changing the plate potential. The values of plate potential are indicated in Fig. 8 below the current values. The current was limited by space charge up to approximately 1.2 milliamperes. When the current was limited by emission, the current varied with the plate potential because of the characteristic poor saturation of these oxide cathodes.

These data show that the oxide is positive, regardless of whether the current reaching the plate is limited by space charge or by emission, as was predicted on the basis of our theory. However, the observed curve differs from the predicted in two respects.

In the first place the curve does not pass through the origin. When the plate current is zero, the probe has a negative potential with respect to the core. Since there is a constant flow of energy across the oxide, there must exist a temperature difference between the core and probe. The intercept, therefore, measures the thermal e.m.f. generated by the two nickel-barium oxide junctions at the two temperatures. The temperature difference is estimated to be something like 20 degrees. All of our conduction current voltage curves show this intercept. It does not appear in Fig. 7, however, due to the low temperature and the large voltage range plotted.

That the intercept is due to a thermal e.m.f. was demonstrated in the following manner: The core and probe were connected together through a variable resistance and a galvanometer. The current indicated by the galvanometer was changed by varying the external resistance. A plot was made of the reciprocal of the current versus the external resistance. The plot gave a straight line relation whose slope was equal to the floating probe potential at this temperature. Furthermore, the oxide resistance, as determined from this plot, agrees with the resistance determined from the slope of a current voltage curve at this temperature. This means that the core-oxide-probe system acts just like a source of e.m.f. with a definite internal resistance. The value of the e.m.f. or resistance varies with the temperature. It was found that the intercept of Fig. 8 varied linearly with the power input to the cathode as is to be expected if the temperature difference between any two points in a medium conducting heat is directly proportional to the rate at which energy flows through the medium.

The second deviation from the predictions is the fact that the curve in Fig. 8 is linear only in the region which is well defined by space charge. Over the portion of the curve in which the current is limited by emission, the potential increases more slowly than the current. This is due to the fact that the probe potential varies with the time and the points shown on the curve represent equilibrium values. Thus, when the plate current was suddenly changed from a low value to 4.3 milliamperes, by raising and maintaining the plate potential to approximately 80 volts, the probe potential changed rapidly with time, as illustrated by points 1, 2, 3 and 4, which were taken 5, 25, 80 and 300 seconds respectively after the plate current was increased.

This phenomenon is the same as that observed when conduction current

is drawn between core and probe and which was described above. If instantaneous values of probe potential had been taken, the straight dashed line would have been obtained. The slope of this line represents the resistance of the oxide between the core and a point in the plane of the probe.

If this interpretation is correct, the resistance as thus determined should be somewhat less than the resistance obtained from the initial line of a conduction current-voltage curve at the same temperature. From Fig. 8 the oxide-resistance is 105 ohms. The resistance determined from the slope of a conduction current voltage curve at the same temperature is 268 ohms. The ratio of these resistances is 2.65. At a temperature of 756°K, the resistance obtained from the probe potential plate current curve is 0.54×10^4 ohms and the resistance determined from the slope of the conduction current-voltage curve is 1.15×10^4 ohms. The ratio between these resistances is 2.12. Since the ratios of the cross-sections of the current paths in the two types of curves is somewhat greater than 1 and somewhat less than 3, it is to be expected that the ratio of the resistances would be somewhere between these values. The observed ratios 2.65 and 2.12 are entirely reasonable. Furthermore, the plate current-probe potential curves are similar to the conduction current-voltage curves as regards their deviation from linearity. This deviation from linearity occurs at the same potential difference between core and probe for the two curves. The magnitude of the deviation at any probe potential is approximately the same in the two cases.

These results fully confirm the prediction that the potential of a point in the oxide with respect to the core should be positive and should be directly proportional to the current through the oxide. It is therefore reasonably certain that the electrons pass through the oxide as they would through a metal of a high resistivity and that they do not become occluded on the oxide particles and thus set up a pseudo space charge.

The conclusion that the active layer is on the oxide surface and that the current is not carried thermionically between core and coating is based thus far on tests in special experimental tubes. It can be extended to numerous other tubes by a consideration of the potential distribution between two insulated bodies both of which are thermionic emitters. Let us assume that the electrons are transferred thermionically from the core to the coating and then reemitted thermionically from the coating to the plate. Let us further assume that the electron emissivity of the core is considerably less than that of the coating. Before any potential is applied to the plate, the potential of the oxide will differ from that of the core by a potential equal to the contact potential difference at the core-oxide interface. At the instant when a positive plate potential is applied, the coating will give up more electrons to the plate than it receives from the core. Consequently the coating will become positively charged with respect to the core and the potential difference between coating and plate will decrease. As long as this potential difference between coating and plate is sufficient to keep the current from the coating saturated, the electron emission from the coating will exceed that received by the coating, and the coating will become more and more positively charged. This process

will continue until the current from the coating is limited by space charge and is just equal to the emission limited current from the core to the coating. When this steady state is reached, an appreciable part if not most of the potential difference applied between core and plate will be used up between the core and the coating. Consequently, when the space current is limited by emission; (1) the potential of a probe embedded in the oxide should be an appreciable fraction of the applied potential; (2) an appreciable part if not the major part of the energy dissipated in the tube should be dissipated in the coating, which should consequently get very hot.

These predictions are not confirmed by experiment. The data for Fig. 8 show that the probe potential is only about 0.3 volt even when the plate potential is 100 volts and even this 0.3 volt is to be ascribed to an iR drop rather than to a potential difference across the core-oxide interface. Furthermore, it is a well-known fact that in commercial tubes, a negligible part of the energy represented by the product of the space current and the applied plate potential is dissipated in the filament. It is only in unusual filaments with very thick, shaggy coatings that any appreciable part of the applied potential is used up in the oxide and in this case the resistance of the coating is sufficient to account for the energy dissipated in the filament. These facts make it appear improbable that the emission is ever limited by the core in ordinary oxide coated filaments.

Do the Electrons Come from the Adsorbed Barium Atoms or from the Underlying Oxide?

While it is obviously impossible to observe directly whether the emitted electrons come from the adsorbed barium or from the underlying oxide, nevertheless experiment can indirectly decide between these two views. The predictions made on these two views are quite distinct and can be tested by experiments.

If the thermions come from the adsorbed barium, the activity or emission current at a fixed temperature should be directly proportional to the number of monatomically adsorbed atoms and should increase steadily from a low value characteristic of a bare surface to a value characteristic of solid barium. On the other hand if the electrons come from the underlying oxide and if the barium is ionized and thus helps the electrons escape, one might reasonably expect the activity to increase at a rate which is much more than proportional to the concentration of adsorbed barium and that it might reasonably reach an optimum value for a monatomic layer before it decreases to its value characteristic of sold barium. Of course, eventually as the concentration of barium increases, the electrons must originate in the barium.

The experiments described above and in previous publications in which barium was deposited on the oxide surface either by electrolysis or by evaporation from an outside source, decidedly favor the second hypothesis and definitely contradict the predictions of the first hypothesis.

The behavior of barium on the oxides is strikingly similar to that of barium on tungsten. In both cases as the surface concentration increases log i

increases rapidly at first then more and more slowly, passes through an optimum and then decreases to approach the value for solid barium; when the surface concentration is subsequently decreased, log i again increases to the same optimum and then decreases toward its original value. This striking similarity in behavior points to a similarity in the mechanism of emission in the two cases.

For a layer of barium or other electropositive elements adsorbed on tungsten, it is generally held that at least some of the adsorbed barium is ionized and that the emitted electrons come from the underlying tungsten rather than from the adsorbed barium. On this adion grid theory one can readily explain: (1) Why the work function decreases,[14] passes through a minimum and then increases,[15] (2) why the contact potential changes correspondingly,[14] (3) why the current voltage curves saturate poorly if the surface is not uniformly covered,[16] (4) why the barium sticks to the tungsten at relatively high temperatures,[15] (5) why the adsorbed elements sometimes come off as positive ions,[14] (6) why the rate of positive ion emission decreases as the surface concentration increases.[14]

Because this adion grid theory is capable of interpreting these experimental facts we believe that for one or perhaps even two layers of barium the emitted electrons come from the tungsten or oxide rather than from the barium.

There is one aspect in which barium on the oxides differs from barium on tungsten. In tungsten the number of "free" electrons or those available for emission is fixed; in the oxides this number probably increases by large factors as the amount of barium dispersed through the oxide increases. This view is based on the observation that the conductivity of oxides increases by large factors when the amount of free metal dispersed in the oxide increases. Presumably the electrons that take part in the conduction are also "free" to leave the surface of the oxide if they have sufficient kinetic energy when close enough to the surface. Consequently it is to be expected that the emission will depend not only on the amount of barium on the surface but also on the amount dispersed through the oxide. The barium on the surface makes it easier for each electron to leave the surface: It decreases the work function ϕ in Richardson's equation, $i = AT^2\epsilon^{-\phi\epsilon/kT}$. The barium dispersed through the oxide increases the number of electrons that approach the surface: It increases the "A" in Richardson's equation.

We arrive at this view partly as a result of the following experiment. In the tube described in Fig. 1, the cathode was glowed at 1040°K until its activity as tested at 500°K reached a steady and reproducible value. A measured electron current was then sent into the cold oxide coating from an external filament for a measured time. The activity of the oxide filament as tested at 500°K was determined periodically. It was found that the activity increased, passed through an optimum and then decreased. Following this treatment,

[14] Becker, Trans. Amer. Electrochem. Soc. **55,** 153–175 (1929).
[15] Becker, Bell Laboratories Record **9,** 54–58, Oct. 1930.
[16] Becker, Phys. Rev. **35,** 1431 (1930).

the cathode was glowed at 1040°K while its activity at 500°K was again tested periodically. It was found that the activity increased at first, came to an optimum, which differed slightly from the preceding optimum, and then decreased until it approached a steady value. This steady value was greater than the preceding steady value on glowing at 1040°K. Electrons were then again sent into the oxide until the activity passed through an optimum and decreased. This treatment was again followed by a glowing treatment. Both processes were repeated again and again.

Fig. 9 shows some of the results. The various activities are plotted as a function of the total number of milliampere minutes (m.a.m.) of current sent into the oxide cathode. At any value of m.a.m. there are, in general, four characteristic activities shown in the figure. The first set of points do not

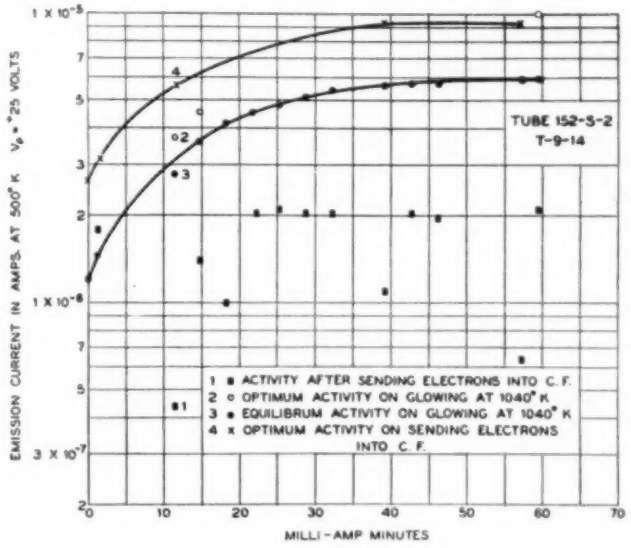

Fig. 9.

and should not form a smooth curve since the m.a.m. between successive glowings at 1040°K was irregular. If the interval between two successive glowings is unusually long, the initial activity is unusually low as it should be. The other sets of points form smooth curves as they should. The most important curve is the uppermost one for the optima on sending electrons into the oxide since each point represents the emission when the surface is covered with a monatomic layer of barium. This confirms the previously known fact, that the concentration of barium on the surface is not the only factor determining the activity.

We interpret this experiment as follows: After the initial glowing at 1040°K the concentrations of barium in the oxide and on the surface had reached a steady state. When electrons were sent into the oxide, oxygen was deposited on the core while barium was brought to the surface by electrolysis. The oxygen combined with the core since it is well known that a Konel core is readily oxidized. When the concentration of barium on the sur-

face reached a monatomic layer, the activity had an optimum value. We estimate that as the electrolysis continued in some cases several layers of barium were deposited on the surface. During the glowing at 1040°K this barium diffused back into the oxide and thus increased the concentration of barium dispersed through the oxide. After each treatment this concentration in the oxide was greater than after the preceding treatment. This is the reason why the optima and the steady value glowing curves increased with the m.a.m.

This experiment seems to us to be a crucial test between the two hypotheses; (1) that the electrons originate in the adsorbed barium itself, (2) they originate in the oxide underneath the adsorbed barium. On the first hypothesis it is difficult or impossible to see why there should be any optimum and why the optima should depend on the treatments to which the oxide was subjected. On the other hand, the second hypothesis is able to explain readily the observed facts.

The Rôle of the Core Metal

In this laboratory it has long been recognized that the nature of the core material has a very great influence on the activities that can be attained and the ease with which they can be attained. King[17] has shown that the average electron emissivity of a number of "combined" coated filaments with platinum-nickel core was higher than the emissivity of similar coatings on platinum-iridium cores. More recently Lowry[4] has shown that uncombined coated filaments with Konel metal cores were better electron emitters than some coated filaments with platinum cores. The emission from oxide coated nickel is also usually much better than from oxide coated platinum. According to Beese,[18] if 0.1 percent of barium is alloyed with the core, the easily attainable activity is appreciably improved.

The influence of the core material on the easily attainable activities is thus a well established fact. It has usually been assumed that this influence is an indirect one. Recently Lowry[4] has expressed the belief that the core material directly affects the activity. As a result he, "assumes that the source of the emission is the composite layer formed by occlusion of alkaline earth metal on the surface of the core". He admits however, "that no crucial tests of this explanation have been offered except that of showing the pronounced influence of the core metal". The experiments described above constitute such a crucial test since they show that the activity is determined by the outer oxide surface. It is well known that thermionic properties are directly affected by only a few atomic layers near the surface. It is also well known that the oxide coating is thousands of layers deep. Consequently the effect of the core material must be an indirect one.

The ways in which the core material may indirectly affect the activity are numerous. Anything which increases the concentration of barium adsorbed on the surface of the oxide or dispersed through the oxide, or anything which changes the composition or physical structure of the oxide will affect the ac-

[17] King, Bell Tech. Jrl. **2**, 31–100 (1923).
[18] Beese, Phys. Rev. **36**, 1309–1313 (1930).

tivity. The oxide very likely reacts chemically with some core constituents to form metallic barium some of which reaches the surface by diffusion. Carbon which is frequently present in cores as an impurity almost certainly reacts with the oxides. In some cases certain core materials, nickel for example, may be dispersed through the oxides. Such dispersed materials change the conductivity of the oxide and the ease with which electrolytic decomposition takes place. It is quite likely that such impurities in the oxide affect the crystal size of the oxide and thus influence diffusion, adsorption, and electrolytic phenomena which in turn affect the activity. If the core is purposely made to contain metallic barium, this barium will diffuse through the oxide and become adsorbed on the surface. The core material may also influence the ease with which the carbonates are decomposed to the oxides when the filament is first heated. Finally, the core material certainly affects the composition of the compounds which are formed when oxide filaments are heated in air to make "combined" filaments. The nature of these compounds and the products of their decompostion when the filament is heated in a vacuum, certainly affects the activity. In these and numerous other cases the core affects the activity in a round-about way rather than directly.

Conclusions

From these experimental results we conclude that: (1) The active layer is at the outer oxide surface.[19] The activity depends upon the concentration of barium and oxygen on this surface and also upon the amount of metallic barium dispersed through the oxide. The core material does not directly affect the emission but it does greatly affect the ease with which free barium is produced by heat treatment or electrolysis. (2) The thermionic electrons originate in the oxide just underneath the adsorbed barium. (3) Most of the current through the oxide is conducted by electrons, a small portion being carried by barium and oxygen ions.

[19] Huxford (Phys. Rev. **38,** 379–395 (1931)) comes to this same conclusion as a result of his work on the photoelectric emission from oxide cathodes.

WAVE-LENGTH STANDARDS IN THE SPECTRA OF ALUMINUM, SILICON AND BISMUTH IN THE SCHUMANN REGION

By R. V. Zumstein
Mendenhall Laboratory, Ohio State University

(Received October 5, 1931)

Abstract

The second order spectra of these elements have been photographed along with first order iron lines with a two meter vacuum grating. Between 1900 and 1500A values are found for the aluminum lines which check very closely the work of Bowen and Ingram. The silicon wave-lengths are 1816.922, 1808.01, 1533.42 and 1526.71. For bismuth the values are 1902.33, 1823.71, 1791.82, 1787.39 and 1777.01. These values are believed to be accurate to within about 0.02A.

IN A previous communication[1] certain wave-lengths in the spectra of carbon and tin were determined to about 0.02A. With a few improvements the same method has been used to obtain standard wave-lengths in the spectra of aluminum, silicon and bismuth. The details of the method may be obtained from the above mentioned article. The results obtained are recorded in Table I. Each measurement is the average of about five plates.

Aluminum

The source of light was a carbon arc in an atmosphere of hydrogen or nitrogen at 1 cm pressure. The lower carbon was 3.5 cm diameter with a shallow hole in the center. About 4 gm aluminum and 0.5 gm of very pure iron wire were placed in the lower electrode. The upper electrode was a solid carbon rod 1 cm diameter with a distance between the electrodes of about 3 mm. The current of 80 amperes was obtained from a 110 volt d.c. generator. The lower electrode was positive and the exposure lasted about 8 minutes. A fluorite window was cemented over the slit in order to allow a good vacuum to be maintained in the spectrometer and any desired gas pressure in the arc chamber. Bowen and Ingram[2] have also made measurements of aluminum lines by direct comparison with iron and their results are included in the table. Although the two sources of light and the methods of producing the spectra were different yet the agreement is very good. The aluminum arc works best in the nitrogen atmosphere. It was, however, necessary to use hydrogen when the lines were near the strong cyanogen band at 3884A. Recent measurements of these lines have also been made by Sawyer and Paschen,[3] Selwyn[4] and Fowler.[5]

[1] R. V. Zumstein and D. S. Marston, Phys. Rev. **38,** 305 (1931).
[2] I. S. Bowen and S. B. Ingram, Phys. Rev. **28,** 444 (1926).
[3] R. A. Sawyer and F. Paschen, Ann. d. Physik **84,** 1 (1927).
[4] E. W. H. Selwyn, Proc. Phys. Soc. **41,** 402 (1929).
[5] A. Fowler, Proc. Roy. Soc. **A123,** 427 (1929).

TABLE I. *Wave-length standards (I.A. vac).*

Bowen and Ingram			Zumstein			Classification	
				Aluminum II and III			
Int.	λ	error	Int.	λ	error		
10	1862.775	0.02	5	1862.782	0.02	III	$3s^2S_{\frac{1}{2}}-3p^2P_{\frac{1}{2}}^0$
			6	1862.34	0.03	II	$3s3p^3P_2^0-3s4s^3S_1$
			4	1858.05	0.03	II	$3s3p^3P_1^0-3s4s^3S_1$
			2	1855.95	0.03	II	$3s3p^3P_0^0-3s4s^3S_1$
10	1854.715	0.02	6	1854.722	0.02	III	$3s^2S_{\frac{1}{2}}-3p^2P_{1\frac{1}{2}}^0$
4	1767.730	0.01	2	1767.76	0.02	II	$3s3p^3P_2^0-3p^2\,{}^3P_1$
4	1765.814	0.01	1	1765.84	0.02	II	$3s3p^3P_1^0-3p^2\,{}^3P_0$
5	1763.939	0.01	5	1763.95	0.02	II	$3s3p^3P_{21}^0-3p^2\,{}^3P_{21}$
4	1761.973	0.01	1	1762.00	0.02	II	$3s3p^3P_0^0-3p^2\,{}^3P_1$
4	1760.101	0.01	2	1760.13	0.02	II	$3s3p^3P_1^0-3p^2\,{}^3P_2$
5	1724.982	0.01	5	1724.981	0.01	II	$3s3p^3P_2^0-3s3d\,{}^3D_{321}$
5	1721.273	0.01	3	1721.279	0.01	II	$3s3p^3P_1^0-3s3d\,{}^3D_{21}$
4	1719.455	0.01	1	1719.459	0.01	II	$3s3p^3P_0^0-3s3d\,{}^3D_1$
6	1670.802	0.03	4	1670.78	0.03	II	$3s^2\,{}^1S_0-3s3p\,{}^1P_1^0$
	Fowler			*Silicon II* Zumstein			
10	1816.98		4	1816.922	0.01		$3s^23p^2P_{1\frac{1}{2}}^0-x?$
8	1808.09		3	1808.01	0.02		$3s^23p^2P_{\frac{1}{2}}^0-x?$
10	1533.55		7	1533.42	0.02		$3s^23p^2P_{1\frac{1}{2}}-3s^24s^2S_{\frac{1}{2}}$
8	1526.38		5	1526.71	0.02		$3s^23p^2P_{\frac{1}{2}}^0-3s^24s^2S_{\frac{1}{2}}$
	McLennan, etc.			*Bismuth II* Zumstein			
100U	1902.42		25	1902.33	0.02		$6p_{\frac{1}{2}}6p_{1\frac{1}{2}}3_2-6p_{\frac{1}{2}}7s\;2_1^0$
80	1823.80		5	1823.71	0.02		$6p_{1\frac{1}{2}}6p_{1\frac{1}{2}}4_2-6p_{1\frac{1}{2}}7s\;9_2^0$
70	1791.93		9	1791.82	0.02		$6p_{\frac{1}{2}}6p_{1\frac{1}{2}}2_1-6p_{\frac{1}{2}}7s\;1_0^0$
80	1787.47		4	1787.39	0.02		$6p_{1\frac{1}{2}}6p_{1\frac{1}{2}}4_2-6p_{1\frac{1}{2}}7s\;10_1^0$
90u	1777.13		10	1777.01	0.02		$6p_{\frac{1}{2}}6p_{1\frac{1}{2}}2_1-6p_{\frac{1}{2}}7s\;2_1^0$

U Very diffuse, u diffuse

Silicon

There are two strong pairs of lines due to Si II. They should be very useful standards because a small quantity of silicon brings them out in the arc. I frequently find them in the spectra of vacuum tubes from the glass or quartz wall of the tube. Fowler's[5,6] wave-lengths are included in the table. His value 1526.38 seems to be a misprint of 1526.83, the silicon lines were obtained from an arc with a smaller lower carbon, about 1 cm diameter having a hole 0.5 cm diameter which contained the silicon and iron. It was necessary to use the hydrogen atmosphere as bands were always present in the nitrogen atmosphere. The current was 60 amperes d.c.

Bismuth

There are five Bi II lines which are very strong in the arc and spark. They may also be obtained from a fused quartz vacuum tube if a small piece of bis-

[6] A. Fowler, Phil. Trans. **A225,** 46 (1925).

muth is placed in the tube. The most recent measurement of the bismuth lines seems to be by McLennan, McLay and Crawford[7] and their values are given in the table. The classification is also taken from their paper. The second order bismuth and first order iron spectra were obtained from an arc in which the lower electrode was a 2.5 cm iron rod with a hole 0.5 cm diameter and 3 cm deep to contain the bismuth. The upper electrode was carbon as before. The current was 35 amperes d.c. in hydrogen at 1 cm pressure for most of the plates. A few were taken with 60 and 90 ampere alternating current arcs in nitrogen. Because there was no systematic shift of the wavelength with increase of current it is felt that the iron lines are free from pole effect in spite of the large current used (to the order of accuracy that may be obtained from a spectrum having the dispersion of 6A/mm).

At present there is great interest in the fine structure of the bismuth lines. 1902.33 was very intense and broad if there was much bismuth present. It is only of value as a standard where there is a slight concentration of bismuth atoms. 1777.01 was always slightly diffuse even at small concentrations. It would perhaps resolve into components in a higher order or with a finer slit. The other bismuth lines are sharp. It may be mentioned that our spectroscope has a slit 0.05 mm wide and clearly resolves the carbon lines 1658.12 and 1657.90. It is hoped that others will publish similar (or better) wavelength determinations. We should have a much larger number of lines in this region of the spectrum for which at least three independent observers check to within 0.02A. I am indebted to Dr. J. B. Green for helpful discussion of the classification of these lines.

[7] McLennan, McLay and Crawford, Proc. Roy. Soc. **A129,** 587 (1930).

CERTAIN SPECTRA IN THE VANADIUM I ISO-ELECTRONIC SEQUENCE

By Helen T. Gilroy
Physical Laboratory, Cornell University
(Received July 24, 1931)

Abstract

Displacement of multiplets in the iso-electronic sequence which begins with the arc spectrum of vanadium.—Regular displacements were observed for analogous quartets and sextets in the spectra of Mn III, Fe IV, Co V and Ni VI, continuing those already known for V I and Cr II. In addition a new sextet sequence has been found for V I to Co V. The configuration changes investigated were $3d^4\,4p$ to $3d^4\,4s$, $3d^4\,4d$ to $3d^4\,4p$, $3d^4\,4p$ to $3d^5$ and $3d^3\,4sp$ to $3d^3\,4s^2$.

Moseley diagrams and the irregular doublet law.—The irregular doublet law was applied to systems of sextets and quartets due to electronic changes in atoms having five electrons in outer shells. When the change did not involve a change in total quantum number, the law was closely followed.

Centroid diagram.—Shifts of energy levels for sextets and quartets of (P° D° F°) $3d^4\,4p$ have been calculated for V I to Co V, using the centroid method. Values are not absolute because not all the levels of this configuration are known. But relative values are useful for predicting higher states in the sequence.

Landé interval rule.—Typical tests of the Landé interval rule are given.

Regular doublet law.—The $(\Delta\nu)^{1/4}$ is linear with atomic number in some cases, but not in all.

Tables are given for the new lines and new term values.

THE regular and irregular doublet laws have been shown to hold for several iso-electronic sequences in the first long period of the table of elements.[1,2,3]. This report gives the results of a further application of these laws to the iso-electronic sequence which starts with the arc spectrum of vanadium, and also of an attempt to find radiated lines due to changes in energy level involving L values which are less than the maximum.

The neutral vanadium atom has, in addition to the closed sub-shells of electrons called $1s^2\,2s^2\,2p^6$ and $3s^2\,3p^6$, five valence electrons which, for this iso-electronic sequence, may have the configuration $3d^3\,4s^2$. Lines in the arc spectrum of vanadium will be due then, to excitation of any one or more of these valence electrons and their subsequent return to a lower energy state. Several sextets and quarters have previously been found in this spectrum, due to changes in electron configuration from $3d^4 4p$ to $3d^4 4s$, $3d^4 4p$ to $3d^5$, $3d^3 4sp$ to $3d^3 4s^2$, $3d^3 4sp$ to $3d^4 4s$ and $3d^4 4p$ to $3d^3 4s^2$.[4,5,6].

[1] Gibbs and White, Phys. Rev. **29,** 426 and 655 (1927); Gibbs and White, Phys .Rev. **33,** 157 (1929).

[2] Gibbs and White, Proc. Nat. Acad. Sci. **13,** 525 (1927); and **12,** 598 and 448 (1926).

[3] White, Phys. Rev. **33,** 538, 672 and 914 (1929).

[4] W. F. Meggers, J. of Wash. Acad. of Sci. **13,** 317 (1923); **14,** 151 (1924).

[5] O. Laporte, Die Naturwissenschaften **11,** 779 (1923).

[6] H. N. Russell, Astrophys. J. **66,** 184 (1927).

Of the second member of this sequence, the first spark spectrum of chromium, only quartets and sextets of the electron changes $3d^44p$ to $3d^44s$ and $3d^44p$ to $3d^5$ have been reported.[6,7,8]. Since the chromium atom which is emitting the first spark spectrum has lost one electron, it will have as many electrons outside the completed sub-shells as the neutral vanadium atom. Hence the spectra have been found to be similar in several respects, though the relative order of energy levels may differ. This will be shown later in one of the graphs. Very few data have been published about the remaining spectra of

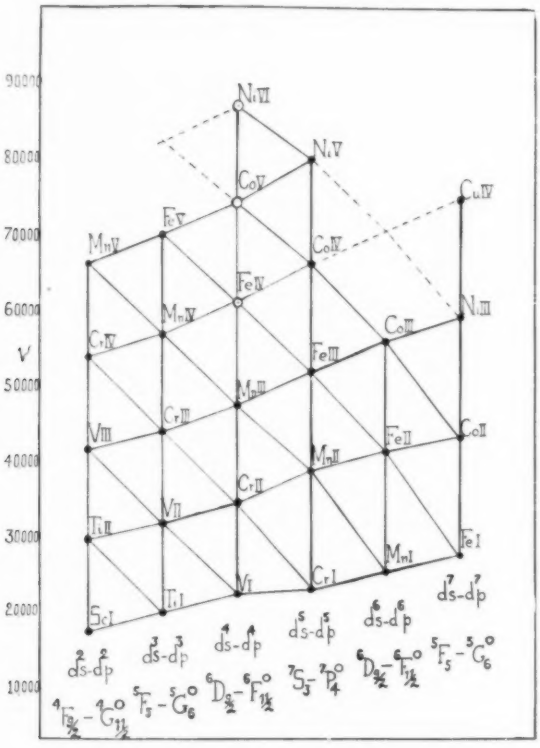

Fig. 1. Regular displacement of multiplets.

this sequence, Mn III, Fe IV, Co V and Ni VI. One sextet group in Mn III, $3d^44s\ {}^6D-3d^44p\ {}^6F^\circ$, has been identified.[2]

According to the present theory of atomic structure and line spectra, a space quantization of the electrons $3d^44s$ give the following energy levels;— $^2(S, D, G)$, $^{2,4}(P, F)$, $^2(S, D, F, G, I)$, $^{2,4}(P, D, F, G, II)$ and $^{4,6}(D)$. Of these, only the $^{4,6}(D)$ which are involved in the emission of the more intense lines, have been considered in this investigation. Similarly, from the $3d^44p$ configuration only those levels which are derived from the ^5D level of a d^4 configuration, have been studied, that is $^{4,6}(P^\circ, D^\circ, F^\circ)$. In the next higher configuration, $3d^44d$, we have levels $^{4,6}(S, P, D, F, G)$ from the same $d^4\ {}^5D$ limit. In the d^5

[7] Meggers, Kiess and Walters Jr., J. Opt. Soc. Amer. **9**, 361 (1924).
[8] C. C. Kiess and O. Laporte, Science **63**, 234 (1926).

configuration there are levels $^4(D, G)$ and ^6S from the same limit. Since there are two possible methods of ionizing an atom having valence electrons d^4s, one by the removal of an s electron and the other by the removal of a d electron, we might build a five-electron system on the $3d^34s$ configuration, whose lowest energy levels should be $^5(P, F)$. The addition of an s electron to this configuration gives levels $^{4,6}(P, F)$ of the $3d^34s^2$ configuration, while the addition of a p electron gives $3d^34sp\ ^{4,6}(S^\circ, P^\circ, D^\circ, F^\circ, G^\circ)$. This report includes the wave-lengths of a few multiplets due to the electronic change ($3d^34s^2 - 3d^34sp$).

Displacement of Multiplets

The method employed for predicting the spectral regions in which these multiplets should be found, is that of Gibbs and White.[1,2] Figure 1 is in part a reproduction of their graph showing the regular displacement of multiplets with increasing atomic number but the same number of outer electrons, and with increasing number of d electrons in the incompleted sub-shell but in the same state of ionization. For one electron transition, $3d^44s - 3d^44p$, and one multiplet group, $^6D - {}^6F^\circ$, radiated frequencies have been found for V I[4], Cr II[7] and Mn III[2] with separations of about 13,000 cm^{-1}. From this regularity one may expect that the corresponding line for Fe IV will be at about 61,000 cm^{-1}, for Co V at about 74,000 cm^{-1} and for Ni VI at about 87,000 cm^{-1}. These points are indicated by circles instead of solid dots in Figure 1. In Fe V the line $3d^34s\ ^5F_5 - 3d^34p\ ^5G^\circ_6$ found by White[3] at 69,905 cm^{-1} fits into this diagram, as do $3d^54s\ ^7S_3 - 3d^54p\ ^7P^\circ_4$ for Co IV and Ni V at 66,573 cm^{-1} and 80,376 cm^{-1} respectively, both determined by Morell.[9] With these frequencies and those now identified for lines $^6D - {}^6F^\circ$ in Fe IV, Co V and Ni VI, it is possible to predict with a fair degree of accuracy the most intense lines in parallel sequences. For instance, the line $3d^34s\ ^5F_5 - 3d^34p\ ^5G^\circ_6$ of Co VI should be at 82,500 cm^{-1} and $3d^64s\ ^6D_{9/2} - 3d^64p\ ^6F^\circ_{11/2}$ of Ni IV at 70,700 cm^{-1}.

Photographs taken with a vacuum spectrograph in the regions indicated for the five-electron sequences, show the head line of $(^6D - {}^6F^\circ)$ $(3d^44s - 3d^44p)$ from Fe IV at 61,312 cm^{-1}, from Co V at 74,312 cm^{-1} and from Ni VI at 87,388 cm^{-1}. These are plotted in Figure 2. In the same manner, from a knowledge of quartets and sextets in the spectra of V I and Cr II, corresponding multiplets have been found for the remainder of the sequence. Some of these are shown in Fig. 2. This completes the multiplet groups produced by the electron change $3d^44s - 3d^44p$, which approach the limit $3d^4\ ^5D$, a multiplet arising from the configuration $3d^4$ of the corresponding atom, in the next higher state of ionization.

Another possible configuration change involved in this same iso-electronic sequence is from $3d^44p$ to $3d^5$. Since ^6S is the only sextet in the $3d^5$ configuration the only probable sextet group of lines of any intensity is $^6S - {}^6P^\circ$. This results in three lines, $^6S_{5/2} - {}^6P^\circ_{3/2,5/2,7/2}$ whose term differences are already known for all the elements in the sequence, having been found in one of the

[9] Morell, Thesis, Cornell, 1928.

sets of multiplets mentioned above; i.e ($3d^4 4s - 3d^4 4p$) ($^6D - {}^6P^\circ$). This group of lines has been followed through the sequence except in Ni VI, where the lines should appear at about 318A. At this very short wave-length the lines are so faint and the probable error in reciprocal cm so large, that this group has been omitted from the tables of wave-lengths and term values, although two lines were found approximately in this position. Lines due to two more changes in electronic configuration, $3d^4 4p - 3d^4 4d$ and $3d^3 4s^2 - 3d^3 4sp$, have been found for the sequence to Co V. The group $^6F^\circ - {}^6G$ from the $3d^4 4p - 3d^4 4d$ change, involving the largest L values, contains the strongest lines of the first configuration change, though much weaker than the strong lines of the $3d^4 4s - 3d^4 4p$ groups. For Mn III two additional sextet groups, $^6F^\circ - {}^6F$ and $^6F^\circ - {}^6D$, have been found for $3d^4 4p - 3d^4 4d$.

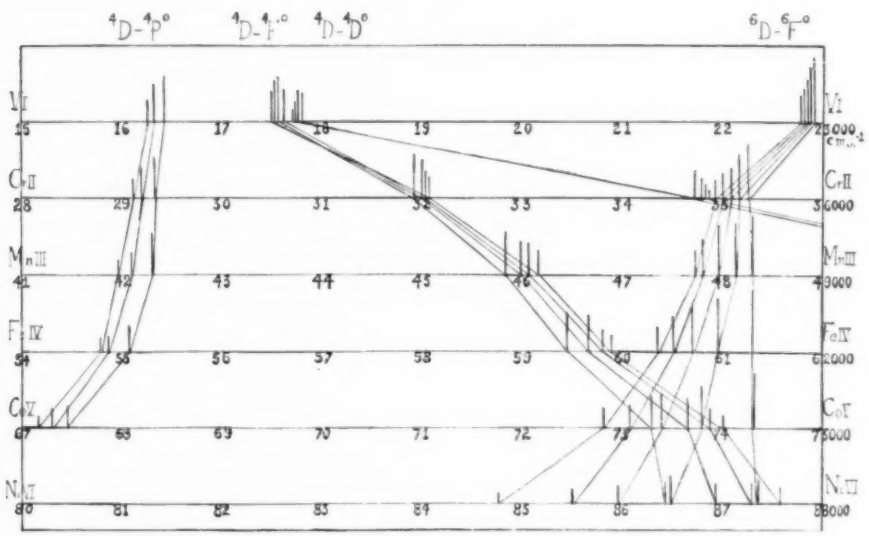

Fig. 2. Displacement of multiplets. Iso-electronic sequence $3d^4 4s - 3d^4 4p$.

In Figure 2 the nearly linear increase in radiated frequency with increasing atomic number, can be observed from the small change in direction of the connecting lines. This is also true of other multiplets not shown in this chart. A $3d^4 4p - 3d^4 4d$ change involves approximately 20,000 cm^{-1} shift in frequency from any element to the next higher in the sequence, a $3d^4 4s - 3d^4 4p$ change involves 13,000 cm^{-1} shift and a $3d^3 4s^2 - 3d^3 4sp$, about 13,500 cm^{-1}. Where the change in electronic configuration involves a change in total quantum number, the lines are displaced somewhat irregularly toward the shorter wave-lengths. In the case of a $3d^5 - 3d^4 4p$ change the displacement is about 60,000 cm^{-1} between any two members of the sequence.

One of the tests which has been used throughout to distinguish between lines due to high and low stages of atomic ionization, is apparently not absolutely reliable when adjacent lines belong to different sequences. In general, the presence of an inductive resistance in series with the spark gap very

greatly reduces the intensity of the high ionization lines.[10,11] In the manganese spectrum the $(3d^44p-3d^44d)$ $(^6F^\circ-{}^6G)$ group of Mn III is closely adjacent to $(3d^34s-3d^34p)$ $(^5F-{}^5G^\circ)$ of Mn IV and $(3d^24s-3d^24p)$ $(^2F-{}^2F^\circ)$ of Mn V. An inductance which is sufficient nearly to efface the strongest line and completely to efface the other lines of the Mn III group, reduces the intensities of the lines of the Mn IV and Mn V groups to a much less extent. Without the inductance the intensities of the latter two groups are nearly the same as that of the strongest Mn III line in the multiplet under discussion.

Irregular Doublet Law

These same data may be combined in another manner to illustrate the irregular doublet law. Bowen and Millikan[12] have shown that the irregular doublet law for x-rays may be transferred to doublets of the second and third periods which are due to one-electron systems. Gibbs and White[1,2,3,13] have extended this application to doublets of the fourth, fifth and sixth periods and to triplets, quartets and quintets in the first and second long periods of the elements. Table I gives the results of a test of this law for systems of lines due to five electrons in outer shells, quartets and sextets having the largest L

TABLE I. *Irregular doublet law.* Values of $\nu^{1/2}$ referred to $3d^4\ {}^5D_0$ of V II, Cr III, Mn IV, etc.

Config.	T.	V I	Δ	Cr II	Δ	Mn III	Δ	Fe IV	Δ	Co V	Δ	Ni VI
$3d^44s$	$^6D_{9/2}$	228	120	348	122	470	122	592	122	714	122	836
$3d^44p$	$^6F^\circ_{11/2}$	171	122	293	122	415	123	538	122	660	122	782
$3d^44d$	$^6G_{13/2}$	90	126	216	121	337	122	459	122	581	122	703
$3d^5$	$^6S_{5/2}$	182	184	366	162	528	150	678	143	821	129	(950)
Values of $\nu^{1/2}$ referred to $3d^4\ {}^5D_0$ of V II, Cr III, Mn IV, etc.												
$3d^44s$	$^4D_{7/2}$	214	124	338	123	461	124	585	122	707	123	830
$3d^44p$	$^4F^\circ_{9/2}$	167	120	287	121	408	123	531	122	653	123	776
Values of $\nu^{1/2}$ referred to $3d^34s\ {}^5F_1$ of V II, Cr III; etc.												
$3d^34s^2$	$^4F_{9/2}$	237.5	77.5	315	77.5	392.5	77.5	470	78	548		
$3d^34sp$	$^4G^\circ_{11/2}$	158	78	236	77.5	313.3	77.3	390.6	77.8	468.4		

values being selected to represent each system. Graphically this can be shown in a Moseley diagram, as in Fig. 3. In this figure are plotted the square roots of term values referred to $3d^4\ {}^5D_0$ of the corresponding atom in the next higher state of ionization. In the case of V I, for instance, Russell's[14] value of 52,300 for the limit of $3d^44s\ {}^6D_{1/2}$ was assumed, giving 51,988 for $3d^44s\ {}^6D_{9/2}$. The square root of 51,988, that is 228, was then used as the starting point for the graph. Knowing the radiated frequency of $3d^44s\ {}^6D_{9/2}-3d^44p\ {}^6F^\circ_{11/2}$ we may

[10] Fowler, Phil. Trans. Roy. Soc. **A225,** 1 (1925).

[11] Gibbs, Vieweg and Gartlein, Phys. Rev. **34,** 406 (1929).

[12] Bowen and Millikan, Phys. Rev. **24,** 209 (1924); Phys. Rev. **25,** 295, and **26,** 150 (1925); **27,** 144 (1926).

[13] Gibbs and White, Proc. Nat. Acad. Sci. **12,** 551 and 675 (1926); **14,** 345 and 559 (1928); Phys. Rev. **29,** 359 (1927); **31,** 520 (1928); **33,** 157 (1929).

[14] Russell, Astrophys. J. **66,** 233 (1927).

determine the term value of $3d^4p\ {}^6F^\circ_{11/2}$ referred to the same limit. The square root of this term value gave the first point on the $3d^44p\ {}^6F^\circ_{11/2}$ curve. For the Cr II spectrum Russell's approximate value of 122,000 for $3d^44s\ {}^6D_{1/2}$ referred to $3d^4\ {}^5D_0$ of Cr III, was used and the square roots of term values for $3d^44s\ {}^6D_{9/2}$ and $3d^44p\ {}^6F^\circ_{11/2}$ were determined as in the case of V I. The limits of the sextet series are not known for Mn III, so an extrapolated number for the square root of the term value was read from the graph, assuming that

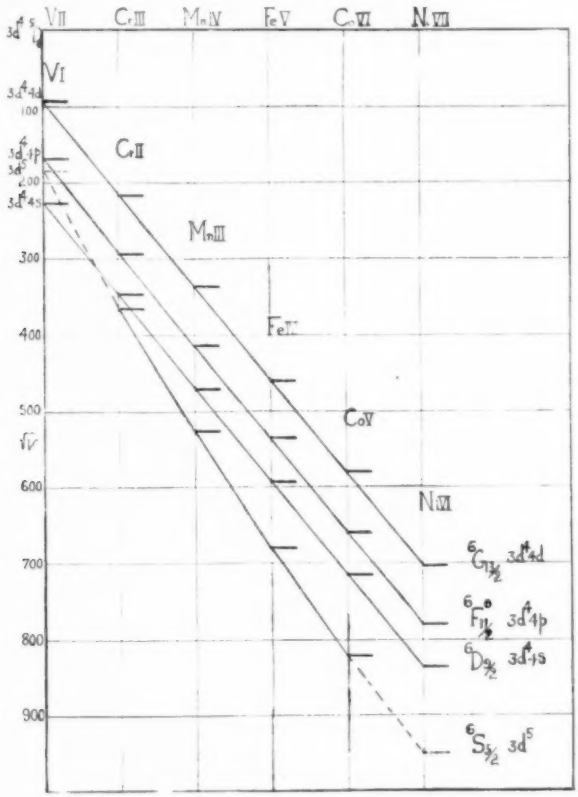

Fig. 3. Moseley Diagram. $\nu^{1/2}$ vs. atomic number.

$3d^44s\ {}^6D_{9/2}$ could be represented by a straight line. This assumption was made on the strength of curves for four sequences reported by White.[3] Since the radiated frequency $3d^44s\ {}^6D_{9/2}-3d^44p\ {}^6F^\circ_{11/2}$ is known, the square root of the term value for $3d^44p\ {}^6F^\circ_{11/2}$ can be readily calculated. A continuation of this method for the remaining elements in the sequence resulted in parallel lines, showing that $\Delta\nu^{1/2}$ is constant, independent of the atomic number, as required by the irregular doublet law. When the same method was applied to the lines $3d^44d\ {}^6G_{13/2}$ and $3d^5\ {}^6S_{5/2}$ corresponding curves were obtained. In the former case the curve is very nearly parallel to those for $3d^44p\ {}^6F^\circ_{11/2}$ and $3d^44s\ {}^6D_{9/2}$,but not in the latter case. Since the irregular or screening doublet law in x-ray spectra holds only for levels between which the transition involves no change in total quantum number of the electrons, the line representing

$\nu^{1/2}$ for $3d^5\ {}^6S_{5/2}$ should not be parallel to those for $3d^4 4s$, $3d^4 4p$ and $3d^4 4d$, in all of which the total quantum numbers of all the electrons involved in the electronic configuration, are the same.

The term values for the quartets, recorded in Table I, are referred to the lowest level, $3d^4\ {}^5D_0$, of the sextet limits, and the same method was used in calculating the $\nu^{1/2}$ for successive elements. A slightly different method was

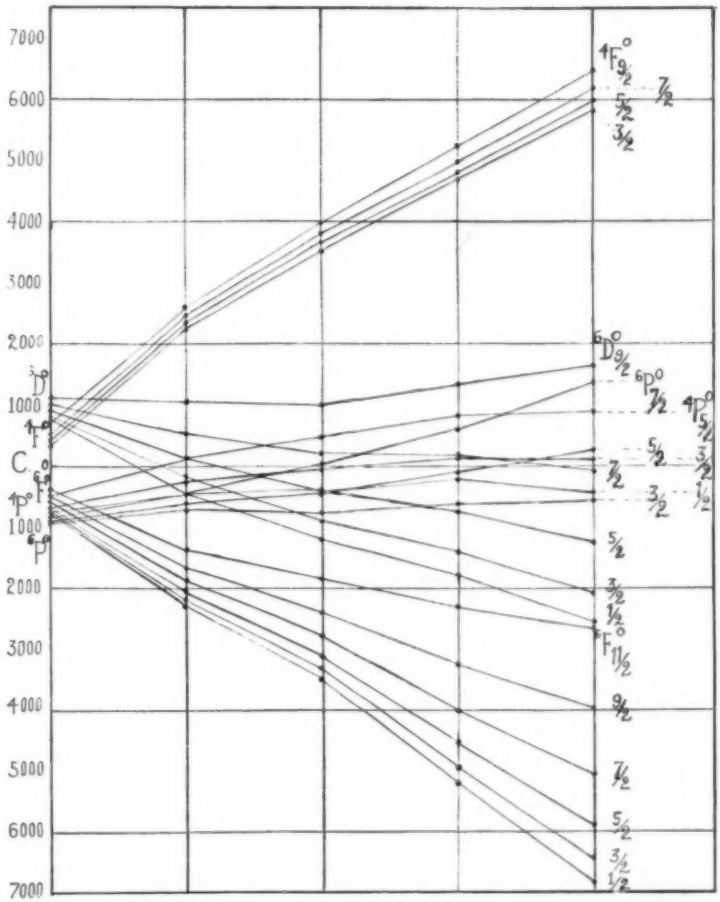

Fig. 4. Shift of Energy Levels. $3d^4 4p\ {}^4(F^\circ P^\circ)\ {}^6(P^\circ D^\circ F^\circ)$

used for the second set of quartets in Table I, because the limits were known only in the case of $3d^3 4s^2\ {}^4F_{9/2}$ of V I. For convenience, the reference level taken is $3d^3 4s\ {}^5F_1$ of V II rather than the actual limit, $3d^3 4s\ {}^5F_5$. From the radiated frequency $3d^3 4s^2\ {}^4F_{9/2} - 3d^3 4sp\ {}^4G^\circ_{11/2}$ and the known term value of $3d^3 4s^2\ {}^4F_{9/2}$, the term value for $3d^3 4sp\ {}^4G^\circ_{11/2}$ can be found and hence the $\nu^{1/2}$ for each level. Assuming that $\Delta\nu^{1/2}$ is constant and knowing the values of $3d^3 4s^2\ {}^4F_{9/2} - 3d^3 4sp\ {}^4G^\circ_{11/2}$ for the remainder of the sequence, values for $\nu^{1/2}$ can be calculated. With these values plotted for both $3d^3 4s^2\ {}^4F_{9/2}$ and $3d^3 4sp\ {}^4G^\circ_{11/2}$, the lines are observed to be straight, which is in agreement with the

results for the sextets and the first set of quartets having the same total quantum number. The one exception is the $3d^5\ {}^6S_{5/2}$ line, already mentioned, which is related to the others by means of an electronic change involving a change in total quantum number and hence not a violation of the irregular doublet law.

A comparison of Table I with Fig. 3, shows that $3d^34s^2\ {}^4F_{9/2}$ represents the lowest energy level of V I, but does not for the remainder of the sequence. Instead, $3d^5\ {}^6S_{5/2}$ has dropped slightly below $3d^34s^2\ {}^4F_{9/2}$ for Cr II and with rapidly increasing frequency difference, continues to be the lowest level for the rest of the sequence. The level $3d^5\ {}^6S_{5/2}$ for Ni VI has not been definitely determined, but there is small probability that the $\nu^{1/2}$ will not be in the position indicated by the dotted line in Fig. 3.

TABLE II. *Landé interval rule.* Term separations of $3d^34s$ in cm^{-1}.

Spectrum	${}^6D_{9/2}$	${}^6D_{7/2}$	${}^6D_{5/2}$	${}^6D_{3/2}$	${}^6D_{1/2}$	
V I	113 (4.5)	91 (3.6)	67 (2.7)	41 (1.6)		(4)
Cr II	192.7 (4.5)	156 (3.6)	115 (2.7)	70.8 (1.7)		(7)
Mn III	296 (4.5)	241 (3.7)	180 (2.7)	132 (2.0)		
Fe IV	594.5 (4.5)	476 (3.6)	341 (2.6)	253 (1.9)		
Co V	851 (4.5)	678 (3.6)	524 (2.7)	314 (1.66)		
Ni VI	1272 (4.5)	976 (3.5)	642 (2.3)	341 (1.2)		
Theory	4.5	3.5	2.5	1.5		

	${}^4D_{7/2}$	${}^4D_{5/2}$	${}^4D_{3/2}$	${}^4D_{1/2}$	
V I	137 (3.5)	102 (2.6)	63 (1.6)		(4)
Cr II	226 (3.5)	166.7 (2.6)	103 (1.6)		(7)
Mn III	328 (3.5)	241 (2.6)	146 (1.6)		
Fe IV	448 (3.5)	307 (2.4)	184 (1.4)		
Co V	626 (3.5)	428 (2.4)	265 (1.5)		
Ni VI	852 (3.5)	625 (2.6)	373 (1.5)		
Theory	3.5	2.5	1.5		

Centroid Diagram

Greater detail in analysing the shift of energy levels is presented in Fig. 4. The zero line in this figure is the centroid of the configuration under consideration for each element, in so far as the levels have been determined. Vertical distances are the frequency differences between this centroid and each level. The centroid, according to the usual method[15] is calculated as the mean of all the levels weighted in proportion to $2j+1$, where j is the inner quantum number of the level. The final grouping of the levels in Co V indicates a possible coupling which differs from the Russell-Saunders but is not sufficiently different to follow the jj coupling of much heavier elements.[15,16] Addition of other quartet and doublet levels, now unknown, will change the values of the levels given, but should not appreciably change their relative shift. The relative values are useful in predicting higher states in the sequence.

The Landé Interval Rule

The Landé interval rule was found useful in locating most of these multiplets. Though it does not hold for all cases, Table II gives a typical illustration of the extent of variation in the spectra studied. In this table term separations are given in reciprocal centimeters; in brackets under each separation is a number to be compared with the theoretical ratios of term separations given at the bottom of the table. The spread of the multiplets, which appears

Table III. *Regular doublet law.*

			$\Delta\nu$	$\Delta\nu^{1/4}$	s
$3d^4 4s$	$^4D_{7/2}-{}^4D_{5/2}$	V I	137	3.42	14.36
		Cr II	226	3.88	14.20
		Mn III	328	4.28	14.18
		Fe IV	448	4.61	14.34
		Co V	626	5.02	14.31
		Ni VI	852	5.41	14.32
$3d^4 4s$	$^6D_{9/2}-{}^6D_{7/2}$	V I	113	3.26	17.85
		Cr II	193	3.73	18.22
		Mn III	296	4.16	18.50
		Fe IV	594	4.92	18.30
		Co V	851	5.41	18.55
		Ni VI	1272	5.98	18.68
$3d^4 4p$	$^6F^\circ_{11/2}-{}^6F^\circ_{9/2}$	V I	142	3.46	17.65
		Cr II	287	4.12	17.62
		Mn III	490	4.71	17.78
		Fe IV	935	5.54	17.63
		Co V	1374	6.10	17.62
		Ni VI	2183	6.82	17.50
$3d^4 4d$	$^6G_{13/2}-{}^6G_{11/2}$	V I	99	3.15	17.83
		Cr II	159	3.56	18.14
		Mn III	317	4.24	18.05
		Fe IV	575	4.90	17.96
		Co V	929	5.53	17.93

[15] Mack, Laporte and Lang, Phys. Rev. **31,** 748 (1928).
[16] Mack, Phys. Rev. **34,** 17 (1929).

TABLE IV. *Configuration change* $3d^34s^2-3d^34sp$.

Mn III.

sp \ s^2	$^4F_{9/2}$	632	$^4F_{7/2}$	460	$^4F_{5/2}$	340	$^4F_{3/2}$
$^4G^\circ_{11/2}$	55850.6 50 1790.49						
495							
$^4G^\circ_{9/2}$	55355.7 23 1806.50		55987.9 50 1786.10				
338							
$^4G^\circ_{7/2}$	55017.6 18 1817.60		55650.2 25 1798.05		56110.1 40 1782.19		
292							
$^4G^\circ_{5/2}$					55818.2 12 1793.57		56158.3 6 1780.68

Fe IV.

sp \ s^2	$^4F_{9/2}$	824	$^4F_{7/2}$	626	$^4F_{5/2}$	450	$^4F_{3/2}$
$^4G^\circ_{11/2}$	68268.2 40 1464.81						
595							
$^4G^\circ_{9/2}$	67673.2 5 1477.69		68496.9 40 1459.92				
425							
$^4G^\circ_{7/2}$	67246.8 5 1487.35		68071.7 37-x 1469.04		68697.4 25 1455.66		
356							
$^4G^\circ_{5/2}$					68341.0 4 1463.25		68791.4 15 1453.67

Co V.

sp \ s^2	$^4F_{9/2}$	1088	$^4F_{7/2}$	966	$^4F_{5/2}$	544	$^4F_{3/2}$
$^4G^\circ_{11/2}$	80844.0 20 1236.95						
846							
$^4G^\circ_{9/2}$	80198.2 8 1246.91		81186.6 15 1231.73				
532							
$^4G^\circ_{7/2}$			80654.9 2 1239.85		81420.6 8 1228.19		
419							
$^4G^\circ_{5/2}$					81001.2 2 1234.55		81545.4 3 1226.31

in Fig. 2, is here shown in the increasing value of $\Delta\nu$ with increasing atomic number.

Regular Doublet Law

The other doublet law which has already been mentioned, the relativity or regular doublet law in x-ray spectra, serves as another check on the selection of multiplets. This "doublet" must be tested by the $\Delta\nu$ between levels having the same L values but different inner quantum numbers.[17] Landé first noticed that this relation could be applied to optical spectra.[18] Bowen and

Table V. *Mn III. Configuration change* ($3d^4 4s - 3d^4 4p$).

	s	$^4D_{7/2}$	329	$^4D_{5/2}$	242	$^4D_{3/2}$	145	$^4D_{1/2}$
p								
$^4F^\circ_{9/2}$		45818.2 80 2182.54						
167								
$^4F^\circ_{7/2}$		45641.0 30 2190.53		45979.9 70 2174.86				
149								
$^4F^\circ_{5/2}$		45503.9 1 2197.61		45830.4 3 2181.96		46072.5 90 2170.49		
59								
$^4F^\circ_{3/2}$						46013.4 2 2173.28		46158.7 25 2166.44
$^4D^\circ_{7/2}$		51348.9 80 1947.46		51677.4 5 1935.08				
209								
$^4D^\circ_{5/2}$				51468.4 45 1942.94		51707.9 4 1933.94		
168								
$^4D^\circ_{3/2}$						51539.5 30 1940.26		51684.9 1 1934.80
91								
$^4D^\circ_{1/2}$						51450.6 2 1943.61		51593.5 1 1938.23
$^4P^\circ_{5/2}$		42328.76 40 2362.46		42657.93 12 2344.23		42898.39 2 2331.09		
542								
$^4P^\circ_{3/2}$				42113.06 50-x 2374.56		42357.45 50 2360.86		42504.18 8 2357.72
390								
$^4P^\circ_{1/2}$						41967.96 30 2382.77		42113.06 x 2374.56

[17] Sommerfeld, "Atombau" 4th Ed. p. 420.

[18] Landè, Zeits. f. Physik **16**, 394 (1923).

Millikan[13] and Gibbs and White[14] have tested the law for one-electron systems and the latter have applied it to the location of similar multiplets in higher electronic states. One form of this law is

$$\Delta\nu = K(Z - s)^4$$

Table III gives the values of $\nu^{1/4}$ for a few multiplets reported in this investigation. Column 1 gives the configuration, column 2, the levels whose $\Delta\nu$ is used in the calculation and column 6 gives the screening constant. The increase in $\nu^{1/4}$ is nearly linear, but not exactly so in all cases. The introduction of Landé's correction for penetrating orbits does not eliminate the variations from linearity.

TABLE VI. *New term values for V I and Cr II.*

V I. Referred to $3d^34s^2\ {}^4F_{3/2}$ (Russell, Astrophys. J. **66**, 233, 1927)			Cr II Referred to $3d^5\ {}^6S_{5/2}$ (C. C. Kiess, Bur. of St. J. of Res. **5**, 775 (1930))		
$3d^44d$	${}^6G_{3/2}$	45850.3	$3d^44d$	${}^6G_{3/2}$	86571.0
	${}^6G_{5/2}$	45883.6		${}^6G_{5/2}$	86629.0
	${}^6G_{7/2}$	45938.5		${}^6G_{7/2}$	86715.7
	${}^6G_{9/2}$	46007.1		${}^6G_{9/2}$	86827.8
	${}^6G_{11/2}$	46085.2		${}^6G_{11/2}$	86964.9
	${}^6G_{13/2}$	46183.7		${}^6G_{13/2}$	87124.2

TABLE VII. *Term values of Mn III, referred to the limit of the sextets, estimated from the Moseley diagram.*

Config.	T.	Value	Config.	T.	Value	Config.	T.	Value
$3d^44d$	${}^6F_{11/2}$	111,373	$3d^44p$	${}^4D^\circ_{7/2}$	161,172	$3d^44p$	${}^6F^\circ_{11/2}$	172,583
		314			209			490
	${}^6F_{9/2}$	111,687		${}^4D^\circ_{5/2}$	161,381		${}^6F^\circ_{9/2}$	173,073
		207			168			400
	${}^6F_{7/2}$	111,894		${}^4D^\circ_{3/2}$	161,549		${}^6F^\circ_{7/2}$	173,473
		151			91			313
	${}^6F_{5/2}$	112,045		${}^4D^\circ_{1/2}$	161,640		${}^6F^\circ_{5/2}$	173,786
		90						224
	${}^6F_{3/2}$	112,135		${}^4F^\circ_{9/2}$	166,703		${}^6F^\circ_{3/2}$	174,010
		52			167			158
	${}^6F_{1/2}$	112,187		${}^4F^\circ_{7/2}$	166,870		${}^6F^\circ_{1/2}$	174,168
					149			
	${}^6D_{9/2}$	112,595		${}^4F^\circ_{5/2}$	167,019	$3d^44s$	${}^4D_{7/2}$	212,521
		207			59			328
	${}^6D_{7/2}$	112,802		${}^4F^\circ_{3/2}$	167,078		${}^4D_{5/2}$	212,849
		160						242
	${}^6D_{5/2}$	112,962		${}^6D^\circ_{9/2}$	169,684*		${}^4D_{3/2}$	213,091
		157		${}^4P^\circ_{5/2}$	170,192 *			146
	${}^6D_{3/2}$	113,119		${}^6D^\circ_{7/2}$	170,467*		${}^4D_{1/2}$	213,237
		84		${}^6P^\circ_{7/2}$	170,682 *			
	${}^6D_{1/2}$	113,203		${}^4P^\circ_{3/2}$	170,734 *		${}^6D_{9/2}$	220,900
	${}^6G_{13/2}$	113,701		${}^6D^\circ_{5/2}$	171,103*			298
		317		${}^6P^\circ_{5/2}$	171,118 *		${}^6D_{7/2}$	221,198
	${}^6G_{11/2}$	114,018		${}^4P^\circ_{1/2}$	171,124 *			241
		275		${}^6P^\circ_{3/2}$	171,466 *		${}^6D_{5/2}$	221,439
	${}^6G_{9/2}$	114,293		${}^6D^\circ_{3/2}$	171,567*			178
		211		${}^6D^\circ_{1/2}$	171,855*		${}^6D_{3/2}$	221,617
	${}^6G_{7/2}$	114,504						132
		102					${}^6D_{1/2}$	221,749
	${}^6G_{5/2}$	114,606						
		33				$3d^5$	${}^6S_{5/2}$	278,552
	${}^6G_{3/2}$	114,639						

TABLE VIII. *Term values of Fe IV, referred to the limit of the sextets, estimated from the Moseley diagram.*

Config.	T.	Value	Config.	T.	Value	Config.	T.	Value
$3d^54d$	$^6G_{13/2}$	210,479	$3d^54p$	$^6D^\circ_{9/2}$	283,473*	$3d^54p$	$^6F^\circ_{5/2}$	291,379
		575						388
	$^6G_{11/2}$	211,054		$^4P^\circ_{5/2}$	285,994 *		$^6F^\circ_{3/2}$	291,767
		509						240
	$^6G_{9/2}$	211,563		$^6P^\circ_{7/2}$	286,217 *		$^6F^\circ_{1/2}$	292,007
		417						
	$^6G_{7/2}$	211,980		$^6D^\circ_{7/2}$	286,633*	$3d^54s$	$^4D_{7/2}$	341,056
		247						448
	$^6G_{5/2}$	212,227		$^4P^\circ_{3/2}$	286,639 *		$^4D_{5/2}$	341,504
		88		$^6P^\circ_{5/2}$	286,921 *			308
	$^6G_{3/2}$	212,315		$^4P^\circ_{1/2}$	287,032 *		$^4D_{3/2}$	341,812
$3d^54p$	$^4D^\circ_{7/2}$	273,472		$^6P^\circ_{3/2}$	287,446 *			184
		265					$^4D_{1/2}$	341,996
	$^4D^\circ_{5/2}$	273,737		$^6D^\circ_{5/2}$	287,566*		$^6D_{9/2}$	350,464
		143			663			597
	$^4D^\circ_{3/2}$	273,880		$^6D^\circ_{3/2}$	288,231*		$^6D_{7/2}$	351,061
		111			391			476
	$^4D^\circ_{1/2}$	273,991		$^6D^\circ_{1/2}$	288,622*		$^6D_{5/2}$	351,537
				$^6F^\circ_{11/2}$	289,152			342
	$^4F^\circ_{9/2}$	281,584			935		$^6D_{3/2}$	351,879
		246		$^6F^\circ_{9/2}$	290,087			253
	$^4F^\circ_{7/2}$	281,830			736		$^6D_{1/2}$	352,132
		180		$^6F^\circ_{7/2}$	290,823			
	$^4F^\circ_{5/2}$	282,010			556	$3d^5$	$^6S_{5/2}$	460,278
		97						
	$^4F^\circ_{3/2}$	282,107						

TABLE IX. *Term values of Co V referred to the limit of the sextets, estimated from the Moseley diagram.*

Config.	T.	Value	Config.	T.	Value	Config.	T.	Value
$3d^54d$	$^6G_{13/2}$	337,287	$3d^54p$	$^6D^\circ_{9/2}$	431,194*	$3d^54p$	$^6F^\circ_{5/2}$	438,762
		929						573
	$^6G_{11/2}$	338,216		$^6P^\circ_{7/2}$	431,488 *		$^6F^\circ_{3/2}$	439,335
		785						376
	$^6G_{9/2}$	339,001		$^4P^\circ_{5/2}$	431,976 *		$^6F^\circ_{1/2}$	439,711
		631						
	$^6G_{7/2}$	339,632		$^6P^\circ_{5/2}$	432,622 *	$3d^54s$	$^4D_{7/2}$	501,264
		425						626
	$^6G_{5/2}$	340,057		$^4P^\circ_{3/2}$	432,757 *		$^4D_{5/2}$	501,890
		312						428
	$^6G_{3/2}$	340,369		$^6D^\circ_{7/2}$	432,934*		$^4D_{3/2}$	502,318
								265
$3d^54p$	$^4F^\circ_{9/2}$	426,409		$^4P^\circ_{1/2}$	433,306 *		$^4D_{1/2}$	502,583
		274						
	$^4F^\circ_{7/2}$	426,683		$^6P^\circ_{3/2}$	433,437 *		$^6D_{9/2}$	509,796
		197						851
	$^4F^\circ_{5/2}$	426,880		$^6D^\circ_{5/2}$	434,130*		$^6D_{7/2}$	510,647
		145						677
	$^4F^\circ_{3/2}$	427,025		$^6D^\circ_{3/2}$	434,977*		$^6D_{5/2}$	511,324
								524
				$^6D^\circ_{1/2}$	435,463*		$^6D_{3/2}$	511,848
								314
				$^6F^\circ_{11/2}$	435,484		$^6D_{1/2}$	512,162
					1,374			
				$^6F^\circ_{9/2}$	436,858	$3d^5$	$^6S_{5/2}$	673,859
					1,073			
				$^6F^\circ_{7/2}$	437,931			
					831			

Tables of Term Values and Wave-lengths

Two illustrations of multiplet groups of lines are given in Tables IV and V. Each line is represented by its frequency, intensity and wave-length in a vacuum. About fifty lines have been traced for the change in configuration $3d^44s - 3d^44p$ through the sequence which starts with V I. Approximately half of these go through to Ni VI, the remainder to Co V. In the other three electronic changes, $3d^44p - 3d^44d$, $3d^5 - 3d^4p$ and $3d^44s^2 - 3d^34sp$, twenty lines have been traced to Co V, and in addition some fainter multiplet lines found in Mn III. Tables VI, VII, VIII, IX and X give the energy level values referred to the lowest level, $3d^4\ {}^5D_0$ of the corresponding atom which has lost one more electron. These values depend on the limits of the sextets in V I and

Table X. *Term values of Ni VI referred to the limit of the sextets, estimated from the Moseley diagram.*

Config.	T.	Value	Config.	T.	Value	Config.	T.	Value
$3d^44d$	${}^6G_{13/2}$	494,090	$3d^44p$	${}^6F^\circ_{9/2}$	613,691	$3d^44s$	${}^4D_{3/2}$	692,038
		1,286			1,485			373
	${}^6G_{11/2}$	495,376		${}^6F^\circ_{7/2}$	615,176		${}^4D_{1/2}$	692,411
					1,146			
$3d\ 4p$	${}^4F^\circ_{9/2}$	604,140		${}^6F^\circ_{5/2}$	616,322		${}^6D_{9/2}$	698,896
		333			1,045			1,273
	${}^4F^\circ_{7/2}$	604,473		${}^6F^\circ_{3/2}$	617,367		${}^6D_{7/2}$	700,169
		270			507			976
	${}^4F^\circ_{5/2}$	604,743		${}^6F^\circ_{1/2}$	617,874		${}^6D_{5/2}$	701,145
		100						642
	${}^4F^\circ_{3/2}$	604,843	$3d^44s$	${}^4D_{7/2}$	690,561		${}^6D_{3/2}$	701,787
					852			341
	${}^6P^\circ_{7/2}$	606,982		${}^4D_{5/2}$	691,413		${}^6D_{1/2}$	702,128
		1,727			625			
	${}^6P^\circ_{5/2}$	608,709						
		1,154						
	${}^6P^\circ_{3/2}$	609,863						
	${}^6F^\circ_{11/2}$	611,508						
		2,183						

Table XI. *Wave-lengths of new lines.*

Vanadium I				Chromium II			
λ(I.A. air)	Int.	ν (vac.)	Origin	λ (I.A. air)	Int.	ν (vac.)	Origin
			$3d^44p \quad 3d^44d$				$3d^44p \quad 3d^43d$
4799.01	8	20831.9	${}^6F^\circ_{11/2} - {}^6G_{11/2}$	2558.28	12	39075.3	${}^6F^\circ_{11/2} - {}^6G_{9/2}$
4785.46	1	20890.8	${}^6F^\circ_{7/2} - {}^6G_{5/2}$	2549.43	40	39211.2	${}^6F^\circ_{11/2} - {}^6G_{11/2}$
4784.48	30-x	20895.1	${}^6F^\circ_{9/2} - {}^6G_{9/2}$	2539.76	10	39360.8	${}^6F^\circ_{9/2} - {}^6G_{9/2}$
4776.44	60	20930.3	${}^6F^\circ_{11/2} - {}^6G_{13/2}$	2539.11	60	39370.8	${}^6F^\circ_{11/2} - {}^6G_{13/2}$
4773.06	10	20945.1	${}^6F^\circ_{7/2} - {}^6G_{7/2}$	2537.60	12	39392.7	${}^6F^\circ_{7/2} - {}^6G_{5/2}$
4766.68	50	20973.1	${}^6F^\circ_{9/2} - {}^6G_{11/2}$	2531.79	40	39485.0	${}^6F^\circ_{7/2} - {}^6G_{7/2}$
4764.13	4	20984.3	${}^6F^\circ_{5/2} - {}^6G_{5/2}$	2530.93	60	39498.4	${}^6F^\circ_{9/2} - {}^6G_{11/2}$
4757.48	50	21013.7	${}^6F^\circ_{7/2} - {}^6G_{9/2}$	2525.47	8	39583.9	${}^6F^\circ_{5/2} - {}^6G_{5/2}$
4756.01	1	21020.2	${}^6F^\circ_{3/2} - {}^6G_{3/2}$	2524.52	40	39598.8	${}^6F^\circ_{7/2} - {}^6G_{9/2}$
4751.58	35	21039.8	${}^6F^\circ_{5/2} - {}^6G_{7/2}$	2520.42	20	39663.3	${}^6F^\circ_{3/2} - {}^6G_{3/2}$
4748.51	38	21053.4	${}^6F^\circ_{3/2} - {}^6G_{5/2}$	2519.79	40	39673.6	${}^6F^\circ_{5/2} - {}^6G_{7/2}$
4746.66	35	21061.6	${}^6F^\circ_{1/2} - {}^6G_{3/2}$	2516.70	30	39722.1	${}^6F^\circ_{3/2} - {}^6G_{5/2}$
				2515.20	8	39745.8	${}^6F^\circ_{1/2} - {}^6G_{3/2}$

Cr II as calculated by Russell,[14] and the Moseley diagram of Fig. 3. From the most recent values of the constants involved in the relation between principal ionization potential and term value, the ionization potentials were calculated from the equation,

$$V = 0.00012336 \times \text{term value in cm}^{-1}.$$

In this case "principal ionization potential" is used to designate the potential necessary to remove, completely, one electron, changing the atom from the lowest energy in the state under discussion to the lowest energy in the next

TABLE XII. *Wave-lengths of Mn III, in order of increasing frequency.*

λ(I.A.)	Int.	ν (vac.)	Origin
			$3d^14s$ $3d^14p$
2382.77	30	41967.9	$^4D_{3/2}-{}^4P^\circ_{1/2}$
2374.56	50-x	42113.1	$^4D_{5/2}-{}^4P^\circ_{3/2}$
2362.46	40	42328.8	$^4D_{7/2}-{}^4P^\circ_{5/2}$
2360.86	50	42357.4	$^4D_{3/2}-{}^4P^\circ_{3/2}$
2352.72	8	42504.2	$^4D_{1/2}-{}^4P^\circ_{3/2}$
2344.23	12	42657.9	$^4D_{5/2}-{}^4P^\circ_{5/2}$
2331.09	2	42898.4	$^4D_{3/2}-{}^4P^\circ_{5/2}$
2197.61	1	45503.9	$^4D_{7/2}-{}^4F^\circ_{5/2}$
2190.53	30	45651.0	$^4D_{7/2}-{}^4F^\circ_{7/2}$
2182.54	80	45818.2	$^4D_{7/2}-{}^4F^\circ_{9/2}$
2181.96	3	45830.4	$^4D_{5/2}-{}^4F^\circ_{5/2}$
2174.86	70	45979.9	$^4D_{5/2}-{}^4F^\circ_{7/2}$
2173.28	2	46013.4	$^4D_{3/2}-{}^4F^\circ_{3/2}$
2170.49	90	46072.5	$^4D_{3/2}-{}^4F^\circ_{5/2}$
2166.44	28	46158.7	$^4D_{1/2}-{}^4F^\circ_{3/2}$
2009.80	1	49756.2	$^6D_{3/2}-{}^6D^\circ_{1/2}$
2005.27	3	49868.6	$^6D_{5/2}-{}^6D^\circ_{3/2}$
2004.45	2	49889.0	$^6D_{1/2}-{}^6D^\circ_{1/2}$
2001.32	20	49967.0	$^6D_{5/2}-{}^6P^\circ_{3/2}$
1998.16	30	50046.0	$^6D_{3/2}-{}^6D^\circ_{3/2}$
1997.04	25	50074.1	$^6D_{7/2}-{}^6P^\circ_{5/2}$
1996.30	1	50092.7	$^6D_{7/2}-{}^6D^\circ_{5/2}$
1994.19	25	50145.7	$^6D_{3/2}-{}^6P^\circ_{3/2}$
1992.94	5	50177.1	$^6D_{1/2}-{}^6D^\circ_{3/2}$
1991.32	25	50217.9	$^6D_{9/2}-{}^6P^\circ_{7/2}$
1987.57	4	50312.7	$^6D_{5/2}-{}^6P^\circ_{5/2}$
1986.86	30	50330.7	$^6D_{5/2}-{}^6D^\circ_{5/2}$
1982.83	40	50433.0	$^6D_{9/2}-{}^6D^\circ_{7/2}$
1979.78	1	50510.7	$^6D_{7/2}-{}^6P^\circ_{7/2}$
1971.29	40	50728.2	$^6D_{7/2}-{}^6D^\circ_{7/2}$
1962.07	40	50966.6	$^6D_{5/2}-{}^6D^\circ_{7/2}$
1952.52	50	51215.7	$^6D_{9/2}-{}^6D^\circ_{9/2}$
1947.46	80	51348.9	$^4D_{7/2}-{}^4D^\circ_{7/2}$
1943.61	2	51450.6	$^4D_{3/2}-{}^4D^\circ_{1/2}$
1942.94	45	51468.4	$^4D_{5/2}-{}^4D^\circ_{5/2}$
1941.34	40	51510.8	$^6D_{7/2}-{}^6D^\circ_{9/2}$
1940.26	30	51539.5	$^4D_{3/2}-{}^4D^\circ_{3/2}$
1938.23	1	51593.5	$^4D_{1/2}-{}^4D^\circ_{1/2}$
1935.08	5	51677.4	$^4D_{5/2}-{}^4D^\circ_{7/2}$
1934.80	1	51684.9	$^4D_{1/2}-{}^4D^\circ_{3/2}$
1933.94	4	51707·9	$^4D_{5/2}-{}^4D^\circ_{3/2}$

λ(I.A.)	Int.	ν (vac.)	Origin
			$3d^34s^2$ $3d^34sp$
1817.60	15	55017.6	$^4F_{9/2}-{}^4G^\circ_{7/2}$
1806.50	18	55355.7	$^4F_{9/2}-{}^4G^\circ_{9/2}$
1798.05	18	55650.2	$^4F_{7/2}-{}^4G^\circ_{7/2}$
1793.57	10	55818.2	$^4F_{5/2}-{}^4G^\circ_{5/2}$
1790.49	50	55850.6	$^4F_{9/2}-{}^4G^\circ_{11/2}$
1786.10	50	55987.9	$^4F_{7/2}-{}^4G^\circ_{9/2}$
1782.19	40	56110.1	$^4F_{5/2}-{}^4G^\circ_{7/2}$
1780.68	6	56158.3	$^4F_{3/2}-{}^4G^\circ_{5/2}$
			$3d^14p$ $3d^13d$
1707.46	35	58566.5	$^6F_{11/2}-{}^6G^\circ_{11/2}$
1701.12	2	58784.8	$^6F^\circ_{9/2}-{}^6G_{9/2}$
1698.31	35	58882.1	$^6F^\circ_{11/2}-{}^6G_{13/2}$
1695.55	1	58977.9	$^6F^\circ_{7/2}-{}^6G_{7/2}$
1693.22	40	59059.1	$^6F^\circ_{9/2}-{}^6G_{11/2}$
1689.52	15	59188.1	$^6F^\circ_{7/2}-{}^6G_{9/2}$
1686.62	25	59290.2	$^6F^\circ_{5/2}-{}^6G_{7/2}$
1684.10	1	59378.5	$^6F^\circ_{3/2}-{}^6G_{3/2}$
1683.17	20	59411.7	$^6F^\circ_{3/2}-{}^6G_{5/2}$
1679.69	10	59534.8	$^6F^\circ_{1/2}-{}^6G_{3/2}$
1666.99	60	59988.4	$^6F^\circ_{11/2}-{}^6D_{9/2}$
1659.21	25	60269,6	$^6F^\circ_{9/2}-{}^6D_{7/2}$
1653.50	40	60477.8	$^6F^\circ_{9/2}-{}^6D_{9/2}$
1652.66	10	60508.5	$^6F^\circ_{7/2}-{}^6D_{5/2}$
1648.30	15	60668.6	$^6F^\circ_{7/2}-{}^6D_{7/2}$
1644.39	5	60812.8	$^6F^\circ_{3/2}-{}^6D_{1/2}$
1644.05	tr.	60825.4	$^6F^\circ_{5/2}-{}^6D_{5/2}$
1642.72	18	60874.6	$^6F^\circ_{7/2}-{}^6D_{9/2}$
1642.14	1	60896.2	$^6F^\circ_{3/2}-{}^6D_{3/2}$
1640.13	tr	60970.0	$^6F^\circ_{1/2}-{}^6D_{1/2}$
1639.77	10	60984.2	$^6F^\circ_{5/2}-{}^6D_{7/2}$
1633.71	45	61210.4	$^6F^\circ_{1/2}-{}^6F_{11/2}$
1629.15	30	61383.6	$^6F^\circ_{9/2}-{}^6F_{9/2}$
1623.89	25	61580.5	$^6F^\circ_{7/2}-{}^6F_{7/2}$
1619.59	20	61744.0	$^6F^\circ_{5/2}-{}^6F_{5/2}$
1618.46	2	61787.1	$^6F^\circ_{7/2}-{}^6F_{9/2}$
1615.96	10	61882.7	$^6F^\circ_{3/2}-{}^6F_{3/2}$
1615.62	8	61895.7	$^6F^\circ_{5/2}-{}^6F_{7/2}$
1613.63	5	61972.1	$^6F^\circ_{3/2}-{}^6F_{5/2}$
1613.22	1	61987.8	$^6F^\circ_{1/2}-{}^6F_{1/2}$
1611.86	2	62040.1	$^6F^\circ_{1/2}-{}^6F_{3/2}$
			$3d^5$ $3d^14p$
925.2	10	108081.	$^6S_{5/2}-{}^6P^\circ_{3/2}$
922.2	40	108431	$^6S_{5/2}-{}^6P^\circ_{5/2}$
918.5	100	108870	$^6S_{5/2}-{}^6P^\circ_{7/2}$

higher state of ionization. Since $3d^5\ {}^6S$ is the lowest level for Mn III, Fe IV and Co V, the value of this level referred to $3d^4\ {}^5D_0$ of each atom in its next higher state of ionization, was used in the calculation. The results are; Mn III 34.4 volts, Fe IV 56.8 volts and Co V 83.1 volts.

The final tables, XI to XV, give the new lines for this sequence. For each element studied, the values of wave-length, intensity, frequency and origin are given, the order being that of increasing frequency.

The writer wishes to take this opportunity to express her thanks for the use of the vacuum spectrograph and her appreciation of the very helpful advice of Professor R. C. Gibbs during the progress of this investigation.

TABLE XIII. *Wave-lengths of Fe IV in order of increasing frequency.*

λ (I.A.)	Int.	ν (vac.)	Origin	λ (I.A.)	Int.	ν (vac.)	Origin
			$3d^34s \quad 3d^34p$				$3d^34s^2 \quad 3d^34sp$
1825.55	8	54778.0	${}^4D_{3/2}-{}^4P^\circ_{1/2}$	1487.35	5	67246.8	${}^4F_{9/2}-{}^4G^\circ_{7/2}$
1822.72	2	54863.1	${}^4D_{5/2}-{}^4P^\circ_{3/2}$				$3d^34s \quad 3d^34p$
1819.29	1	54966.5	${}^4D_{1/2}-{}^4P^\circ_{1/2}$	1485.48	12	67318.3	${}^4D_{7/2}-{}^4D^\circ_{5/2}$
1815.61	25	55061.8	${}^4D_{7/2}-{}^4P^\circ_{5/2}$	1479.65	38	67583.6	${}^4D_{7/2}-{}^4D^\circ_{7/2}$
1812.53	1	55171.5	${}^4D_{3/2}-{}^4P^\circ_{3/2}$				$3d^34s^2 \quad 3d^34sp$
1801.53	5	55508.4	${}^4D_{5/2}-{}^4P^\circ_{5/2}$	1477.69	5	67673.2	${}^4F_{9/2}-{}^4G^\circ_{9/2}$
1688.44	2	59226.3	${}^4D_{7/2}-{}^4F^\circ_{7/2}$				$3d^34s \quad 3d^34p$
1681.45	25	59472.5	${}^4D_{7/2}-{}^4F^\circ_{9/2}$	1475.67	28	67765.8	${}^4D_{5/2}-{}^4D^\circ_{5/2}$
1680.86	1	59493.4	${}^4D_{5/2}-{}^4F^\circ_{5/2}$	1474.52	2	67818.7	${}^4D_{3/2}-{}^4D^\circ_{1/2}$
1675.78	25	59673.7	${}^4D_{5/2}-{}^4F^\circ_{7/2}$	1472.13	35	67928.8	${}^4D_{3/2}-{}^4D^\circ_{3/2}$
1674.89	5	59705.4	${}^4D_{3/2}-{}^4F^\circ_{3/2}$	1470.54	2	68002.2	${}^4D_{1/2}-{}^4D^\circ_{1/2}$
1672.18	5	59802.2	${}^4D_{3/2}-{}^4F^\circ_{5/2}$	1469.92	20	68030.9	${}^4D_{5/2}-{}^4D^\circ_{7/2}$
1669.73	2	59889.9	${}^4D_{1/2}-{}^4F^\circ_{3/2}$	1469.04	37-x	68071.7	${}^4D_{3/2}-{}^4D^\circ_{5/2}$
1663.52	10	60113.4	${}^6D_{3/2}-{}^6F^\circ_{3/2}$				$3d^34s^2 \quad 3d^34sp$
1663.21	10	60124.7	${}^6D_{1/2}-{}^6F^\circ_{1/2}$	1469.04	x	68071.7	${}^4F_{7/2}-{}^4G^\circ_{7/2}$
1662.26	20	60159.1	${}^6D_{5/2}-{}^6F^\circ_{5/2}$				$3d^34s \quad 3d^34p$
1660.07	20	60238.4	${}^6D_{7/2}-{}^6F^\circ_{7/2}$	1468.11	2	68114.8	${}^4D_{1/2}-{}^4D^\circ_{3/2}$
1656.61	15	60364.2	${}^6D_{1/2}-{}^6F^\circ_{3/2}$				$3d^34s^2 \quad 3d^34sp$
1656.25	10	60377.5	${}^6D_{9/2}-{}^6F^\circ_{9/2}$	1464.81	40	68268.2	${}^4F_{9/2}-{}^4G^\circ_{11/2}$
1652.85	20	60501.6	${}^6D_{3/2}-{}^6F^\circ_{5/2}$	1463.25	4	68341.0	${}^4F_{5/2}-{}^4G^\circ_{5/2}$
1647.05	45	60714.6	${}^6D_{5/2}-{}^6F^\circ_{7/2}$	1459.92	40	68496.9	${}^4F_{7/2}-{}^4G^\circ_{9/2}$
1640.03	65	60974.5	${}^6D_{7/2}-{}^6F^\circ_{9/2}$	1455.66	25	68697.4	${}^4F_{5/2}-{}^4G^\circ_{7/2}$
1630.99	75	61312.4	${}^6D_{9/2}-{}^6F^\circ_{11/2}$	1453.67	15	68791.4	${}^4F_{3/2}-{}^4G^\circ_{5/2}$
1579.73	3	63302.0	${}^6D_{5/2}-{}^6D^\circ_{3/2}$				$3d^34p \quad 3d^34d$
1574.68	8	63505.0	${}^6D_{1/2}-{}^6D^\circ_{1/2}$	1280.43	10	78098.8	${}^6F^\circ_{11/2}-{}^6G_{11/2}$
1571.21	10	63645.2	${}^6D_{3/2}-{}^6D^\circ_{3/2}$	1273.49	2	78524.4	${}^6F^\circ_{9/2}-{}^6G_{9/2}$
1566.54	3	63834.9	${}^6D_{9/2}-{}^6D^\circ_{7/2}$	1271.08	15	78673.2	${}^6F^\circ_{11/2}-{}^6G_{13/2}$
1565.05	2	63895.7	${}^6D_{1/2}-{}^6D^\circ_{3/2}$	1268.40	2	78839.5	${}^6F^\circ_{7/2}-{}^6G_{7/2}$
1563.30	10	63967.2	${}^6D_{5/2}-{}^6D^\circ_{5/2}$	1265.28	15	79033.9	${}^6F^\circ_{9/2}-{}^6G_{11/2}$
1560.26	15	64091.8	${}^6D_{5/2}-{}^6P^\circ_{3/2}$	1263.47	15	79147.1	${}^6F^\circ_{5/2}-{}^6G_{5/2}$
1559.08	15	64140.4	${}^6D_{7/2}-{}^6P^\circ_{5/2}$	1261.72	10	79256.9	${}^6F^\circ_{7/2}-{}^6G_{9/2}$
1556.48	15	64247.4	${}^6D_{9/2}-{}^6P^\circ_{7/2}$	1259.54	30	79394.1	${}^6F^\circ_{5/2}-{}^6G_{7/2}$
1555.01	1	64308.2	${}^6D_{3/2}-{}^6D^\circ_{5/2}$	1258.68	2	79448.3	${}^6F^\circ_{3/2}-{}^6G_{3/2}$
1552.11	15	64428.3	${}^6D_{7/2}-{}^6D^\circ_{7/2}$	1257.29	6	79536.1	${}^6F^\circ_{3/2}-{}^6G_{5/2}$
1547.58	15	64616.9	${}^6D_{5/2}-{}^6P^\circ_{5/2}$	1254.80	10	79694.0	${}^6F^\circ_{1/2}-{}^6G_{3/2}$
1546.03	8	64681.6	${}^6D_{1/2}-{}^6P^\circ_{3/2}$				$3d^5 \quad 3d^34p$
1542.15	15	64844.4	${}^6D_{7/2}-{}^6P^\circ_{7/2}$	587.6	2	172829.	${}^6S_{5/2}-{}^6P^\circ_{3/2}$
1540.77	1	64902.5	${}^6D_{5/2}-{}^6D^\circ_{7/2}$	576.8	40	173368.	${}^6S_{5/2}-{}^6P^\circ_{5/2}$
1538.67	25	64991.1	${}^6D_{9/2}-{}^6D^\circ_{9/2}$	574.5	50	174061	${}^6S_{5/2}-{}^6P^\circ_{7/2}$
1524.67	15	65587.9	${}^6D_{7/2}-{}^6D^\circ_{9/2}$				

TABLE XIV. *Wave-lengths of Co V in order of increasing frequency.*

λ(I.A.)	Int.	ν (vac.)	Origin.
		$3d^34s$ $3d^34p$	
1488.73	20	67171.4	$^4D_{3/2}-{}^4P^\circ_{1/2}$
1486.02	25	67293.8	$^4D_{5/2}-{}^4P^\circ_{3/2}$
1482.91	20	67435.0	$^4D_{1/2}-{}^4P^\circ_{1/2}$
1482.62	25	67448.2	$^4D_{7/2}-{}^4P^\circ_{5/2}$
1476.65	30	67720.8	$^4D_{3/2}-{}^4P^\circ_{3/2}$
1468.98	35	68074.4	$^4D_{5/2}-{}^4P^\circ_{5/2}$
1459.77	15	68503.9	$^4D_{3/2}-{}^4P^\circ_{5/2}$
1389.11	32	71988.5	$^6D_{5/2}-{}^6F^\circ_{3/2}$
1380.21	10	72452.2	$^6D_{1/2}-{}^6F^\circ_{1/2}$
1379.05	10	72513.7	$^6D_{3/2}-{}^6F^\circ_{5/2}$
1378.12	25	72562.1	$^6D_{5/2}-{}^6F^\circ_{5/2}$
1375.20	30	72716.7	$^6D_{7/2}-{}^6F^\circ_{7/2}$
1373.09	30	72828.4	$^6D_{1/2}-{}^6F^\circ_{3/2}$
1371.01	10	72938.9	$^6D_{9/2}-{}^6F^\circ_{9/2}$
1369.30	4	73030.0	$^4D_{7/2}-{}^4F^\circ_{7/2}$
1368.24	30	73086.6	$^6D_{3/2}-{}^6F^\circ_{5/2}$
1364.17	30	73304.6	$^4D_{7/2}-{}^4F^\circ_{9/2}$
1362.46	30	73393.9	$^6D_{5/2}-{}^6F^\circ_{7/2}$
1361.32	20	73458.3	$^4D_{5/2}-{}^4F^\circ_{5/2}$
1357.67	30	73655.6	$^4D_{5/2}-{}^4F^\circ_{7/2}$
1356.09	tr.	73741.9	$^4D_{3/2}-{}^4F^\circ_{3/2}$
1355.20	40	73789.8	$^6D_{7/2}-{}^6F^\circ_{9/2}$
1353.42	15	73886.9	$^4D_{3/2}-{}^4F^\circ_{5/2}$
1351.22	6	74007.2	$^4D_{1/2}-{}^4F^\circ_{1/2}$
1345.67	50	74312.4	$^6D_{9/2}-{}^6F^\circ_{11/2}$
1301.12	35	76856.9	$^6D_{5/2}-{}^6D^\circ_{5/2}$
1295.87	40	77168.2	$^6D_{3/2}-{}^6D^\circ_{5/2}$
1295.55	25	77187.3	$^6D_{7/2}-{}^6D^\circ_{7/2}$
1286.95	28	77703.2	$^6D_{9/2}-{}^6D^\circ_{9/2}$
1284.00	15	77881.6	$^6D_{5/2}-{}^6P^\circ_{3/2}$
1281.63	30	78025.6	$^6D_{7/2}-{}^6P^\circ_{5/2}$
1277.01	50	78307.9	$^6D_{9/2}-{}^6P^\circ_{7/2}$
1275.52	2	78399.4	$^6D_{3/2}-{}^6P^\circ_{3/2}$
1272.23	20	78602.1	$^6D_{11/2}-{}^6D^\circ_{11/2}$
1270.70	20	78696.8	$^6D_{5/2}-{}^6P^\circ_{5/2}$
1270.44	tr.	78712.9	$^6D_{1/2}-{}^6P^\circ_{3/2}$
1263.28	5	79159.0	$^6D_{7/2}-{}^6P^\circ_{7/2}$
1258.61	6	79452.7	$^6D_{9/2}-{}^6D^\circ_{11/2}$
1246.91	8	80198.2	$^4F_{9/2}-{}^4G^\circ_{9/2}$
1239.85	2	80654.9	$^4F_{7/2}-{}^4G^\circ_{7/2}$
1236.95	20	80844.0	$^4F_{9/2}-{}^4G^\circ_{11/2}$
1234.55	2	81001.2	$^4F_{5/2}-{}^4G^\circ_{5/2}$
1231.73	15	81186.6	$^4F_{7/2}-{}^4G^\circ_{9/2}$
1228.19	8	81420.6	$^4F_{5/2}-{}^4G^\circ_{7/2}$
1226.31	3	81545.4	$^4F_{3/2}-{}^4G^\circ_{5/2}$
		$3d^34s^2$ $3d^34sp$	
			$3d^34p$ $3d^34d$
1028.08	1	97268.7	$^6F^\circ_{11/2}-{}^6G_{11/2}$
1021.14	10	97853.1	$^6F^\circ_{9/2}-{}^6G_{9/2}$
1018.36	10	98197.1	$^6F^\circ_{11/2}-{}^6G_{13/2}$
1017.43	1	98286.9	$^6F^\circ_{7/2}-{}^6G_{7/2}$
1013.80	10	98638.8	$^6F^\circ_{9/2}-{}^6G_{11/2}$
1010.94	10	98917.8	$^6F^\circ_{7/2}-{}^6G_{9/2}$
1009.02	15	99106.1	$^6F^\circ_{5/2}-{}^6G_{7/2}$
1007.51	10	99254.6	$^6F^\circ_{3/2}-{}^6G_{5/2}$
1006.86	4	99318.7	$^6F^\circ_{1/2}-{}^6G_{3/2}$
			$3d^5$ $3d^34p$
415.94	1	240419.	$^6S_{5/2}-{}^6P^\circ_{3/2}$
414.52	5	241243	$^6S_{5/2}-{}^6P^\circ_{5/2}$
412.59	10	242371	$^6S_{5/2}-{}^6P^\circ_{7/2}$

TABLE XV. *Wave-lengths for Ni VI in order of increasing frequency.*

λI.A.	Int.	ν (vac.)	Origin.
		$3d^34s$ $3d^34p$	
1191.72	5	83912.3	$^6D_{3/2}-{}^6F^\circ_{1/2}$
1186.90	2	84253.1	$^6D_{1/2}-{}^6F^\circ_{1/2}$
1184.56	4	84419.5	$^6D_{3/2}-{}^6F^\circ_{3/2}$
1179.80	20	84760.2	$^6D_{1/2}-{}^6F^\circ_{3/2}$
1170.08	15	85464.2	$^6D_{3/2}-{}^6F^\circ_{5/2}$
1163.20	10	85969.7	$^6D_{5/2}-{}^6F^\circ_{7/2}$
1161.61	2	86088.2	$^4D_{7/2}-{}^4F^\circ_{7/2}$
1157.13	15	86420.7	$^4D_{7/2}-{}^4F^\circ_{9/2}$
1156.36	12	86478.3	$^6D_{9/2}-{}^6F^\circ_{9/2}$
1153.79	2	86670.9	$^4D_{5/2}-{}^4F^\circ_{5/2}$
1150.22	10	86940.6	$^4D_{5/2}-{}^4F^\circ_{7/2}$
1146.85	8	87195.4	$^4D_{3/2}-{}^4F^\circ_{3/2}$
1145.53	15	87295.8	$^4D_{3/2}-{}^4F^\circ_{5/2}$
1144.32	18	87388.1	$^6D_{9/2}-{}^6F^\circ_{11/2}$
1141.96	10	87568.7	$^4D_{1/2}-{}^4F^\circ_{3/2}$
1095.49	8	91283.3	$^6D_{5/2}-{}^6P^\circ_{3/2}$
1093.37	40	91460.4	$^6D_{7/2}-{}^6P^\circ_{5/2}$
1087.97	50	91914.3	$^6D_{9/2}-{}^6P^\circ_{7/2}$
1083.98	5	92252.6	$^6D_{1/2}-{}^6P^\circ_{3/2}$
1081.82	1	92436.8	$^6D_{3/2}-{}^6P^\circ_{5/2}$
1074.51	15	93065.7	$^6D_{3/2}-{}^6P^\circ_{5/2}$
1073.11	12	93187.1	$^6D_{7/2}-{}^6P^\circ_{7/2}$
			$3d^34p$ $3d^34d$
861.09	2	116132	$^6F^\circ_{11/2}-{}^6G_{11/2}$
851.66	20	117418	$^6F^\circ_{11/2}-{}^6G_{13/2}$
844.69	20	118386	$^6F^\circ_{9/2}-{}^6G_{11/2}$

A NEW TYPE OF CRYSTAL FINE-STRUCTURE: LITHIUM FERRITE ($Li_2O \cdot Fe_2O_3$)

By E. Posnjak and Tom. F. W. Barth
Geophysical Laboratory, Carnegie Institution, Washington, D. C.
(Received October 9, 1931)

Abstract

The interpretation of the x-ray diffraction obtained from the isometric modification of lithium ferrite resulted in the conclusion that the smallest "unit" of this structure contains four anions and four cations. The anions, oxygens, occupy the four equivalent points 4*b* while the cations, iron and lithium, occupy together the four equivalent points 4*c*. The large difference in the scattering power of iron and lithium makes it possible to arrive at the definite conclusion that in the structure of lithium ferrite the same set of equivalent positions is occupied by the two chemically different elements (variate atom equipoints). It is shown that the distribution of iron and lithium in this set of equipoints is not regular, that is, there are not always two of each cation present in the "unit"; the distribution is one of chance, which, however, must comply with the requirement that an equal number of each of the cations is always present within a relatively small space. In view of these findings the conception of the unit cell loses its traditional chemical significance and becomes strictly a geometric conception. The "unit cell" of lithium ferrite has a meaning only if its lattice be regarded as geometric points in space. The lattice of lithium ferrite is then identical with the one of the "sodium chloride" structure (4b, 4c); the unit cube contains one molecule of $Li_2O \cdot Fe_2O_3$, and the length of its edge is 4.141 ± 0.005A. The density of lithium ferrite is 4.368 and its refractive index $n_{Li} = 2.40 \pm 0.04$.

Introduction

In the course of studies of ferrites it became of interest to prepare and examine the properties of the alkali ferrites. Although sodium and potassium ferrites have been described in the literature, there is apparently no record of the preparation of lithium ferrite. It will be appropriate therefore to mention that the experiments showed that this compound could be prepared in two modifications, an isotropic and an anisotropic one. The latter resulted from the interaction of a concentrated solution of lithium hydroxide and ferric oxide when heated in a pressure bomb somewhat below 600°C, while above this temperature the cubic modification was formed. The isometric modification was also prepared by heating the appropriate mixture consisting of lithium carbonate and ferric oxide, at red heat. The relation of the two modifications of lithium ferrite has not been determined. In this paper we shall be concerned only with the one formed at the higher temperature which is isotropic, and which was found not to invert when cooled to and kept at room temperature. The optical examinations were kindly made by Dr. George Tunell of this Laboratory, who found that the isotropic modification has a refractive index $n_{Li} = 2.40 \pm 0.04$. The determination of the density of this modification by the pycnometer method[1] resulted in the value of 4.368.

[1] J. Johnston and L. H. Adams, J. Am. Chem. Soc. **34**, 563 (1912).

X-ray Diffraction Measurements

When lithium ferrite was prepared in the bomb by crystallization from solution, minute single octahedral crystals were obtained, the edges and corners of which were modified by rounded faces which were apparently dodecahedra and cubes. They were, however, too small to be utilized singly for x-ray measurements. Diffraction was therefore obtained only by the powder method. The apparatus was one made by the General Electric Company, equipped for using K_α radiation of molybdenum. The spacings were standardized in the usual way by exposure of sodium chloride on the same film alongside of lithium ferrite. Data obtained from such a powder spectrogram are given in Table I. By using the customary equation

TABLE I. *Powder diffraction data from lithium ferrite* ($Li_2O \cdot Fe_2O_3$).

Planar spacing	Intensity (estimated)	Indices	a_0
2.39	4	111(1)	4.143
2.07	10	100(2)	4.142
1.461	9	110(2)	4.128
1.247	3	113(1)	4.144
1.195	4	111(2)	4.144
1.035	2	100(4)	4.141
0.949	1	133(1)	4.140
0.925	5	120(2)	4.139
0.845	4	112(2)	4.143
0.798	1	111(3) 115(1)	4.150
0.732	1−	110(4)	4.144
0.690	2	100(6) 122(2)	4.132
0.654	2	130(2)	4.139
0.624	1	113(2)	4.141
0.575	1−	230(2)	4.145
0.553	1	123(2)	4.138
			$a_0 = 4.141 \pm 0.005$A

$m = a_0^3\rho/M$, where m is the number of molecules of $Li_2O \cdot Fe_2O_3$ within the unit, M the mass of a molecule of the substance, ρ its density, and a_0 the length of the edge of the unit cube, we find $m = 0.993$. This is, within experimental error, a whole number, as it should be, and one may therefore assume that one molecule of $Li_2O \cdot Fe_2O_3$ is associated with the unit cube.

Application of Space Group Criteria

From the reflections given in Table I it is immediately obvious that the lattice underlying the structure of lithium ferrite is a face-centered one. An examination of the tabulation of the results of the theory of space groups shows, however, that there is no space group with an underlying face-centered lattice, or for that matter of any other cubic lattice, which would accommodate two lithium, two iron, and four oxygen ions. This fact would suggest that it may be necessary to multiply the number of molecules of $Li_2O \cdot Fe_2O_3$, and therefore the length of the edge of the unit cell in which they are contained, by a simple integer, as for instance by two; however, we shall show later that this will be found to conflict with the experimental data.

Atomic Arrangement of $Li_2O \cdot Fe_2O_3$

The comparison of the diffraction data from lithium ferrite with those of magnesium and ferrous oxides presents a clue for the solution of the problem. Thus it was found that the diffraction from lithium ferrite bore a very close similarity to that of the two substances just mentioned. The powder diffraction patterns of all three are reproduced in Fig. 1 and it will be readily seen how small the differences in spacings and intensities are. In view of recent experience in the study of spinels[2] in which the present authors had shown that different elements occupy crystallographically equivalent positions, it was thought not to be improbable that lithium ferrite presented another case of variate atom equipoints. Both magnesium oxide[3] and ferrous oxide[4] had been shown to have the sodium chloride structure containing four cations and four anions per unit cell in a face-centered arrangement (4*b*, 4*c*). In the case of lithium ferrite it was thought that by analogy lithium and iron together may occupy four equivalent positions and the oxygens the other four; thus com-

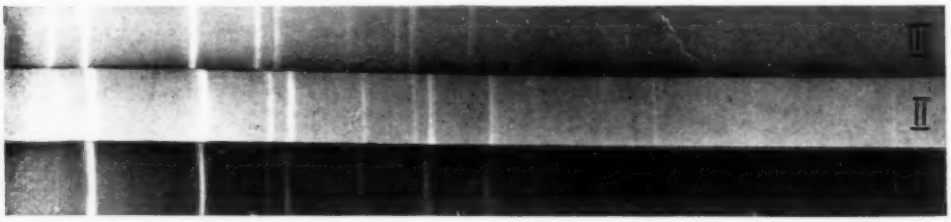

Fig. 1. Spectrograms of I, MgO; II, $Li_2O \cdot Fe_2O_3$; and III, FeO.

plying with the experimental evidence of the presence of two lithium, two iron, and four oxygen ions per unit cell of the lithium ferrite structure.

By making this assumption, the next question that arises concerns the interrelation between the lithium and iron ions within the crystal: are the points in arrangement 4*c* occupied in a regular or an irregular fashion by the two different kinds of ions? The following discussion will prove that it is necessary to conclude that the distribution of lithium and iron among the points of arrangement 4*c* must be one of chance, complying only with the requirement of an equal number of each within a relatively very small space.

The simplest regular arrangement which we may assume would be obtained by placing the lithium and iron ions alternately between the oxygens. Then in the direction of the edge of the cube we would have O–Fe–O–Li–O—. It is quite obvious that in this case the length of the edge of the unit cube would be twice that of the "sodium chloride" arrangement where it extends only from one oxygen over a cation to the next oxygen. The length of the edge of the unit cell given in Table I corresponds to the one in the "sodium chloride" structure, and if we assume the regular distribution of iron and

[2] Tom. F. W. Barth and E. Posnjak, J. Wash. Acad. Sci. **21,** 255 (1931).

[3] W. P. Davey and E. O. Hoffmann, Phys. Rev., [2], **15,** 333 (1920); W. Gerlach and O. Pauli, Zeits. f. Physik **7,** 116 (1921); R. W. G. Wyckoff, Am. J. Sci. [5], **1,** 138 (1921).

[4] R. W. G. Wyckoff and E. D. Crittenden, J. Am. Chem. Soc. **47,** 2876 (1925).

lithium it would therefore be necessary to conclude that the true length of the edge of the cube is $2a_0$. This would of course result in the necessity of reassigning all our indices to higher orders—they would all be multiplied by two, which means that no first order reflections at all would occur in the lithium ferrite structure. However, such a conclusion can be shown to be incompatible with the established theory of the interaction of x-rays and crystals. The proof in this case is identical with that advanced by L. Vegard and H. Schjelderup[5] and more precisely brought out by M. v. Laue[6] in clearing up the theory of diffraction in the case of mixed crystals. The discussion may be confined to the consideration of the structure factor of the face-centered cubic crystal resulting from the regular arrangement of lithium and iron mentioned above, the length of the edge of the unit cell of which is $A_0 = 2a_0$. The structure factor can be expressed as the product of the following three parts:

$$F_1 = \left[1 + e^{2\pi i(h+k)/2} + e^{2\pi i(h+l)/2} + e^{2\pi i(k+l)/2}\right]^2$$

$$F_2 = \left[1 + e^{2\pi i(h+k)/4} + e^{2\pi i(h+l)/4} + e^{2\pi i(k+l)/4}\right]^2$$

$$F_3 = \left[\overline{\mathrm{O}}(1 + e^{2\pi i(h+k+l)/2}) + \overline{\mathrm{Li}} \cdot e^{-2\pi i(h+k+l)/2} + \overline{\mathrm{Fe}} \cdot e^{2\pi i(h+k+l)/2}\right]^2.$$

The part F_1 is due to the fact that the whole lattice is made up of face-centered lattices; the part F_2 because from such a lattice three other identical lattices will be developed by the displacements $A_0/4$, 0, $A_0/4$; 0, $A_0/4$, $A_0/4$ and $A_0/4$, $A_0/4$, 0; and part F_3 shows that in the direction parallel to a body diagonal there are situated equally spaced O–Li–O–Fe. With the help of this structure factor all reflections which can occur may be calculated. When this is done it is found that while all the reflections which have been observed should occur in this structure, there should in addition be present reflections which, however, were not found in the spectrogram. For instance, the reflection from 111(1), the spacing of which would be 4.78A, has the structure factor 16.16 ($\overline{\mathrm{Fe}} - \overline{\mathrm{Li}}$) and, owing to the difference in the scattering power of iron and lithium, the intensity of this reflection should be stronger than any of those observed. As a matter of fact there is no indication of a diffraction line in this position, and therefore the assumption of the regular distribution of iron and lithium which required doubling the length of the edge of our unit cell must be discarded.

We now have to evaluate our experimental data in regard to the other assumption, namely, the chance distribution of iron and lithium in the four equipoints (4*c*) of the "sodium chloride" arrangement. Taking into consideration not too small a portion of the crystal an equal number of points is occupied by iron and by lithium. Therefore in calculating the intensities the average of the scattering power of the two may be taken, (Fe+Li)/2. The position of the atoms are: O in (4*b*) i.e. 0 0 0 , $\frac{1}{2}\ \frac{1}{2}\ 0$, $\frac{1}{2}\ 0\ \frac{1}{2}$, $0\ \frac{1}{2}\ \frac{1}{2}$; and 2Fe+2Li in (4*c*) i.e. $\frac{1}{2}\ \frac{1}{2}\ \frac{1}{2}$, $\frac{1}{2}\ 0\ 0$, $0\ \frac{1}{2}\ 0$, $0\ 0\ \frac{1}{2}$. The intensities of reflection were calculated on the basis of the equation

[5] L. Vegard and H. Schjelderup, Phys. Zeits. **18,** 93 (1917).

[6] M. v. Laue, Ann. d. Physik [4], **56,** 497 (1918).

$$I = j\frac{1 + \cos^2 2\theta}{\sin 2\theta}F^2,$$

employing the F-values published by W. L. Bragg and J. West[7] for iron and oxygen. For lithium the F-curve given recently by R. W. James and G. W. Brindley[8] was used. The results are given in Table II from which it will be

TABLE II. *Comparison of observed and calculated diffraction intensities from lithium ferrite ($Li_2O \cdot Fe_2O_3$).*

Indices	Estimated	Calculated	Indices	Estimated	Calculated
(111)	4	1.4	(333)}	1	1.3
(200)	10	10.4	(115)}		
(220)	9	8.8	(440)	1−	0.8
(113)	3	2.3	(600)}	2	1.6
(222)	4	3.1	(244)}		
(400)	2	1.3	(260)	1	1.0
(133)	1	1.5	(226)	1	0.8
(240)	5	4.0	(460)	1−	0.5
(422)	4	2.8	(246)	1	0.8

seen that the calculated intensities are in very good agreement with the estimates made from the spectrogram. Therefore we must conclude that this is the correct structure and that iron and lithium together occupy four equipoints of the "sodium chloride" arrangement filling these points in equal molecular ratio by chance distribution. The holohedral symmetry required by the "sodium chloride" arrangement is in accord with the observed external crystal faces and it may also be mentioned that the lattice dimensions of lithium ferrite agree well with the accepted values of the atomic radii.

CONCLUSIONS

In a recent study of the structure of spinels the authors[9] have shown that the 16 equivalent positions (16*c*) of this structure are not all occupied by chemically equivalent ions, but that eight of them are of one kind, such as the trivalent Fe^{+++}, Al^{+++}, Ga^{+++}, etc., while the other eight are bivalent ions like Mg^{++}, Fe^{++}, etc. The present study of the structure of lithium ferrite, which structurally is the simplest possible case and therefore an even more convincing one, again proves that crystallographically equivalent positions in a crystal may be occupied by chemically different ions (Fe^{+++} and Li^{+}). Such crystals with variate atom equipoints challenge in a certain way our usual conceptions of "crystal" and "chemical compound." Crystallographically, in crystals with variate atom equipoints we find that the usual symmetry requirements (symmetry operations) cannot be extended to its smallest unit, that is, the unit cell. Such an extension can only be accomplished if the atoms are regarded purely as geometrical points in space. Crystals with variate atom equipoints do not exhibit in their lattice the regular

[7] W. L. Bragg and J. West, Zeits. f. Krist. **69**, 118 (1929).
[8] R. W. James and G. W. Brindley, Phil. Mag. [7] **12**, 81 (1931).
[9] Tom. F. W. Barth and E. Posnjak, J. Wash. Acad. Sci. **21**, 255 (1931).

periodicity in regard to the chemical character of the atoms composing it, which is usually associated with our conception of compounds. However, it should be remembered that the conception of the molecule also found no support from the crystal structure of such simple substances as the alkali halides, some oxides, etc.; indeed, the conception of the "unit cell" was introduced and in a sense replaced it, but only as a convenient descriptive term, for it would be very arbitrary to think of the chemical molecule as being identical with the unit cell. In the solid state the only logical limitation of the molecule is the macrocrystal itself.

It may be suggested that the structure with variate atom equipoints be regarded as representing the general case of which the other structures are special cases. We know that the possession of a (geometrical) unit cell of indefinite chemical composition (which is identical with having variate atom equipoints) is apparently the property of all mixed crystals and is therefore a very common phenomenon. There seems to be no obvious reason from the point of view of geometrical and descriptive crystallography why compounds would not require similar treatment.

Several cases are on record in which the same problem arose. For instance, ammonium-oxy-fluoro-molybdate,[10] $(NH_4)_3MoO_3F_3$, whose x-ray diffraction data indicate that the O and F ions occupy crystallographically equivalent positions. In this case it was possible to explain the structure by assuming a larger unit cell, the existence of which, however, could not be brought out by the x-ray spectrograms on account of the similarity of the scattering power of O and F. Other cases were potassium cyanate,[11] KCNO, in which C and N seemed to occupy crystallographically equivalent positions and $Co(NH_3)_5H_2OSO_4I$,[12] in which the NH_3 groups are partly replaced by H_2O. In these cases again the explanation given for ammonium-oxy-fluoro-molybdate appeared reasonable. In the case of lithium ferrite, however, it can be shown in view of the large difference in the scattering power of the cations that an enlargement of the unit cell is inadequate to explain this structure, and thus it becomes much more reasonable to assume that the iron and lithium ions are irregularly distributed within the same set of equipoints.

While very few cases of this type of structure have so far been encountered in compounds, and it is also impossible at present to say what significance attaches to this fact, further studies will show whether or not these cases are fortuitous.

[10] L. Pauling, J. Am. Chem. Soc. **46**, 2738 (1924).
[11] S. B. Hendricks and L. Pauling, J. Am. Chem. Soc. **47**, 2904 (1925).
[12] O. Hassel, Norsk. Geol. Tidsskrift. **10**, 33 (1928). See also *idem*, p. 92.

NATURAL UNITS FOR ATOMIC PROBLEMS

By Arthur E. Ruark
University of Pittsburgh

(Received September 16, 1931)

Abstract

This paper deals principally with two systems of units, designated A and B. In both, the velocity of light and the rest mass of the electron are taken as units. In A, the length unit is $h^2/4\pi^2 m_0 e^2$, which is the radius of the first Bohr hydrogen orbit, in B, it is $h/2\pi m_0 c$, which is $(2\pi)^{-1}$ times the Compton shift in scattering at 90°. In each system, the choice of the above units determines the unit of charge through the equation for the Coulomb force, $f = e^2/r^2$. In system A, the electronic charge is numerically equal to the fine structure constant, α; in system B, the square of the electronic charge is numerically equal to α, and h is equal to 2π. It is shown that many formulas of quantum theory are greatly simplified when written in terms of system B; the coefficients of the Schrödinger and Dirac equations contain only small integers and the electronic charge. The use of these units provides a consistent scheme for simplifying the algebra associated with problems of quantum theory.

§1

WE ARE all familiar with numerous cases in which the mathematical treatment of physical problems is simplified by a suitable choice of units. In the computation of atomic energy levels Hylleraas[1] and others have found it very useful to employ a unit of length of the same order of magnitude as the radius of the first Bohr orbit. Sometimes also, the energy required to ionize the hydrogen atom from its lowest state is taken as the unit of energy. However, when the relativistic wave equations are used, the self-energy of the electron is a more convenient unit. This circumstance led the writer to consider the whole question of natural units for use in problems of atomic and nuclear physics. It soon appeared that rather striking simplifications of the wave-mechanical equations can be achieved by proper choice of units. The determination of the most convenient unit systems was not straightforward, but required considerable searching. The writer's conclusions are presented in this brief paper, which is devoted to methodology, and contains no new physical result.

One of the best-known attempts to simplify the equations of quantum theory and related subjects is that of Planck,[2] who chose new units of length, time, mass and temperature, of such sizes that the velocity of light, the quantum of action, the universal constant of gravitation, and the gas constant are all numerically equal to one. The rounded values of the units of length, time and mass are as follows:

[1] Hylleraas, Zeits. f. Physik **65**, 209 (1930), and earlier papers.
[2] Planck, Heat Radiation, English translation by Masius, p. 175.

Unit of length: 4×10^{-33} centimeter
Unit of time: 1.3×10^{-43} second
Unit of mass: 5.4×10^{-5} gram.

We leave the gas constant out of consideration, since it may always be made unity by properly choosing the unit of temperature.

Obviously, the difficulty with this system is that the new units are not convenient in size for use in atomic problems. The same criticism may be directed against many similar attempts. The writer tried, therefore, to obtain systems of units which fulfill, as far as possible, the following requirements: The fundamental units of length, time and mass must be of such magnitude that atomic lengths, times, and masses are expressible by fairly small numbers, as long as we deal with small quantum numbers; and the coefficients in the principal equations of atomic physics should be simplified when the new units are used. Two of the systems examined will be discussed in detail.

§2

In setting up a system of natural units almost every step consists in abandoning some artificial relation associated with the c.g.s. system. We try to proceed as a Maxwell demon probably would if he were entrusted with the construction of a natural and universal scheme of units. In this section we concern ourselves with two systems, designated A and B. In both, the velocity of light, c, is taken as the unit of velocity. In extranuclear problems, the units of length adopted are as follows:

A: $h^2/4\pi^2m_0e^2$, the radius of the first hydrogen orbit if the motion of the nucleus is neglected.

B: $h/2\pi m_0c$, the Compton wave-length change in scattering at 90°, divided by 2π.

The corresponding units of time are fixed by the choices already made. They are,

A: $h^2/4\pi^2m_0e^2c$.

B: $h/2\pi m_0c^2$.

In both systems we take the rest mass of the electron as the mass unit. At first sight it might seem better to assign the value unity to e, the electronic charge, but this does not simplify the more important equations of quantum theory as much as the choice we have made.[3]

It will often be convenient to prime a quantity measured in c.g.s. units, the unprimed symbol being reserved for the same quantity measured in the new units. Thus $h' = 6.547\times10^{-27}$ erg sec., the conventional value of Planck's constant, while it happens that in system B the numerical value of h is 2π.

[3] The essential point is, we cannot make both the elementary charge and the electronic mass *simultaneously* equal to unity, unless we are willing to modify the classical equation for the force between two charges by introducing a constant analogous to the constant of gravitation. The expression $f = \epsilon^2/r^2$, giving the force between two equal charges, ϵ, serves to define the unit of charge. If the numerical values of f and r are unity, then ϵ is the unit of charge. But it is readily verified that the force between two electrons at unit distance is not one in either of the schemes considered here, so the electronic charge cannot be one in these systems.

The unit of action in B is $m_0' \cdot c' \cdot (h'/2\pi m_0' c') = h'/2\pi = (1.042 \pm .0013) \times 10^{-27}$ erg second. This is the quantum of action adopted by Dirac, Weyl and others, in preference to Planck's constant. The use of the symbol h for this quantity has led to so much confusion that a new one seems desirable. Perhaps h_0 would be an acceptable designation. The desire to employ $h'/2\pi$ as the unit of action constituted the writer's reason for choosing $h'/2\pi m_0' c'$ as the new unit of length in system B. Anyone who wishes to employ Planck's constant as the unit of action may do so by taking $h'/m_0' c'$ as the length unit; but then the factor 2π, or some power of it, will appear in many equations.

In Table I we give the c.g.s. numerical values of the new units of certain important physical quantities. These are rounded, since it is not necessary to

TABLE I. *Approximate c.g.s. values of natural units.*

Physical quantity	c.g.s value of unit in system A	c.g.s value of unit in system B
Length	$h'^2/4\pi^2 m_0' e'^2 = 0.5 \times 10^{-8}$	$h'/2\pi m_0' c' = 3.9 \times 10^{-11}$
Time	$h'^2/4\pi^2 m_0' e'^2 c' = 0.17 \times 10^{-18}$	$h'/2\pi m_0' c'^2 = 1.3 \times 10^{-21}$
Velocity	$c' = 3 \times 10^{10}$	$c' = 3 \times 10^{10}$
Mass	$m_0' = 9 \times 10^{-28}$	$m_0' = 9 \times 10^{-28}$
Momentum	$m_0' c' = 2.7 \times 10^{-17}$	$m_0' c' = 2.7 \times 10^{-17}$
Energy	$m_0' c'^2 = 8.1 \times 10^{-7}$	$m_0' c'^2 = 8.1 \times 10^{-7}$
Action	$\alpha h'/2\pi = 1.4 \times 10^{-25}$	$h'/2\pi = 1.0 \times 10^{-27}$
Charge	$e'/\alpha = 6.5 \times 10^{-8}$	$e'/\alpha^{1/2} = 5.6 \times 10^{-9}$

use them in recasting the equations of quantum theory. In the table, α represents the fine structure constant, which is dimensionless. According to Birge,[4] we have

$$\alpha = \frac{2\pi e^2}{hc} = (7.283 \pm 0.006) \times 10^{-3} \tag{1}$$

and

$$\frac{1}{\alpha} = \frac{hc}{2\pi e^2} = 137.29 \pm 0.11. \tag{2}$$

The numerical value of the unit of charge in any system may readily be found with the aid of these relations. In system B, for example, $c = 1$, and $2\pi/h = 1$. Therefore,

$$e^2 = \alpha. \quad (\textit{system } B \textit{ only}) \tag{3}$$

and the new unit of charge measured in c.g.s. electrostatic units must be $e'/\alpha^{1/2} = 4.770 \times 10^{-10}/8.533 \times 10^{-2} = 5.59 \times 10^{-9}$ e.s.u. Similarly,

$$e = \alpha. \quad (\textit{system } A \textit{ only}). \tag{4}$$

It is reasonable to suppose that in nuclear problems it will prove convenient to use units exactly like those of Table I, except that the mass of the proton, or possibly that of the alpha-particle, will replace the electronic mass in the definitions of the units. Attention may be directed to the quantity $e^2/m_0 c^2$, which has the dimensions of length (it is equal to $\alpha h/2\pi m_0 c$) and is of the same order of magnitude as the classical radius of the Lorentz electron.

[4] Birge, Phys. Rev. Supplement **1**, 1 (1929).

Systems involving the so-called gravitational radius of the electron have also been considered by the writer, but will not be discussed here.

§3

It is now possible to state the relative advantages of the proposed systems. Atomic diameters are of the order unity in system A, and frequencies associated with the outer electron shells are of the same order as the corresponding c.g.s. wave numbers. It appears that the units of system A are well adapted in size to the discussion of the outer electrons and of wave-lengths in the optical region, while system B is more useful in dealing numerically with fast electrons and x-ray phenomena. However, the chief benefits to be derived from the use of these units are associated with the facts that algebra is often simplified, and that many atomic constants have small numerical values. For example, in both systems the numerical measures of a mass and of the corresponding energy are identical, since $c=1$. The self energy of the electron is unity. Wave number and frequency are numerically identical and further the electrostatic and electromagnetic units of any quantity are the same. The expression for the Lorentz force per unit charge is $E+[vH]$ and many other electrodynamic formulae are less complex than in c.g.s. units.

It is interesting to note the simple forms assumed by certain equations of atomic theory when the system B is employed. All quantities belonging to the electron have values expressible in terms of integers and of the electronic charge, provided the customary expressions for the electronic angular momentum and magnetic moment are rigorously correct. Thus, the angular momentum is numerically $1/2$, and the magnetic moment $e/2$. Of all electronic properties, then, only the charge requires experimental determination, from the standpoint of both our new unit systems.[5] In both of them, its numeric is connected in a simple way with the fine structure constant, as we see from Eqs. (1) to (4).

Further, in system B the energy, mass and momentum of a photon are all given numerically by $2\pi\nu$, and exponential factors in wave functions are simplified. Thus, numerically $e^{-2\pi iEt/h}$ becomes e^{-iEt}. Such examples could be indefinitely multiplied.

We now illustrate the application of system B to several important equations. Heisenberg's commutation relation is

$$pq - qp = \frac{hI}{2\pi i}. \tag{5}$$

But $h=2\pi$, and (5) may be rewritten as

$$pq - qp = -iI. \quad (\textit{system } B \textit{ only}). \tag{5a}$$

[5] Of course it is not implied that the determination of electronic constants other than the charge can be avoided in connection with *practical* problems. For example, in order to express a length of the order of a few centimeters in terms of the new unit of length, that unit would first have to be found in terms of some familiar unit, such as the centimeter. The new systems are designed to reduce labor for the theoretical and not the experimental physicist.

In this form, the physical units of the right member are submerged, but the algebra of any matrix problem is simplified, and the "lost" constants can easily be reinserted in the final result. It is not necessary to go through laborious transformations in obtaining (5a) or other simplified equations. For example, in the new units as in the old, Schrödinger's equation has the form

$$\Delta\psi + \frac{8\pi^2}{h^2}(E - V)\psi = 0; \tag{6}$$

but in system B, $4\pi^2/h^2 = 1$, numerically, and (6) becomes,

$$\Delta\psi + 2(E - V)\psi = 0. \quad (system\ B\ only). \tag{6a}$$

The relativistic Schrödinger equation and the Dirac equations are also simplified. To summarize, when we use system B, the general equations of quantum mechanics have rational coefficients, except for the occurrence of the electronic charge, which is numerically equal to $\alpha^{1/2}$.

Eddington[6] has brought forward a theory involving space of sixteen dimensions, which indicates that $1/\alpha$ may be exactly 137, that is, $1+1/2$ (17.16). If this were substantiated, all coefficients in the wave equation would be rational. However, Birge's value of $1/\alpha$, cited in Eq. (2), disagrees with Eddington's 137 by more than twice the probable error. Other interpretations of α have been suggested by Lewis and Adams,[7] by Perles,[8] and by Fürth;[9] but such matters, important as they may be, lie outside our present scope.

In conclusion, it may be worth while to note that the use of the natural units discussed focuses attention on certain unsolved problems of quantum theory. The only empirical constants which occur when we apply the Schrödinger Eq. (6a) to the problem of the hydrogen atom are α and m/M. The former enters through the fact that $V = -Ze^2/r = -Z\alpha/r$, in accordance with Eq. (3). No doubt the value of α is connected with the internal mechanism of the electron, as we can see by examining classical electronic models, while it appears probable that m/M will eventually be interpreted as the ratio of two eigenwerte of a still-to-be-discovered wave equation. Pending the elucidation of these matters, the use of our system B reduces the wave equation to very simple terms.

[6] Eddington, Proc. Roy. Soc. **A126,** 696 (1930) and earlier papers.
[7] Lewis and Adams, Phys. Rev. **3,** 92 (1914).
[8] Perles, Naturwiss. **16,** 1094 (1928).
[9] Fürth, Zeits. f. Physik **57,** 429 (1929).

SOME PHYSICAL PROPERTIES OF COMPRESSED GASES. II, CARBON MONOXIDE

By W. Edwards Deming and Lola E. Shupe
Fertilizer and Fixed Nitrogen Investigations
Bureau of Chemistry and Soils
Washington, D. C.

(Received September 5, 1931)

Abstract

The writers have adjusted and extrapolated the compressibility data obtained by Bartlett and his collaborators on carbon monoxide, so that accurate $p-v-T$ relations from $-70°$ to $400°$ and up to 1200 atm. are available. The relatively low pressure isotherms of Scott at 25° and of Goig-Botella at 0°, 12.44°, and 20.22° are included. Derivatives are obtained by the graphical scheme used for similar calculations on nitrogen. The specific volume, density, expansion coefficients $-(p/v)(dv/dp)_T$ and $(T/v)(dv/dT)_p$ fugacity, C_p, C_p-C_v, C_v, Joule-Thomson coefficient μ are calculated and shown in curves and a table for 14 pressures and 11 temperatures in the range $-70°$ to $400°$ and 25 to 1200 atm. In particular, C_p vs. p isotherms, C_v vs. t isobars, t vs. $p\,\mu=$const. graphs are shown; among the last, the $\mu=0$ curve is the inversion curve. There are no direct experimental data for comparison. On account of similarity in the molecular structure and the spectra of the molecules CO and N_2, one might look for some correspondence in the physical properties of the two gases. In general, the trends of the two are qualitatively similar. The C_p-C_v vs. p isotherms all show a maximum. This maximum is very flat at the highest temperatures and comes at about 700 atm. As the temperature decreases, the maximum becomes pronounced and moves to lower pressures; it comes at about 200 atm. along the $-50°$ and $-70°$ curves. Along the $-70°$ isotherm a second maximum appears at about 550 atm., but it is not evident at higher temperatures. C_p-C_v approaches R, of course, along all isotherms as the pressure is decreased to zero. C_p is obtained by adding ΔC_p to C_p^*. C_p^* denotes the heat capacity for a given temperature at zero pressure; ΔC_p is the change in C_p with pressure along a given isotherm. It is evaluated thru $\int_0^p -T(d^2v/dT^2)_p dp$. The derivative occurring under the integral sign is obtained by the authors' graphical scheme at a sufficient number of points for mechanical integration under the isotherm. Along isotherms at 50° and lower, C_p increases rapidly with pressure and reaches a maximum at about 300 atm. Changes in pressure above 500 atm. cause only relatively small changes in C_p at any temperature. Above 200 atm. and below 0°, C_p increases rapidly as the temperature is lowered. The C_v vs. t isobars show that from 300 to 1200 atm. C_v has a minimum at about 100°. On the low temperature side of this minimum the curves are very steep; along the 1200 atm. isobar C_v drops from 4.4 R at $-70°$ to 2.57 R at 100°. Above 100°, C_v is only a few hundredths cal./mole deg. higher than C_v^* for pressures up to 400 atm; further increase in pressure to 1200 atm. raises C_v only a few tenths. Below 25°, C_v for $p=25$ is slightly less than C_v^*. Below 0°, C_v at 100, 150, and 200 atm. drops far below C_v^* as the temperature is lowered. A graph showing $\Delta\equiv v(pv/RT-1)$ vs. ρ isotherms and isobars is shown, the data for which are listed in the table. This graph is very convenient for interpolating $p-v-T$ data. Having given two of the three $p-v-T$ coordinates, the third is quickly estimated from the graph, or is readily computed more exactly by reading the ordinate Δ and solving $\Delta=v(pv/RT-1)$ for the unknown desired. Values for the second virial coefficient are found. They are expressible by $B=58.03-19.84\ T^{-1}$ cc/mole between $-70°$ and 400°.

FAIRLY complete compressibility data for several gases over considerable range of pressure and temperature are now available. The work of Bartlett and his collaborators and of others on nitrogen, hydrogen, and their mixtures,[1] carbon monoxide,[2] methane,[3] and helium[4] form valuable extensions of hitherto existing data. A method of determining derivatives such as $(dv/dp)_T$, $(dv/dT)_p$, $(d^2v/dT^2)_p$ from compressibility data enables various physical properties to be computed. The writers have been using a graphical scheme for evaluating derivatives. Curves and a table showing specific volume, density, fugacity, expansion coefficients $-(p/v)(dv/dp)_T$ and $(T/v)(dv/dT)_p$, ΔC_p, C_p, $C_p - C_v$, C_v, and μ for nitrogen over the range $-70°$ to $600°$ and from 20 to 1200 atm. have been published.[5] In the present paper we give the results for carbon monoxide.

This graphical scheme depends on the fact that

$$\Delta \equiv v(pv/RT - 1) \tag{1}$$

and

$$\alpha \equiv RT/p - v \tag{2}$$

and their derivatives with respect to p, v, T express the deviation from Boyle's law; and that any departure of $-(p/v)\ (dv/dp)_T$ and $(T/v)\ (dv/dT)_p$ from unity is evidenced by Δ and α and their derivatives being different from zero. In addition to the relations between the derivatives of v, Δ, and α given by Eqs. (3) to (10), we shall need[6]

$$(T/v)(dv/dT)_p = \frac{pv/RT - (d\Delta/dT^{-1})_p/vT}{1 + 2\rho\Delta} \tag{15}$$

$$(T/v)(dv/dT)_p = pv/RT[\rho^2(d\Delta/d\rho)_p + (1 + 2\rho\Delta)] \tag{16}$$

$$(T/v)(dv/dT)_p = (d\alpha/dT^{-1})_p/vT + RT/pv \tag{17}$$

$$-T(d^2v/dT^2)_p = \frac{T}{v}\left\{\left(\frac{dv}{dT}\right)^2 - \frac{1}{p}\,\frac{d}{dT}\left(pv\,\frac{dv}{dT}\right)\right\}_p, \tag{18}$$

[1] Bartlett, J. Amer. Chem. Soc. **49,** 687 (1927); **49,** 1955 (1927); Bartlett, Cupples, Tremearne, ibid. **50,** 1275 (1928); Bartlett, Hetherington, Kvalnes, Tremearne, ibid. **52,** 1363 (1930).

[2] Bartlett, Hetherington, Kvalnes, Tremearne, J. Amer. Chem. Soc., **52,** 1374 (1930); G. A. Scott, Proc. Roy. Soc. **125A,** 330 (1929); Severian Goig-Botella, Anales soc. espan. fisquim **27,** 315 (1929); one set of his measurements at 0° is published in duplicate in the Comptes Rendus **189,** 246 (1929).

[3] Kvalnes and Gaddy, J. Amer. Chem. Soc. **53,** 394 (1931). This publication gives data from $-70°$ to 200° and up to 1000 atm. Isotherms at 300° and 400° will soon be undertaken by Dr. Wiebe on the same apparatus.

[4] Wiebe, Gaddy, Heins, J. Amer. Chem. Soc. **53,** 1721 (1931). This publication gives data from $-70°$ to 200° and up to 1000 atm. Isotherms at 300° and 400° will soon be undertaken by Dr. Wiebe on the same apparatus.

[5] W. Edwards Deming and Lola E. Shupe, Phys. Rev. **37,** 638 (1931).

[6] In this paper, the equations, figures, and tables will be numbered as continuations from those in the paper on nitrogen.

because it is more accurate to use Δ and α in isobars against T^{-1} than against T, and because the second derivative is conveniently found from $pv(dv/dT)_p$ vs. T isobars, as will be explained later.

After Bartlett's[2] data on carbon monoxide were published a recalibration of his thermocouple showed that the temperatures recorded as $-25°$, $-50°$, $-70°$ should have been $-24.99°$, $-49.93°$, $-69.90°$. The slight corrections necessary at these temperatures were made, and then Δ vs. p isotherms were plotted from Bartlett's data at $-70°$, $-50°$, $-25°$, $0°$, $25°$, $50°$, $100°$, $150°$, $200°$ to 1000 atm., and from Scott's 25° isotherm, which goes to 170 atm.,

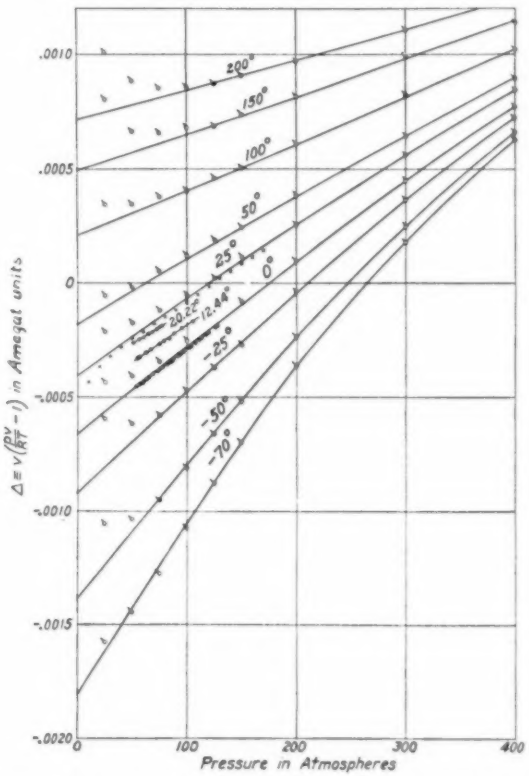

Fig. 7. Δ vs. p isotherms for carbon monoxide to 400 atmospheres. Bartlett's points are flagged circles, Goig-Botella's are circles, Scott's are crosses. Scott's isotherm is at 25°, Goig-Botella's are at 0°, 12.44°, and 20.22°. The data were smoothed according to the curves.

and from Goig-Botella's isotherms at 0°, 12.44°, and 20.22°, which go from 50 to 130 atm. The low pressure portion of these isotherms are shown in Fig. 7. We also plotted Δ vs. T^{-1} isobars obtained from Bartlett's data, at 25, 50, 75, 100, 150, 200, 300, 400, 500, 600, 800, 1000 atm., from $-70°$ to 200°. On these curves were also placed points from Scott's and Goig-Botella's data where they could be used. By trial and error smooth isotherms and isobars were finally placed so that the same value of Δ would be read from a curve on either plot at a given temperature and pressure. This is equivalent to fixing a smooth Δ, p, T^{-1} surface in space.

The $pv/(pv)_0$ value for 800 atm. and 25° was misprinted in Bartlett's paper as 1.9915. It should be 1.0115.

Bartlett's isobars were extrapolated to 1200 atm. and his isotherms to 400°; this is a 20 percent extrapolation with regard to pressure and a 22 percent extrapolation with regard to T^{-1}. Since Bartlett gives nine isotherms and twelve isobars in the range $25 \leqq p \leqq 1000$ atm. and $0.002113 \leqq T^{-1} \leqq 0.004922$, extrapolation to 1200 atm. and to $0.001485°K^{-1}$ should be trustworthy. The value of these extrapolations, if they are any where near as reliable as we think they are, must be considerable; to extend the p-v-T observations to 300° and 400° and to 1200 atm. would require some changes in the apparatus; in fact serious difficulties would have to be overcome in experiments with carbon monoxide at 300° and 400° under high pressure.

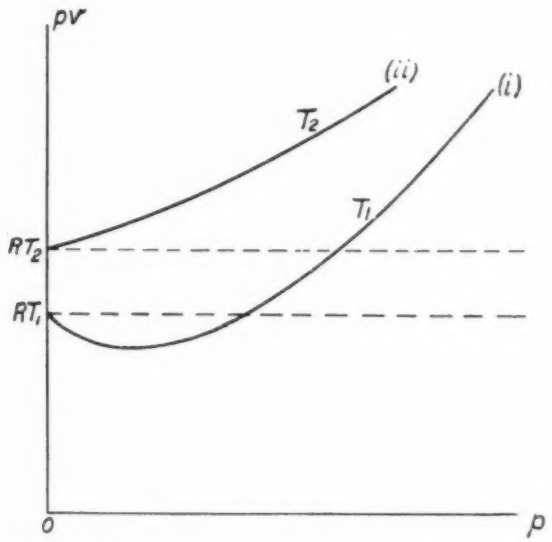

Fig. 8. The isothermal variation of pv with p at low pressure for an actual gas. Carbon monoxide takes the form of (*i*) at 50° or lower, and takes the form of (*ii*) at 100° or higher.

As with nitrogen, the close proximity of the plotted (experimental) values of Δ to the final smooth curves, on which lie the adjusted values of Δ, attests to the high precision of the compressibility data and gives promise that the derived calculations should be reliable. An exception occurs at Bartlett's low pressure observations, as is seen in Fig. 7. The curves shown were drawn from the following considerations.

Holborn and Otto[7] found that the expression

$$pv = RT + ap + bp^2 + cp^4 \tag{19}$$

is capable of following the data of most of the permanent gases along an isotherm from about 20 to 100 atm. Recently William Wild[8] has observed that

[7] Holborn and Otto, Zeits. f. Physik **33,** 1 (1925).

[8] William Wild, Phil. Mag. **12,** 41 (1931).

this power series, when used with constants obtained from data between roughly 20 and 100 atm., extrapolated to 1 atm. gives the "compressibility" (usually denoted by $1+\lambda$, the ratio of the pv product at zero pressure to the product at 1 atm., both at 0°C) in agreement better than 1 in 10,000 with the value obtained from low pressure data where a linear equation $pv = RT + ap$ suffices. These facts mean that the series (19) is capable of expressing the trends of the isotherms from zero pressure up to 50 or 100 atm.

From Eq. (19),

$$\Delta = a + (a^2/RT + b)p + (2ab/RT)p^2 + (b^2/RT + c)p^3 + \cdots \quad (20)$$

A pv vs. p isotherm will take the form (*i*) or (*ii*) in Fig. 8, depending on whether the temperature is below or above the Boyle temperature; at the

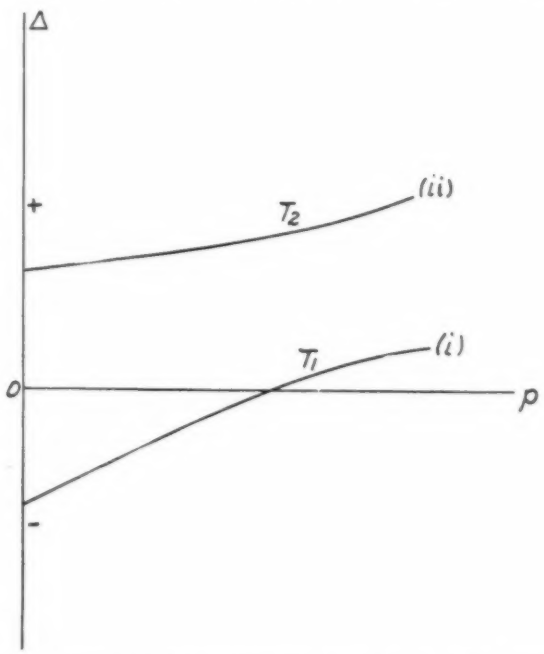

Fig. 9. The graphs of Δ vs. p corresponding to the pv vs. p isotherms in Fig.6.

Boyle temperature $pv = RT$ and the curve is a horizontal line, at least for some distance. Along (*ii*) $a>0$ and $b>0$, hence the corresponding Δ vs. p graph will begin as a straight line with a positive intercept and positive slope and will then curve upward as indicated in Fig. 9, since the coefficients of p and p^2 in (20) are positive. Along (*i*) $a<0$ and $b>0$, so the corresponding Δ curve will begin as a straight line with a negative intercept and positive slope and will then curve downward as shown, since in (20) the coefficients of p and p^2 are positive and negative respectively. The trends thus predicted for the Δ curves are beautifully followed by Goig-Botella's and Scott's points in Fig. 7, but not by Bartlett's. Goig-Botella's and Scott's apparatuses were designed for the low pressure region, but Bartlett's was designed primarily for

work from 100 to 1000 atm., and the upward curl of his points may come from a small systematic error, active only at low pressure. This explanation of the deviation is satisfactory according to a private communication from Dr. Bartlett.

It should be noted that this discrepancy is only slight. The Δ curves are magnified residuals; further, $(dp/d\Delta)_{v,T} = RT\rho^2$ is very small at the low pressure (or low density) end—at 25 atm. and 0° a change in Δ of 0.0001 Amagat units affects the calculated pressure only 0.06 atm.; therefore the points in Fig. 7, instead of showing the data to be unreliable, really show them to be remarkably systematic.

The family of Δ *vs.* T^{-1} isobars (not shown) become nearly straight lines at the higher temperatures and at the lower pressures. The zero pressure isobar is fitted well enough by a straight line, and

$$\Delta = b - (a/R)T^{-1} \tag{21}$$

may be taken for its equation. When Δ is replaced by $v(pv/RT-1)$, this becomes closely

$$(p + a/v^2)(v - b) = RT, \tag{22}$$

which is van der Waals' equation. From this,

$$-T(d^2v/dT^2)_p = 2a/RT^2 \text{ at } p = 0. \tag{23}$$

The slope $-a/R$ of the zero pressure isobar is -0.8856 Amagat units, so

$$\begin{aligned} -T(d^2v/dT^2)_p &= 2 \times 0.8856T^{-2} \text{ Amagat units} \\ &= 960.7T^{-2} \text{ cal./mole atm. deg.} \end{aligned} \tag{24}$$

This quantity will be used later in calculating the heat capacities. It is the value of $(dC_p/dp)_T$ at zero pressure. A more accurate equation of state would give the same result for this purpose, since we need the derivative $-T(d^2v/dT^2)_p$ only at zero pressure.

Eq. (1) can be rewritten as

$$pv/RT = 1 + \Delta\rho. \tag{25}$$

Δ at low pressures is then the second virial coefficient, usually denoted by B; so the Δ vs. T^{-1} zero pressure isobar is really a plot of B. It is expressed by statistical theory in terms of the interaction energy ϵ of two molecules, and the temperature, by

$$B = 2\pi N \int_0^\infty (1 - e^{-\epsilon/kT})r^2 dr. \tag{26}$$

According to London,[9] $-\epsilon$ lies between $3\alpha^2 V_a/4r^6$ and $3\alpha^2 V_i/4r^6$. α here denotes the polarizability of the molecule, and is not the α of Eq. (2). V_a and V_i are the excitation and ionization energies, and r is the molecular separation.

[9] Eisenschitz and London, Zeits. f. Physik **60**, 491 (1930); London, Zeits. f. Physik **63**, 245 (1930).

Margenau[10] evaluated the above integral by assuming that $\epsilon = \infty$ for $r \leqq d$, and $-\epsilon = 3\alpha^2 V_i/4r^6$ when $r > d$. His result is

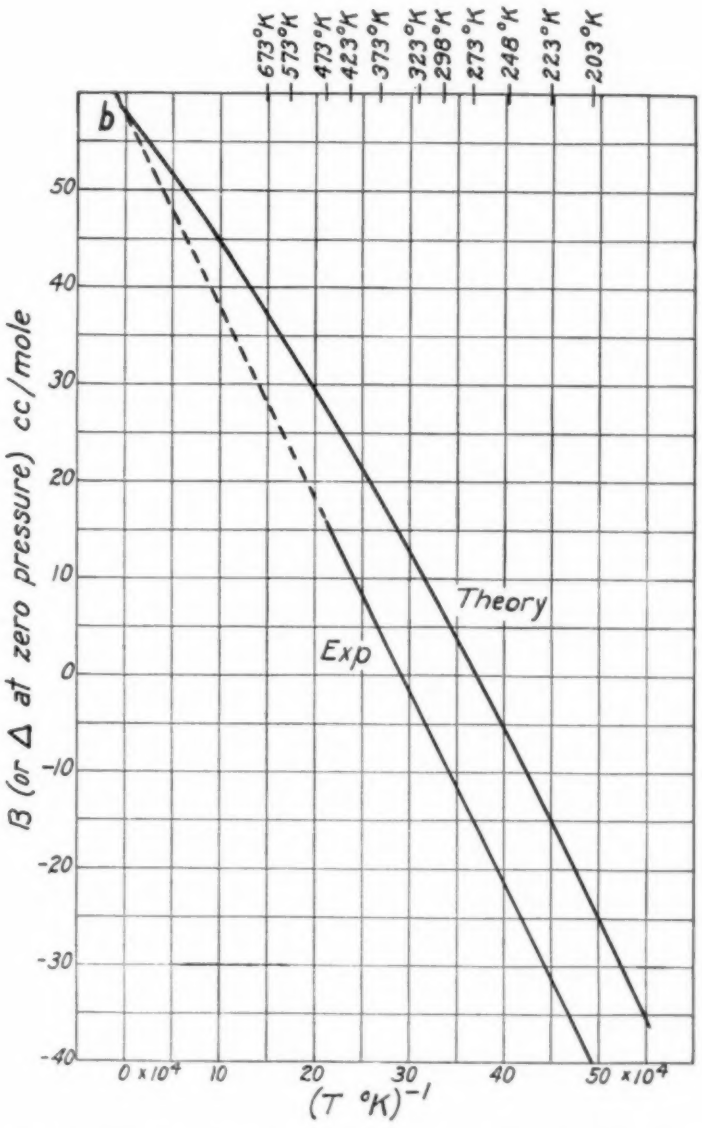

Fig. 10. Carbon monoxide. The curve marked "Exp." shows the experimental values of the second virial coefficient from $-70°$ to 200°C. The extrapolation (dashed) gives $b = 58.03$ cc/mole. This value in Eq. (27) gives the curve marked "Theory".

$$B = b(1 - 0.75y - 0.094y^2 - 0.014y^3 - 0.0019y^4 - 0.00022y^5 - 0.000022y^6 - \cdots) \tag{27}$$

[10] H. Margenau, Phys. Rev. **36**, 1782 (1930).

where

$$b = 2\pi N d^3/3, \quad y = \alpha^2 V_i/d^6 kT = 4\pi^2 N^2 \alpha^2 V_i/9kb^2 T.$$

b is thus four times the volume of N spheres of diameter d. If N is the number of molecules per mole, b is in cc/mole. b can be evaluated by extrapolating the zero pressure Δ vs. T^{-1} isobar back to $T^{-1}=0$. The value so obtained is $b=0.002590$ Amagat units or $22403\times 0.002590 = 58.03$ cc/mole. Zahn and Miles[11] give information from which it is possible to deduce that the polariz-

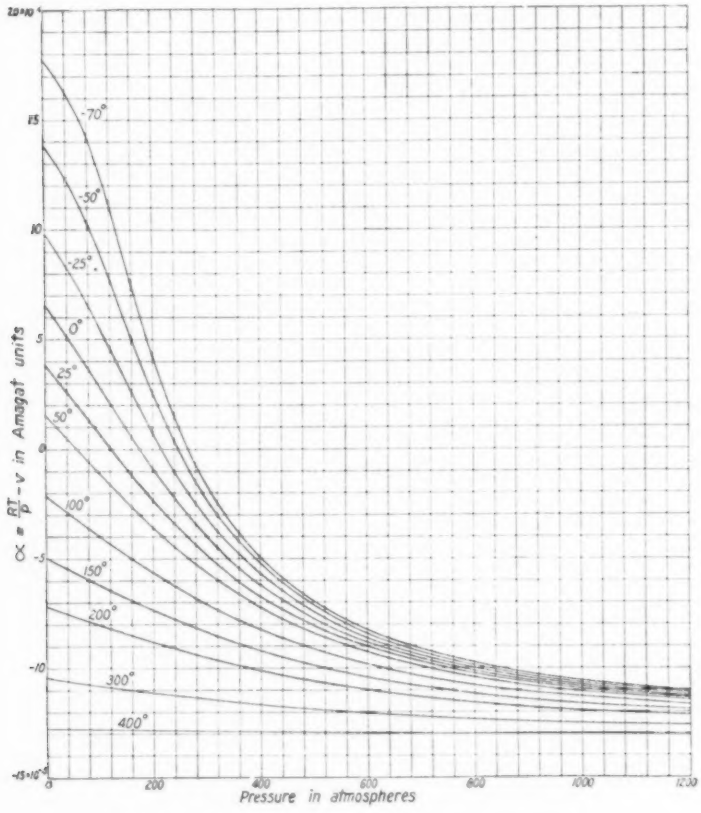

Fig. 11. α vs. p isotherms for carbon monoxide.

ability of CO is 1.97×10^{-24}cc per molecule. John T. Tate and P. T. Smith[12] found 14.20 electron volts for the ionization potential of CO.

With these, $y=177.7T^{-1}$. The curve given by the series (27) is marked "Theory" in Fig. 10. The curve marked "Exp." is our Δ vs. T^{-1} zero pressure isobar. The agreement is fairly good. The theoretical curve has a perceptible curvature over the range of experiment, $-70° \leqq t \leqq 200°$, while the other does not. According to a recent paper by Kirkwood and Keyes,[13] the second virial

[11] C. T. Zahn and J. B. Miles Jr., Phys. Rev. **32**, 497 (1928).

[12] From a paper read at the Washington meeting of the American Physical Society, May 2, 1931.

[13] J. G. Kirkwood and F. G. Keyes, Phys. Rev. **37**, 832 (1931).

coefficient for He goes through a maximum at about $-100°$, and the same phenomenon should appear at sufficiently high temperatures for other gases. This would imply that the experimental curve should not be extrapolated as a straight line to $T^{-1}=0$ and that $b<58.03$; also that the assumptions underlying the development of Eq. (27) are not fully valid at high temperatures, and that perfect agreement of the curves in Fig. 10 is not to be expected. The experimental curve in Fig. 10, or the list of Δ at zero pressure at the bottom of Table II are probably as good values for the second virial coefficient from $-70°$ to $400°$ as can be gotten from the data available.

The α vs. p isotherms of Fig. 11 might be of some interest. There has been some conjecture[14] concerning the shape of these curves for a real gas, and Fig. 11 is probably the first publication for an extended range for any gas.[14a] The areas under the curves are used in determining fugacities by Eq. (28).

The tables published by Bartlett and others show compressibility factors $pv/(pv)_0$ at the different pressures and temperatures. The denominator $(pv)_0$ is the value of pv at S. T. P. Baxter[15] gives 1.00048 for $pv/(pv)_0$ at zero pressure. Using Birge's value 22414.1 cc for the volume of a mole of an ideal gas at S. T. P. we have $22414.1/1.00048=22403.3$ for the factor to convert Amagat units of volume into cc/mole. Multiplication of densities in mole/cc by 28.006 converts them into g/cc. We also use $R=82.0489$ cc atm./mole deg. or 1.9864 cal./mole deg., and 273.18° for the ice point, after Birge.

The final values of the physical properties are shown in Table II and in the figures. Care has been taken in each entry to give only as many figures as we consider significant; the last figure is considered doubtful. No points are shown on the curves because they are drawn through the plotted point in every case. Each physical property listed will now be discussed.

Specific volume v, column 2; density ρ, column 3; Δ, column 10 and Fig. 12.

The values of Δ were read from the Δ vs. p isotherms or from the Δ vs. T^{-1} isobars. Those for zero pressure or zero density constitute the second virial coefficient, and are shown at the bottom of the table and in Fig. 10. Eq. (1) solved for v then gives the specific volume for any pressure and temperature at which Δ is known. The densities in column 3 are in g/cc and were obtained by dividing 28.006 by the corresponding v in cc/mole.

The Δ vs. ρ isotherms and isobars of Fig. 12 are convenient for exhibiting and interpolating the p-v-T data, as is described in the title to the figure. Any one of the p-v-T coordinates can be quickly estimated when the other two are given; when greater accuracy is desired, the value of Δ, as read from the graph corresponding to the two given coordinates (ρ and T, v and p, etc.), is substituted in Eq. (1) to obtain the third coordinate. The values of Δ are listed so that anyone desiring to make interpolations in the p-v-T data with more accuracy than can be gotten from the Fig. 12 appearing here can construct a

[14] Lewis and Randall, Thermodynamics, p. 195 (McGraw-Hill Book Company, 1923).

[14a] Added in proof. Since this was written, a table of α for nitrogen from $-148°$ to 300° and to about 100 atm. has appeared in a paper by George Tuncll, J. Phys. Chem. **35**, 2885 (1931).

[15] Baxter *et al.*, J. Amer. Chem. Soc. **53**, 1627 (1931).

TABLE II. *Some physical properties of compressed carbon monoxide derived from experimental data on compressibility.*

1 p	2 v	3 ρ	4 f	5 $-\frac{p}{v}\left(\frac{dv}{dp}\right)_T$	6 $\frac{T}{v}\left(\frac{dv}{dT}\right)_p$	7 ΔC_p	8 C_p	9 C_v	10 Δ
atm.	cc/mole	g/cc	atm.			calories/mole degree			cc/mole
			$t=-70°$	$C_p^*=6.953$,	$C_v^*=4.967$	cal./mole deg.			
25	629.0	.04453	23.59	1.057	1.220	.63	7.58	4.94	−35.62
50	298.1	.09395	44.67	1.100	1.465	1.37	8.32	4.86	−31.57
75	189.8	.1475	63.68	1.118	1.710	2.21	9.16	4.71	−27.71
100	138.3	.2025	81.13	1.076	1.899	3.11	10.06	4.54	−23.64
150	92.40	.3031	113.4	.881	1.943	4.57	11.53	4.45	−15.57
200	73.95	.3787	144.9	.667	1.706	5.38	12.34	4.64	−8.33
300	59.32	.4721	214.5	.446	1.188	5.76	12.72	6.01	4.01
400	52.77	.5307	299.5	.366	.888	5.52	12.47	7.05	14.05
500	48.91	.5726	405.9	.320	.780	5.26	12.21	6.67	22.85
600	46.23	.6058	539.7	.293	.708	5.31	12.26	6.62	30.69
800	42.69	.6561	917.8	.257	.552	5.52	12.47	7.63	44.76
1000	40.35	.6941	1509	.238	.467	5.62	12.57	8.17	57.31
1100	39.43	.7103	1917	.231	.426	5.65	12.60	8.54	63.16
1200	38.62	.7252	2422	.223	.396	5.67	12.62	8.75	68.73
			$t=-50°$	$C_p^*=6.953$,	$C_v^*=4.967$	cal./mole deg.			
25	703.6	.03980	24.00	1.038	1.168	.51	7.46	4.95	−27.69
50	339.9	.08239	46.22	1.062	1.352	1.07	8.02	4.85	−24.40
75	220.6	.1269	67.00	1.064	1.500	1.67	8.63	4.83	−21.24
100	162.9	.1719	86.70	1.037	1.619	2.28	9.23	4.77	−17.99
150	109.3	.2561	124.3	.909	1.655	3.28	10.23	4.87	−11.40
200	86.02	.3256	161.7	.751	1.528	3.87	10.82	5.02	−5.20
300	66.20	.4231	242.9	.551	1.172	4.16	11.11	5.74	5.60
400	57.44	.4876	339.4	.433	.942	4.01	10.96	5.86	14.63
500	52.60	.5325	457.9	.374	.810	3.86	10.81	5.80	22.94
600	49.36	.5674	604.6	.337	.710	3.88	10.83	6.02	30.47
800	45.00	.6224	1010	.291	.569	4.02	10.97	6.63	43.46
1000	42.16	.6643	1624	.271	.484	4.08	11.03	7.08	54.91
1100	41.07	.6819	2038	.262	.447	4.10	11.05	7.31	60.27
1200	40.13	.6979	2544	.251	.417	4.11	11.06	7.44	65.42
			$t=-25°$	$C_p^*=6.954$	$C_v^*=4.968$	cal./mole deg.			
25	794.6	.03524	24.36	1.022	1.124	.40	7.36	4.96	−19.33
50	389.7	.07186	47.62	1.032	1.245	.82	7.78	4.93	−16.76
75	256.4	.1092	70.01	1.029	1.348	1.26	8.22	4.90	−14.23
100	191.3	.1464	91.80	1.007	1.421	1.69	8.64	4.90	−11.58
150	128.9	.2173	134.5	.925	1.454	2.36	9.31	5.00	−6.50
200	100.3	.2791	177.5	.808	1.392	2.76	9.71	5.02	−1.46
300	74.75	.3747	270.5	.629	1.152	2.99	9.95	5.31	7.84
400	63.62	.4403	378.8	.509	.969	2.93	9.88	5.30	15.88
500	57.35	.4883	509.2	.432	.833	2.84	9.80	5.36	23.41
600	53.26	.5258	667.6	.393	.724	2.83	9.78	5.61	30.33
800	47.86	.5852	1094	.342	.591	2.86	9.81	5.99	42.14
1000	44.45	.6301	1720	.314	.504	2.87	9.82	6.31	52.58
1100	43.13	.6494	2132	.303	.469	2.88	9.83	6.48	57.35
1200	42.01	.6666	2628	.285	.441	2.88	9.84	6.48	62.01
			$t=0°$	$C_p^*=6.956$,	$C_v^*=4.970$	cal./mole deg.			
25	884.0	.03168	24.62	1.012	1.094	.33	7.28	4.96	−12.55
50	437.6	.06400	48.60	1.015	1.183	.66	7.62	4.94	−10.44
75	290.3	.09649	72.13	1.008	1.255	1.00	7.95	4.94	−8.33
100	217.8	.1286	95.38	.989	1.305	1.32	8.27	4.95	−6.25
150	147.4	.1900	141.7	.926	1.334	1.83	8.79	5.02	−2.02
200	114.2	.2453	189.0	.843	1.299	2.14	9.10	5.05	2.15
300	83.71	.3346	290.8	.674	1.135	2.36	9.32	5.07	10.08
400	69.96	.4003	408.3	.566	.980	2.35	9.31	5.10	17.39
500	62.19	.4504	547.6	.493	.851	2.31	9.27	5.22	24.08
600	57.13	.4902	714.1	.443	.748	2.27	9.23	5.39	30.24
800	50.72	.5521	1152	.380	.616	2.20	9.16	5.57	41.11
1000	46.72	.5995	1778	.352	.531	2.16	9.12	5.81	50.65
1100	45.18	.6199	2183	.340	.496	2.15	9.11	5.93	55.00
1200	43.90	.6380	2663	.319	.467	2.15	9.10	5.92	59.28
			$t=25°$	$C_p^*=6.959$,	$C_v^*=4.973$	cal./mole deg.			
25	971.8	.02882	24.80	1.005	1.073	.27	7.23	4.97	−6.72
50	484.2	.05784	49.31	1.003	1.140	.54	7.50	4.96	−5.04
75	322.8	.08675	73.64	.994	1.193	.81	7.77	4.96	−3.32
100	243.1	.1152	97.94	.977	1.229	1.07	8.02	4.98	−1.52
150	165.1	.1696	147.0	.926	1.248	1.47	8.43	5.04	2.03

TABLE II. (*Continued*).

1	2	3	4	5	6	7	8	9	10
p	v	ρ	f	$-\frac{p}{v}\left(\frac{dv}{dp}\right)_T$	$\frac{T}{v}\left(\frac{dv}{dT}\right)_p$	ΔC_p	C_p	C_v	Δ
atm.	cc/mole	g/cc	atm.			calories/mole degree			cc/mole
200	127.6	.2195	197.5	.851	1.229	1.72	8.68	5.08	5.51
300	92.40	.3031	306.2	.724	1.116	1.93	8.89	5.02	12.30
400	76.25	.3673	430.8	.612	.984	1.95	8.91	4.99	18.82
500	67.04	.4177	576.4	.540	.869	1.93	8.89	5.08	24.82
600	60.94	.4596	748.1	.488	.772	1.89	8.84	5.22	30.13
800	53.55	.5230	1191	.417	.644	1.80	8.76	5.30	40.24
1000	48.97	.5719	1808	.387	.555	1.73	8.69	5.52	49.06
1100	47.22	.5930	2201	.373	.522	1.71	8.66	5.59	53.05
1200	45.77	.6119	2661	.348	.493	1.67	8.63	5.52	56.97
			$t=50°$	$C_p^*=6.965$,	$C_v^*=4.979$	cal./mole deg.			
25	1059	.02645	24.94	1.000	1.058	.23	7.19	4.98	−1.90
50	529.8	.05286	49.82	.995	1.109	.46	7.42	4.97	−.45
75	354.5	.07899	74.74	.985	1.149	.68	7.64	4.97	1.01
100	267.7	.1046	99.81	.969	1.176	.88	7.85	4.99	2.53
150	182.2	.1537	150.8	.925	1.193	1.21	8.17	5.03	5.58
200	140.6	.1992	203.7	.871	1.177	1.42	8.39	5.04	8.54
300	101.0	.2773	317.8	.755	1.097	1.62	8.59	4.97	14.43
400	82.47	.3396	447.5	.650	.984	1.68	8.65	4.97	20.14
500	71.87	.3896	597.7	.580	.883	1.68	8.64	5.02	25.54
600	64.92	.4314	772.9	.527	.796	1.65	8.61	5.11	30.45
800	56.53	.4955	1218	.454	.673	1.58	8.54	5.16	39.88
1000	51.27	.5462	1826	.418	.580	1.50	8.46	5.37	47.88
1100	49.28	.5684	2207	.402	.551	1.46	8.42	5.36	51.46
1200	47.65	.5877	2649	.376	.518	1.42	8.38	5.33	55.11
			$t=100°$	$C_p^*=6.987$,	$C_v^*=5.001$	cal./mole deg.			
25	1231	.02276	25.11	.994	1.037	.17	7.16	5.00	5.94
50	619.3	.04522	50.48	.986	1.069	.34	7.33	5.00	7.03
75	416.2	.06730	76.18	.974	1.092	.50	7.49	5.00	8.07
100	315.1	.08889	102.3	.959	1.108	.64	7.63	5.01	9.16
150	215.0	.1303	155.9	.924	1.119	.87	7.86	5.02	11.43
200	165.7	.1690	211.9	.881	1.112	1.04	8.02	5.01	13.67
300	117.9	.2375	333.1	.792	1.064	1.24	8.22	4.94	18.34
400	95.04	.2947	469.8	.705	.980	1.32	8.31	4.95	22.96
500	81.70	.3428	625.9	.643	.898	1.34	8.33	5.00	27.31
600	73.04	.3835	805.1	.588	.831	1.33	8.32	4.98	31.50
800	62.44	.4485	1249	.514	.715	1.27	8.26	5.04	39.43
1000	55.91	.5009	1835	.470	.635	1.21	8.20	5.08	46.20
1100	53.54	.5231	2194	.453	.600	1.18	8.16	5.13	49.44
1200	51.56	.5431	2604	.428	.569	1.15	8.14	5.10	52.65
			$t=150°$	$C_p^*=7.024$,	$C_v^*=5.038$	cal./mole deg.			
25	1401	.02000	25.21	.991	1.024	.13	7.16	5.04	11.96
50	707.0	.03961	50.86	.980	1.044	.26	7.28	5.04	12.88
75	476.2	.05881	77.00	.968	1.058	.38	7.41	5.04	13.67
100	361.1	.07755	103.7	.954	1.067	.49	7.52	5.05	14.52
150	246.8	.1146	158.8	.923	1.074	.67	7.70	5.05	16.31
200	190.1	.1473	216.6	.888	1.070	.81	7.84	5.03	18.10
300	134.5	.2082	341.9	.814	1.037	1.01	8.03	4.98	21.87
400	107.4	.2607	482.5	.741	.971	1.11	8.13	5.01	25.54
500	91.60	.3057	641.5	.685	.906	1.15	8.17	5.03	29.24
600	81.19	.3449	821.9	.634	.848	1.16	8.19	5.03	32.72
800	68.42	.4093	1260	.562	.743	1.16	8.18	5.10	39.45
1000	60.72	.4612	1825	.514	.668	1.13	8.15	5.13	45.48
1100	57.86	.4840	2164	.495	.638	1.12	8.14	5.14	48.21
1200	55.50	.5046	2548	.473	.606	1.11	8.13	5.17	50.97
			$t=200°$	$C_p^*=7.076$,	$C_v^*=5.090$	cal./mole deg.			
25	1569	.01784	25.26	.989	1.015	.11	7.18	5.09	16.76
50	793.5	.03529	51.08	.977	1.028	.21	7.28	5.09	17.47
75	535.2	.05233	77.48	.964	1.035	.31	7.38	5.10	18.21
100	406.3	.06893	104.5	.951	1.040	.39	7.47	5.10	18.93
150	277.7	.1008	160.5	.923	1.045	.54	7.62	5.09	20.32
200	213.9	.1309	219.4	.892	1.038	.66	7.74	5.09	21.82
300	150.7	.1858	347.1	.830	1.014	.84	7.91	5.04	24.82
400	119.7	.2340	489.8	.769	.962	.94	8.02	5.07	27.91
500	101.4	.2763	649.9	.718	.908	.99	8.07	5.09	30.96
600	89.28	.3137	830.1	.671	.859	1.03	8.10	5.09	33.91
800	73.39	.3765	1261	.600	.767	1.06	8.14	5.15	39.65
1000	65.50	.4276	1805	.550	.692	1.08	8.15	5.24	45.01
1100	62.22	.4501	2128	.531	.664	1.08	8.16	5.25	47.47
1200	59.51	.4706	2488	.510	.632	1.08	8.16	5.30	49.96

TABLE II.—(*Continued*)

1 p	2 v	3 ρ	4 f	5 $\frac{p}{v}\left(\frac{dv}{dp}\right)_T$	6 $\frac{T}{v}\left(\frac{dv}{dT}\right)_p$	7 ΔC_p	8 C_p	9 C_v	10 Δ
atm.	cc/mole	g/cc	atm.			calories/mole degree			cc/mole
			$t=300°$	$C_p^*=7.218$,	$C_v^*=5.232$	cal./mole deg.			
25	1905	.01470	25.31	.988	1.006	.07	7.29	5.23	23.86
50	964.3	.02905	51.27	.975	1.009	.14	7.36	5.23	24.35
75	651.0	.04302	77.88	.962	1.010	.20	7.42	5.24	24.89
100	494.5	.05664	105.2	.950	1.010	.26	7.48	5.24	25.45
150	338.0	.08285	161.9	.924	1.010	.36	7.58	5.21	26.46
200	257.8	.1086	221.6	.900	1.000	.45	7.66	5.22	27.56
300	182.2	.1537	350.8	.850	.976	.58	7.80	5.21	29.60
400	143.6	.1951	494.1	.803	.946	.68	7.90	5.20	31.77
500	120.6	.2322	653.2	.763	.904	.76	7.98	5.25	34.03
600	105.3	.2659	829.7	.722	.864	.82	8.04	5.28	36.20
800	86.42	.3241	1243	.655	.792	.92	8.14	5.34	40.64
1000	75.02	.3733	1749	.606	.721	.99	8.21	5.49	44.67
1100	70.87	.3952	2042	.586	.698	1.01	8.23	5.49	46.62
1200	67.40	.4155	2372	.567	.670	1.03	8.25	5.54	48.53
			$t=400°$	$C_p^*=7.386$,	$C_v^*=5.400$	cal./mole deg.			
25	2238	.01252	25.32	.987	1.000	.05	7.44	5.40	28.90
50	1133	.02472	51.31	.975	.999	.10	7.49	5.40	29.26
75	765.0	.03661	77.96	.962	.997	.15	7.54	5.41	29.68
100	581.0	.04821	105.3	.950	.996	.19	7.58	5.40	30.16
150	396.9	.07057	162.1	.927	.987	.26	7.65	5.40	30.92
200	304.9	.09186	221.8	.905	.978	.33	7.71	5.40	31.70
300	212.9	.1316	350.6	.864	.954	.44	7.82	5.40	33.27
400	166.9	.1678	492.4	.823	.931	.53	7.92	5.39	34.86
500	139.4	.2009	648.6	.790	.897	.62	8.00	5.45	36.52
600	121.0	.2314	820.3	.758	.861	.69	8.08	5.52	38.11
800	98.18	.2852	1215	.696	.793	.83	8.21	5.66	41.45
1000	84.41	.3318	1688	.649	.733	.93	8.32	5.81	44.61
1100	79.42	.3527	1958	.626	.716	.97	8.35	5.78	46.20
1200	75.25	.3722	2252	.605	.696	1.00	8.38	5.78	47.79

$\Delta \equiv v(pv/RT-1)$ in cc/mole extrapolated to zero pressure

t°C	Δ	t°C	Δ
−70	−39.65	100	4.84
−50	−30.89	150	11.09
−25	−21.96	200	16.09
0	−14.63	300	23.37
25	−8.51	400	28.50
50	−3.38		

larger scale chart for that purpose. It is planned to publish large size plots of Δ vs. ρ isotherms and isobars for the gases nitrogen, carbon monoxide, hydrogen, 3:1 hydrogen nitrogen mixture, methane, and helium, as a U. S. Department of Agriculture publication.

Fugacity f, column 4.

Fugacities are computed from the equation

$$f = p \exp(-1/RT) \int_0^p \alpha dp. \tag{28}$$

The integral was evaluated by mechanical integration of the α vs. p isotherms of Fig. 11.

Expansion coefficients $-(p/v)(dv/dp)_T$ and $(T/v)(dv/dT)_p$, columns 5 and 6.

The Δ vs. p, α vs. p, and Δ vs. ρ isotherms and the Δ vs. T^{-1}, α vs. T^{-1}, and Δ vs. ρ isobars are now used to get derivatives. The slopes of these curves can be determined at any point by the graphical method described in the paper

on nitrogen.[5] This method consists of estimating the slope of an α or Δ curve by mechanical means, and then using this slope as a correction term to find the corresponding derivative of v, by Eqs. (3) *et seq.* The three determinations of $-(p/v)\ (dv/dp)_T$ obtained through Eqs. (6), (7), (8) at each point were plotted in isotherms against pressure and in isobars against temperature, and

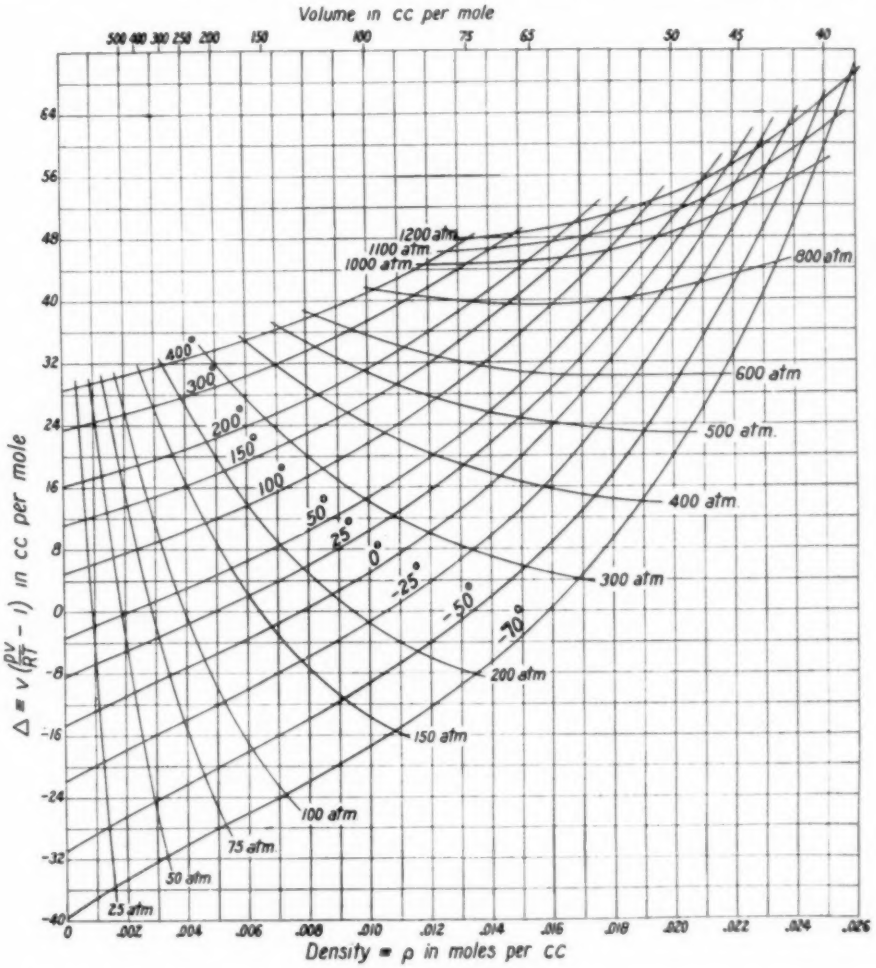

Fig. 12. Δ vs. ρ isotherms and isobars for carbon monoxide. By means of this graph one can readily interpolate the $p-v-T$ data. Thus, for $\rho=0.010$ moles per cc and $t=0°C$, the pressure can be roughly estimated as 240 atm. By reading off $\Delta=5.0$ cc per mole at this point and using $v=1/\rho=100$ cc per mole, $T=273.18°$, $R=82.049$ cc atm./mole deg., the equation $\Delta=v(pv/RT-1)$ gives $p=235.3$ atm.

were adjusted by placing smooth curves that have the same ordinate on both plots at any pressure and temperature, just as the Δ and α curves were smoothed. The ordinates read from either plot are given in column 5.

Likewise there are three determinations of $(T/v)(dv/dT)_p$ at each point, through Eqs. (15), (16), (17). They were adjusted by plotting $pv(dv/dT)_p$ vs.

T isobars at 25, 50, 75, 100 atm.; these isobars turn out to be straight lines. At higher pressures the adjustment was made by drawing smooth curves to $pv(dv/dT)_p$ vs. T and $(dv/dT)_p$ vs. T^{-1} isobars and $(T/v)\ (dv/dT)_p$ vs. p isotherms, and taking the average of $(T/v)\ (dv/dT)_p$ obtained from the three ordinates at a given temperature and pressure.

It should be noted that, at every point, the determinations of an expansion coefficient obtained through the different equations agreed very closely and consequently little smoothing was necessary. Agreement to three figures in all three determinations was not unusual.

ΔC_p, and the heat capacity C_p, columns 7 and 8 and Fig. 14.

ΔC_p is the change in C_p caused by a change in pressure at constant temperature. It is obtained through the thermodynamic equation

$$(dC_p/dp)_T = -T(d^2v/dT^2)_p, \tag{11}$$

which when integrated between 0 and p along an isotherm gives

$$C_p = C_p^* + \Delta C_p = C_p^* + \int_0^p -T(d^2v/dT^2)_p dp. \tag{12}$$

C_p^* is the heat capacity at zero pressure, and it is necessary to assume some value for it at each temperature in order to complete the calculations.

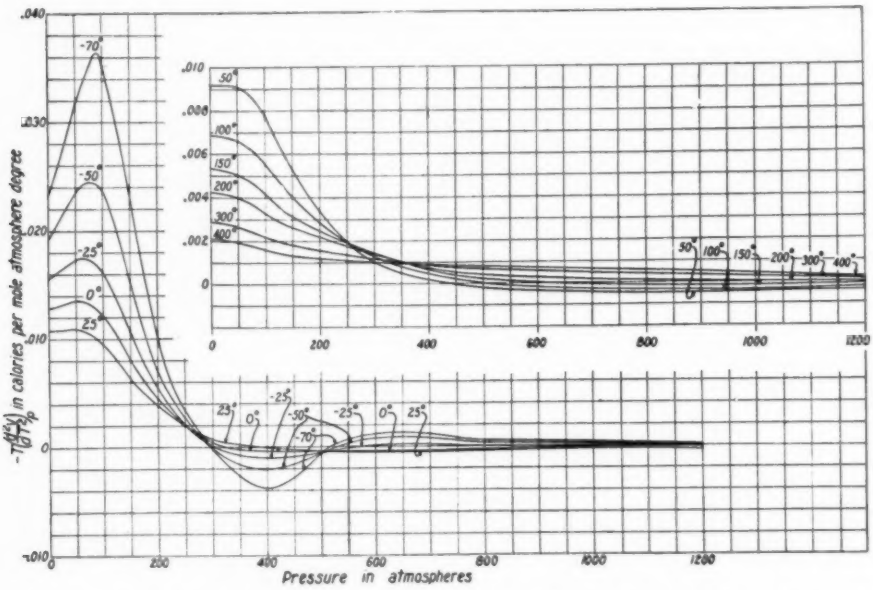

Fig. 13. $-T(d^2v/dT^2)_p = (dC_p/dp)_T$ vs. p isotherms. The area under a curve between any two pressures is the change in heat capacity (at constant pressure) in cal./mole degree between these two pressures, at that temperature.

There are some experimental determinations of C_p at 1 atm., but they are scattered. When corrected to zero pressure by an equation of state they all agree pretty well with the quantum equation

$$C_p^* = 7R/2 + R(3090/T)^2 e^{3090/T}/(e^{3090/T} - 1)^2, \quad (29)$$

which we have accordingly used for C_p^*. $C_v^* = C_p^* - R$. We have assumed that the rotational states remain fully excited down to $-70°$. We wish to thank Dr. W. M. D. Bryant of the Du Pont Ammonia Corporation for advice concerning the choice of a formula for C_p^*.

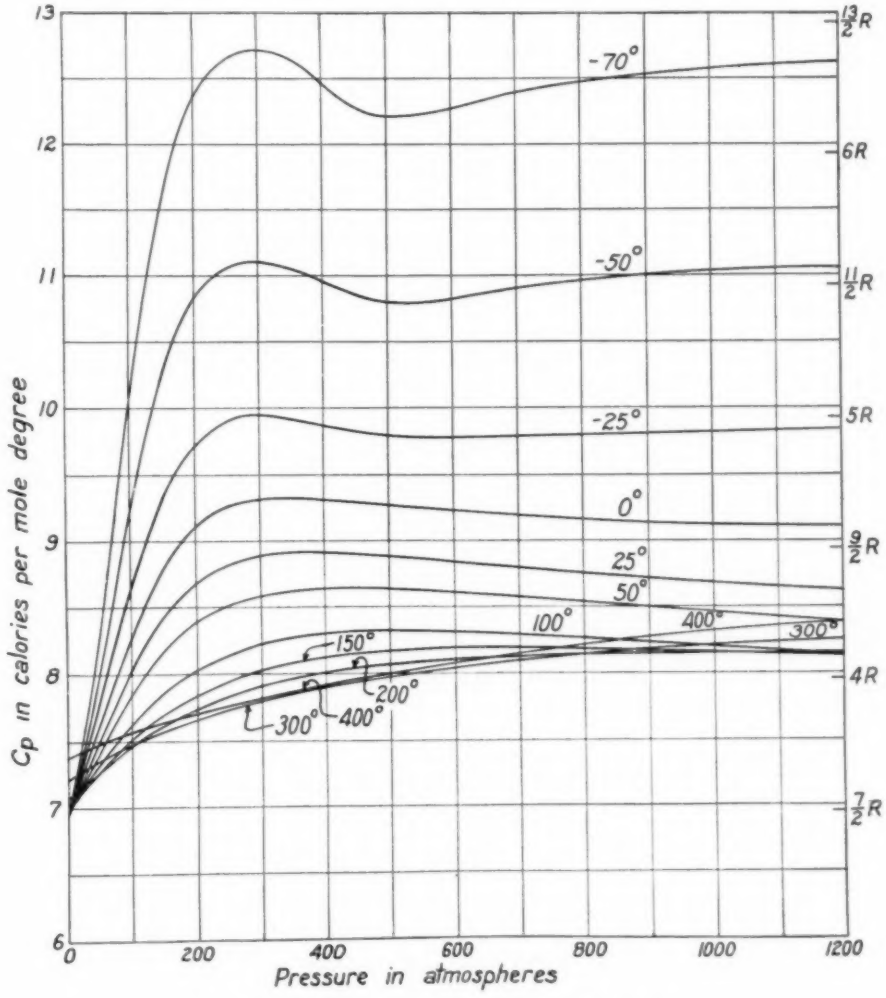

Fig. 14. Carbon monoxide. C_p vs. p isotherms.

The integral in Eq. (12) was evaluated by a mechanical integration under the $-T(d^2v/dT^2)_p$ vs. p isotherms, which are shown in Fig. 13. For these curves at 25, 50, 75, 100 atm., the ordinate was obtained at any point through Eq. (18) from the slope and ordinate of the corresponding $pv(dv/dT)_p$ vs. T isobar, which for the four low pressures was always a straight line, as was previously noted. There is little doubt that the values of $-T(d^2v/dT^2)_p$ therefrom obtained are very accurate, since the slopes and ordinates of straight

lines can be definitely determined. This means that C_p must be quite accurately calculated through these pressures.

Beyond 100 atm. the determination of the second derivative by means of the $pv(dv/dT)_p$ vs. T isobars was supplemented at each point by taking the slopes of the $(dv/dT)_p$ vs. T^{-1} isobars. The two determinations agreed well enough to lead one to expect ΔC_p to be correct to within a few hundredths cal./mole deg. throughout the whole range.

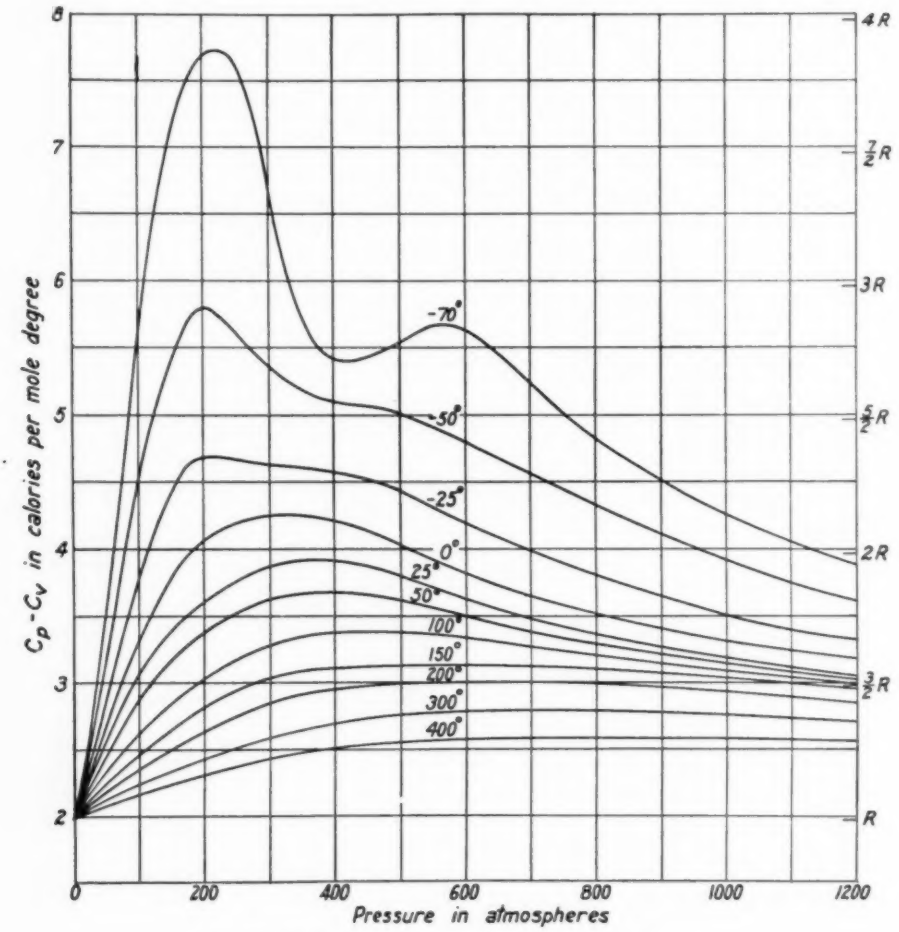

Fig. 15. Carbon monoxide. $C_p - C_v$ vs. p isotherms.

Eq. (24) was used for the zero pressure intercept in Fig. 13. Some time ago the question was raised by the writers[16] whether $-T(d^2v/dT^2)_p$ or $(dC_p/dp)_T \to 0$ as $p \to 0$, as would happen if the behavior of the heat capacity of the actual gas approaches that of a perfect gas. As the gas expands, $pv \to RT$ and $C_p - Cv \to R$, but Eq. (22) shows that $-T(d^2v/dT^2)_p \to 2a/RT^2 \neq 0$, as $p \to 0$.

[16] W. Edwards Deming and Lola E. Shupe, Phys. Rev. **37**, 220 (1931).

Since $(dC_p/dp)_T \neq 0$ at very low pressures, the limiting heat capacity C_p^* is not reached except at zero pressure. As the gas expands, there is no

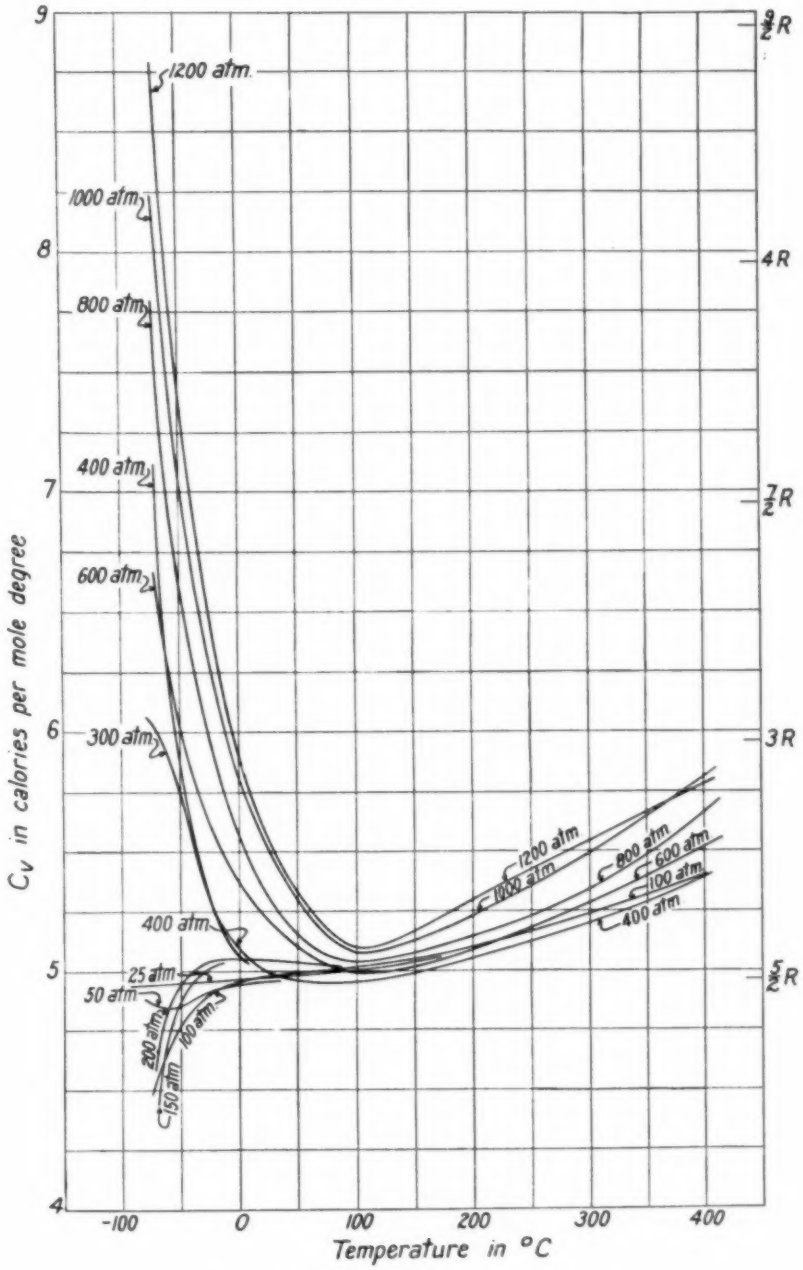

Fig. 16. Carbon monoxide. C_v vs. t isobars.

point reached beyond which further expansion is accompanied by changes in C_p that are infinitesimal compared with the changes in p.

The curves in Fig. 13 show that at low temperatures $(dC_p/dp)_T$ varies considerably with pressure, the lower the temperature the greater the variation. At 25° and above, this derivative is nearly constant through 50 atm.

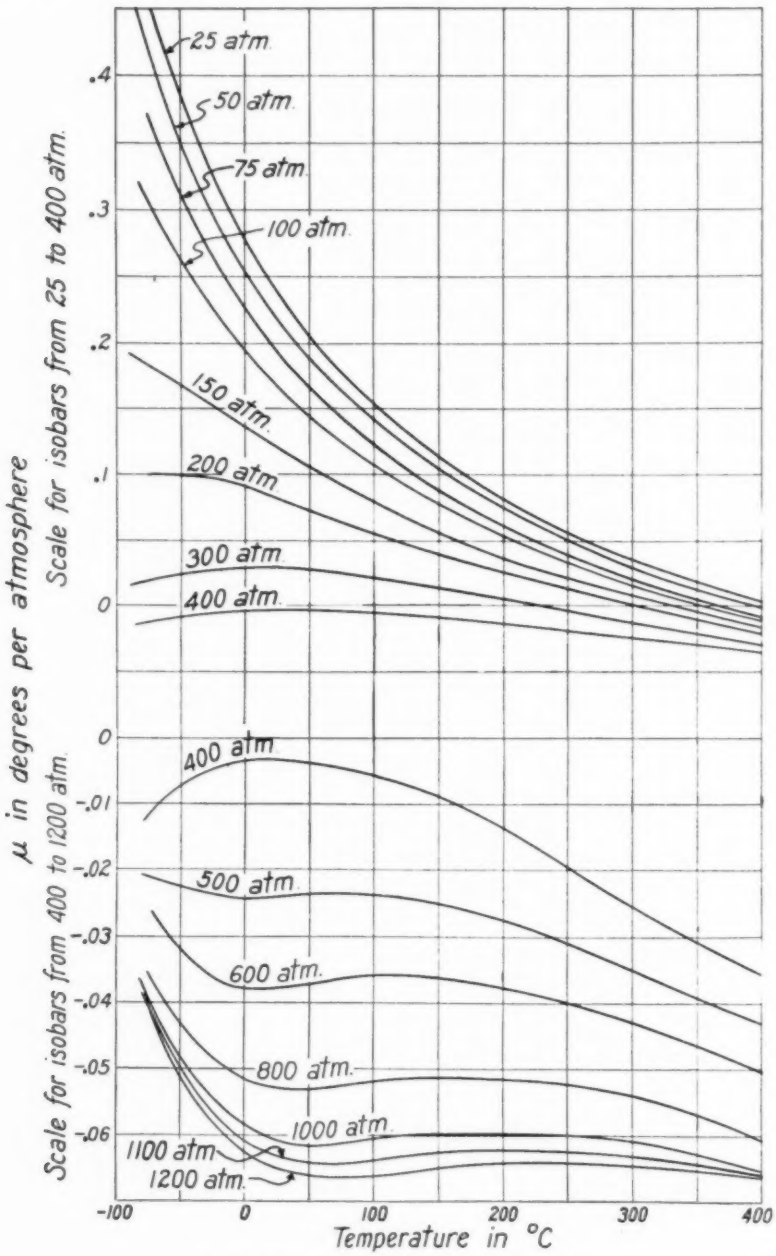

Fig. 17. Carbon monoxide. μ vs. t isobars.

and then decreases with further increase in pressure. Beyond 500 atm. this derivative is small at all temperatures, so very little change in C_p is produced at any of our temperatures by compression beyond 500 atm.

There are no experimental data available on carbon monoxide, but there are the authors'[5] calculations on nitrogen to compare with. Fig. 3 for nitrogen and Fig. 14 for carbon monoxide show that the C_p curves are very similar. At $-50°$ and $-70°$, C_p for carbon monoxide is slightly higher than it is for nitrogen, but at $-25°$ and above, the reverse is true. The difference is nowhere greater than some tenths cal./mole deg.

The quantity $C_p - C_v$, Fig. 15; the heat capacity C_v, column 9 and Fig. 16.

$$C_p - C_v = -T(dv/dT)_p^2/(dv/dp)_T \tag{13}$$

The derivatives in this equation are simply related to the expansion coefficients in columns 5 and 6, so $C_p - C_v$ can be calculated for each pressure and

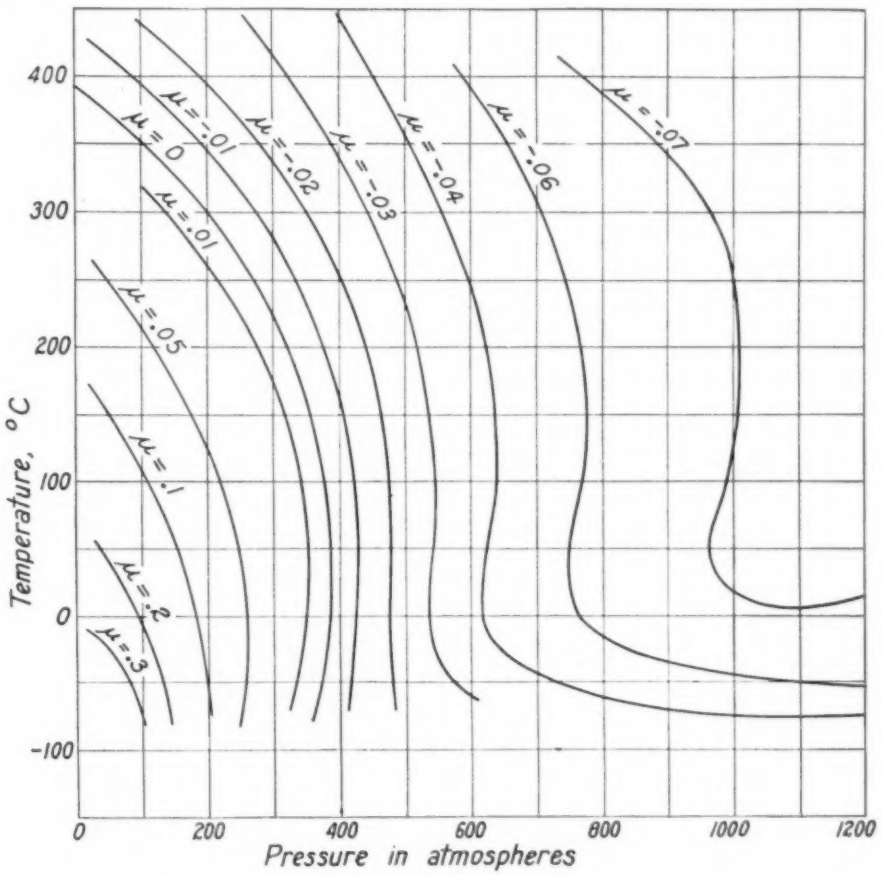

Fig. 18. Carbon monoxide. t vs. p μ = constant curves. μ is given in °C per atm. $\mu > 0$ means that the gas is heated by an adiabatic compression.

temperature. The results are shown in Fig. 15. According to Eq. (22), $C_p - C_v \to R$ as $p \to 0$, at all temperatures.

C_v is calculated by subtracting $C_p - C_v$ from C_p. Some of the C_v vs. t isobars are shown in Fig. 16. More of them could not be drawn without causing

confusion. Above 50°, isobars for $p=0, 25, \ldots, 400$ almost coincide. At higher pressures C_v is higher. Below 50°, C_v at 25 atm. falls a few hundredths cal./mole deg. under C_v*. Below 50°, C_v at 50, 75, 100, 150, 200 atm. deviates considerably from C_v*. The isobars for 100, 150, 200 atm. take peculiar quick descents as the temperature drops below −25°; this is most pronounced for 150 atm. The isobars for 300, 400, . . . , 1200 atm. have a minimum at about 100°. On the low temperature side of this minimum the curves are very steep. The graph for nitrogen in Fig. 5 shows the same characteristics.

Joule-Thomson coefficient μ, Figs. 17 and 18.

The Joule-Thomson coefficient can be calculated from the equation

$$\mu\rho C_p = (T/v)(dv/dT)_p - 1. \tag{14}$$

The values of μ can be read from the curves of Figs. 17 or 18. The latter is a family of μ curves obtained from the μ vs. t isobars (Fig. 17) and μ vs. p isotherms (not shown). The $\mu=0$ curve in Fig. 18 is the inversion curve.

The ultimate accuracy of calculations made by the present method is the accuracy of the p-v-T relations. Data from the various laboratories that have undertaken compressibility work agree very closely, and thus give assurance that calculations made from them should be reliable provided the derivatives can be accurately evaluated. Compressibility data over a wide range of temperature and pressure for a number of gases are now available, and the present method is a quick and accurate means for the determination of a number of physical properties. Calculations for other gases are in progress.

RECIPROCAL RELATIONS IN IRREVERSIBLE PROCESSES. II.

By Lars Onsager
Department of Chemistry, Brown University

(Received November 9, 1931)

Abstract

A general reciprocal relation, applicable to transport processes such as the conduction of heat and electricity, and diffusion, is derived from the assumption of microscopic reversibility. In the derivation, certain average products of fluctuations are considered. As a consequence of the general relation $S=k \log W$ between entropy and probability, different (coupled) irreversible processes must be compared in terms of entropy changes. If the displacement from thermodynamic equilibrium is described by a set of variables $\alpha_1, \cdots, \alpha_n$, and the relations between the rates $\dot{\alpha}_1, \cdots, \dot{\alpha}_n$ and the "forces" $\partial S/d\alpha_1, \cdots, \partial S/d\alpha_n$ are linear, there exists a quadratic dissipation-function,

$$2\Phi(\dot{\alpha}, \dot{\alpha}) \equiv \Sigma \rho_{ij} \dot{\alpha}_i \dot{\alpha}_i = dS/dt = \dot{S}(\alpha, \dot{\alpha}) \equiv \Sigma (\partial S/d\alpha_j)\dot{\alpha}_j$$

(denoting definition by $\equiv$). The symmetry conditions demanded by microscopic reversibility are equivalent to the variation-principle

$$\dot{S}(\alpha, \dot{\alpha}) - \Phi(\dot{\alpha}, \dot{\alpha}) = \text{maximum},$$

which determines $\dot{\alpha}_1, \cdots, \dot{\alpha}_n$ for prescribed $\alpha_1, \cdots, \alpha_n$. The dissipation-function has a statistical significance similar to that of the entropy. External magnetic fields, and also Coriolis forces, destroy the symmetry in past and future; reciprocal relations involving reversal of the field are formulated.

I. Introduction

In A previous communication[1] a reciprocal theorem for heat conduction in an anisotropic medium was derived from the principle of microscopic reversibility, applied to fluctuations. In the following we shall derive reciprocal relations for irreversible processes in general, particularly transport processes: conduction of electricity and heat, and diffusion.

As before we shall assume that the average regression of fluctuations will obey the same laws as the corresponding macroscopic irreversible processes. In (I) we considered fluctuations in "aged" systems, i.e., systems which have been left isolated for a length of time that is normally sufficient to secure thermodynamic equilibrium. For dealing with the conduction of heat we naturally considered the fluctuations of the distribution of heat, and we studied the behavior of the quantities $\alpha_1, \alpha_2, \alpha_3 =$ the total displacements of heat in the directions x_1, x_2 and x_3, respectively.

We brought the laws of irreversible processes into the theory of fluctuations by studying averages

$$\overline{\alpha_1(t)\alpha_2(t+\tau)} = \lim_{t'' \to \infty} \frac{1}{t''-t'} \int_{t=t'}^{t=t''} \alpha_1(t)\alpha_2(t+\tau)dt \qquad (1.1)$$

[1] L. Onsager, Phys. Rev. **37**, 405 (1931). Cited in the following as (I).

of the values of two fluctuating quantities α_1 and α_2 (in this particular case displacements of heat in two perpendicular directions) observed with a prescribed time interval τ. The condition of microscopic reversibility we applied in the form:

$$\overline{\alpha_1(t)\alpha_2(t+\tau)} = \overline{\alpha_2(t)\alpha_1(t+\tau)}\,. \tag{1.2}$$

The calculation of averages of the type (1.1) involves several steps. First of all, something must be known about the distribution of values of the fluctuating quantities $\alpha_1, \alpha_2 \cdots$; we shall employ standard methods for calculating the average products:

$$\overline{\alpha_1^2}, \quad \overline{\alpha_1\alpha_2}, \cdots \tag{1.3}$$

with but a slight variation. In addition, we must know the average changes (of quantities $\alpha_2, \alpha_3 \cdots$) which accompany a given deviation α_1' of a quantity α_1 from its normal value $\bar{\alpha}_1(=0)$. On this basis a certain *initial state* of an irreversible process is associated with the displacement $\alpha_1=\alpha_1'$; the average regression towards the normal state will obey the ordinary macroscopic laws governing such processes.

The average regression is described by the functions:

$$\overline{\alpha_i}(\tau, \alpha_j')$$

defined as the average of the quantity α_i, taken over all cases, (picked at random for an aged system), in which, τ seconds earlier, the quantity α_j *had* the value α_j'. Whenever these functions are linear in α_j', which will be the common case when reasonable variables α are chosen, the knowledge of the averages (1.3) suffices for evaluating (1.1).

In (I), §4, we derived reciprocal relations for heat conduction in an anisotropic body, showing that the conducting properties of the most general (triclinic) crystal can be represented by a *symmetrical tensor* (ellipsoid). In that particular case it was not necessary to calculate the averages (1.3), nor to determine completely the state associated with a displacement $\alpha_1=\alpha_1'$, because the necessary information could be derived from considerations of symmetry. Even so, these considerations were based on the proposition that, in regard to the probability for a given distribution of energy, the different volume elements of a *homogeneous* crystal would be equivalent, so that the anisotropy of the crystal could be neglected in this particular connection. This proposition involves the fundamental principles of statistical mechanics although it obviates a part of the general mathematical apparatus.

We shall review the derivation briefly. If J_1, J_2, J_3 denote the components of the heat flow along the coordinate axes x_1, x_2, x_3, respectively, and T the absolute temperature, the phenomenological laws of heat conduction in a triclinic crystal take the general form

$$\begin{aligned} J_1 &= L_{11}X_1 + L_{12}X_2 + L_{13}X_3 \\ J_2 &= L_{21}X_1 + L_{22}X_2 + L_{23}X_3 \\ J_3 &= L_{31}X_1 + L_{32}X_2 + L_{33}X_3 \end{aligned} \tag{1.4}$$

where X_1, X_2, X_3 are the components of the "force" on the heat flow

$$X_1 = -(1/T)\partial T/dx_1; \quad X_2 = -(1/T)\partial T/dx_2; \quad X_3 = -(1/T)\partial T/dx_3 \tag{1.5}$$

(Carnot). In order to derive the reciprocal relations

$$L_{12} = L_{21}; \; L_{23} = L_{32}; \; L_{31} = L_{13}$$

we considered the fluctuations of the moments

$$\begin{aligned} \alpha_1 &= \int \epsilon x_1 dV \\ \alpha_2 &= \int \epsilon x_2 dV \end{aligned} \tag{1.6}$$

of the distribution of energy, $\epsilon = \epsilon(x_1, x_2, x_3)$. When we chose the external boundary of the crystal spherical, center at the origin, all questions pertaining to the *instantaneous* distribution of energy have spherical symmetry (cf. above). Thus

$$\overline{\alpha_1} = \overline{\alpha_2} = 0; \; \overline{\alpha_1^2} = \overline{\alpha_2^2}; \; \overline{\alpha_1\alpha_2} = 0, \tag{1.7}$$

and with a displacement of energy there is associated a temperature gradient in the same direction:

$$\begin{aligned} \overline{\partial T/dx_1}^{\alpha_1', \alpha_2'} &= -T\overline{X}_1(\alpha_1', \alpha_2') = CT\alpha_1' \\ &\quad -T\overline{X}_2(\alpha_1', \alpha_2') = CT\alpha_2' \end{aligned} \tag{1.8}$$

where C is for our immediate purposes a mere constant. (Certain rather trivial considerations are needed to justify our assumption of a *linear* relation between displacement (α_1', α_2') and gradient $(T\overline{X}_1, T\overline{X}_2)$. When we take that much for granted, the more special form (1.8) follows from the spherical symmetry.)

The gradient (1.8) determines the heat flow J according to (1.4), and the rate of change $\dot{\alpha}$ of the displacement α is the same as the total flow

$$\begin{aligned} \dot{\alpha}_1(\alpha_1', \alpha_2', \alpha_3') &= d\alpha_1/dt = \int J_1 dV = -CV(L_{11}\alpha_1' + L_{12}\alpha_2' + L_{13}\alpha_3') \\ \dot{\alpha}_2(\alpha_1', \alpha_2', \alpha_3') &= -CV(L_{21}\alpha_1' + L_{22}\alpha_2' + L_{23}\alpha_3'). \end{aligned} \tag{1.9}$$

Then in a short interval of time Δt

$$\overline{\alpha_2}(\Delta t, \alpha_1') = \overline{\alpha_2}(0, \alpha_1') + \dot{\alpha}_2(\alpha_1')\Delta t = 0 - L_{21}CV\alpha_1'\Delta t,$$

where $\bar{\alpha}_2(0, \alpha_1')$ vanishes by symmetry. From this, obviously

$$\overline{\alpha_1(t)\alpha_2(t + \Delta t)} = \overline{\alpha_1'\alpha_2(\Delta t, \alpha_1')} = -L_{21}CV\overline{\alpha_1'^2}\Delta t$$

and, by analogy

$$\overline{\alpha_2(t)\alpha_1(t + \Delta t)} = -L_{12}CV\overline{\alpha_2^2}\Delta t.$$

Since, by (1.7): $\overline{\alpha_1^2}=\overline{\alpha_2^2}$, the requirement:

$$\overline{\alpha_1(t)\alpha_2(t+\Delta t)} = \overline{\alpha_2(t)\alpha_1(t+\Delta t)}$$

for microscopic reversibility imposes the condition:

$$L_{12} = L_{21}.$$

The more general case of simultaneous transport of heat, electricity and matter (diffusion) in isotropic or anisotropic media leads us to consider the fluctuations of a set of variables $\alpha_1, \alpha_2 \cdots$, measuring displacements of heat, electricity and matter, eventually in different directions. We shall have to actually evaluate the averages (1.3); symmetry considerations can yield the necessary information only in a few cases, as above. The calculation of (1.3) involves directly Boltzmann's fundamental relation between entropy S and probability W:

$$S=k \log W+\text{constant}$$

The exceedingly general character of this relation is the reason that the *rates* of irreversible processes, not solely the ultimate equilibrium, are subject to reciprocal laws, in which *different processes have to be compared in terms of the entropy changes involved.*

Sometimes, of course, it may be more convenient to employ other thermodynamic potentials, particularly the free energy, the main reason being that conditions of *mechanical* equilibrium (pressure, elastic) frequently enter into the laws of irreversible processes, and that the description in terms of energy involves more familiar derived functions (thermodynamic potential, electromotive force, electrical resistance). Above, we purposely considered the "force" on heat, although the concept was not necessary for dealing with the problem in hand, just to demonstrate how the concept of "force" could be extended beyond the familiar.

Fundamentally, however, the *entropy* is the simplest among the thermodynamic potentials, and it is the only one that will serve our purposes in all cases. In our example, where displacements α_1, α_2, α_3 of heat are considered, the state of the system being determined by these displacements, so that

$$S = \sigma(\alpha_1, \alpha_2, \alpha_3),$$

the temperature gradients are essentially the same as $\partial S/d\alpha_1$ etc., or rather

$$\partial\sigma/d\alpha_r = \partial(1/T)/dx_r.$$

In order to see this, we recall the fundamental thermodynamic relation

$$\delta S=(1/T)(\delta E-\delta A)-(\mu/T)\delta m,$$

where E = energy; A = work; m = amount of substance; μ = Gibbs' thermodynamic potential. The amount of heat added to a volume element is $\delta Q=\delta E-\delta A$. Now if there is a uniform gradient of temperature (or $1/T$ in the r-direction, then an amount of heat δQ transported a distance Δx_r changes the entropy by the amount

$$\delta S=\delta Q\cdot\Delta(1/T)=\delta Q\cdot\Delta x_r\cdot\partial(1/T)/dx_r=\delta\alpha_r\cdot\partial(1/T)/dx_r,$$

whereby $\delta\alpha_r$ measures a displacement of heat (in units cm $\times$ cal.).

Similarly, where a displacement α of matter (in the x direction) is considered,

$$\partial\sigma/d\alpha = -\partial(\mu/T)/dx,$$

and if α is a displacement of electricity, then

$$\partial\sigma/d\alpha = X/T,$$

where X is the intensity of the electric field.

According to the empirical laws of transport processes the flow J of matter, heat or electricity is proportional to the gradient of the corresponding specific potential, that is

$$J \sim -\operatorname{grad} T$$

for heat conduction and

$$J \sim X;\ J \sim -\operatorname{grad} \mu,$$

respectively, for electrical conduction (Ohm's law) and isothermal diffusion (alternative form of Fick's law). In the following we shall write these empirical relations in the general form

$$d\alpha_r/dt = \dot{\alpha}_r \sim \partial S/d\alpha_r,$$

where the rate of displacement $\dot{\alpha}$ is essentially the same as the flow J, (by definition), except for a volume factor. Whenever different transport processes interfere with each other the simple proportionality is replaced by a system of linear relations

$$\dot{\alpha}_r = G_{r1}\partial\sigma/d\alpha_1 + \cdots + G_{rn}\partial\sigma/d\alpha_n, \quad (r = 1, \cdots, n), \tag{1.11}$$

where again $S=\sigma(\alpha_1, \cdots \alpha_n)$. In taking for granted the linear form (1.11) we are still making use of empirical laws, mostly familiar, which are understood and expected from simple and equally familiar kinetic considerations of very wide scope. Examples have been enumerated in (I), §§ 1–2, and need not be repeated here.

Our object is to show that the condition (1.2) for microscopic reversibility leads to the general reciprocal relation

$$G_{rs} = G_{sr}. \tag{1.12}$$

2. General Theory of Fluctuations

It was shown by L. Boltzmann that a mechanical theory of molecules requires a statistical interpretation of the second law of thermodynamics. Thermodynamic equilibrium is explained as a statistical equilibrium of elementary processes, and Boltzmann gave a direct relation between the entropy S and the "thermodynamic probability" W of a thermodynamic state:

$$S = k \log W + \text{const.}, \tag{2.1}$$

where k is the gas constant per molecule (1.371×10^{-16} erg/degree). The apparent rest associated with thermodynamic equilibrium is explained by the

smallness of the factor k. According to (2.1), under circumstances which normally lead to such equilibrium, the probability

$$e^{\Delta S/k}$$

for a deviation involving an entropy change ΔS (necessarily negative), is appreciable only when ΔS is (at the outmost) of the order of magnitude of k. The *fluctuations* permitted by this restriction can be observed only in very favorable cases, for example the opalescence of liquids near the critical point[2] and Brownian motion of small particles in liquids,[3] or of a mirror in delicate elastic suspension.[4]

The premises and the consequences of Boltzmann's principle (2.1) have been discussed by A. Einstein[5] to an extent which will be practically sufficient for our purposes. It is essential that a thermodynamic equilibrium state, specified in terms of energy and external parameters (volume etc.), is incompletely specified from a molecular point of view; the quantity W measures the number (or extent) of different possibilities for realizing a given thermodynamic state. In order to calculate W one needs a complete (molecular) theory of the system in hand: If one assumes that molecules obey the laws of classical mechanics, then W equals an extension in phase-space, while on the basis of quantum theory W equals the number of stationary states corresponding to the prescribed energy. However, as Einstein has pointed out, the calculation of fluctuations according to (2.1) is *independent of all special assumptions regarding the laws which may govern elementary processes* (we must of course assume that these laws do permit statistical equilibrium of some kind).

We shall have to make certain *general assumptions* about *aged systems*, i.e., systems which have been left isolated for a length of time that is normally sufficient to secure thermodynamic equilibrium. We expect that such a system will in the course of time pass through *all* the (thermodynamic) states $\Gamma^1, \Gamma^2, \cdots \Gamma^l$ that are compatible with the conditions of isolation, whereby the energy, the values of external parameters (volume, etc.) and the numbers of indestructible elementary particles (atoms, molecules) are prescribed.[6] In the course of a long time t the system will spend a total t_r of time intervals in the state Γ^r; we expect that $t_1, t_2 \cdots t_l$ will be proportional to the regions W_1, $W_2 \cdots W_l$. This statement contains an assumption even if W_1, $W_2 \cdots$ are considered as unknown, namely that t_1/t, $t_2/t \cdots$ will be fully determined by the nature of the system, (and the conditions of isolation), independently of the initial state. Granted this assumption, we may define W_1, $W_2 \cdots$ as pro-

[2] M. v. Smoluchowski, Ann. d. Physik [4], **25,** 205 (1909). Theory accompanied by a general discussion of fluctuations is given by A. Einstein, Ann. d. Physik [4], **33,** 1275 (1910).

[3] A. Einstein, Ann. d. Physik [4], **17,** 549 (1905). M. v. Smoluchowski, Ann. d. Physik [4], **21,** 756 (1906).

[4] P. Zeeman and O. Houdyk, Proc. Acad. Amsterdam **28,** 52 (1925). W. Gerlach, Naturwiss. **15,** 15 (1927). G. E. Uhlenbeck and S. Goudsmit, Phys. Rev. **34,** 145 (1929).

[5] Einstein, reference 2.

[6] In a discussion of the fundamental questions involved, W. Schottky introduces the term "resistent groups." Ann. d. Physik [4], **68,** 481 (1922).

portional t_1/t, $t_2/t \cdots$, without reference to any detailed theory of the system. (On the basis of the underlying picture, every W is still a large integer, equal to the number of "microscopic" states contained in a given thermodynamic state. Here, however, we are only interested in the ratios of $W_1, W_2, \cdots$). The various assumptions involved in this application of Boltzmann's principle may be summarized in the formula:

$$S_r = k \log (t_r/t) + \text{const.} \tag{2.2}$$

where S_r is the entropy of the state Γ^r; we shall refer to t_r/t as the *probability* for this state.

A thermodynamic state $\Gamma^r = \Gamma(\alpha_1^r, \cdots \alpha_n^r)$ may be defined in terms of given values $\alpha_1^r, \cdots \alpha_n^r$ for such variables $\alpha_1, \cdots \alpha_n$ as can be measured by ordinary means. From a statistical point of view we must allow latitudes $\Delta\alpha_1, \cdots \Delta\alpha_n$ in this specification (the probability for a region of no extension equals zero). We have to introduce a distribution-function

$$f(\alpha_1, \cdots, \alpha_n)$$

and the probability for the state Γ^r becomes equal to the integral of $f(\alpha_1, \cdots \alpha_n)$ over the region

$$\alpha_1^{(r)} < \alpha_1 < \alpha_1^{(r)} + \Delta\alpha_1$$

$$\cdots\cdots\cdots\cdots$$

$$\alpha_n^{(r)} < \alpha_n < \alpha_n^{(r)} + \Delta\alpha_n.$$

Then (2.2) takes the form

$$S_r = k \log f(\alpha_1^{(r)}, \cdots \alpha_n^{(r)}) + k \log (\Delta\alpha_1 \cdots \Delta\alpha_n) + \text{const.} \tag{2.3}$$

Our only direction for the appropriate choice of latitudes $\Delta\alpha$ is that they ought to be taken of the same order of magnitude as the common fluctuations of the quantities α in the state Γ^r. This convention takes care of all important cases; because thermodynamic measurements of entropy are possible only for equilibrium states.[7] A more accurate specification of $\Delta\alpha_1, \cdots \Delta\alpha_n$ is unnecessary because, say, doubling each $\Delta\alpha$ will change the right side of (2.3) only by the amount $nk \log 2$, where $k = 1.371 \times 10^{-16}$ erg/degree, and an entropy difference of this magnitude is far too small to affect any measurement. Actually, where reasonable variables $\alpha_1, \cdots \alpha_n$ are chosen, the order of magnitude of the product $\Delta\alpha_1, \Delta\alpha_2 \cdots \Delta\alpha_n$ varies so little that the contribution $k \log (\Delta\alpha_1' \cdots \Delta\alpha_n'/\Delta\alpha_1'' \cdots \Delta\alpha_n'')$ to the entropy difference between two thermodynamic states is entirely negligible in comparison with $k \log(f(\alpha_1', \cdots \alpha_n')/f(\alpha_1'', \cdots \alpha_n''))$; it is the factor $f(\alpha_1, \cdots \alpha_n)$ that causes the tremendous difference in the probabilities of different thermodynamic states, and is responsible for measurable entropy differences. Thus, as long as we restrict ourselves to cases where S_r is a measured entropy, we may neglect the variability of the term $k \log (\Delta\alpha_1 \cdots \Delta\alpha_n)$ on the right side of (2.3) and write

[7] We allow ourselves, following the custom of thermodynamics, to consider states that may be approximated in some way by equilibrium states. Cf. Schottky, reference 6.

$$S_r = k \log f(\alpha_1^{(r)}, \cdots \alpha_n^{(r)}) + \text{const.} \tag{2.4}$$

So far we have assumed that the variables $\alpha_1, \cdots \alpha_n$ define the state of the system in hand *completely* from the thermodynamic (phenomenological) point of view. As pointed out by Einstein[8] the relation (2.4) remains valid in cases where this definition is incomplete. We merely have to adopt the convention that among all the states which fulfill the given specifications, we select the one with the greatest entropy. This theorem again depends on the probabilities for different states being of different order of magnitude, so that the given set of values of $\alpha_1, \cdots \alpha_n$ will be realized by the chosen state much more frequently than by all other states taken together. We shall summarize these results for subsequent applications. The greatest entropy allowed by a given set $\alpha_1', \cdots \alpha_n'$ of values of the variables $\alpha_1, \cdots \alpha_n$ we denote by

$$\sigma_{1\cdots n}(\alpha_1', \cdots \alpha_n').$$

The corresponding (thermodynamic) state we denote by

$$\Gamma'_{1\cdots n} = \Gamma_{1\cdots n}(\alpha_1', \cdots \alpha_n').$$

Then

$$\sigma_{1\cdots n}(\alpha_1', \cdots \alpha_n') = k \log f(\alpha_1', \cdots \alpha_n') + \text{const.} \tag{2.5}$$

gives the probability for finding the variables $\alpha_1, \cdots \alpha_n$ with a given set of values $\alpha_1', \cdots \alpha_n'$. Practically every time when $\alpha_1, \cdots \alpha_n$ assume this set of values, the system will be in the state $\Gamma_{1\cdots n}(\alpha_1', \cdots \alpha_n')$.

We shall calculate at once certain averages which will be needed for the subsequent derivations. We denote by $f_p(\alpha_p)$ the distribution-function for the variable α_p. We have according to (2.5):

$$k \log f_p(\alpha_p) = \sigma_p(\alpha_p) + \text{const.}, \tag{2.6}$$

where $\sigma_p(\alpha_p')$ is the greatest entropy possible when $\alpha_p = \alpha_p'$, realized by the state $\Gamma_p(\alpha_p')$. The function f_p is determined by (2.6) together with the condition

$$\int_{-\infty}^{\infty} f_p(\alpha_p) d\alpha_p = 1.$$

We obtain from (2.6) by differentiation

$$k df_p/d\alpha_p = f_p(\alpha_p) d\sigma_p/d\alpha_p,$$

assuming that the differential quotient exists. We shall also assume that the entropy $\sigma_p(\alpha_p)$ attains its maximum for a finite value α_p^0 of α_p, corresponding to the equilibrium state Γ^0, and that $(\alpha_p - \alpha_p^0) f_p(\alpha_p)$ approaches zero for large values of $|\alpha_p - \alpha_p^0|$.[9] Then it is easy to calculate the average

$$\begin{aligned} \overline{(\alpha_p - \alpha_p^0) d\sigma_p/d\alpha_p} &= \int_{-\infty}^{\infty} (\alpha_p - \alpha_p^0)(d\sigma_p/d\alpha_p) f_p(\alpha_p) d\alpha_p \\ &= k \int_{-\infty}^{\infty} (\alpha_p - \alpha_p^0)(df_p/d\alpha_p) d\alpha_p. \end{aligned}$$

[8] Einstein, reference 2.

[9] Otherwise this function must have an infinite number of maxima. All the conditions stated are fulfilled whenever α_p is a resonable thermodynamic variable.

Integration by parts yields

$$k\left[(\alpha_p - \alpha_p{}^0)f_p(\alpha_p)\right]_{-\infty}^{\infty} - k\int_{-\infty}^{\infty} f_p(\alpha_p)d\alpha_p.$$

The first term vanishes, and the second equals $-k$; thus

$$\overline{(\alpha_p - \alpha_p{}^0)d\sigma_p/d\alpha_p} = -k. \tag{2.7}$$

In the same manner, and under the same assumptions we find

$$\overline{(\alpha_p - \alpha_p{}^0)\partial\sigma_{1\ldots n}/d\alpha_p}$$

$$= \int_{-\infty}^{\infty}\cdots\int(\alpha_p - \alpha_p{}^0)(\partial\sigma/d\alpha_p)f_{1\ldots n}d\alpha_1\cdots d\alpha_n = -k, \tag{2.8a}$$

and

$$\overline{(\alpha_q - \alpha_q{}^0)\partial\sigma_{1\ldots n}/d\alpha_p} = 0, \quad (p \neq q). \tag{2.8b}$$

In the following we shall find it convenient to apply the simple formula (2.7) directly. However, it seems desirable to show the connection with the ordinary formulas for the averages of the products $(\alpha_p-\alpha_p{}^0)(\alpha_q-\alpha_q{}^0)$. We must assume that the entropy $\sigma_{1..n}$ can be expressed by a multiple power series, and that the abridged Taylor development

$$\sigma_{1\ldots n}(\alpha_1,\cdots\alpha_n) = S_0 + \tfrac{1}{2}\sum_{p,q=1}^{n}\eta_{pq}(\alpha_p - \alpha_p{}^0)(\alpha_q - \alpha_q{}^0), \tag{2.9}$$

where

$$\eta_{pq} = \eta_{qp} = \left[\partial^2\sigma_{1\ldots n}/d\alpha_p d\alpha_q\right]_{\alpha_1=\alpha_1{}^0;\ \cdots;\ \alpha_n=\alpha_n{}^0}, \tag{2.10}$$

will suffice in the entire region of values of $\alpha_1,\cdots\alpha_n$, for which the contribution to any of the averages (2.8 a, b) is at all appreciable. (Since $f\sim\exp(\sigma/k)$, the maximum of $f_{1\ldots n}$ is very sharp). Then we may substitute in (2.8 a, b):

$$\partial\sigma_{1\ldots n}/d\alpha_p = \sum_{p=1}^{n}\eta_{pq}(\alpha_q - \alpha_q{}^0), \tag{2.11}$$

and we obtain a system of linear equations

$$\sum_{r=1}^{n}\eta_{pr}\overline{(\alpha_r - \alpha_r{}^0)(\alpha_q - \alpha_q{}^0)} = -k\delta_{pq} = \begin{cases} -k, & (p=q) \\ 0, & (p\neq q), \end{cases} \tag{2.12}$$

from which the mean squares and products of fluctuations may be computed.

3. The Regression of Fluctuations

We are accustomed to observe that the course of an irreversible process taking place in an isolated system is entirely determined by the initial thermodynamic state according to definite laws, such as the laws for conduction of heat. On the basis of a statistical interpretation of the second law of thermodynamics, no process can be completely predetermined by an initial thermodynamic state; because such a state is itself incompletely defined (from a

molecular point of view; cf. §2). However, we can understand a predetermination with practical certainty, within limits of the order of magnitude of ordinary fluctuations, whereby much greater deviations will be very rare. From this statistical point of view we may still interpret the predictions of irreversible processes from empirical laws as valid for averages taken over a large number of similar cases, which in this connection means cases of irreversible processes starting from the same initial *thermodynamic* state.

Strictly speaking, this rule does not specify uniquely the more refined "microscopic" (molecular) interpretation of laws derived from relatively crude "macroscopic" observations. It makes a considerable difference whether we take an average of the type $\bar{\alpha}=(\alpha'+\alpha'')/2$ or one of the type $\bar{\alpha}=[(\alpha'^5+\alpha''^5)/2]^{1/5}$. However, in all important concrete cases the natural answer to this question will be obvious. For example, if α is a total displacement of heat, itself the sum of many local displacements whose changes depend on local conditions, there may be no doubt that the straight average $\bar{\alpha}=(\alpha'+\alpha'')/2$ is correct.

Now we are able to solve the problem of predicting the *average regression* of fluctuations: Suppose that we start out with a certain isolated system, and watch the fluctuations of the variables $\alpha_1, \cdots \alpha_n$ for a great length of time. Whenever the values of $\alpha_1, \cdots \alpha_n$ happen to be (simultaneously) $\alpha_1', \cdots \alpha_n'$, we make a record of the values which these variables (and perhaps other quantities $\alpha_{n+1}, \cdots \alpha_{n+p}$) assume τ *seconds later*. The averages of such records we denote by

$$\overline{\alpha_1}(\tau, \alpha_1', \cdots \alpha_n'), \cdots \overline{\alpha_{n+p}}(\tau, \alpha_1', \cdots \alpha_n').$$

We know that almost every time when $\alpha_1=\alpha_1'; \cdots ; \alpha_n=\alpha_n'$, the system will be in the (phenomenological) state $\Gamma'_{1\ldots n}=\Gamma(\alpha_1', \cdots \alpha_n')$, and the average course of an irreversible process following that state, described by the functions

$$\overline{\alpha_1}(\tau, \Gamma'_{1\ldots n}), \cdots \overline{\alpha_{n+p}}(\tau, \Gamma'_{1\ldots n}),$$

we know from macroscopic experiments. These functions may be considered as properties (in an extended sense) of the state $\Gamma'_{1\ldots n}$. The "normal" (common) properties of states corresponding to prescribed values $\alpha_1', \cdots \alpha_n'$ of the fluctuating quantities $\alpha_1, \cdots \alpha_n$ are certainly those of the state $\Gamma_1' \cdots {}_n$. The question whether we are allowed to interchange "normal" and average properties must be decided from the consideration of individual cases, as outlined above.

Assuming that the variables $\alpha_1, \cdots \alpha_n$ are suitable in this regard, we have:

$$\overline{\alpha_i}(\tau, \alpha_1', \cdots \alpha_n') = \overline{\alpha_i}(\tau, \Gamma'_{1\ldots n}), \quad (i = 1, \cdots, n+p), \tag{3.1}$$

as a general rule for predicting the average regression of fluctuations from the laws of irreversible processes.

4. Reciprocal Relations

For a discussion of the requirements of microscopic reversibility the averages

$$A_{ji}(\tau) = \overline{\alpha_j(t)\alpha_i(t+\tau)} = \overline{\alpha_j'\bar{\alpha}_i(\tau, \alpha_j')} \tag{4.1}$$

afford a convenient point of attack. The quantities $A_{ij}(\tau)$ may also be defined as time averages (1.1)

$$A_{ji}(\tau) = \lim_{t''\to\infty} \frac{1}{t''-t'} \int_{t=t'}^{t=t''} \alpha_j(t)\alpha_i(t+\tau)dt.$$

In the following it will be convenient to assume that the variables $\alpha_1, \cdots \alpha_n$ measure deviations from the thermodynamic equilibrium, whereby their averages $\bar{\alpha}_1, \cdots \bar{\alpha}_n$ for this state (and also the "normal" values α_j^0) vanish:

$$\overline{\alpha_i} = \alpha_i^0 = 0, \quad (i = 1, \cdots n). \tag{4.2}$$

The assumption of microscopic reversibility requires that, if α and β be two quantities which depend only on the configuration of molecules and atoms, *the event* $\alpha=\alpha'$, *followed* τ *seconds later by* $\beta=\beta'$, *will occur just as often as the event* $\beta=\beta'$, *followed* τ *seconds later by* $\alpha=\alpha'$. The same will be true if α and β depend on the velocities of elementary particles in such a manner that they are not changed when the velocities are reversed, for example, when α depends on the distribution of energy in a system.[10] If α_j and α_i are two such "reversible" variables of a reversible system, then obviously

$$A_{ji}(\tau) = \overline{\alpha_j(t)\alpha_i(t+\tau)} = \overline{\alpha_i(t)\alpha_j(t+\tau)} = A_{ij}(\tau). \tag{4.3}$$

We shall consider cases where the course of an irreversible process starting from any state of the type $\Gamma_{1\ldots n}$ can be described by a set of linear differential equations of the form (1.11):

$$\frac{d\overline{\alpha_i}}{dt} = \dot{\bar{\alpha}}_i = \sum_{r=1}^{n} G_{ir} \frac{\partial\sigma_{1\ldots n}(\alpha_1, \cdots \alpha_n)}{d\alpha_r}, \quad (i = 1, \cdots n). \tag{4.4}$$

According to (3.1) we have

$$\overline{\alpha_i}(\tau, \alpha_j') = \overline{\alpha_i}(\tau, \Gamma_j'),$$

where Γ'_j is the state of maximum entropy for a given value α_j' of the variable α_j. Mathematically this state is characterized by the relations

$$\begin{aligned} \alpha_j &= \alpha_j' \\ \partial\sigma_{1\ldots n}/d\alpha_r &= 0, \quad (r \neq j), \end{aligned} \tag{4.5}$$

and we have for the set of values of $\alpha_1, \cdots \alpha_n$ determined by these conditions:

$$\partial\sigma_{1\ldots n}/d\alpha_j = [d\sigma_j/d\alpha_j]_{\alpha_j=\alpha_j'}. \tag{4.6}$$

[10] Cf. (I) p. 418.

From (4.4) we have in a short interval of time Δt

$$\overline{\alpha_i}(\Delta t, \alpha_j') = \overline{\alpha_i}(0, \alpha_j') + \dot{\alpha}_i \Delta t = \overline{\alpha_i}(0, \alpha_j') + \sum_{r=1}^{n} G_{ir}(\partial \sigma_{1 \cdots n}/d\alpha_r)\Delta t,$$

or substituting (4.5) and (4.6):

$$\overline{\alpha_i}(\Delta t, \alpha_j') = \overline{\alpha_i}(0, \alpha_j') + G_{ij}(d\sigma_j(\alpha_j')/d\alpha_j')\Delta t.$$

Calculating according to (4.1) the average $A_{ji}(\Delta t)$ we obtain

$$A_{ji}(\Delta t) = \overline{\alpha_j(t)\alpha_i(t + \Delta t)} = \overline{\alpha_j' \overline{\alpha_i}(0, \alpha_i')} + G_{ij}\Delta t \overline{\alpha_j d\sigma_j / d\alpha_j},$$

or, observing (2.7) and the convention (4.2):

$$A_{ji}(\Delta t) = A_{ji}(0) - k\Delta t G_{ij}. \tag{4.7}$$

Similarly, of course

$$A_{ij}(\Delta t) = A_{ij}(0) - k\Delta t G_{ji}.$$

Applying the condition (4.3) for microscopic reversibility we find

$$G_{ij} = G_{ji}, \tag{4.8}$$

as announced at the end of §1. The importance of considering fluctuations for the derivation of this result is apparent from the occurrence of Boltzmann's constant k in (4.7).

5. The Principle of the Least Dissipation of Energy

The symmetry relation (4.8) contains the important reciprocal relations in transport processes. An alternative form of (4.8) is convenient for many applications, and commands considerable intrinsic interest. The description (4.4) of a set of simultaneous irreversible processes may be rewritten in the form

$$\frac{\partial \sigma_{1 \cdots n}(\alpha_1, \cdots \alpha_n)}{d\alpha_i} = \sum_{r=1}^{n} \rho_{ir}\dot{\alpha}_r, \quad (i = 1, \cdots n), \tag{5.1}$$

where, according to the equations

$$\sum_{r=1}^{n} \rho_{ir}G_{rj} = \sum_{r=1}^{n} G_{ir}\rho_{rj} = \delta_{ij} = \begin{cases} 1, & (i = j) \\ 0, & (i \neq j), \end{cases} \tag{5.2}$$

the coefficients (ρ_{ij})form the inverse matrix of (G_{ij}), which enter into (4.4). The symmetry relations (4.8) may be replaced by the equivalent

$$\rho_{ij} = \rho_{ji}, \quad (i = 1, \cdots n). \tag{5.3}$$

We introduce the *dissipation-function*

$$\Phi(\dot{\alpha}, \dot{\alpha}) \equiv \tfrac{1}{2} \sum_{i,j} \rho_{ij}\dot{\alpha}_i\dot{\alpha}_j, \tag{5.4}$$

and incorporate the symmetry relations (5.3) into the description of irreversible processes by writing

$$\partial \sigma_{1 \cdots n}(\alpha_1, \cdots \alpha_n)/d\alpha_i = \partial \Phi(\dot{\alpha}, \dot{\alpha})/d\dot{\alpha}_i, \tag{5.5}$$

in place of (5.1). Further, if we define a function

$$\dot{S}(\alpha, \dot{\alpha}) \equiv \sum_{r=1}^{n} (\partial \sigma_{1 \ldots n}/d\alpha_r)\dot{\alpha}_r, \tag{5.6}$$

representing the rate of increase of the entropy, we can formulate a *variation-principle*, namely

$$\delta[\dot{S}(\alpha, \dot{\alpha}) - \Phi(\dot{\alpha}, \dot{\alpha})] = 0. \tag{5.7}$$

Our convention is that only the velocities $\dot{\alpha}_1, \cdots \dot{\alpha}_n$ should be varied, thus

$$\delta[\dot{S}(\alpha, \dot{\alpha}) - \Phi(\dot{\alpha}, \dot{\alpha})] = \sum_{i=1}^{n} \left(\frac{\partial \sigma_{1 \ldots n}}{d\alpha_i} - \frac{\partial \Phi}{d\dot{\alpha}_i} \right) \delta\dot{\alpha}_i = 0,$$

according to (5.5). The variation principle (5.7), which we shall call the *principle of the least dissipation of energy*, for reasons mentioned in (I), §6, provides convenient means for transforming the reciprocal relations (5.3), or (4.8), to cases where the conventional description of irreversible processes involves an infinite number of variables, for example the temperatures in all parts of a space. The dissipation-function equals half the rate of production of entropy

$$2\Phi(\dot{\alpha}, \dot{\alpha}) = \dot{S}(\alpha, \dot{\alpha}), \tag{5.8}$$

because of (5.5), (5.6) and (5.4), which may be written

$$\Phi(\dot{\alpha}, \dot{\alpha}) = \tfrac{1}{2} \sum_{i,j} \rho_{ij}\dot{\alpha}_i\dot{\alpha}_j = \tfrac{1}{2} \sum_{i} \dot{\alpha}_i \partial\Phi/d\dot{\alpha}_i.$$

It is evident from (5.8) that $\Phi(\dot{\alpha}, \dot{\alpha})$ must be essentially positive (definite or semidefinite), because the second law of thermodynamics demands $\dot{S} \geqq 0$. Therefore the extremum given by (5.7) is always a maximum

$$\dot{S}(\alpha, \dot{\alpha}) - \Phi(\dot{\alpha}, \dot{\alpha}) = \text{maximum}. \tag{5.9}$$

Applications of this principle will be given in a later publication; in (I), §§4–5, a special result was derived by a direct method.

It is worth pointing out that in the dissipation-function has a direct statistical significance. A detailed discussion would be out of place in this article, where a compact presentation of important theorems is intended, but we may state without derivation the result, which is an extension of Boltzmann's principle (2.1). The equilibrium condition of thermodynamics

$$S = \text{maximum}$$

characterizes the most probable state, and the probability W for a state $\Gamma(\alpha_1, \cdots \alpha_n)$ is given by Boltzmann's principle

$$k \log W(\alpha_1, \cdots \alpha_n) = S(\alpha_1, \cdots \alpha_n) + \text{const.};$$

for the precise interpretation of this theorem we must refer to the discussion in §2. In a similar manner, Eq. (5.9) describes the most probable course of an

irreversible process. It is also possible to show, under assumptions approximately equivalent to those that are necessary for deriving, (simultaneously), (5.5) and (2.12), that the probability

$$W(\Gamma', \Delta t, \Gamma'') = W(\alpha_1', \cdots \alpha_n', \Delta t, \alpha_1'', \cdots \alpha_n'')$$

for the states $\Gamma' = \Gamma(\alpha_1', \cdots \alpha_n')$ and $\Gamma'' = \Gamma(\alpha_1'', \cdots \alpha_n'')$ occurring at the times t' and $t'' = t' + \Delta t$, respectively, is given by the formula

$$k \log W(\Gamma', \Delta t, \Gamma'') = S' + S'' - \frac{\Phi(\Delta\alpha, \Delta\alpha)}{\Delta t} + \text{const.}, \qquad (5.10)$$

where $S' = S(\alpha_1', \cdots \alpha_n')$, $S'' = S(\alpha_1'', \cdots \alpha_n'')$, and

$$\Phi(\Delta\alpha, \Delta\alpha) = \tfrac{1}{2} \sum_{i,j} \rho_{ij} (\alpha_i'' - \alpha_i')(\alpha_j'' - \alpha_j').$$

(Needless to say, we assume that we are dealing with an aged system.)

6. Nonreversible Systems

As mentioned in (I), §7, we know from our macroscopic experience certain conservative dynamical systems which do not exhibit dynamical reversibility, namely systems where external magnetic fields are acting, and systems whose motion is described relatively to a rotating frame of coordinates, the rotation being equivalent to a field of Coriolis forces. In such cases, where the macroscopic laws of motion are non-reversible, the microscopic motion cannot be reversible.

In dealing with cases of this kind it is advantageous to consider the intensities of magnetic and Coriolis fields as variable external parameters of the system in hand. Then macroscopic dynamical systems subject to external magnetic and Coriolis forces have the following symmetry with regard to reversal of the time: If $[q] = [Q(t - t_0)]$ is a possible motion (succession of configurations $[q]$) of a system left to itself in a magnetic (or Coriolis) field of intensity Θ, then the reverse succession of configurations $[q] = [Q(t_0 - t)]$ is a possible motion of the same system when placed in a field of intensity $-\Theta$. Further, let α and β be two functions of the state (and of the parameters) of the system in hand, such that their values are not changed when all the velocities in the system are reversed, (simultaneously with Θ). Then, when we consider the fluctuations in an aged system, as in §4, the succession of events $\alpha = \alpha'$, $\beta = \beta'$, with an intervening lapse of time τ, will occur in a system placed in a field of intensity $+\Theta$, just as often as the succession of events $\beta = \beta'$, $\alpha = \alpha'$, (with a time-interval τ), will occur in a system placed in a field of intensity $-\Theta$.

If we may apply this symmetry condition to the motion of elementary particles, and α_i, α_j are two "reversible" dynamical variables, the averages (4.1) will be functions of the time τ and the field intensity Θ:

$$A_{ji}(\Theta, \tau),$$

and we have the symmetry condition

$$A_{ji}(\Theta, \tau) = A_{ji}(-\Theta, -\tau) = A_{ij}(-\Theta, \tau). \tag{6.1}$$

Supposing that a certain irreversible process can be described in the form (4.4), the coefficients G_{ji} being functions of Θ,

$$\frac{d\alpha_i}{dt} = \dot{\alpha}_i = \sum_{j=1}^{n} G_{ij}(\Theta) \frac{\partial \sigma_{1\cdots n}(\alpha_1, \cdots \alpha_n)}{d\alpha_j}, \quad (i = 1, \cdots n), \tag{6.2}$$

we can derive (4.7) as before

$$A_{ji}(\Theta, \Delta t) = A_{ji}(\Theta, 0) - k\Delta t G_{ij}(\Theta)$$
$$A_{ij}(-\Theta, \Delta t) = A_{ij}(-\Theta, 0) - k\Delta t G_{ji}(-\Theta),$$

and upon applying the symmetry condition (6.1) we find

$$G_{ij}(\Theta) = G_{ji}(-\Theta). \tag{6.3}$$

This theorem contains a reciprocal relation between the Nernst effect and the Ettingshausen effect, which has been derived previously by P. W. Bridgman[11] and by H. A. Lorentz[12] on a quasi-thermodynamic basis.

[11] P. W. Bridgman, Phys. Rev. **24,** 644 (1924); Fourth Solvay Congress ("Conductibilité Electrique des Metaux"), 352 (1924).

[12] H. A. Lorentz, Fourth Solvay Congress, 354 (1924).

THE PROBLEM OF ROTATING MAGNETS

By W. B. Pietenpol and E. C. Westerfield
University of Colorado

(Received September 1, 1931)

Abstract

Ampere's problem of a cylindrical magnet free to rotate about its axis when a current enters at some point on the side of the magnet and leaves along the axis is treated by applying Ampere's original formula directly to the amperian currents which, according to the most commonly accepted theory, account for the magnetic properties of a body. For the torque on a symmetrically magnetised magnet, an expression in agreement with that of Zeleny and Page, and Kimball is obtained. However, this method of attack indicates that this torque is due only to the current in the portions of the circuit not attached to the magnet, contrary to the conclusion of Zeleny and Page. In the case of an asymmetrically magnetised magnet, it is found that the same expression holds provided only that the current is symmetrical in the portion of the circuit not mechanically attached to the magnet. This shows that the expression is more general than indicated by Zeleny and Page, in that they employed a symmetrical distribution of current within as well as without the magnet.

Introduction

THE problem of rotating magnets, which is the converse of unipolar induction, has received considerable attention in recent publications. Ampere first showed that when an electric current is allowed to traverse a cylindrical magnet, entering at some point on the side of the magnet and leaving along the axis of symmetry, the magnet experiences a torque. He explained this effect qualitatively by assuming the magnetism of the magnet to be due to tiny amperian currents and applying his law for the direction of the force between current elements.

In a recent article[1] in which Zeleny and Page have derived the quantitative expression for the torque experienced by the magnet, they conclude that only the current in the portion of the circuit attached to the magnet can contribute to this torque. Kimball[2] obtained the identical expression by deducing the torque exerted on the external circuit by the magnet, and, applying the law of action and reaction, assuming an equal and opposite torque on the magnet. This method of attack seems to imply that only the unattached portions of the current circuit could contribute to the torque on the magnet. These results seem incompatible. However, it is difficult to show experimentally which is correct, since the experimental conditions as well as the resultant expressions are identical.

Zeleny and Page find that when the magnet is asymmetrically magnetised

[1] Zeleny and Page, Phys. Rev. **24,** 544 (1924); Phys. Rev. **27,** 470 (1926); See also, Kennard and Wang, Phys. Rev. **27,** 460 (1926).

[2] A. L. Kimball, Phys. Rev. **28,** 1302 (1926).

the original expression still holds, provided the current both within and without the magnet be symmetrically distributed. Kimball did not treat this case; but, if his original assumption is correct, we readily see that the expression still holds provided only that the current in the portions of the circuit not attached to the magnet be symmetrically distributed. It becomes, therefore, a matter of some importance to determine whether Kimball's assumption is correct.

The present authors have considered this matter theoretically by applying Ampere's original formula[3] directly to the tiny amperian currents which are supposed to account for the properties peculiar to a magnet.

I. Force on a Vector Current Element

In the vector notation, Ampere's formula for the force between two current elements $\mathbf{e}$ and $d\mathbf{r}$[4] separated by the vector distance $\mathbf{r}$ becomes

$$d\mathbf{F} = I_e I_r(2\mathbf{re}\cdot d\mathbf{r} - 3\mathbf{r}\cdot\mathbf{e}dr)(\mathbf{r}:r^4) \tag{1}$$

Taking $\mathbf{e}=r\mathbf{i}$ and $\mathbf{r}=\mathbf{i}u+\mathbf{j}v+\mathbf{k}w$, we have $\mathbf{e}\cdot d\mathbf{r}=e\,du$ and $\mathbf{r}\cdot\mathbf{e}=eu$, and Eq. (1) becomes

$$d\mathbf{F} = eI_e I_r(2rdu - 3udr)(\mathbf{r}:r^4). \tag{2}$$

From this we obtain as the u, v, and w components of the force

$$dF_u = eI_e I_r d(u^2:r^3) \tag{3}$$

$$dF_v = eI_e I_r(d(uv:r^3) + (vdu - udv):r^3) \tag{4}$$

$$dF_w = eI_e I_r(d(uw:r^3) + (wdu - udw):r^3). \tag{5}$$

II. Axial Torque on an Amperian Current

Formula (3) gives the force along the vector current element $\mathbf{e}$ when $\mathbf{e}$ is directed along the u-axis, and if this expression be integrated between (u_a, r_a) and (u_b, r_b) we obtain

$$F_e = F_u = eI_e I_r(u_b^2:r_b^3 - u_a^2:r_a^3) \tag{6}$$

$$= eI_e I_r(r_b^{-1}\cos^2\phi_b\cos^2\theta_b - r_a^{-1}\cos^2\phi_a\cos^2\theta_a) \tag{7}$$

as the force along $\mathbf{e}$ due to the partial circuit along the path of integration, ϕ being the angle between $\mathbf{r}$ and the (u, v)-plane and θ being the angle between the u-axis and the $(\mathbf{r}, w)$-plane. (Fig. 1). Now suppose $\mathbf{e}$ is translated a small distance $\mathbf{c}$ perpendicular to itself (Fig. 2), then e may be represented by $(c\text{-}d\theta)$; and if c is sufficiently small to permit us to neglect the change in distances between $\mathbf{e}$ and the termini of the partial circuit, we may express the torque on $\mathbf{e}$ about the w-axis as

$$dT = c^2 I_c I_r(r_b^{-1}\cos^2\phi_b\cos^2\theta_b - r_a^{-1}\cos^2\phi_a\cos^2\theta_a)d\theta \tag{8}$$

[3] Carl Cinnamon has applied Ampere's formula to a solenoid, (Abstract, Journal of the Colorado-Wyoming Academy of Science **1**, 41 (1930).

[4] $d\mathbf{r}$=the differential of vector $\mathbf{r}$; ds=the scalar length of $d\mathbf{r}$; dr=the differential of the scalar r.

If we consider $\mathbf{e}$ to be an element of an amperian current lying in the (u, v)-plane and having the w-axis as its axis, we may obtain the total torque (about the w-axis) on this amperian current by integrating Eq. (8) as the θ's vary

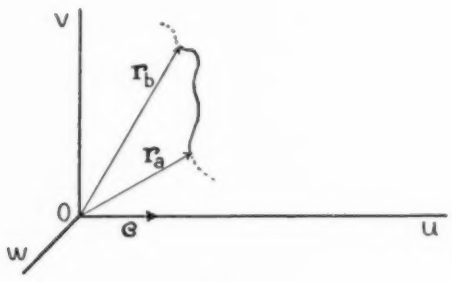

Fig. 1.

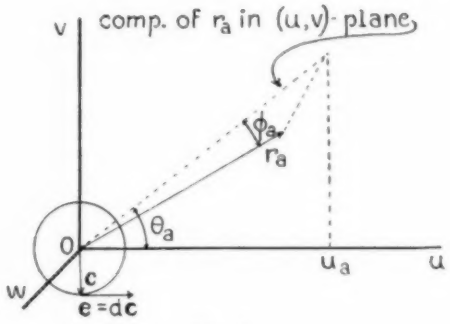

Fig. 2.

through an angle 2π. Since, from symmetry, the initial values of θ_a and θ_b cannot affect the final result, we may replace each by θ. We then have

$$T = c^2 I_c I_r (r_b^{-1} \cos^2 \phi_b - r_a^{-1} \cos^2 \phi_a) \int_0^{2\pi} \cos^2 \theta d\theta$$

$$= 4c^2 I_c I_r (r_b^{-1} \cos^2 \phi_b - r_a^{-1} \cos^2 \phi_a) \int_0^{\pi/2} \cos^2 \theta d\theta \tag{9}$$

$$= \pi c^2 I_c I_r (r_b^{-1} \cos^2 \phi_b - r_a^{-1} \cos^2 \phi_a). \tag{10}$$

If we allow r_b to approach r_a as a limit and ϕ_b to approach ϕ_a as a limit, our partial circuit again approaches the vector element $d\mathbf{r}$ as a limit, and our differential expression for the torque on the amperian circuit becomes (from Eq. (10))

$$dT = \pi c^2 I_c I_r d(u^2 : r^3 + v^2 : r^3). \tag{11}$$

III. Force on a Closed Circuit

First assume $\mathbf{e}$ to be directed along the u-axis, i.e., $\mathbf{e} = e\boldsymbol{i}$. Since Newton's third law is satisfied by Ampere's formula, we may apply formulae (3), (4), and (5) after reversing the signs. We see that the right member of Eq. (3) and the first term of the right members of Eqs. (4) and (5), being perfect differentials, vanish when integrated around a closed circuit; hence, for the closed circuit o we have

$$F_u = 0.$$

$$F_v = eI_e I_r \int_0 (u dv - v du) : r^3 = eI_e I_r \int_0 \boldsymbol{k} \times \mathbf{r} \cdot d\mathbf{r} : r^3$$

$$= eI_e I_r \boldsymbol{k} \cdot \int_0 \mathbf{r} \times d\mathbf{r} : r^3,$$

$$F_w = eI_eI_r \int_0 (udw - wdu):r^3 = - eI_eI_r \int_0 j \times \mathbf{r}\cdot d\mathbf{r}:r^3$$

$$= - eI_eI_r j \cdot \int_0 \mathbf{r} \times d\mathbf{r}:r^3,$$

or replacing $I_eI_r\int_0 \mathbf{r}\times d\mathbf{r}:r^3$ by $\boldsymbol{A}$, we may write[5]

$$\boldsymbol{F} = e(\boldsymbol{A}\cdot kj - \boldsymbol{A}\cdot jk) = e\boldsymbol{A} \times j \times k = e\boldsymbol{A} \times i = \boldsymbol{A} \times \boldsymbol{e}. \tag{12}$$

(See Fig. 3.) Since $\mathbf{r}$ is a general vector, Eq. (12) is obviously valid even when $\mathbf{e}$ is not directed along the u-axis; and if $\mathbf{e}$ is located at $\boldsymbol{q}$ and $\mathbf{s} = \mathbf{r} - \boldsymbol{q}$. Then, $\boldsymbol{q}$ being constant, we have, replacing $\mathbf{r}$ in $\boldsymbol{A}$ by $\mathbf{s}$,

$$\boldsymbol{A} = I_eI_r \int_0 \mathbf{s} \times d\mathbf{s}:s^3 = I_eI_r \int_0 \mathbf{s} \times d\mathbf{r}:s^3, \qquad d\mathbf{s} = d\mathbf{r},$$

and may write

$$\boldsymbol{F} = - I_eI_r\mathbf{e} \times \int_0 \mathbf{s} \times d\mathbf{r}:s^3. \tag{13}$$

IV. Force on an Amperian Current

Suppose now, in Eq. (13), we replace $\mathbf{r}$ by $\mathbf{c}$, where $\mathbf{c}$ is the radius vector which traces out an amperian current lying in the (u, v)-plane with center at origin. (See Fig. 4.) Then $d\mathbf{r} \equiv d\mathbf{c}$ will be a vector current element of this

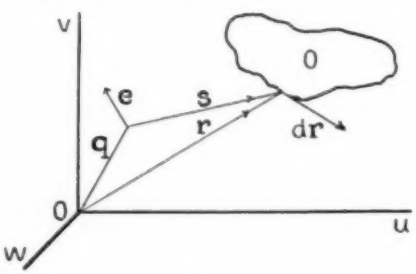

Fig. 3.

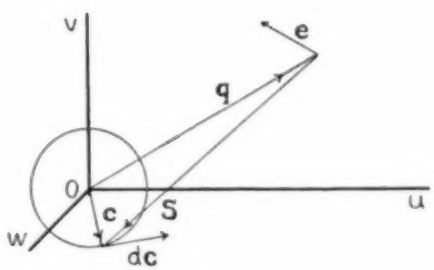

Fig. 4.

amperian current. If we assume the amperian current to be circular, c, being the radius, will be constant. Eq. (13) now becomes

$$\boldsymbol{F} = I_eI_c\mathbf{e} \times \int_c (\boldsymbol{q} - \mathbf{c}) \times d\mathbf{c}:s^3 = I_eI_c\mathbf{e} \times \left(\boldsymbol{q} \times \int_c d\mathbf{c}:s^3 - \int_c \mathbf{c} \times d\mathbf{c}:s^3\right)$$

$$= I_eI_c\mathbf{e} \times \left(\boldsymbol{q} \times i \int_c du:s^3 + \boldsymbol{q} \times j \int_c dv:s^3 - c^2k \int_c d\theta:s^3\right), \tag{14}$$

[5] Triple and higher vector cross-products will be written without parentheses when the operations are to be carried out in inverse order. For example, the expression $\mathbf{a}\times(\mathbf{b}\times(\mathbf{c}\times\mathbf{d}))$ will be indicated by $\mathbf{a}\times\mathbf{b}\times\mathbf{c}\times\mathbf{d}$, while the expression $(\mathbf{a}\times\mathbf{b})\times(\mathbf{c}\times\mathbf{d})$ will be written $(\mathbf{a}\times\mathbf{b})\times\mathbf{c}\times\mathbf{d}$, etc.

where θ is the angle between $\mathbf{c}$ and the u-axis. It remains then to evaluate the three integrals involved in Eq. (14). Since $d\mathbf{c}$ is perpendicular to $\mathbf{c}$ in the (u, v)-plane, it follows that $du = c \sin \theta d\theta$, and $dv = c \cos \theta d\theta$. Moreover, since $\mathbf{s} = \mathbf{c} - \mathbf{q}$, we have, taking $\mathbf{q}$ in the (u, w)-plane, $s^3 = (q^2 + c^2 - 2q_u c \cos \theta)^{3/2}$. Whence, expanding by the binomial theorem and neglecting the third and higher powers of c, (c being small compared to q) we obtain

$$s^{-3} = \frac{2q^4 + 6q^2 q_u c \cos\theta - 3q^2 c^2 + 15 q_u^2 c^2 \cos^2\theta}{2q^7}. \tag{15}$$

Or, neglecting the second and higher powers of c, we have the simpler expression

$$s^{-3} = (q^2 + 3q_u c \cos\theta) : q^5. \tag{16}$$

By making use of the above relations, we see that the first integral in Eq. (14) vanishes when integrated around a closed circuit, the integrand being a perfect differential. Applying approximation (16), the second integral becomes

$$\begin{aligned} \int_c dv : s^3 &= (c : q^3) \int_0^{2\pi} \cos\theta d\theta + 3(q_u c^2 : q^5) \int_0^{2\pi} \cos^2\theta d\theta \\ &= 12(q_u c^2 : q^5) \int_0^{\pi/2} \cos^2\theta d\theta = 3\pi(q_u c^2 : q^5). \end{aligned} \tag{17}$$

It is worth while noticing that while we have used only the terms of approximation (16) in obtaining Eq. (17), yet approximation (15) would have added nothing to this result.

Treating the third integral of Eq. (14) in a similar manner, we obtain

$$\begin{aligned} c^2 \int_c d\theta : s^3 &= (c^2 : q^3) \int_0^{2\pi} d\theta + 3(q_u c^3 : q^5) \int_0^{2\pi} \cos\theta d\theta \\ &= 2\pi(c^2 : q^3). \end{aligned} \tag{18}$$

And again we observe that approximation (15) would merely give additional terms in the fourth power of c. Thus Eqs. (17) and (18) are accurate to and including the third power of c.

Setting the expressions obtained in (17) and (18) back in Eq. (14) now, we obtain

$$\begin{aligned} \boldsymbol{F} &= 3\pi q_u (c^2 : q^5) I_e I_c \boldsymbol{e} \times \boldsymbol{q} \times \boldsymbol{j} - 2\pi(c^2 : q^3) I_e I_c \boldsymbol{e} \times \boldsymbol{k} \\ &= I_e I_c (\pi c^2 : q^5)(3\boldsymbol{e} \times \boldsymbol{q} \times \boldsymbol{k} \times \boldsymbol{q} - 2q^2 \boldsymbol{e} \times \boldsymbol{k}). \end{aligned} \tag{19}$$

And since $\pi c^2 \boldsymbol{k} = \boldsymbol{a}$ is the vector area of the amperian current, we may write Eq. (19) in the somewhat more elegant form

$$\boldsymbol{F} = (I_e I_c : q^5) \boldsymbol{e} \times (3\boldsymbol{q} \times \boldsymbol{a} \times \boldsymbol{q} - 2q^2 \boldsymbol{a}). \tag{20}$$

This equation is independent of the coordinate axes; and, since in obtaining this result our only restrictions have been on the position of the coordinate axes, not on the relative position of the amperian current and the vector cur-

rent element, it follows that Eq. (20) is perfectly general,—the only restriction being that q be large compared to c, (i.e., compared to a).

V. Total Axial Torque

If, in Eq. (20), we take our amperian current to lie in the (u, v)-plane with center at $\boldsymbol{r}$; and take the general vector current element $\boldsymbol{e}$ to lie at $\boldsymbol{b}$: then we

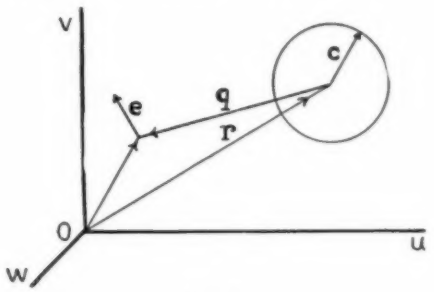

Fig. 5.

have $\boldsymbol{q}=\boldsymbol{b}-\boldsymbol{r}$ (i.e., $\boldsymbol{r}=\boldsymbol{b}-\boldsymbol{q}$), and $\boldsymbol{a}=\pi c^2\boldsymbol{k}$. (See Fig. 5.) Eq. (20) will then become

$$\boldsymbol{F} = K(2q^2\boldsymbol{k}\times\boldsymbol{e} - 3\boldsymbol{e}\times\boldsymbol{q}\times\boldsymbol{q}\times\boldsymbol{k}), \tag{21}$$

where $K=(\pi c^2{:}\,q^5)I_eI_c$. The torque about the w-axis due to this force will be

$$\begin{aligned}
T_1 &= \boldsymbol{k}\cdot\boldsymbol{r}\times\boldsymbol{F}, && \boldsymbol{r}=\boldsymbol{b}-\boldsymbol{q},\\
T_1 &= K(2q^2\boldsymbol{k}\cdot\boldsymbol{r}\times\boldsymbol{k}\times\boldsymbol{e} - 3\boldsymbol{k}\cdot\boldsymbol{r}\times\boldsymbol{e}\times\boldsymbol{q}\times\boldsymbol{q}\times\boldsymbol{k})\\
&= K(2q^2\boldsymbol{k}\cdot\boldsymbol{b}\times\boldsymbol{k}\times\boldsymbol{e} - 2q^2\boldsymbol{k}\cdot\boldsymbol{q}\times\boldsymbol{k}\times\boldsymbol{e} - 3\boldsymbol{k}\cdot\boldsymbol{b}\times\boldsymbol{e}\times\boldsymbol{q}\times\boldsymbol{q}\times\boldsymbol{k}\\
&\quad + 3\boldsymbol{k}\cdot\boldsymbol{q}\times\boldsymbol{e}\times\boldsymbol{q}\times\boldsymbol{q}\times\boldsymbol{k})\\
&= K(2q^2\boldsymbol{k}\cdot\boldsymbol{b}\times\boldsymbol{k}\times\boldsymbol{e} - 2q^2\boldsymbol{k}\cdot\boldsymbol{q}\times\boldsymbol{k}\times\boldsymbol{e} - 3\boldsymbol{k}\cdot\boldsymbol{b}\times\boldsymbol{e}\times\boldsymbol{q}\times\boldsymbol{q}\times\boldsymbol{k}\\
&\quad - 3\boldsymbol{k}\cdot\boldsymbol{q}\times\boldsymbol{q}\times\boldsymbol{k}\ \boldsymbol{q}\cdot\boldsymbol{e}).
\end{aligned} \tag{22}$$

This last result comes from the expansion

$$\begin{aligned}
\boldsymbol{k}\cdot\boldsymbol{q}\times\boldsymbol{e}\times\boldsymbol{q}\times\boldsymbol{q}\times\boldsymbol{k} &= \boldsymbol{k}\cdot(\boldsymbol{q}\cdot\boldsymbol{q}\times\boldsymbol{q}\times\boldsymbol{k}\,\boldsymbol{e} - \boldsymbol{q}\cdot\boldsymbol{e}\,\boldsymbol{q}\times\boldsymbol{q}\times\boldsymbol{k})\\
&= \boldsymbol{k}\cdot(\boldsymbol{q}\times\boldsymbol{q}\cdot\boldsymbol{q}\times\boldsymbol{k}\,\boldsymbol{e} - \boldsymbol{q}\cdot\boldsymbol{e}\,\boldsymbol{q}\times\boldsymbol{q}\times\boldsymbol{k})\\
&= -\,\boldsymbol{k}\cdot\boldsymbol{q}\times\boldsymbol{q}\times\boldsymbol{k}\,\boldsymbol{q}\cdot\boldsymbol{e}.
\end{aligned}$$

Now, returning to Eq. (11), we find the expression for the torque on the amperian current about its own axis to be

$$\begin{aligned}
T_2 &= \pi c^2 I_e I_r d(u^2{:}\,r^3 + v^2{:}\,r^3)\\
&= (\pi c^2{:}\,r^4)I_eI_r(2r(u\,du + v\,dv) - 3(u^2+v^2)dr)\\
&= (\pi c^2{:}\,r^4)I_eI_r(2r\boldsymbol{k}\times\boldsymbol{r}\cdot\boldsymbol{k}\times d\boldsymbol{r} - 3\boldsymbol{k}\times\boldsymbol{r}\cdot\boldsymbol{k}\times\boldsymbol{r}dr)\\
&= (\pi c^2{:}\,r^5)I_eI_r(2r^2\boldsymbol{k}\cdot\boldsymbol{r}\times\boldsymbol{k}\times d\boldsymbol{r} - 3\boldsymbol{k}\cdot\boldsymbol{r}\times\boldsymbol{k}\times\boldsymbol{r}\,\boldsymbol{r}\cdot d\boldsymbol{r}).
\end{aligned}$$

Whence, replacing $\boldsymbol{r}$ by $\boldsymbol{q}$ and $d\boldsymbol{r}$ by $\boldsymbol{e}$ to make the notation agree with that of Eq. (22), we have

$$\begin{aligned} T_2 &= K(2q^2\boldsymbol{k}\cdot\boldsymbol{q}\times\boldsymbol{k}\times\boldsymbol{e} - 3\boldsymbol{k}\cdot\boldsymbol{q}\times\boldsymbol{k}\times\boldsymbol{q}\,\boldsymbol{q}\cdot\boldsymbol{e}) \\ &= K(2q^2\boldsymbol{k}\cdot\boldsymbol{q}\times\boldsymbol{k}\times\boldsymbol{e} + 3\boldsymbol{k}\cdot\boldsymbol{q}\times\boldsymbol{q}\times\boldsymbol{k}\,\boldsymbol{q}\cdot\boldsymbol{e}). \end{aligned} \tag{23}$$

Combining Eqs. (22) and (23), we have for the total torque about the w-axis

$$\begin{aligned} T &= T_1 + T_2 \\ &= K(2q^2\boldsymbol{k}\cdot\boldsymbol{b}\times\boldsymbol{k}\times\boldsymbol{e} - 3\boldsymbol{k}\cdot\boldsymbol{b}\times\boldsymbol{e}\times\boldsymbol{q}\times\boldsymbol{q}\times\boldsymbol{k}) \\ &= K\boldsymbol{k}\cdot\boldsymbol{b}\times\boldsymbol{e}\times(3\boldsymbol{q}\times\boldsymbol{k}\times\boldsymbol{q} - 2q^2\boldsymbol{k}) \\ &= K\boldsymbol{k}\cdot\boldsymbol{b}\times\boldsymbol{e}\times(q^2\boldsymbol{k} - 3\boldsymbol{q}\cdot\boldsymbol{k}\,\boldsymbol{q}) \\ &= K\boldsymbol{k}\cdot\boldsymbol{b}\times\boldsymbol{e}\times(\boldsymbol{q}\times\boldsymbol{k}\times\boldsymbol{q} - 2\boldsymbol{q}\cdot\boldsymbol{k}\,\boldsymbol{q}), \end{aligned} \tag{24}$$

where, as before, $K = (\pi c^2 : q^5) I_e I_c$.

Suppose now, for comparison, we develop the vector expression for the field of the short magnet to which the amperian current may be supposed to correspond. The field along $\boldsymbol{q}$ at a vector distance $\boldsymbol{q}$ from the center of a short magnet is given by $(2M:q^3)\cos\theta$, where M is the magnetic moment of the magnet, and θ is the angle between $\boldsymbol{q}$ and the normal vector. Also, the component of the field perpendicular to $\boldsymbol{q}$ in the plane determined by $\boldsymbol{q}$ and the normal vector, is given by $(M:q^3)$ sine θ. If $\boldsymbol{k}$ is the normal vector (as it is in the case under consideration), then from the above expressions we may write as the vector expression of the total field strength at $\boldsymbol{b}$ (where as before $\boldsymbol{q} = \boldsymbol{b} - \boldsymbol{r}$, $\boldsymbol{r}$ being the vector position at the midpoint of the short magnet)

$$\begin{aligned} \boldsymbol{H} &= (2M:q^5)\boldsymbol{q}\cdot\boldsymbol{k}\,\boldsymbol{q} + (M:q^5)\boldsymbol{q}\times\boldsymbol{q}\times\boldsymbol{k} \\ &= (M:q^5)(2\boldsymbol{q}\cdot\boldsymbol{k}\,\boldsymbol{q} + \boldsymbol{q}\times\boldsymbol{q}\times\boldsymbol{k}). \end{aligned} \tag{25}$$

But M is equivalent to $\pi c^2 I_c$ in accordance with the idea of equivalent magnetic shells; hence, combining Eqs. (24) and (25), we may write

$$T = I_e\boldsymbol{k}\cdot\boldsymbol{b}\times\boldsymbol{H}\times\boldsymbol{e}. \tag{26}$$

Or, interchanging dot and cross,

$$T = I_e\boldsymbol{k}\times\boldsymbol{b}\cdot\boldsymbol{H}\times\boldsymbol{e}. \tag{27}$$

This equation really deals with differentials (if we think of the tiny amperian current as an infinitesimal element of the cross-sectional area of a magnet of finite proportions), and should be written

$$dT = I_e\boldsymbol{k}\times\boldsymbol{b}\cdot d\boldsymbol{H}\times\boldsymbol{e} = I_e\boldsymbol{e}\times\boldsymbol{k}\times\boldsymbol{b}\cdot d\boldsymbol{H}, \tag{28}$$

but if we integrate (28) over any finite area in the (u, v)-plane we obtain

$$T = I_e\boldsymbol{e}\times\boldsymbol{k}\times\boldsymbol{b}\cdot\int_A d\boldsymbol{H} = I_e\boldsymbol{e}\times\boldsymbol{k}\times\boldsymbol{b}\cdot\boldsymbol{H}; \tag{29}$$

hence, Eq. (27) is true for any finite area in the (u, v)-plane, being identical in form to Eq. (29).

It follows that if the area under consideration is a right section of a uniformly magnetized, cylindrical magnet whose axis of symmetry coincides with the w-axis, then Eq. (29) may be written

$$T = I_e(N:2\pi), \tag{30}$$

where N is the number of lines of flux which would be cut by $\mathbf{e}$ if it were rigidly attached to a radius vector and swept about the w-axis once. Again, Eq. (30) is really a differential equation (in fact, a second order differential equation), the correct formulation being

$$d^2T = (I_e:2\pi)d^2N. \tag{31}$$

Integrating Eq. (31) along the length of the magnet, we have

$$dT = (I_e:2\pi)\int_L d^2N = (I_e:2\pi)dN. \tag{32}$$

Again, integrating Eq. (32) along the circuit of which $\mathbf{e}$ is an element, we have

$$T = (I_e:2\pi)\int_{b_1}^{b_2} dN = (I_e:2\pi)(N_2 - N_1),$$

or, for simplicity of statement,

$$T = (I_e:2\pi)N, \tag{33}$$

where N is understood to mean the algebraic sum of the lines of flux cutting the annular surface which would be swept out by rotating the segment of circuit in question about the w-axis, (i.e., about the axis of symmetry of the magnet).

The above expression applies to a uniformly magnetised, cylindrical magnet. To treat the case of an asymmetrically magnetised magnet, we may return to Eq. (29). If $\mathbf{e}$ is now considered to be a differential length of a filament of current symmetrically distributed about the axis of the magnet, then (29) becomes

$$dT = I_e r H e_r = r H e_r dI \tag{34}$$

where r is the perpendicular distance from the axis to $\mathbf{e}$, H is the scalar magnitude of the field at $\mathbf{e}$, and e_r is the component of $\mathbf{e}$ along r. But $dI = (I:2\pi)d\theta$, and $dN = He_r rd\theta$; hence (34) may be written

$$dT = (I:2\pi)rHe_r d\theta = (I:2\pi)dN. \tag{35}$$

Integrating this expression around a ring having as its axis the axis of the magnet, we obtain

$$T = IN:2\pi \tag{36}$$

corresponding to (30). In this expression, I is the current and N the flux through the ring.

Tracing through steps corresponding to Eqs. (31), (32), and (33), we see that (36) is the right form also for the equation corresponding to (33), where, now, N signifies the flux of a magnet of finite length through a ring region of finite dimensions,—formula (36) holding provided only that the current in this ring region be symmetrically distributed. Since throughout this work we have been dealing with expressions which satisfy Newton's third law, it follows that the torque must be due to the reaction between the amperian currents of the magnet and the current in the portions of the circuit not attached to the magnet. Thus for each infinitesimal force derived for an amperian current, there was an equal and opposite force on the current element e. If both the current element and the amperian current are seated in the same solid body (as they would be in the case of the current traversing the magnet), their mutual reaction could only produce mechanical stresses in the body and could not produce a motion of the body as a whole. It follows that (36) gives the torque on an asymmetrically magnetised magnet provided only that the current in the unattached portions of the circuit be symmetrically distributed, and N represent the total flux which cuts them.

Conclusion

Formula (33) has the same form as the expression obtained by Zeleny and Page, the distinction being that Zeleny and Page were led to attribute the torque to the reaction of the flux of the magnet with the current traversing the magnet and attached arm. In the light of the results contained in the present paper, this seems subject to logical objections; since, as has been pointed out, the reaction between a current element and an amperian circuit situated in the same solid body could only produce mechanical stresses in that body and not rotation of the body as a whole.

Zeleny and Page obtained an expression identical to that of (36) when the entire current sheet was symmetrical, whereas it is shown in the present paper that the current in the portions of the circuit attached to the magnet need not be symmetrical. Zeleny and Page have not treated the case of an asymmetrically magnetised magnet and asymmetrically distributed current within the magnet; however, since in this more general case the torque exerted by the current circuit on the poles would, in general, not be zero, it seems possible that they would find it somewhat difficult to apply their method; and, of course, the logical objections mentioned above would still apply.

It should be pointed out that while there is some doubt as to the validity of Ampere's original formula as applied to partial circuits, it is admittedly valid when one of the circuits is complete as in the present case.

In the experiment performed by Zeleny and Page in which the magnet is replaced by the brass cylinder in a fixed solenoid, the torque on the brass cylinder may be calculated by again applying Ampere's formula for the force between current elements. Here, however, the current-bearing conductors of

the solenoid are not mechanically attached to the cylinder, hence, the torque on it is due to the reaction between the current traversing the brass cylinder and the current in the solenoid. In this case the authors are in agreement with Zeleny and Page. If the solenoid is mechanically attached to the brass cylinder, then the reaction of the current within the brass cylinder with the current in the solenoid can no longer contribute to the torque, and the torque is due to the reaction between the current in the solenoid and the current in the portions of the circuit not attached to the brass cylinder.

In the present paper, only the major torque of the ordinary set-up has been calculated. Actually, the reaction of the current in the portions of the circuit attached to the magnet with that in the portions of the circuit not attached thereto may contribute to the torque, though, as pointed out by Zeleny and Page, this contribution is negligible in the experiments considered. It is obvious, however, that an experiment could be arranged in which this contribution would not be negligible. In asymmetrical cases, external magnetic fields would also affect the torque. To include these factors and extend the treatment to any rigid system, the following general law may be stated: *The torque on any rigid system may be obtained from the integrated reactions of all the current elements mechanically attached, with all the current elements not mechanically attached to the system.* It is understood that magnets are to be treated in terms of the corresponding amperian currents.

LETTERS TO THE EDITOR

Prompt publication of brief reports of important discoveries in physics may be secured by addressing them to this department. Closing dates for this department are, for the first issue of the month, the twenty-eighth of the preceding month; for the second issue, the thirteenth of the month. The Board of Editors does not hold itself responsible for the opinions expressed by the correspondents.

On the Interpretation of the Selective Photoelectric Effect from Two-Component Cathodes

A paper by Mr. A. R. Olpin with the above title appeared in the November 1st issue of the Physical Review. [**38,** 1745, 1931] Mr. Olpin calculates the wave-length of maximal response for a series of alkali hydrides, alkali oxides and alkali sulphides with a striking precision. His interpretation is based upon the Campbell-Fowler theory with the modification that the distance d between successive atomic layers occurring in the expression derived by Fowler has been correlated to the interplanar spacings in crystals of the compounds dealt with.

The object of this letter is to point out that the amazing agreement which Mr. Olpin finds is purely accidental.

Recently Zintl and Harder (Zeits. f. physik. Chemie B. **14,** 265, 1931) have determined the crystal structures of the alkali hydrides. The lattice constants which they give are rather different from those used in Mr. Olpin's calculations as the following table shows:

	Zintl and Harder	Olpin
LiH	4.084A	4.10A
NaH	4.880	4.50
KH	5.700	5.20
RbH	6.037	5.52
CsH	6.376	5.84

The next table shows the wave-lengths of maximal response as calculated on the basis of the correct spacings as compared to the observed wave-lengths.

	Calc.	Obs.
LiH	2750A	2800A
NaH	3930	3400, 3300
KH	5360	4350
RbH	6010	4800
CsH	6710	5400

It will be seen that there is no quantitative agreement except for LiH.

The spacings which Mr. Olpin uses in his calculations for the oxides and sulphides are not correct either, so that the agreement which he finds also for these substances is fictive.

W. H. ZACHARIASEN

Ryerson Physical Laboratory.
University of Chicago,
December 3, 1931.

"Regular Reflection of X-rays from Quartz Crystals Oscillating Piezoelectrically." Some Interpretations

Fox and Cork (Phys. Rev. **38,** 1420 (1931)), with a Y-cut quartz plate as the reflecting crystal in a Bragg spectrometer failed to detect any effect of piezoelectric oscillations on either the intensity or width of the reflected line. In view of the magnitude of the intensity effect usually observed this null result requires explanation.

An important fact to be considered in connection with this result is that it was obtained by surface reflection from the quartz plate, while all other positive results (Fox and Carr; Barrett; Nishikawa, Sakisaka and Sumoto; Barrett and Howe) were obtained by transmission through the quartz plate. It has been shown (Sakisaka, Proc. Phys.-Math. Soc.

Japan **12,** 190 (1930)) that with Mo$K\alpha$ rays reflecting from the surface of quartz, there is no appreciable contribution to the reflected beam from depths in the crystal greater than about 0.12 mm, either when the crystal had a "clean natural face" or when it has a ground surface. Fox and Cork, then, observed in their experiment the reflecting characteristics of the outer tenth millimeter or so of their half-millimeter thick crystal.

In grinding crystals to shape the surfaces become imperfect and intensely reflecting. These imperfect surface layers extend to a depth of about 0.1 mm (Sakisaka, Jap. Jour. Phys. **4,** 171 (1927)) and are not entirely removed by etching for a few minutes, nor by polishing. It is likely that such a layer on the reflecting surface was the seat of practically all of the reflected energy in Fox and Cork's experiment. Their result could be explained by saying that the reflecting layer was already so imperfect that oscillations could not add appreciably to this imperfection and therefore could not appreciably alter the line width and intensity. Sakisaka and Sumoto (Proc. Phys.-Math. Soc. Japan **13,** 211 (1931)) explain in this manner the unchanged surface reflection from quartz when the quartz is subjected to a temperature gradient.

Another interpretation of the negative result is possible that might be valid even with a thoroughly etched surface. Barrett and Howe found the reflecting power of oscillating quartz to be such as to indicate not a condition of random imperfection in the lattice, but, instead, a condition resulting from directed strain gradients. Regions of a crystal may be found where the reflecting power of a plane is practically unchanged by oscillations. The condition of strain in Fox and Cork's oscillating crystal may have been such as to have no effect on their reflected beam. There is too little known at present about the distribution of reflecting power as a function of mode of oscillation, type of cut, accuracy of cut, crystal dimensions and circuit interactions to be able definitely to accept or reject this interpretation.

CHARLES S. BARRETT
CARL E. HOWE

Naval Research Laboratory,
Bellevue, Anacostia, D.C.,
December 1, 1931.

Note on "The Range of Fast Electrons and Neutrons"

In the Physical Review, November 1st, 1931, Messrs. J. F. Carlson and J. R. Oppenheimer,[1] writing on the range of electrons and hypothetical neutrons, make a number of statements which more extensive knowledge of the published experimental facts would have prevented.

(1) To speak of the thinness of the tracks of fast β-rays is misleading; one can really only refer to the line density of droplets which are individually observed in photographs taken under properly controlled conditions.

(2) In 1929, Skobelzyn[2] pointed out from the evidence of track photographs that the number of ions produced per centimeter of a cosmic straight track differs, if at all, but slightly from the number observed under the same conditions in the case of the fastest β particles of radioactive origin.

(3) In the case of radioactive β-rays the exact variation of ionization per centimeter with $\epsilon=(1-v^2/c^2)^{-1/2}$ is known experimentally,[3] and instead of ionization per centimetre increasing with log ϵ, as theory requires according to Messrs. Carlson and Oppenheimer, it decreases. Nevertheless, they say that their "result makes it hard to believe that the particles observed with cosmic rays are electrons or protons since they are observed to ionize less than slower β particles". This reasoning is based on obvious contradiction of the experimental facts.

(4) With regard to the radioactive emission of neutrons from nuclei they write, "it would be of extreme interest to see whether in such a disintegration (radioactive β-ray) thin tracks of the kind observed by Mott-Smith could be found". For the benefit of the writers of this sentence it seems necessary to point out that this experiment has been performed on every occasion in which a β-ray source has been used in an expansion chamber, and that no evidence whatsoever for the emission of neutrons has been obtained.

[1] Carlson and Oppenheimer, Phys. Rev. **38,** 1787 (1931).

[2] Skobelzyn, Zeits. f. Phys. **54,** 686 (1929).

[3] Williams and Terroux, Proc. Roy. Soc., **A, 126,** 289 (1930).

Surely it is hardly necessary to insist that the object of physical theories is to describe accurately the experimental facts to which they refer, and to point out that such a purpose is defeated at the outset by neglect of the facts.

W. H. WATSON
F. R. TERROUX
Macdonald Physics Laboratory,
McGill University,
Montreal, Canada,
November 23, 1931.

Neutrons and Cosmic Rays

It has been suggested that cosmic rays are neutrons of high energy.[1] The neutron proposed by Pauli has a magnetic moment and hence should be deflected in a nonhomogeneous magnetic field. This suggests the possibility of an observational verification of the neutron hypothesis, either by a Stern-Gerlach experiment or by displacements in the earth's magnetic field. An exact treatment would require the solution of a wave equation but an approximate result can be obtained classically.

In a Stern-Gerlach experiment the displacement s normal to the original velocity is given by

$$s = \tfrac{1}{4}\,\frac{\mu}{E}\,l^2\frac{\partial H}{\partial s}$$

where μ is the magnetic moment of the particle and E is its energy. The ratio of the displacements of a neutron and an atom is

$$s_N/s_A = (\mu_N/\mu_A)(E_A/E_N).$$

If μ_N and μ_A are of the same order of magnitude S_N will not be measurable since E_N (for cosmic rays) is large compared to E_A, and s_A is almost at the limit of measurability.

Neutrons approaching the earth might be deflected by the earth's magnetic field so that they would not be distributed uniformly over the earth's surface. This would be analogous to the effect found by Epstein[2] for electrons.

For a neutron with a magnetic moment μ and energy E moving radially toward a dipole whose moment is M the component of force perpendicular to the direction of motion is

$$F = \frac{-6\mu M}{r^4}\,\frac{\sin\theta\cos\theta}{(1+3\cos^2\theta)^{1/2}}$$

where r is the distance from the dipole and θ the angle between the axis of the dipole and the direction of motion. An approximate integration gives

$$s = -\mu M/3ER^2$$

for the deflection normal to r for the value of θ giving maximum deflection. If μ is one Bohr magneton, M the magnetic moment and R the radius of the earth and E one million volt-electrons we find s to be approximately 10^{-6} centimeters.

We conclude that it is impossible to distinguish between neutrons and photons by magnetic effects if the energies are of cosmic-ray magnitudes. It is doubtful if neutrons with energy small enough to be appreciably deflected in a magnetic field would produce enough ionization to be observed at all.

L. D. HUFF
Clemson College,
South Carolina.
November 25, 1931.

[1] L. M. Mott-Smith and G. L. Locher, Phys. Rev. **38,** 1399 (1931); J. F. Carlson and J. R. Oppenheimer, Phys. Rev. **38,** 1787 (1931).

[2] P. S. Epstein, Proc. Nat. Acad. **16,** 658 (1930).

Conservation of Energy and the Disintegration of RaE.

The disintegration of RaE is accompanied by the emission of a more or less continuous spectrum of β-rays and by little high-frequency γ-radiation. Since the energy difference between RaE and RaF would be expected to have *some* unique value this peculiar β-ray emission has been cited by Bohr, at the recent meeting of the British Association for the Advancement of Science, as rendering doubtful the conservation of energy in the process of disintegration. There is, however, another mode of escape from the apparent dilemma.

The change from RaD to RaE raises the atomic number by unity and may be regarded as increasing the linear dimensions of the nucleus while decreasing the linear dimensions of the extra-nuclear electron structure. The probability of capture by the nucleus of an extra-nuclear electron is thus increased and we may

regard this event as initiating the next transformation. The captured electron, considered as a projectile entering the nucleus with a definite energy, can transfer this energy, together with the energy difference between that of RaE^+ and RaF^+, to *two* electrons within the nucleus, both of which might thus be emitted with different energies subject only to the condition that the sum of these energies is constant. These are obviously conditions for a continuous β-ray spectrum with a maximum intensity corresponding to the most probable velocity of emergence. The subsequent return of an electron to the shell from which it had been captured would give rise to some x-ray characteristic of RaF. The question whether or not the captured electron is one of the two emitted is probably meaningless.

The idea that a β-ray disintegration may be initiated by the instability of an extra-nuclear electron is not new, since it was proposed by H. T. Wolff as early as 1915.[1] This seems to be the first case in which such an extra-nuclear electron is needed for other reasons. It will be noticed that we must assume so much independence of the intra-nuclear and extra-nuclear systems as may be necessary to provide a certain degree of randomness in the impacts of captured electrons. On these views the number of β-rays emitted in the process should be twice the number of RaE atoms disintegrating.

This note is based upon a discussion with Professor A. H. Compton, who suggested, in particular, that the initial event in the proposed two-electron emission should be the capture of a third electron by the nucleus of RaE.

L. W. McKeehan
Sloane Physics Laboratory,
Yale University,
November 16, 1931.

[1] H. T. Wolff, Phys. Zeits. **16**, 416–419 (1915).

Distribution of Mobilities of Ions in Air

In the last issue of the Physical Review [**38**, 1716 (1931)] Loeb and Bradbury in discussing a paper of mine [Phys. Rev. **34**, 310 (1929)], in which I showed that aged ions in moist air have mobilities spread over a considerable range of values, make the following statement: "In this investigation most sources of error have been critically analyzed with the possible exception of the action of the moving air stream in aspirating more ions (and perhaps a larger spatial extent of ionization) into his chamber than is evident from the measurements". I should like to show that this hypothesized source of error was not present in my experiments. It should be recalled that in these experiments a *slow*, non-turbulent system of air was made to flow axially in the space between two concentric cylinders and that a relatively small amount of air, partially ionized in an auxiliary chamber, was gently forced into the main air stream through 102 small holes along a circumference of the outer of the two cylinders. The rate at which this ionized air entered the apparatus was controlled by water flowing under a constant pressure head into a gasometer and after a steady state of flow was reached this rate could not be affected by an aspiratory action of the main air stream. Moreover, this rate, which entered the calculations as a small quantity, was actually measured during the progress of each set of observations while the main air stream was flowing continuously. Incidentally the rate was found to be the same whether the main air stream was flowing or not. It should be noted, too, that the behavior of the jets of air as they entered the apparatus was carefully studied in a duplicate apparatus made partly of glass. The jets were made visible by an admixture of smoke and showed no widening such as is mentioned in the above quotation as having possibly been present.

John Zeleny
Sloane Physics Laboratory,
Yale University,
November 20, 1931.

The Deepest Term in the Au II Spectrum

The first spark spectrum of gold was analyzed by McLennan and McLay (Trans. Roy. Soc. Can. **22**, 103 (1928)) who did not locate the lowest term, $d^{10}\,{}^1S_0$, because of lack of range of the fluorite spectrograph used in their investigation. In the course of an investigation in this laboratory of the excitation of the gold spectrum in an atmosphere of helium, the spectrum of a gold hollow cathode discharge in helium has been photographed

with a 1 meter vacuum spectrograph. Only three combinations between $d^{10}\ {}^1S_0$ and known terms are possible, *viz.*, combinations with ${}^3P_1{}^0$, ${}^3D_1{}^0$, and ${}^1P_1{}^0$ of the d^9p configuration. Only three lines with the expected frequency differences appear in the region and thus locate ${}^1S_0$ with certainty. The lines are:

Int.	λ	ν	Classification
4	1362.44	73398	${}^1S_0 - d^9p\ {}^3P_1{}^0$
7	1224.65	81655	${}^1S_0 - d^9p\ {}^1P_1{}^0$
5	1166.81	85704	${}^1S_0 - d^9p\ {}^3D_1{}^0$

The wave-lengths are believed good to somewhat better than one-tenth of an Angstrom and the separations somewhat better. The frequency differences agree with McLennan's analysis to within 2 frequency units. The value of ${}^1S_0$ based on McLennan's term values is -15036.

This value of the low level is further confirmed from a study of the spectrum of the low voltage arc in helium and gold vapor. In this excitation lines from the two levels $d^97S\ {}^3D_1$ and ${}^1D_2$, which are respectively 24.11 and 24.15 volts above the normal state of the gold atom and thus nearly in resonance with the He ion (24.47 volts), are very strongly excited.

R. A. Sawyer
Kenneth Thomson
University of Michigan,
November 25, 1931.

A Band Spectrum due to the Molecule N_2O_3

During a study of the absorption of light by N_2O (Abstract No. 19 Chicago Meeting of the American Physical Society, Nov. 27–28, 1931), the authors were lead to an investigation of mixtures of NO and NO_2, and have observed, in the near ultraviolet, an absorption spectrum consisting of apparently diffuse bands, due in all probability to the molecule N_2O_3. The bands are observed in relatively large amounts of NO when small amounts of NO_2 are added, the new bands predominating over the absorption of NO_2 under these conditions. Their centers are located approximately at wave-lengths 3843, 3682, 3539, 3509, 3417, 3386, 3305, 3279. The bands do not appear to possess sharp edges nor to show any pronounced tendency to degrade one way or the other. The first member is exceptionally diffuse. The third member appears most intense. The bands grow weaker as they proceed to shorter wave-lengths suggesting that there may be further weaker members among the NO_2 absorption. The new bands show qualitatively the dependence to be expected upon the pressures of NO and NO_2, and upon the temperature, decreasing noticeably with increasing temperature. A more detailed description of this spectrum will be published later.

Eugene H. Melvin
Oliver R. Wulf
U. S. Bureau of Chemistry and Soils,
November 23, 1931.

A. Effect of Crystal Symmetry on the Energy Levels of Solids. B. Experimental Evidence of Definite Orientation of Coordinated Water Molecules About Rare Earth Ions in Solution

Because of its interest to physicists, who perhaps would not see the complete paper in a chemical journal, we think that it is desirable to publish a brief summary of an article which we shall submit soon to the Journal of the American Chemical Society.

A. Photographs were taken of the absorption spectra of the Gd^{+++} ion in monoclinic crystals of $GdCl_3 \cdot 6H_2O$, $GdBr_3 \cdot 6H_2O$, $Gd_2(SO_4)_3 \cdot 8H_2O$; in hexagonal crystals of $Gd(BrO_3)_3 \cdot 9H_2O$, $Gd(C_2H_5SO_4)_3 \cdot 9H_2O$, and in a triclinic crystal, $Gd(NO_3)_3 \cdot 6H_2O$. Gadolinium IV was chosen because it is by far the most desirable ion for this type of work. It gives sharp lines at room temperature, it has the simplest spectrum of any of the rare earths, its lines and multiplets being well separated from one another, and its basic level, ${}^8S_{7/2}$, is known to be single. Its chief disadvantage is that its absorption lines occur in the ultraviolet.[1]

In all cases the same multiplets were observed at approximately the same frequencies, although a slight shift of the multiplets toward shorter wave-lengths was noticeable in the case of crystals of higher symmetry. The lines within the multiplets were, however, greatly affected by changes in the crystal system.

[1] Freed and Spedding, Nature **123,** 525 (1929); Phys. Rev. **34,** 945 (1929); ibid. **38,** 670 (1931); Spedding, Phys. Rev. **37,** 777 (1931).

From the monoclinic crystals the number and spacing of the lines was almost identical, the differences between the spectra of $Gd_2(SO_4)_3 \cdot 8H_2O$ and $GdCl_3 \cdot 6H_2O$ being of the same order as those between $GdCl_3 \cdot 6H_2O$ and $GdBr_3 \cdot 6H_2O$.[2] Only in two cases were distinct differences observed and both occurred in multiplets in which the lines were very closely spaced. The differences were caused by a single line of the chloride spectrum becoming two lines in the case of the sulphate. On the other hand, between the hexogonal and monoclinic crystals, there were notable differences both in the number and spacing of the lines. The over-all spread of the multiplets was less than half that shown by the monoclinic crystals, and in many cases fewer lines were observed. The spectrum of the triclinic crystal was similar to that of the monoclinic type, but its multiplets were farther spread out. Unfortunately, only two groups of lines were obtained from $Gd(BrO_3)_3 \cdot 9H_2O$ and $Gd(NO_3)_3 \cdot 6H_2O$ owing to continuous absorption by the negative ions in the region below 3000A.

In a previous letter[3] to this journal experimental evidence was presented which showed that all the lines arise from a single basic level, $^8S_{7/2}$, which is not appreciably affected by the crystal field. For this reason the position of the lines and multiplets is effectively an energy level diagram of the excited levels. The absence of sensitivity to variations in the crystal field of the mean positions of the multiplets and the great sensitivity of their component lines to this field proves that the multiplets arise from an excited electronic level which has become non-degenerate because of the electric fields of the crystal. To a first approximation, the type and magnitude of the splitting depends only on the symmetry of the crystal, and the chemical differences of the surrounding ions have only a second order effect, except for that which aids in determining the crystal form.

These facts are in good agreement with those predicted by Bethe,[4] who, from considerations of wave mechanics and group theory has shown that degeneracy of the levels of rare earth ions, caused by the force fields of the neighboring ions in the crystal, should depend on the symmetry of the fields about the ions, and that the degeneracy should become less in fields of lower symmetry. In his calculations Bethe has made many simplifying assumptions which are not applicable here, so that better than qualitative agreement should not be expected. While the unique structures are still unknown, careful crystallographic measurements of all our crystals have been made by Professor Adolph Pabst of this university. In general the crystals are from the class of highest symmetry of the system to which they belong. In the case of the hexagonal crystals which we have used, the symmetry about the Gd^{+++} ion appears certainly to be greater than that about the Gd^{+++} ion in the monoclinic crystals.

B. Photographs were taken of the absorption spectra of Gd^{+++} ion in solutions of $GdCl_3 \cdot 6H_2O$ and $Gd(C_2H_5SO_4)_3 \cdot 9H_2O$ of various concentrations. The positions and general spacings of the lines in all cases were very similar to those of the $GdCl_3 \cdot 6H_2O$ crystals except that the lines were very much wider and the multiplets were shifted slightly toward higher frequencies. The fact that the lines of the multiplets can be clearly resolved shows that the water molecules must take definite positions about the Gd^{+++} ion in order to give a field of definite symmetry. If random distribution is assumed, there would be all types of symmetry and the multiplets would become broad, blurred bands on account of the overlapping of the various spectra. The great width of the lines does, however, show that there is considerable thermal agitation and that the water molecules vibrate about their mean positions.

A study of the number of lines in the multiplets, together with their shifts, widths, and so on, should give a great deal of information concerning the effect which temperature, concentration, additional ions, various solvents and the like have on the force fields which surround the ions in solution.

We are continuing this work and hope soon to have more detailed information concerning it.

F. H. SPEDDING
(*National Research Fellow in Chemistry*)
G. C. NUTTING

Chemical Laboratory of the University of California,
Berkeley, California,
November 18, 1931.

[2] Freed and Spedding, J. Am. Chem. Soc. **52,** 3747 (1930).

[3] F. H. Spedding, Phys. Rev. **38,** 2080 (1931).

[4] Bethe, Ann. d. Physik **3,** 133 (1929).

The Heat Capacity of Methane

D. S. Villars and G. Schultze (Phys. Rev. **38,** 998 (1931)) have recently published a paper on the rotational heat capacity of methane gas. By applying the results of Hund and Elert, they obtained the *a priori* probabilities of the rotational states and the series expression for $Q=\sum_i P_i e^{-\epsilon_{ri}/kT}$. According to Villars and Schultze, symmetry and nuclear spin result in the existence of three non-combining types of methane, quintet, triplet and singlet. They have calculated rotational heat capacities for each of the three varieties; for the metastable mixture of 5/16 quintet, 9/16 triplet and 2/16 singlet, and for the equilibrium mixture. The heat capacity of the metastable mixture is that of what we might call "ordinary" methane, while the equilibrium heat capacity is that which would obtain in the presence of some hypothetical catalyst. The results of Villars and Schultze indicate that the rotational heat capacity of methane reaches a maximum around 50°K and then falls off to about 0.6 R at 175°, where it is apparently still decreasing. This result was very surprising, since it seemed to us that the equipartition value of 3/2 R should have been reached by this temperature. If their results were correct, the experimental value of the entropy of methane at 298.1° would be considerably in error, since it has been obtained from the third law value at the boiling point by assuming the rotational heat capacity of the gas to be 3/2 R from the latter temperature to 298.1°K.

The fact that the experimental entropy agrees with that calculated from the Tetrode equation equally well at the boiling point and at room temperature led us to recalculate the results of Villars and Schultze.

Assuming methane to be a regular rigid tetrahedron, the rotational energy levels are given by the equation:

$$E_r = \frac{h^2}{8\pi^2 I} j(j+1).$$

From the definition, $\sigma = h^2/8\pi^2 IkT$, we have the following expression for the rotational heat capacity:

$$C_r = \sigma^2 \frac{d^2 \ln Q}{d\sigma^2} = \sigma^2 \left[\frac{Q \dfrac{d^2Q}{d\sigma^2} - \left(\dfrac{dQ}{d\sigma}\right)^2}{Q^2} \right].$$

For I, the moment of inertia, we have used the Raman value, 5.17×10^{-40} gm cm² (Dickinson, Dillon and Rasetti, Phys. Rev. **34,** 582 (1929)), which was also used by Villars and Schultze. We have used the same *a priori* probabilities as those given by Villars and Schultze.

An evaluation of Q, $(dQ/d\sigma)$, $(d^2Q/d\sigma^2)$ by summing, and substitution in the above equation for C_r, gives the results in Table I, and those plotted in Figs. 1 and 2. In Fig. 1, the three curves represent the heat capacity of the three kinds of methane, while in Fig. 2, the two curves are for the equilibrium mixture and the metastable frozen mixture. Above the temperature range of the plots, the heat capacity curves are virtually straight lines, coincident with $C_r/R=1.5$.

Our results differ considerably from those of Villars and Schultze. Below 40°, the two

TABLE I. *Rotational heat capacity of methane.*

T°K	Quintet C_r/R	Triplet C_r/R	Singlet C_r/R	Equilibrium C_r/R	5/16 Quintet 9/16 Triplet 2/16 Singlet C_r/R
3.84	0	0.035	0	0.499	0.020
7.68	0.006	0.481	0.003	0.941	0.290
12.80	0.276	0.981	0.030	1.347	0.642
19.20	1.354	1.328	0.219	1.733	1.198
25.60	2.255	1.457	0.537	1.838	1.592
30.72	2.432	1.487	0.794	1.798	1.696
38.40	2.198	1.498	1.101	1.688	1.667
43.89	1.971	1.499	1.250	1.621	1.615
51.20	1.747	1.500	1.374	1.563	1.561
61.44	1.589	1.500	1.456	1.527	1.527
76.80	1.516	1.500	1.492	1.504	1.504
153.60	1.500	1.500	1.500	1.500	1.500

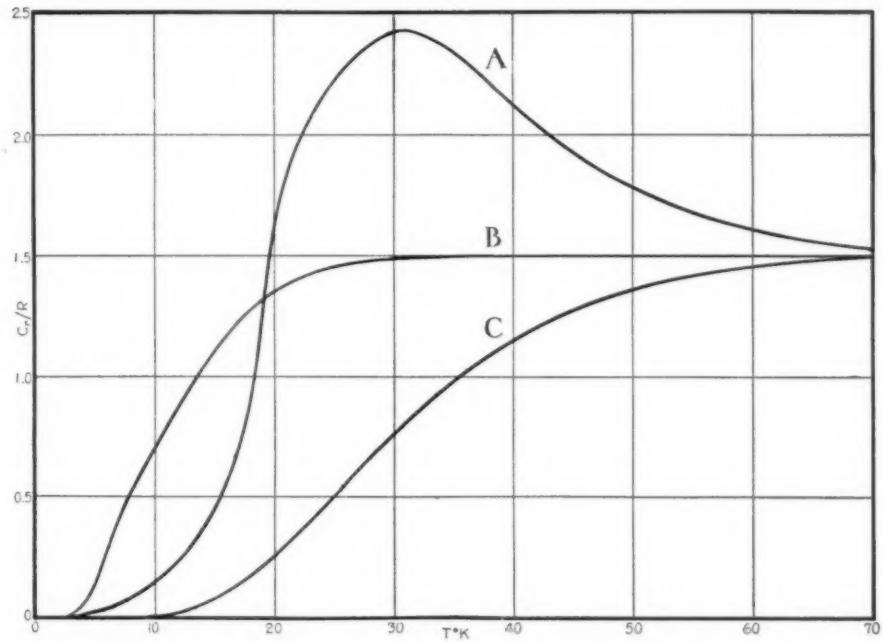

Fig. 1. Rotational heat capacities of methane. *A*, quintet. *B*, triplet. *C*, singlet.

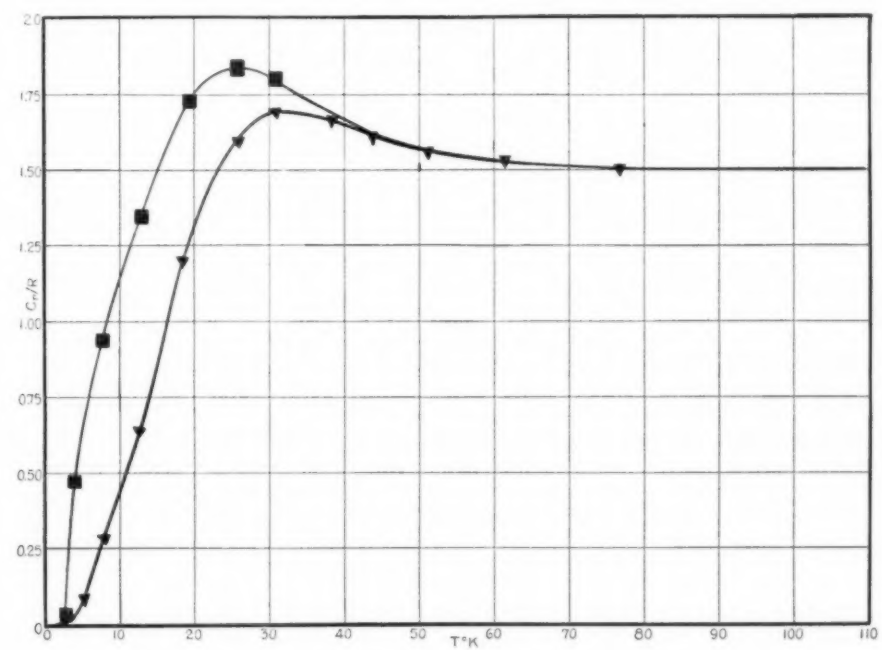

Fig. 2. Rotational heat capacities of methane. Squares, equilibrium. Triangles frozen.

sets of results agree fairly well, except for the case of the equilibrium mixture, but at higher temperatures the difference is very marked. As may be seen from Fig. 2, according to our calculations, the heat capacity after reaching a maximum, descends asymptotically toward the equipartition value, which it reaches, within a few thousandths of a calorie, at a temperature of 100°K. We have been unable to discover the source of the large deviation, but suspect it lies in the evaluation of the sums involved.

For the sake of completeness, we have calculated the vibrational heat capacity at room temperature. Use is made of the same equation as in rotation, namely $C/R=(\sigma^2 d^2 \ln Q/d\sigma^2)$, but in this case we substitute vibrational energies in the expression for Q. With the frequency assignments of Dennison (D. M. Dennison, Astrophy. J. **62,** 84 (1925)) and assuming simple harmonic motion, we obtain $C_v^{(298.1)}/R=0.296$. For the heat capacity of methane at room temperature, therefore, we have $3/2\ R$ for translation, $3/2\ R$ for rotation, R for C_p-C_v and $0.296\ R$ for vibration. Thus

$$C_p^{298.1} = 8.54 \text{ cal. mole}^{-1}.$$

The International Critical Tables gives $C_p=8.47$ at 15°C, and at this temperature our calculated value would be 8.45.

D. P. MacDougall

Chemical Laboratory of the University of California,
Berkeley, California,
November 18, 1931.

An Estimation of the Spectrum of the Element of Atomic Number 87

During the past two years I have been examining the optical spectra of mineral concentrates in an effort to identify the *raies ultimes* of the missing alkali element, eka-caesium. A comparison of alkali spectra shows that the principal series spectrum of this element will be characterized by a widely separated doublet in the red region, and a closer doublet in the violet. K. T. Bainbridge,[1] basing his computations on the similarity of the spectrum of Ra II with that of unionized eka-caesium, has estimated the wave-length of the $1^2S-2^2P_2$ line to be 7600 ± 200A, and that the component of lesser intensity, $1^2S-2^2P_1$, is further in the red at 8720 ± 200A. F. H. Loring[2] has made another estimate, based on Hick's equation for series spectra, which lead to values of 8061A for the $1^2S-2^2P_2$ line, and 4831A as the wave-length of the $1^2S-3^2P_2$ line. Both estimates of the $1^2S-2^2P_2$ line place it in a region of poor photographic sensitivity, indicating that for purposes of identification, the $1^2S-3^2P_2$ transition, though theoretically not the most persistent line in the spectrum of the element, will be more important than the true *raie ultime* in the red. As the approximated wave-lengths of the red line differ considerably from each other, corresponding doubt is placed on the estimate made by Loring of the wave-length of the line in the violet region. In general, a more exact knowledge of the position of the individual lines, together with independent estimates of the doublet separations, are desirable.

Unfortunately, the methods which led to the exact elucidation of the spectra of stripped atoms of the initial series of the periodic table are not applicable to the present case owing to the paucity of analyzed spectra in the 7th period. Spectral regularities in a group of elements, as observed by Ramage[3] among the atomic weights of the alkalis, or by Hicks' for their atomic volumes,[4] cannot be used for extrapolating the spectrum of eka-caesium because of a lack of generality in the correlations.

In an effort to estimate the spectrum of the missing alkali, I observed that for any spectral term T, in a periodic group of elements, the quantum defect Q, is roughly a linear function of the total quantum number n, of the valence electron. If Q is known, T can be calculated from the relationship: (1) $T=r^2R/(n-Q)^2$, where R is the Rydberg constant and $r-1$ is the degree of ionization of the atom. Though this relationship is not precise, it is singularly free from manifest exceptions (see Fig. 1). This generality has been tested and found to be true for the S, P, D, F, G and H levels of the neutral alkali atoms, the singlet and triplet S and P levels in the spectra of the

[1] K. T. Bainbridge, Phys. Rev. **34,** 752 (1929).

[2] F. H. Loring, Chem. News **140,** 178, 202, 242 (1930).

[3] Ramage, Proc. Roy. Soc. **A70,** 1 (1902).

[4] W. N. Hicks, Proc. Roy. Soc. **A83,** 226 (1910).

neutral alkaline earths, the doublet spectra of the neutral atoms of the elements of group III, for the *S*, *P* and *D* levels of the neutral copper, silver and gold atoms, and for the corresponding singlet and triplet levels of zinc, cadmium and mercury. The most marked curvature in the loci is observed in the case of the spectra of the singly ionized alkaline earth atoms, when the levels of radium are included. L. A. Turner[5] observed that if the total quantum numbers assigned by Bohr to the first two groups of elements be given different integral values in the case of the elements of high atomic weight, then the corresponding quantum defects for the *S* and *P* levels are, approximately, a linear function of the atomic number. At the end of his paper he states that H. N. Russell observed: "Straight lines will also be obtained if the quantum defects obtained from Bohr's quantum numbers are plotted against integers". The rule postulated above is more general and exact than Turner's formulation, and is better adapted for purposes of extrapolation in so far that the Bohr quantum numbers differ consistently by unity from element to element.

The utility of the rule, for estimating the spectrum of a heavy element, can be tested by calculating the principal series spectrum of radium, from the energy levels of the known alkaline earths, other than radium, and comparing the result with the known spectrum of the element. If the relationship were exactly linear the first difference Δ, (see Table I) should be a constant and ϵ have the value zero. Since in this case the locus has a marked curvature, the value of Δ is not constant, and it may be assumed that the Δ of radium will probably differ from that of barium by as large an amount as the maximum deviation from constancy observed in that group. On this assumption, the quantum defects of the levels of radium were evaluated from the formula: (2) $Q_{Ra}=Q_{Ba}+\Delta_{Ba}+|\epsilon|_{max}$. The first transition of the principal series so estimated is 3950A for the major line, and 4500A for the component of lesser intensity; the wave-lengths of the observed lines being 3816A and 4683A, respectively.

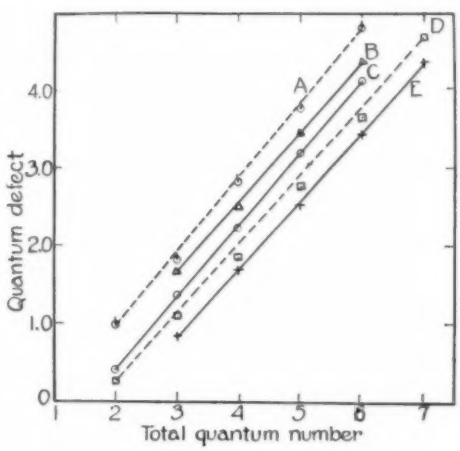

Fig. 1. *S* Levels for the elements of the first three groups. (Data from the Inter. Critical Tables **5,** 392 (1929) 1st ed.) A, 2^2S_1 term for B I, Al I, Ga I, In I and Tl I ($n-1$, instead of n plotted, to avoid intersection with other curves); B, singlet system Mg I, Ca I, Sr I and Ba I (Be I and Ra I spectra not analyzed); C, 1^2S_1 term for Li I, Na I, K I, Rb I and Cs I; D, 1^2S term for Be II, Mg II, Ca II, Sr II, Ba II and Ra II; E, triplet system Be I, Mg I, Ca I, Sr I and Ba I. Dotted lines show marked curvature.

From the law of spectroscopic displacement, the spectrum of eka-caesium may be expected to be similar to that of Ra II; hence, an equation of form (2) may be assumed valid for the extrapolation of its spectrum. The wave-lengths of the *raies ultimes* computed from the energy levels (see Table II) are:

[5] L. A. Turner, Phil. Mag. **48,** 384, 1010 (1924).

$1^2S-2^2P_2=7460$A, $1^2S-2^2P_1=8130$A, $1^2S-3^2P_2=4260$A, and $1^2S-3^2P_1=4310$A. These estimates are in closer agreement with the values of Bainbridge, than with those published by Loring. If Eq. (1) be investigated for the effect on the value of T produced by a small error in the estimation of Q, vis., (3) $\Delta T=-2r^2R\Delta n^*/(n^{*3}+2n^{*2}\Delta n^*)$, it will be observed that the levels of neutral atoms are much less sensitive than those of singly, or doubly ionized atoms. In (3), n^* is the effective quantum number, equal to $n-Q$.

TABLE I. *Estimation of Ra spectrum (example 1^2S term).*

Element	n	Q	Δ	ϵ
Be	2	0.271		
			0.826	
Mg	3	1.097		−0.064
			0.762	
Ca	4	1.859		+0.157
			0.919	
Sr	5	2.778		−0.030
			0.889	
Ba	6	3.667		
Ra	7	(4.713)	Calc.	
		4.699	Observed	

The doublet separations in the principal series of the alkalis increases progressively with increase in nuclear charge. H. Bell[6] has shown that the separations can be accurately represented by empirical equations of the type: $(\Delta\tilde{\nu})^{1/2}=m(N-N_0)$, and $\log\Delta\tilde{\nu}=p\log N+q$, where N is the atomic number, and m, p, q and N_0 are constants. For element 87, the distance between the doublets, computed with the aid of these equations, are $1450\tilde{\nu}$ and $467\tilde{\nu}$ for the multiplets in the red and violet regions, respectively. The separations obtained from the estimated 2^2P_j and 3^2P_j levels, $1100\tilde{\nu}$ and $330\tilde{\nu}$, are in fair agreement with the values calculated from Bell's equations.

TABLE II. *Estimated energy levels of RaII and Ek−Cs I.*

Level	Radium Obs. $\tilde{\nu}$	Radium Calc. $\tilde{\nu}$	Calc. for element 87
1^2S	82,862	83,880	32,930
2^2P_2	56,653	58,600	19,540
2^2P_1	61,510	61,680	20,560
3^2P_2	—	—	9,416
3^2P_1	—	—	9,750

HERMAN YAGODA

New York University,
Washington Square East,
New York, N. Y.
October 27, 1931.

[6] H. Bell, Phil. Mag. **36,** 337 (1918).

Excitation of High Optical Energy Levels. An Erratum

(Phys. Rev. **38,** 193, 1931)

In a letter to the Editor of the above title, line 12, page 194, read $58\cdot10^{-6}$ henrys instead of $6\cdot10^{-5}$ henrys.

J. E. MACK

Department of Physics,
University of Wisconsin,
Madison, Wisconsin,
November 9, 1931.

BOOK REVIEWS

Thermodynamics. ALFRED W. PORTER. Pp. 96+vii, figs. 21. E. P. Dutton and Company New York, 1931. Price, $1.10.

The fundamental principles and equations of classical thermodynamics, and some of their important applications, are developed briefly but clearly in this monograph. The introductory chapter is rendered especially interesting by a presentation of the historical background of the subject. The reviewer is of the opinion that the various empirical equations of state are treated at greater length than their relative importance warrants. The chapter on Irreversible Operations, which includes a comparatively detailed account of the Joule-Thompson effect, is particularly valuable since this phase of thermodynamics frequently receives scant attention. The application of thermodynamics to solutions is treated rather sketchily. No mention is made of the Third Law or of the Nernst Heat Theorem.

ROBERT LIVINGSTON
University of Minnesota

Fortschritte der Chemie, Physik and physikalischen Chemie, Band 20, Heft 3. Bandenspektra und Ihre Bedeutung für die Chemie. R. M. MECKE. Pp. 87, figs. 20. Gebrüder Borntrager, Berlin, 1929, Price 7.60 RM.

This small book includes a discussion of the theory of molecular spectra, helpful but not always accurate. Useful diagrams are given. Rather complete tables of band spectrum data, including heats of dissociation, are presented, including some data for polyatomic molecules. The effects of isotopy in band spectra are discussed in some detail. The author also discusses the use of band spectrum data for the calculation of chemical constants and specific heats.

R. S. MULLIKEN
University of Chicago

The Universe. FRANK ALLEN. Pp. 145+xiv, figs. 31. Harcourt Brace and Company, New York, 1931.

This "little book" gives a very readable, often amusing, and generally instructive account of the successive conceptions of the material universe held since the days of the Greeks. It presents, in bookform, the substance of a popular lecture delivered at the University of Manitoba in 1928, and, suffers somewhat of the general defects of such publications in that it appears to be a little too rambling in places, and goes off on too many by-paths and side-issues. Such may serve their purpose in elevating a lecture above the level of dullness, but often render a published account of it analogous to the "omnibus" article. It is well illustrated with portraits and photographs of the principal philosophers and savants, and adorned with a number of explanatory diagrams and sketches and may well take its place among the already vast number of books which give the uninitiated the impression that they grasp the idea of relativity whereas they have not really touched the meaning of it yet. A more factual criticism one can make is that the author subscribes to the myth that it was Galileo who invented the telescope.

W. J. LUYTEN
University of Minnesota

Dielectric Constant and Molecular Structure. C. P. SMYTH. Pp. 214. Figs. 31. Chemical Catalog Company, New York, 1931. Price $4.00.

This volume is one that will be welcomed by many readers. In the first place, being written by a physical chemist, it naturally stresses the chemical aspects more carefully than does most existing literature, irrespective of language. Also there is a particular dearth of monographs in English on the general subject of dipole-moment. Debye's "Polar Molecules" is perhaps the best known example, and there is almost no duplication of material between this and Professor

Smyth's new book. In the first place, the latter terminates with a very fine and useful 14 page table of the dipole moments of the molecules so far measured. (The English edition of Debye appeared too early to include the table of moments found in the German one, which has since been supplemented by a "Nachtrag" to the table, and then a "Nachtrag" to the "Nachtrag," each sold independently.)

The content of the book is primarily descriptive rather than mathematical. Even the first chapter called "mathematical theory" is more a presentation of the results than details of the mathematical analysis. A valuable feature is a chapter on experimental technique and apparatus, too often overlooked.

The chapters dealing with the relation of dielectric measurements to the structure of organic molecules are particularly complete. It is unfortunate that Professor Smyth's own measurements on ethylene dichloride were available too late to incorporate in the volume, as they have shed much light on the question of free rotation, i.e., as to whether certain carbon bonds are essentially sockets in which the radical can turn freely. The interesting vector addition of constituent dipoles in benzene substituents is discussed in considerable detail.

The two final chapters are on electronic and atomic polarization and on molecular association. In the discussion of electric refraction, some discussion of the calculations of Pauling could very properly have been included, perhaps at the expense of some of the older work. On page 144 the mistake of certain other writers has been followed in stating that the polarizability should vary as the inverse cube rather than inverse fourth power of the effective charge.

The style of the volume is a clear one. The documentation of literature is quite complete, although in Chap. I some minor results are erroneously attributed to Debye rather than Pauli, Manneback, and others.

J. H. Van Vleck
University of Wisconsin

Applications of the Absolute Differential Calculus. A. J. McConnell. Pp. xii+318. Blackie and Son, London 1931. Price 20s.

The avowed purpose of this admirable text is to develop the principles of tensor analysis and the absolute differential calculus, and to apply them to a wealth of relatively elementary subjects. It is to be considered as a text which will enable the student of mathematics or physics to "appreciate the power of tensorial methods . . . by seeing them applied to subjects with which he is already familiar," thus adequately preparing him for the study of more advanced disciplines, such as the general theory of relativity and the geometry of hyperspace.

The first two of the four parts into which the book is divided present the algebraic and geometric treatments of tensor algebra, respectively, and refer in the main to linear transformations. The theory of determinants, including the theory of elementary divisors, is concisely presented in terms of tensor notation. The geometrical applications are concerned with (oblique) rectilinear coordinates, the plane, the straight line and quadric surfaces. The absolute differential calculus proper is developed in the third part, which consists in an introduction to the differential geometry of curves and surfaces in three-dimensional Euclidean space. Finally the fourth part, consisting of the last hundred pages, applies the methods developed to the dynamics of a particle, rigid bodies and continuous media and to the special theory of relativity. An appendix correlates the new with the classical notation in dealing with general orthogonal coordinates in mathematical physics.

This excellent text can be recommended unreservedly to any one who wishes to become acquainted with the methods of tensor analysis; it should also prove a valuable auxiliary or reference text for students learning any of the disciplines with which it deals.

H. P. Robertson
Princeton University

Handbuch der Anorganischen Chemie. Eisenatom und Eisenmetall. Vierter Band, dritte Abteilung, zweiter Teil A, Lieferung I. A. Abegg, F. Auerbach and I. Koppel. Pp. 336, figs. 136. Verlag von S. Hirzel, Leipzig, 1931. Price, 40 RM.

With this second volume on the properties of iron (the first volume was published a year

ago), the excellent handbook of Abegg, started under his direction more than twenty-five years ago, edited after his death by Auerbach and after the latter's passing away by Professor Koppel, is approaching its completion. The publication of the monograph on the properties of iron and its compounds will be welcomed by all the friends of Abegg's Handbook, who have felt a great need for it during a long time.

The present volume dealing with the physical properties of iron will be of special interest to physicists and covers the following subjects:

Atomic weight (by J. Meyer); iron atom (nucleus, electron shells, x-ray spectrum; size of the atom and the ions, etc., by E. Rabinowitsch); preparation of pure iron; pyrophoric and colloidal iron (D. Deutsch); modifications of iron and their stability limits; space lattice and crystal habit; specific gravity; expansion; compressibility; mechanical and thermal properties (by K. Fischbeck); optical properties (by W. Schütz); magnetic and electrical properties (by K. Fischbeck); electromotive and electrochemical behavior (by H. Danneel).

This modern volume is a worthy addition to the well-known "Handbuch."

I. M. KOLTHOFF
University of Minnesota

Gmelins Handbuch der anorganischen Chemie. Eighth edition. Published by the Deutsche Chemische Gesellschaft, Berlin, 1931.

System-Nummer 8, Jod, Vol. 1, pp. 244, price RM 37.

System-Nummer 45, Germanium, pp. 62, price RM 13.

System-Nummer 58, Kobalt, Vol. A, Part I, pp. 220, price RM 34.

System-Nummer 59, Eisen, Vol. B, part 4, pp. 657–872.

It is with gratitude and admiration that new additions to the eighth edition of "Gmelins Handbuch" will be received by physicists, chemists and biologists. The most successful, complete outline of the physical and chemical properties of elements and their compounds, their occurrence in nature, their technical, biological and pharmacological significance is an achievement by which this compilatory work gains a place in any physical or chemical library. The systematic and exhaustive treatment of the literature, in which not only references are made to the original periodicals, but also to the patents published, will be of invaluable aid to scholars in whatever field they may specialize. The four volumes announced above uphold the high scientific standing of the work.

I. M. KOLTHOFF
University of Minnesota

Annales de l'Institut Henri Poincare, Vol. I, sections iv. Pp. 122. Les Presses Universitaires de France, Paris.

In this section of the first volume, there are three articles. An introduction to the subject of band spectra is given by L. Bloch. Dirac discusses several quantum mechanical problems of interest, and Carleman treats the theory of singular integral equations.

The first article is evidently intended merely to give a sketch of the field. After the usual preliminaries, one is introduced to Hund's theory of vector combinations, with the inclusion of case (a) and case (b) only. A few remarks about some typical electronic transitions conclude the treatment. It is clear, but brief.

Dirac points out the similarity between quantum and classical statistics, and obtains the quantum mechanical analogue of Lionville's theorem. Next, the permutation theory is developed, in practically the same form as in his original article. This theory is rather special, since for most actual problems one must consider the rotation group as well as the permutation group. Perhaps a translation of the group theoretical work on rotations into a language similar to that of Dirac (i.e. where space rotations are constants of the motion) would be helpful. Dirac next shows how a hole in a closed shell may be described by means of a wave equation. Heisenberg, a year and a half later, has arrived at this result independently. It is to be regretted that the delay in the publication of these Annales is so great. A discussion of the relativistic electron forms the remainder of this article.

Carleman at first gives examples of singular integral equations. Then it is shown how every analytic function regular in a certain region is a fundamental function for a certain Hermitian kernel. This leads to a study of singular integral equations with Hermitian kernel and complex eigenvalue. They admit of at least one quadratically integrable solution. The concept of spectral function is defined, and the orthogonality properties of such functions discussed.

If the aim of these Annales is to present up to date subjects, then more speedy publication is necessary.

JAMES H. BARTLETT, JR.
University of Illinois

AUTHOR INDEX TO VOLUME 38

References with (A) are to abstracts of papers presented at meetings of the Physical Society and references with (L) are to Letters to the Editor.

Ahearn, A. J. Emission of secondary electrons from tungsten—1858, 1918(A)

Allison, Samuel K. Resolving power attainable in x-ray spectroscopy by photographic methods—203

——— **and Victor J. Andrew.** Experimental test of the ionization chamber method of measuring the relative intensities of x-ray spectrum lines—441

Almy, G. M. and G. D. Rahrer. Faint branches in the OH bands—1816

Almy, John E. Book review—1396

Anderson, O. E. (see More, K. R.)—1995

Andrew, Victor J. (see Allison, Samuel K.)—441

Aughey, Henry (see Kenny, A. W.)—1388(L)

Austin, J. B. Calculation of the characteristic frequency from the coefficient of compressibility—1788(L)

Bacher, R. F. (see Campbell, J. S.)—1906(L)

——— (see Meggers, W. F.)—1258(L)

Badger, Richard M. and John L. Binder. Absorption band in ethylene gas in the near infrared—1442

Badgley, Ralph E. (see Henderson, Joseph E.)—590(A)

Banta, H. E. (see Heaps, C. W.)—195(L)

Barker, E. F. (see Plyler, E. K.)—1827

Barnes, R. Bowling and M. Czerny. Concerning the reflection power of metals in thin layers for the infrared—338

Barrett, Charles S. Laue spots from perfect, imperfect, and oscillating crystals—832(L)

——— **and Carl E. Howe.** Regular reflection of x-rays from quartz crystals oscillating piezoelectrically. Some interpretations—2290(L)

Barth, Tom. F. W. (see Posnjak, E.)—2234

Bartlett, James H., Jr. Many-electron wave functions—1623

——— **and W. H. Furry.** Valence forces in lithium and beryllium—1615

——— Book reviews—1261, 1394, 1395, 2303

Bartlett, Russell S. Thermionic emission from a plane electrode—1566(L)

Bateman, H. On dissipative systems and related variational principles—815

Beams, J. W. (see Stevenson, E. C.)—133

Beams, J. W. (see Street, J. C.)—416

Bearden, J. A. Determination of e/m by the refraction of x-rays—1919(A)

——— Grating constant of calcite crystals—1389(L), 2089

——— Refraction of the copper K-series by quartz—835(L)

Becker, J. A. and R. W. Sears. Phenomena in oxide coated filaments II. Origin of enhanced emission—2193

Beeck, Otto and J. Carlisle Mouzon. Ionization of Kr and Xe by positive alkali ions and the ionization potentials of Ne, A, Kr, and Xe—967

Bender, Wm. Asymmetric Zeeman patterns at intermediate strengths of field in Ca I—588(A)

Bennett, R. D., J. C. Stearns, A. H. Compton. Constancy of cosmic rays—1566(L)

——— (see Compton, A. H.)—1565(L)

Berkey, W. E. and R. C. Mason. Measurements on the vapor stream from the cathode of a vacuum arc—943

——— (see Mason, R. C.)—1783(L)

——— (see Tanberg, R.)—296

Berry, N. E. and G. K. Rollefson. Transition probabilities and quenching in the $3P$ state of sodium—1599

Betsill, J. L. (see Doan, R. L.)—1922(A)

Binder, John L. (see Badger, Richard M.)—1442

Biswas, Susil Chandra. Diamagnetic susceptibility of the rare gas atoms according to Slater's method—1784(L)

Bitter, Francis. Magnetization and the magnetocaloric effect—528, 588(A)

——— Inhomogeneities in the magnetization of ferromagnetic materials—1903(L)

Blue, R. W. (see Giauque, W. F.)—196(L)

Bowen, I. S. Spectrum of doubly ionized carbon, C III—128

Bowers, Harold E. (see Harkins, William D.)—1845

Bozorth, R. M. and J. F. Dillinger. Transverse Barkhausen effect in iron—192(L)

Brackett, Fredrick S. and Urner Liddel. Infrared absorption bands of hydrogen cyanide in gas and liquid—582(A)

Bradbury, Norris. Absolute values of the mobilities of gaseous ions—1905(L)
——— (see Loeb, Leonard B.)—1716
Bradley, Charles A., Jr. (see Urey, Harold C.)—589(A), 718; 1969
Bramley, Arthur. Radioactive disintegration—1567(L)
Breit, G. Hyperfine structure of heavy elements—463
——— **and I. I. Rabi.** Measurement of nuclear spin—2082(L)
Brewer, A. Keith. Effect of adsorbed K^+ ions on the photoelectric threshold of iron—401
Brice, Brooks A. Absorption band spectra of silver bromide and silver iodide vapors—658
Bridgman, P. W. The P-V-T relations of NH_4Cl and NH_4Br, and in particular the effect of pressure on the volume anomalies—182
——— Book review—1082
Briggs, H. B. (see Ives, Herbert E.)—1477, 1917(A)
Brown, Joseph G. Relation of atmospheric space-charge to turbulence and convection—587(A)
Brown, Weldon G. Infrared absorption band system of iodine—1187
——— Note on the heat of dissociation of iodine—709
——— Vibrational quantum analysis of the visible absorption bands of bromine—1179
Brown, W. L. and H. McN. Cowan. Oscillations in discharge tubes—376(L)
Broxon, James W. Residual ionization in nitrogen at high pressures—1704
——— Dielectric constant of commercial nitrogen at high pressures—2049
Brune, O. Equivalent electrical networks—1783(L)
Bryden, Samuel D., Jr. Allowed levels for equivalent (s, p, d, f) electrons with (jj) coupling—1145
——— The structure of the nucleus and its total moment of momentum—1989
Bush, V. and S. H. Caldwell. Thomas-Fermi equation solution by the differential analyzer—1898

Calbick, C. J. (see Davisson, C. J.)—585(A)
Caldwell, S. H. (see Bush, V.)—1898
Callihan, Dixon (see Hatley, C. C.)—909
Campbell, J. S. and R. F. Bacher. Nuclear moments of indium and gallium—1906(L)
——— **and W. V. Houston.** Revision of values of e/m from the Zeeman effect—581(A)
Campbell, J. W. Book review—1910
Cardwell, Alvin B. Photoelectric and thermionic emission from cobalt—2033
——— Photoelectric properties of tantalum—2041
Carlson, J. F. and J. R. Oppenheimer. Range of fast electrons and neutrons—1787(L)
Child, C. D. Absorption of light by flames containing sodium—699
Chow, T. C. and H. D. Smyth. Emission and absorption spectra in sulphur dioxide—838(L)
Christy, Andrew (see Mulliken, Robert S.)—87
Claus, W. D. Effect of temperature on the intensity of x-rays diffusely scattered from rocksalt—604
Compton, A. H., R. D. Bennett, J. C. Stearns. Ionization as a function of pressure and temperature—1565(L)
——— (see Bennett, R. D.)—1566(L)
Condon, E. U. Book reviews—1081, 1909
Constant, F. W. (see Lowance, F. E.)—1547
Cook, S. R. Electromagnetic theory of sight and color vision—587(A)
Cooke, F. W. Ionization of caesium vapor by light—1351
Copley. M. J. (see Guthrie, A. N.)—360
Cork, James M. (see Fox, Gerald W.)—1420
Cotton, J. C. (see Knauss, H. P.)—1190
Coven, Allen W. Scattering of x-rays from paraffin, aluminum, copper and lead—1424
Cowan, H. McN. (see Brown, W. L.)—376(L)
Crigler, Elizabeth A. Intensity of Raman lines in estimating the concentration of the components present in benzene-toluene mixtures—1387(L)
Czerny, M. (see Barnes, R. Bowling)—338

Dahm, Thos. M. Effect of inductance on the electromagnetically damped galvanometer—590(A)
Danforth, W. E., Jr. Dielectric constant of liquids under high pressure—1224
Davey, Wheeler P. (see Phelps, Robert T.)—1919(A)
Davisson, C. J. and C. J. Calbick. Electron lenses—585(A)
——— Book review—1262
Deming, W. Edwards and Lola E. Shupe. Some physical properties of compressed carbon monoxide—1920(A), 2245
Dennison, David M. and Norman Wright. New long wave-length absorption band of CS_2—2077(L)
Dieke, G. H. Perturbations in the helium band spectrum—646
Dillinger, J. F. (see Bozorth, R. M.)—192(L)
Dillon, J. H. Photoelectric properties of zinc single crystals—408
Doan, R. L. and J. L. Betsill. Force relations in drawing copper wire—1922(A)
Doermann, F. W. and Otto Halpern. Elastic scattering of electrons by spherically symmetrical atoms—193(L)
DuMond, Jesse W. M. and Archer Hoyt. A new K-series x-ray line due to Fermi-Sommerfeld electrons—839(L)

DuMond, Jesse W. M. and Harry A. Kirkpatrick. Dependence of Compton line breadth on primary wave-length with the multi-crystal spectrograph —1094

Dunnington, Frank G. Electro-optical shutter—its theory and technique—1506

——— Optical study of the formation stages of spark breakdown—1535

Edwards, Hiram W. Interference in thin metallic films—166

Edwards, R. L. (see Stewart, G. W.)—1575

Eldridge, John A. Book reviews—1793, 1794

Ellett, A. (see Zahl, H. A.)—977

Ellis, Joseph W. Polymers and new infrared absorption bands of water—582(A), 693

Epstein, Paul S. Modern statistics from the Gibbsian point of view—590(A)

Erikson, Henry A. Book review—1396

Estermann, I., R. Frisch and O. Stern. Diffraction experiments with monochromatic molecular beams —584(A)

Fisher, Thomas F. (see Serduke, James T.)—1922 (A)

Focke, A. B. (see Goetz, A.)—1569(L)

Forsythe, W. E. Intercomparison of the high temperature scale—1247

Fowler, R. H. Analysis of photoelectric sensitivity curves for clean metals at various temperatures— 45

Fox, Gerald W. and James M. Cork. Regular reflection of x-rays from quartz crystals oscillating piezoelectrically—1420

Frank, N. H. Theory of thermionic emission—1918 (A)

——— **and L. A. Young.** Transmission of electrons through potential barriers—80

——— (see Young, L. A.)—838(L)

Freed, Simon. Electronic transitions between an inner shell and the virtual outer shells of the ions of the rare earths in crystals—2122

——— **and Frank H. Spedding.** Diagram of some of the energy levels of gadolinium IV in the crystal lattice as obtained from the ultraviolet absorption spectra of $GdCl_3 \cdot 6H_2O$ and $GdBr_3 \cdot 6H_2O$ —670

Frenkel, J. Some remarks on the theory of the photoelectric effect—309

Frisch, R. (see Estermann, I.)—584(A)

Furry, W. H. (see Bartlett, James H., Jr.)—1615

Gartlein, C. W. and R. C. Gibbs. Production of second and third spark spectra in a hollow cathode lamp—1907(L)

Giauque, W. F., R. W. Blue, Roy Overstreet. Entropies of methane and ammonia—196(L)

Gibbs, R. C. and P. G. Kruger. Some evidence indicating the existence of Ba isotopes 136 and 137 —1921(A)

——— (see Gartlein, C. W.)—1907(L)

——— (see Shapiro, C. V.)—1170

Gideon, Edith (see Henderson, Joseph E.)—586(A)

Gilroy, Helen T. Certain spectra in the vanadium I iso-electronic sequence—2217

Glasoe, G. Norris. Contact potential difference between iron and nickel and their photoelectric work functions—1490

Goetz, A. and A. B. Focke. Metamagnetism in bismuth crystals—1569(L)

——— **and R. C. Hergenrother.** Macroscopic and lattice expansion of Bi single crystals—2075(L)

Gortner, R. A. Book reviews—2084, 2088

Goudsmit, S. and L. Gropper. Many-electron selection rules—225

Gray, Newton M. and Lawrence A. Wills. Note on the calculation of zero order eigenfunctions—248

Green, J. B. and R. A. Loring. Multiplet structure and Zeeman effect—1289

——— **and John Wulff.** Paschen-Back effect of hyperfine structure I. Tl II and Tl III—2176

——— **and John Wulff.** Paschen-Back effect of hyperfine structure II. Bi II and Bi III—2186

Gropper, L. (see Goudsmit, S.)—225

Gunn, Ross. Stability of the atmosphere of a rotating star—1052

Guthrie, A. N. and M. J. Copley. Magnetic moment of the palladium atom—360

Hall, Harvey. Relativistic theory of the photoelectric effect. Part I. Theory of the K-absorption of x-rays—57

——— **and J. R. Oppenheimer.** Part II. Photoelectric absorption of ultragamma radiation—57, 589(A)

Halpern, Otto (see Doermann, F. W.)—193(L)

Harder, Oscar E. Book reviews—1573

Hardy, J. D. High resolution in the infrared—2162

Harkins, William D. Periodic system of atomic nuclei and the principle of regularity and continuity of series—1270; a correction—1792(L)

——— **and Harold E. Bowers.** Raman effect and the carbon-halogen bond—1845

Harrington, Marshall C. Secondary emission from nickel by impact of metastable atoms and positive ions in helium—1312

Harrison, George R. Quantitative intensity determinations in the spectra of normal and of singly ionized vanadium, V I and V II—1921(A)

George R. Harrison and M. H. Johnson, Jr. Intensity summation rules and perturbation effects in complex spectra—757
——— **and Philip A. Leighton.** Spectral fluorescence efficiencies of certain substances with applications to heterochromatic photographic photometry—899
Hartig, Henry E. Book review—1081
Harvey, G. G. Diffuse scattering of x-rays from sylvine—593
——— (see Jauncey, G. E. M.)—1071(L); 1925
Hatley, C. C. and Dixon Callihan. Effect of varying concentrations of certain electrolytes on the violet band of the Raman spectra of water—909
Haupt, Curtis R. Probability law governing ionization by electron impact in mercury vapor—282
Heaps, C. W. Thermocouples of longitudinally and transversely magnetized wires—1391(L)
——— **and H. E. Banta.** Effect of internal stress on magnetic susceptibility—195(L)
Heitler, W. Quantum theory and electron pair bond—243
Henderson, Joseph E. and Ralph E. Badgley. Work required to remove a field electron—590(A)
——— **and Edith Gideon.** Effects due to the bombardment of platinum by mercury ions—586(A)
Hergenrother, R. C. (see Goetz, Alexander)—2075(L)
Heyworth, Dorothy. Crystal structure of arsenic triiodide, AsI_3—351
——— Note on the crystal structure of arsenic triodide—1792(L)
Hicks, Victor. Corrected relative intensities of the x-ray lines in the tantalum *L*-series—572(L)
Hiedemann, Egon. Electronic velocities in the positive column of high frequency discharges—198(L)
High, M. E. Raman effect in certain organic compounds—1837
——— **and M. L. Pool.** Removal of continuous background from Raman spectrum of carbon tetrachloride—374(L)
Hill, E. L. Note on the general solution of Schrödinger's equation and the uncertainty principle—2115
——— One-dimensional problems in quantum mechanics—1258(L)
——— Reflection of electrons by a special potential field—1072(L)
——— Book reviews—842, 1260, 1794
Hirsh, F. R., Jr. Satellites of *M*-series x-ray lines—914
Hollaender, Alexander and John Warren Williams. Molecular scattering of light from amorphous and crystalline solids—1739
Holzer, Robert E. Absorption of hydrogen positive rays in helium and argon—585(A)
Houghton, H. G. Transmission of visible light through fog—152
——— (see Stratton, J. A.)—159
Houston, William V. Structure of soft x-ray lines—1797
——— (see Campbell, J. S.)—581(A)
Howe, Carl E. (see Barrett, Charles S.)—2290(L)
Hoyem, A. G. Some electrical properties of spectroscopically pure zinc crystals—1357
——— (see Tyndall, E. P. T.)—820
Hoyt, Archer (see DuMond, Jesse W. M.)—839(L)
Huang, Tzu Ching. Further application of Huang's general equations of energy and entropy of gases: the general adiabatic equation of gases—1385
Hubbard, J. C. Acoustic resonator interferometer: I. the acoustic system and its equivalent electric network—1011
Huff, L. D. Motion of a Dirac electron in a magnetic field—501, 589(A)
——— Neutrons and cosmic rays—2292(L)
Hughes, A. L. Book review—1262
Hughes, D. S. Isotope separation in the spectra of Li I—857
Hulburt, E. O. Temperature of the lower atmosphere of the earth—1876
Hutchisson, Elmer. Band spectrum intensities by graphical methods—1921(A)
Huxford, W. S. Effect of electric fields on the emission of photoelectrons from oxide cathodes—379

Inglis, David R. Energy relations in complex spectra—862
——— **and M. H. Johnson, Jr.** Zeeman effect in intermediate coupling—1642
Ives, Herbert E. Exhibition of parallax panoramagrams made with a large diameter concave mirror—1922(A)
——— Vectorial photoelectric effect in thin films of alkali metals—1209, 1917(A)
——— **and H. B. Briggs.** Photoelectric effect from thin films of alkali metal on silver—1477, 1917(A)

Jackson, Dunham. Book review—1913
Jauncey, G. E. M. Scattering of x-rays by gases and crystals—1
——— Scattering of x-rays from polyatomic gases—194(L)
——— **and G. G. Harvey.** Diffuse scattering of x-rays from sylvine at low temperature—1925
——— **and G. G. Harvey.** Relation between the scattering of x-rays by gases and crystals—1071(L)

Jenkins, F. A., Yale K. Roots and Robert S. Mulliken. Red CN band system—1075(L)
Johnson, J. R. (see Shapiro, C. V.)—1170
Johnson, M. H., Jr. Spectra of two-electron systems—1628
——— (see Harrison, George R.)—757
——— (see Inglis, D. R.)—1642
Johnson, Thomas H. de Broglie wave spectrum from the secondary structure of LiF—586(A)
Johnston, Helen (see Urey, Harold C.)—581(A), 2131
Jones, Arthur Taber. Stability of a single file of straight vortices—2068
Jordan, W. H. (see Roller, Duane)—396

Kaplan, C. Strain-energy function for isotropic bodies—1020
Kaplan, Joseph. Auroral spectrum—582(A)
——— Forced predissociation in nitrogen—373(L)
——— Light of the night sky—1048
——— New criterion for predissociation—1079(L); correction—1792(L)
——— Predissociation in nitrogen and excitation of the green auroral line—1079(L)
——— Book review—1574
Kennard, E. H. (see Roess, Louis C.)—1263
Kennard, R. B. Optical study of heat transfer by convection from solid surfaces to air—1921(A)
Kennedy, Roy J. and Edward M. Thorndike. Search for an electrostatic analogy to the gravitational red shift—591(A)
Kenney, A. W. and Henry Aughey. X-ray diffraction patterns of mixtures—1388(L)
Kenty, Carl. Photoelectric and metastable atom emission of electrons from surfaces—377(L)
——— Photoelectric efficiencies in the extreme ultraviolet—2079(L)
Keyes, F. G. (see Kirkwood, J. G.)—576(L)
King, Arthur S. Features of the spectra of thulium, ytterbium, and lutecium under different excitations—583(A)
——— Spectra of high current vacuum arcs—590(A)
——— (see Meggers, W. F.)—1258(L)
Kingsbury, B. A. Shot effect in photoelectric currents—1458, 1922(A)
Kingsbury, E. F. Thermionic emission in caesium-oxide photocells at room temperatures—1918(A)
Kirkpatrick, Harry A. (see DuMond, Jesse W. M.)—1094
Kirkpatrick, Paul. Lateral space distribution of x-ray photoelectrons—1938
Kirkwood, J. G. and F. G. Keyes. Second virial coefficient—576(L)
Knauss, H. P. and J. C. Cotton. Ultraviolet bands of CO in the electrodeless ring discharge—1190
Knipp, Charles T. and Julian K. Knipp. Electrodeless discharge: Method of measuring induced current, variation of current with pressure for various gases—948
Knipp, Julian K. (see Knipp, Charles T.)—948
Kolthoff, I. M. Book reviews—1793, 2302, 2303
Korff, S. A. Absorption line width in sodium vapor—477
——— Book review—1081
Krishnan, K. S. Magnetic anisotropy of ions of the type XO_3—833(L)
Kruger, P. G. (see Gibbs, R. C.)—1921(A)

Langer, R. M. Absence of spin in nuclear electrons—837(L)
——— Schrödinger potential function—779
——— X-ray reflections from oscillating crystals—573(L)
Langmuir, Irving. Diffusion of electrons back to an emitting electrode in a gas—1656
——— **and K. J. Sixtus.** Regions of reversed magnetization in strained wires—2072(L)
Laporte, Otto, George R. Miller and Ralph A. Sawyer. First spark spectrum of rubidium (Rb II)—843
Lapp, C. J. Book review—1394
Lawrence, Ernest O. and M. Stanley Livingston. Production of high speed protons without the use of high voltages—834(L)
——— **and David H. Sloan.** High velocity mercury ions—586(A)
——— (see Sloan, David H.)—2021
Leighton, Philip A. (see Harrison, George R.)—899
Leland, O. M. Book review—1393
Lewis, Gilbert N. More fundamental thermodynamics—376(L)
Liddel, Urner (see Brackett, Fredrick S.)—582(A)
Linder, Ernest G. Dissociation of water in the glow discharge—679
Lindsay, R. B. Canonical transformation and the vibrations of a loaded string—491
Livingston, M. Stanley (see Lawrence, Ernest O.)—834(L)
Livingston, Robert. Book reviews—1795, 2084, 2301
Llewellyn, F. B. Book review—1397
Locher, G. L. (see Mott-Smith, L. M.)—1399
Loeb, Leonard B. Mobility of Na^+ ions in N_2 and H_2 as a function of time—549, 586(A)
——— Sparking potential and electrode material—1891
——— **and Norris E. Bradbury.** Velocity spectrum of normal gaseous ions in air and the problem of ionic structure—1716

Longden, A. C. Absolute determination of gravity —1920(A)
Loomis, F. W. Rotational structure of the red bands of potassium—2153
——— **and R. E. Nusbaum.** Magnetic rotation spectrum and heat of dissociation of the lithium molecule—1447
——— **and R. W. Wood.** Nuclear spin of potassium —854
Loring, R. A. (see Green, J. B.)—1289
Lowance, F. E. and F. W. Constant. Structure sensitiveness of magnetism in metals—1547
Luhr, Overton. Mass of positive ions in a glow discharge—1730
Luyten, W. J. Book reviews—1911, 1912, 2085, 2301

MacDougall, D. P. Entropies of methane and ammonia—2074(L)
——— Heat capacity of methane—2296(L)
MacDougall, F. H. Book reviews—201, 2086
McKeehan, L. W. Conservation of energy and the disintegration of RaE—2292(L)
McMillan, Edwin. Electrical field giving uniform deflecting force on a molecular beam—1568(L)
Mack, J. E. Excitation of high optical energy levels —193(L), erratum—2300(L)
Mackeown, S. S. Transition from a glow discharge to an arc—584(A)
Margenau, Henry. Equation of state of real gases —1785(L)
——— Role of quadrupole forces in van der Waals attractions—747
——— Surface energy of liquids—365
Marston, D. S. (see Zumstein, R. V.)—305
Mason, R. C. Cathode fall of an arc—427
——— **and W. E. Berkey.** Reaction due to gas molecules leaving the cathode of an arc—1783(L)
——— (see Berkey, W. E.)—943
Matuyama, E. (see Okubo, J.)—1651
Maxwell, Louis R. Average life of the ionized helium atom—1664
Meggers, W. F., A. S. King, R. F. Bacher. Hyperfine structure and nuclear moment of rhenium—1258(L)
Melvin, Eugene H. (see Wulf, Oliver R.)—330
——— **and Oliver R. Wulf.** Band spectra due to the molecule N_2O_3—2294(L)
Meyer, Alfred Wesley. Diffraction of x-rays in organic mixtures—1083
Michels, Walter C. Low voltage excitation of sodium—712
Miller, George R. (see Laporte, Otto)—843
Millis, John S. Zeeman effect in the ortho-helium band spectrum—1148
Milne, W. E. Book review—1913
Mitchell, Allan C. G. Effect of hyperfine structure on the polarization of cadmium resonance radiation—473
Mohler, F. L. Emission spectrum of metallic silver under electron bombardment and its relation to the absorption spectrum—1923(A)
Montgomery, Carol G. Magnetization of colloidal suspensions—1782(L)
More, K. R. and O. E. Anderson. Note on the excitation of the arc spectrum of nitrogen—1995
Morris, Charles S. Raman spectra of certain organic liquids—141
Morton, G. A. Atomic scattering power of copper and oxygen in cuprous oxide—41
Mott-Smith, L. M. and G. L. Locher. New experiment bearing on cosmic-ray phenomena—1399
Mouzon, J. Carlisle (see Beeck, Otto)—967
Mueller, Donald W. and H. D. Smyth. Negative hydrogen ions from H_2O by electrons of a critical velocity—1920(A)
Müller, Hans. Kerr-effect in Rochelle salt—1922(A)
Mulliken, Robert S. Note on the interpretation of the BeF bands—836(L)
——— **and Andrew Christy.** Λ-type doubling and electron configurations in diatomic molecules—87
——— (see Jenkins, F. A.)—1075(L)
——— Book Review—2301
Murphy, George M. (see Urey, Harold C.)—575(L)
Muskat, Morris. Anomalous scattering of alpha-rays—23

Naudé, S. Meiring. Rotational analysis of the first positive nitrogen (N_2) bands—372(L)
Neher, H. V. Scattering of high velocity electrons by thin foils—585(A), 1321
Nettleton, L. L. Book review—1397
Nickerson, John L. Current-intensity relation of the λ600 band of helium—1907(L)
Nielsen, Harald H. Infrared bands of slightly asymmetric molecules—1432
Nielsen, Walter M. Effect of temperature on the continuous band spectrum of mercury vapor—888
Nile, S. W. Calculation of effective nuclear magnetic moments from hyperfine structure—375(L)
Nishikawa, S., Y. Sakisaka and I. Sumoto. Note on "Effect of piezoelectric oscillation on the intensity of x-ray reflections from quartz"—1078(L)
Nottingham, W. B. Transmission of electrons through potential barrier of thoriated filament—1918(A)
Nusbaum, R. E. (see Loomis, F. W.)—1447
Nutting, G. C. (see Spedding, F. H.)—2294

O'Bryan, H. M. Reflecting power and grating efficiency in the extreme ultraviolet—32

Okubo, J. and E. Matuyama. Appearance of the forbidden lines and the intensity modifications of the spectra of mercury, cadmium and zinc under high frequency excitation—1651

Olpin, A. R. Correlating the selective photoelectric effect with the selective transmission of electrons through crystalline surface structures—1917(A)

——— An interpretation of the selective photoelectric effect from two-component cathodes—1745

Onsager, Lars. Reciprocal relations in irreversible processes: II—2265

Oppenheimer, J. R. Note on light quanta and the electromagnetic field—725

——— (see Carlson, J. F.)—1787(L)

——— (see Hall, Harvey)—57, 589(A)

Overstreet, Roy (see Giauque, W. F.)—196(L)

Page, Leigh. Book review—199

Pardue, Louis A. Dispersion of x-rays in calcite—1808

Pauling, Linus. Book review—199

Phelps, Robert T. and Wheeler P. Davey. X-ray study of the nature of solid solutions—1919(A)

Phipps, T. E. (see Shaw, E. J.)—174

Pielemeier, W. H. Supersonic satellites and velocity—1236

Pierce, W. C. Effect of general radiation in the diffraction of x-rays by liquids—1409

——— Higher order effects in the diffraction of x-rays by liquids—1413

Pietenpol, W. B. and E. C. Westerfield. Problem of rotating magnets—2280

Plyler, E. K. Structure of the water vapor molecule—1784(L)

——— **and E. F. Barker.** Infrared spectrum and the molecular configuration of N_2O—1827

Pokrowski, G. I. New effect produced by action of x-rays on matter—925

Pool, M. L. Life of metastable mercury and evidence for a long-lived metastable vibrating nitrogen molecule—955

——— (see High, M. E.)—374(L)

Posnjak, E. and Tom. F. W. Barth. New type of crystal fine-structure lithium ferrite ($Li_2O \cdot Fe_2O_3$)—2234

Potapenko, G. V. Production of ultra-short undamped electromagnetic waves—584(A)

Pyle, W. R. Dielectric constants of certain organic liquids at medium frequency—1057

Rabi, I. I. (see Breit, G.)—2082(L)

Rahrer, G. D. (see Almy, G. M.)—1816

Randall, H. M. and Norman Wright. Infrared spectrum of Sn I—457

Reyerson, L. H. Book review—1910

Rice, Oscar Knefler. Collision problems involving large interactions—1943

Richtmyer, R. D. Upper atomic-number limits for satellites of the x-ray line $L\beta_2$—1802

Rinde, C. A. Note on the relation of wave-length to color sensation—588(A)

Robertson, H. P. Book review—2302

Roess, Louis C. and E. H. Kennard. X-ray absorption by a Thomas-Fermi atom—1263

Rojansky, V. and W. Wetzel. Quantum-mechanical reflection coefficients and their numerical determination—1979

Rollefson, G. K. (see Berry, N. E.)—1599

Roller, Duane, W. H. Jordan and C. S. Woodward. Some photoelectric properties of mercury films—396

Romig, W. Doppler effect in the canal rays in neon—1709

Roots, Yale K. (see Jenkins, F. A.)—1075(L)

Rosen, N. Calculation of interaction between atoms with *s*-electrons—255

——— Normal state of the hydrogen molecule—2099

Ross, William H. Thermocouples whose elements are longitudinally and transversely magnetized wires of nickel and of iron—179

Ruark, Arthur E. Natural units for atomic problems—2240

Rudnick, Philip. Capture and loss of electrons by helium ions in helium—1342

Sakisaka, Y. (see Nishikawa, S.)—1078(L)

Saunders, F. A. Book review—842

Sawyer, Ralph A. (see Laporte, Otto)—843

——— **and Kenneth Thomson.** Deepest term in the Au II spectrum—2294(L)

Schultze, G. (see Villars, D. S.)—998

Schwede, Harold F. (see Struve, Otto)—1195

Sears, R. W. (see Becker, J. A.)—2193

Seass, Stewart. Thermocouples whose elements are longitudinally and transversely magnetized ferromagnetic substances—1254

Serduke, James T. and Thomas F. Fisher. Hall effect in solid mercury—1922(A)

Shapiro, C. V., R. C. Gibbs, and J. R. Johnson. Band spectrum of benzene: existence of a small vibrational frequency in the normal state—1170

Shaw, E. J. and T. E. Phipps. Magnetic moment of the diatomic sulfur molecule—174

Shenstone, A. G. Ultra-ionization potentials in mercury vapor—873

Shih, J. W. Magnetic properties of gold-iron alloys—2051

Shortley, George H. Inverse-cube central force field in quantum mechanics—120
Shrader, J. E. Three-dimensional vibrograph—1923 (A)
Shupe, Lola E. (see Deming, W. Edwards)—1920 (A), 2245
Sixtus, K. J. (see Langmuir, Irving)—2072(L)
Slater, J. C. Molecular energy levels and valence bonds—1109
——— Note on the structure of the groups XO_3—325
——— Quantum theory of the equation of state—237
Sleator, W. W. New absorption bands of ammonia, methyl bromide, methyl iodide and carbon dioxide in the infrared spectrum—147
Sloan, David H. and Ernest O. Lawrence. Production of heavy high speed ions without the use of high voltages—2021
——— (see Lawrence, E. O.)—586(A)
Smith, Lloyd P. Evaluation of the matrix components for helium—1961
Smith, T. Townsend. Book review—578
Smyth, H. D. Emission spectrum of carbon dioxide—2000
——— (see Chow, T. C.)—838(L)
——— (see Mueller, Donald W.)—1920(A)
Soller, Walter. Graphical determination of all crystal lattices from x-ray powder method data—583 (A)
Sommerfeld, A. Angular distribution of photoelectrons—1078(L)
Spedding, Frank H. Zeeman effect in solids—2080(L)
——— **and G. C. Nutting.** A. Effect of crystal symmetry on the energy levels of solids. B. Experimental evidence of definite orientations of coordinated water molecules about rare earth ions in solution—2294
——— (see Freed, Simon)—670
Spencer, Roy G. Absorption of soft x-rays in gases—1932
——— Additional theory of the double x-ray spectrometer—618
——— Study of the shape of the Ag L, Mo K and Cu K lines—630
Stearns, J. C. (see Bennett, R. D.)—1566(L)
——— (see Compton, A. H.)—1565(L)
Stenstrom, K. W. Book reviews—1392, 1398
Stern, O. (see Estermann, I.)—584(A)
Stevens, Daniel S. Rotational analysis of the first negative group of oxygen (O_2^+) bands—1292
Stevenson, E. C. and J. W. Beams. Electro-optical Kerr effect in gases—133
Stewart, G. W. X-ray study of the magnetic character of liquid crystalline para-azoxyanisol and a comparison with the isotropic liquid—931
——— **and R. L. Edwards.** Comparison of viscosity and molecular arrangement in twenty-two liquid octyl alcohols—1575, 2082(L)
Stewart, John Q. Nebular red shift and universal constants—2071(L)
Stewart, O. M. Book review—1794
Stratton, J. A. and H. G. Houghton. Theoretical investigation of the transmission of light through fog—159
Street, J. C. and J. W. Beams. Fall of potential in the initial stages of electrical discharges—416
Strong, John. Investigations in the far infrared—583(A), 1818
Struve, Otto and Harold F. Schwede. Intensities of Balmer emission lines in stellar spectra—1195
Stuart, H. A. Internal molecular potential between the substituent groups in a benzene ring as derived from the heats of combustion—1372
Sumoto, I. (see Nishikawa, S.)—1078(L)
Swann, W. F. G. Book reviews—199, 2086

Tanberg, R. and W. E. Berkey. Temperature of cathode in vacuum arc—296
Terroux, F. R. (see Watson, W. H.)—2291(L)
Thompson, James S. New method producing negative ions—1389(L)
Thomson, Kenneth. (see Sawyer, R. A.)—2293(L)
Thorndike, Edward M. (see Kennedy, Roy J.)—591(A)
Tolman, Richard C. Nonstatic model of universe with reversible annihilation of matter—797
——— On the theoretical requirements for a periodic behaviour of the universe—1758
——— Book review—578
Tonks, Lewi. Increase in surface area due to crystal faces developed by etching—1030
——— Plasma-electron resonance, plasma resonance and plasma shape—1219
Turner, Louis A. Enhancement of predissociation by collisions—574(L)
Tyndall, E. P. T. and A. G. Hoyem. Resistivity of single crystal zinc—820

Uber, Fred M. X-ray absorption coefficients of mercury vapor in the region of its L-absorption discontinuities—217
Uhlenbeck, G. E. (see Van Lear, G. A., Jr.)—1583
——— Book review—1392
Urey, Harold C. The alternating intensities of Na_2 bands—1074(L)
——— **and Charles A. Bradley, Jr.** Relative abundances of isotopes—589(A), 718
——— **and Charles A. Bradley, Jr.** Vibrations of pentatonic tetrahedral molecules—1969

Urey, Harold C. and Helen Johnston. Absorption spectrum of chlorine dioxide—581(A), 2131
——— **and George M. Murphy.** Relative abundance of N^{14} and N^{15}—575(L)
Valasek, Joseph. Book review—1573
Van Atta, L. C. Excitation probabilities for electrons in helium, neon, and argon—876
Van de Graaff, Robert J. 1,500,000 volt electrostatic generator—1919(A)
Van Lear, G. A., Jr. and G. E. Uhlenbeck. Brownian motion of strings and elastic rods—1583
Van Vleck, J. H. Book reviews—1260, 2301
Vaughan, Alfred L. Mass spectrograph analyses, and critical potentials for the production of ions by electron impact, in nitrogen and carbon monoxide —1687
Villars, Donald Statler. Entropy of polyatomic molecules—1552, 1920(A)
——— **and G. Schultze.** Low temperature rotational heat capacities and the relative amounts of the nuclear singlet, triplet and quintet symmetry modifications of methane—998
Vollrath, R. E. 500 kilovolt cathode rays—212

Wahlin, H. B. Emission of positive ions from Cu and Ag—1074(L)
Warner, A. H. Determination of the photoelectric threshold for tungsten by Fowler's method—1871
Warren, B. E. Interpretation of the effect of piezoelectric oscillations on the intensity of x-ray reflections from quartz—572(L)
Washburn, E. W. Crystalline rubber hydrocarbon—1790(L)
Washburn, Harold W. Electro-optical shutter—584(A)
Waterman, A. T. Equilibrium distribution of potential and of electrons outside the surface of a conductor—1497
Watson, David L. Quantization of large scale events —1072(L)
Watson, W. H. and F. R. Terroux. Note on range of fast electrons and neutrons—2291(L)
Webb, J. H. Potential due to a buried spheroid—2056
Weizel, Walter. Broadening of the resonance atomic line of helium—642
Wellman, B. Reaction due to gas molecules leaving the cathode of an arc—1077(L)
Westerfield, E. C. (see Pietenpol, W. B.)—2280
Wetzel, W. Transmission of electrons through an electrical condenser—1205
——— (see Rojansky, V.)—1979
White, H. E. Auto-ionization in the alkaline earth metals and the inert gases—1786(L) 2016
White, H. E. Comparison of the classical electron orbital models with the probability density $\psi\psi^*$ of the Schrödinger and the Dirac solutions of hydrogen-like atoms—589(A)
——— Do protons in the nucleus possess orbital angular momentum?—2078(L)
——— Pictorial representations of the Dirac electron cloud for hydrogen-like atoms—513
Whitmer, Charles A. *M*-series absorption spectrum of tantalum—1164
Williams, E. H. Magnetic properties of copper-nickel alloys—828
Williams, John Warren. (see Hollaender, Alexander) 1739
Williamson, R. C. Book reviews—1909
Wills, Lawrence A. (see Gray, Newton M.)—248
Winans, J. Gibson. New emission bands in mercury vapor—583(A)
Winch, Ralph P. Photoelectric properties of thin unbacked gold films—321
Wollan, E. O. Experimental electron distribution in atoms of monatomic gases—15
Womer, R. L. Ionization of helium, neon and argon —454
Woo, Y. H. Temperature and diffuse scattering of x-rays from crystals—6
Wood, R. W. Absorption spectra of salts in liquid ammonia—1648
——— Raman effect for benzene substitution products by improved technique—2168
——— Selective thermal radiation of colored and pure fused quartz—487
——— Stereophotographic models of electron motion in Stark effect—346
——— (see Loomis, F. W.)—854
Woodcock, K. S. Emission of negative ions under the bombardment of positive ions—1696
Woodward, C. S. (see Roller, Duane)—396
Workman, E. J. Temperature variation of the specific heat (C_p) of CO_2 at 65.3 kg/cm² pressure; the specific heat (C_p) of helium as a function of pressure—587(A)
Wright, Norman (see Dennison, David M.)—2077 (L)
——— (see Randall, H. M.)—457
Wulf, Oliver R. and Eugene H. Melvin. Effect of temperature upon the ultraviolet band spectrum of ozone and the structure of this spectrum—330
——— (see Melvin, Eugene H.)—2294(L)
Wulff, John (see Green, J. B.)—2176, 2186

Yagoda, Herman. Estimation of the spectrum of the element of atomic number 87—2298(L)
Young, Lloyd A. Note on local momentum in wave mechanics—1612

Young, Lloyd A. and N. H. Frank. Temperature dependence of photoelectric effect in metals—838(L)
——— (see Frank, N. H.)—80
Zachariasen, W. H. Interpretation of the selective photoelectric effect from two-component cathodes —2290(L)
Zahl, H. A. and A. Ellett. Reflection of mercury from alkali halide crystals—977
Zahn, C. T. Temperature variation of the electric moment of ethylene chloride—521
Zeleny, John. Aging of ions in air and nitrogen—969
——— Distribution of mobilities of ions in air—2293(L)
Zener, Clarence. Probabilities of low-velocity inelastic collisions—277, 588(A)
Ziegler, G. E. Crystal structure of sodium nitrite, $NaNO_2$—1040
Zumstein, R. V. Wave-length standards in the spectra of aluminum, silicon and bismuth in the Schumann region—2214
——— **and D. S. Marston.** Wave-length standards in the spectra of carbon and tin in the Schumann region—305
Zwicky, F. Permanent electric and magnetic moments of crystals—1772

ANALYTIC SUBJECT INDEX TO VOLUME 38

References marked (A) are to abstracts of papers presented at meetings of the Physical Society, those marked with (L) are to Letters to the Editor.

Absorption of light (see also **Spectra, absorption**)
By flames containing sodium, C. D. Child—699
Transmission of visible light through fog, H. G. Houghton—152; theoretical investigation, J. A. Stratton, H. G. Houghton—159

Acoustics
Resonator interferometer, equivalent electric network, J. C. Hubbard—1011
Supersonic waves, velocity, W. H. Pielemeier—1236

Alpha-particles (see also **Radioactivity**)
Anomalous scattering, Morris Muskat—23

Arcs (see also **Discharge of electricity in gases**)
Cathode fall for thermionic and high field arcs, R. C. Mason—427
Temperature of cathode, vapor stream, R. Tanberg, W. E. Berkey—296
Transition from glow to arc, S. S. Mackeown—584(A)
Velocity of, vapor stream from cathode, R. Tanberg, W. E. Berkey—296, W. E. Berkey, R. C. Mason—943, 1783(L) B. Wellman 1077(L)

Astrophysics
Intensities of Balmer emission lines in stellar spectra, O. Struve, H. F. Schwede—1195
Nebular red shift and universal constants, J. Q. Stewart—2071(L)
Stability of atmosphere of a rotating star, electromagnetic fields, R. Gunn—1052

Atomic and molecular beams
Absorption of H^+, H_2^+, H_3^+ in A and He, R. E. Holzer—585(A)
Diffraction of He by LiF crystals, I. Estermann, R. Frisch, O. Stern—584(A)
Electrical field giving uniform deflecting force on a molecular beam, E. McMillan—1568(L)
Of Pd, A. N. Guthrie, M. J. Copley—360
Reflection of H atom from LiF, T. H. Johnson—586(A)
Reflection of Hg from alkali halide crystals, H. A. Zahl, A. Ellett—977

Atomic structure (see also **Energy states of atoms, Spectra**)
Dirac electron cloud for hydrogen-like atoms, pictorial representation, H. E. White—513,589(A)
Evaluation of the matrix components for He, L. P. Smith—1961
Natural units for atomic problems, A. E. Ruark—2240

Atomic structure factors
Of Cu and O in Cu_2O, G. A. Morton—41
In polyatomic gases, G. E. M. Jauncey—194(L)
Scattering of x-rays by gases and crystals, G. E. M. Jauncey—1; G. E. M. Jauncey, G. G. Harvey—1071(L)
For sylvine, G. G. Harvey—593; at low temperature, G. E. M. Jauncey, G. G. Harvey—1925

Atmosphere (see **Meteorology, atmospheric electricity**)

Atmospheric electricity (see also **Aurora, Meteorology**)
Relation of atmospheric space-charge to turbulence and convection, J. G. Brown—587(A)

Aurora
Auroral spectrum, nitrogen afterglow, J. Kaplan—582(A)
Green line and predissociation in N_2 J. Kaplan—1079(L); a correction 1792(L)
Light of night sky and aurora lines, J. Kaplan—1048

Book reviews
Allen, Frank. The Universe—2301
Annales de l'Institute Henri Poincare, Vol. I, sections i, ii, and iii—1395, section iv—2303
Barr, Guy. A. Monograph of Viscometry—2084
Bauer, O. and M. Hansen. Der aufbau der Kupfer-Zinklegierungen—1573
Becker, Fr. Uber interstellare Massan und die Absorption des Sternlicktes in Weltraum—1081
Berek, M. Gründlagen der Praktischen Optik—1573
Brauns, von Reinhard. Flussige Kristalle und Lebewesen—2088
Courant, R. Voresungern uber Differential-und Integralrechnung. Erster Band: Funktionen einer Veranderlichen—1913
Culver, Charles A. Electricity and Magnetism, an Advanced Textbook for Colleges—1794.
Dadourian, H. M. Analytical Mechanics—1910
Daniels, Mathews, and Williams. Experimental Physical Chemistry—1793
Debye, P. Elektronen Interferenzen Leipziger Vorträge 1930, 1262
Eve, A. S. and D. A. Keyes. Applied Geophysics in Search for Minerals—1397
Ewald, P. P., Th. Poschl, and L. Prandtl. The Physics of Solids and Fluids—578

Book reviews (continued)
Faraday Society Discussion. Photochemical Processes—1795
Ferry, E. S. in collaboration with O. W. Silvey, G. W. Sherman, Jr, D. C. Duncan. A Handbook of Physics Measurements, Vol. II—1394
Fowler, R. H. Statistical Mechanics—1392
Gmelins Handbuch der anorganischen Chemie. 8 Auflage. System-Nummer 8: Jod, Lieferung 1—2303
Gmelins Handbuch der anorganischen Chemie. 8 Auflage. System-Nummer 45: Germanium—2303
Gmelins Handbuch der anorganischen Chemie. 8 Auflage. System-Nummer 58: Kobalt, Teil A, Lieferung 1—2303
Gmelins Handbuch der anorganischen Chemie. 8 Auflage. System-Nummer 59: Eisen, Teil B, Lieferung 4—2303
Handbuch der anorganischen Chemie IV. Band 3, Abt. 2, Teil a 1, Eisenatom und Eisenmetall—A. Abegg, F. Auerbach, I. Koppel. 2302
Handbuch der Astrophysik, Band III, Erste Halfte Grundlagen der Astrophysik—578
Handbuch der Astrophysik, Band III, Zweite Halfte: Grundlagen der Astrophysik, Dritter Teil—1260
Handbuch der Experimentalphysik, Band XXIII. 2 Teil, Phosphoreszenz und Fluoreszenz von P. Lenard, F. Schmidt, und R. Tomaschek; Lichtelektrische Wirkung von P. Lenard and A. Becker—1262
von Helmholtz, H. Counting and Measuring—1909
Hess, Victor F. The Electrical Conductivity of the Atmosphere and its Causes—2086
Houston, R. A. Intermediate Physics—199
Houtermans, F. G. Neuere Arbeiten uber Quantentheorie des Atomkerns—1081
Jeffreys, Harold. Scientific Inference—1911
Kleeman, R. D. The Atomic and Molecular Forces of Chemical and Physical Interaction in Liquids and Gases, and Their Effects—2086
von Kluber, Harald. Das Vorkommen der Chemischen Elemente in Kosmos—2086
Kneser, H. O. Der Aktiv Stickstoff—1574
Kohl, K. Uber ungedanpfte elektrische Ultrakurzwellen—1397
Larmor, Sir Joseph. Mathematical and Physical Papers. Vol. I and II—2086
Laurence, A. C. S. Soap Films—1910
Lichtenstein, L. Vorlesungen uber einige Klassen nichtlinearer Integralgleichungen und Integrodifferentialgleichungen—1394
Luckiesh, N. Artificial Sunlight—1398
Mackaye, James. The Dynamic Universe—199
McConnell, A. J. Applications of the Absolute Differential Calculus—2302
March, Dr. A. Die Grundlagen der Quantenmechanik, zweite Auflage—1261
Mecke, Dr. R. Fortschritte der Chemie, Physik und physikalischen Chemie—2301
Meyer, Kurt H. and H. Mark. Der Aufbau der hochpolymeren organischen Naturstoffe auf Grund Molekular-Morphologischer, Betrachtungen—199
Milne-Thomson. Die elliptischen Funktionen von Jacobi—1913
Milne-Thomson, L. M. and L. J. Comrie. Standard Four-Figure Mathematical Tables—1911
Moulton, Forest Ray. Astronomy—2085
Ollivier, F. La Topographie sans Topographes—1393
Osborn, F. A. Physics of the Home—1909
Planck, Max. Einführung in die Theoretische Optik—842
Poor, V. C. Electricity and Magnetism—842
Porter, A. W. Thermodynamics—2301
Rabinowitsch, Eugen and Erich Thilo. Periodisches System—1793
Rosseland, Svein. Astrophysik (No. XI of Structur der Materie)—1912
Rosenthal, Josef. Das Jahrhundert der Strahlen—1392
Rutherford, Sir Ernest, Dr. James Chadwick and Dr. C. D. Ellis. Radiations from Radioactive Substances—1396
Sauerwald, F. Lehrbuch der Metallkunde—1573
Saunders, Frederick A. A Survey of Physics for College Students—1396
Searborough, J. B. Numerical Mathematical Analysis—1081
Simon, F. Fünfundzwanzig Jahre Nernstscher Wärmesatz—1082
Smith, C. J. Physics for Students of Pharmacy—1909
Smyth, C. P. Dielectric Constant and Molecular Structure—2301
Style, D. W. G. Photochemistry—2084
Ulich, Hermann—Chemische Thermodynamik—201
Warburg, Emil. Lehrbuch der Experimentalphysik fur Studierende—1794
Wigner, Eugen. Gruppentheorie und ihre Anwendung auf die Quantenmechanik der Atomspektren—1794
Wilson, W. Theoretical Physics, Vol. I—1260

Brownian movement
Of strings and elastic rods, G. A. Van Lear, Jr., G. E. Uhlenbeck—1583

Compressibility
Characteristic frequency from compressibility, J. B. Austin—1788(L)
Compton effect (see **X-rays, diffraction, scattering, reflection and refraction**)
Conductivity, thermal (see **Thermal conductivity**)
Contact potentials
Of Fe—Ni compared with photoelectric work function, G. N. Glasoe—1390
Cosmic radiation
Constancy of rays, R. D. Bennett, J. C. Stearns, A. H. Compton—1566(L)
Detection by Wilson cloud apparatus and Geiger-Müller counter, L. M. Mott-Smith, G. L. Locher—1399
Ionization as a function of pressure and temperature, A. H. Compton, R. D. Bennett, J. C. Stearns—1565(L)
Ionization in N_2 at high pressures, J. W. Broxon—1704, and neutronx, L. D. Huff—2292(L)
Range of fast electrons and neutrons, J. F. Carlson, J. R. Oppenheimer—1787(L), criticism, W. H. Watson. F. R. Terroux—2291(L)
Crystals and crystal structure
Of AsI_3, D. Heyworth—351, errata 1792(L)
Crystalline rubber hydrocarbon, E. W. Washburn—1790(L)
Electrical properties of S. P. single crystal zinc, E. P. T. Tyndall, A. G. Hoyem—820 A. G. Hoyem—1357
Fine-structure of lithium ferrite, E. Posnjak, T. F. W. Barth—2234
Graphical determination of crystal lattices from x-ray powder method data, W. Soller—583(A)
Grating constant for calcite crystals, J. A. Bearden—1389(L), 2089
Increase in surface area due to etching, L. Tonks—1030
Magnetic anisotropy of XO_3 ions, K. S. Krishnan—833(L)
Magneto-caloric effect in single crystals, F. Bitter 528, 588(A)
Of $NaNO_2$, G. E. Ziegler—1040
Permanent electric and magnetic moments, F. Zwicky—1772
Photoelectric properties of zinc single crystals, J. H. Dillon—408
Secondary structure of LiF, T. H. Johnson—586(A)
X-ray diffraction patterns of mixtures, A. W. Kenney, H. Aughey—1388(L)
X-ray reflection from crystals oscillating piezoelectrically, G. W. Fox, J. M. Cork—1420; B. E. Warren—572(L) R. M. Langer—573(L); C. S. Barrett—832(L); S. Nishikawa, Y. Sakisaka, I. Sumoto—1078(L) C. S. Barrett, C. E. Howe—2290(L)
Cybotactic state
In isotropic liquids and liquid crystals, G. W. Stewart—931
In octyl alcohols, G. W. Stewart, R. L. Edwards—1575, G. W. Stewart—2082(L)
Various organic mixtures, A. W. Meyer—1083
Diamagnetism (see **Magnetic properties**)
Dielectric constants
Electric moment of crystals, F. Zwicky—1772
Of liquids under high pressure, W. E. Danforth, Jr.—1224
Of N_2 at high pressure, J. W. Broxon—2049
Of organic liquids, W. R. Pyle—1057
Temperature variation of the electric moment of ethylene chloride, C. T. Zahn—521
Diffraction of atoms (see **Atomic and molecular beams**)
Diffusion
Reciprocal relations in irreversible processes: II, L. Onsager—2265
Discharge of electricity in gases (see also **Arcs, Electrons in gases**)
Capture and loss of He ions in He, P. Rudnick—1342
Cathode fall for thermionic and high field arcs, R. C. Mason—427
Diffusion of electrons back to an emitting electrode, I. Langmuir—1656
Dissociation of water in the glow discharge, E. G. Linder—679
Electronic velocities in high frequency discharges, E. Hiedemann—198(L)
Fall of potential in the initial stages, J. C. Street, J. W. Beams—416
Oscillations in discharge tubes, W. L. Brown, H. McN. Cowan—376(L)
Plasma-electron resonance and plasma resonance, L. Tonks—1219
Secondary electrons from Ni in He glow discharge, M. C. Harrington—1312
Discharge of electricity in high vacua (see also **Electrons, thermionic; High voltage tubes, machines**)
Work required to remove a field electron, J. E. Henderson, R. E. Badgley—590(A)
Dissociation
Of H_2O in glow discharge, E. G. Linder—679
Dissociation, heat of (see also **Molecular structure and constants**)
Of AgBr and AgI, B. A. Brice—658
Of H_2O, E. G. Linder—679
Of I_2 from band spectra, W. G. Brown—709
Of Li_2 and Be_2, J. H. Bartlett, Jr. W. H. Furry—1615

Doppler effect
In Ne canal rays, W. Romig—1709
In x-rays, by electrons in scattering body, J. W. M. DuMond, H. A. Kirkpatrick—1094
Dynamics
Canonical transformation for vibrations of loaded strings, R. B. Lindsay—491
Dissipative systems and related variational principles, H. Bateman—815
Elasticity
Characteristic frequency from compressibility, J. B. Austin—1788(L)
Force relations in drawing Cu wire, R. L. Doan, J. L. Betsill—1922(A)
Strain-energy function for isotropic bodies, C. Kaplan—1020
Electrical conductivity and resistance
Reciprocal relations in irreversible processes: II, L. Onsager—2265
Of single crystal zinc, E. P. T. Tyndall, A. G. Hoyem—820, A. G. Hoyem—1357
Electrical circuits
Acoustic resonator interferometer, equivalent electric network, J. C. Hubbard—1011
Equivalent networks, O. Brune—1783(L)
Electrical oscillations and waves
Ultra-short undamped waves, G. V. Potapenko—584(A)
Electric moment (see **Dielectric constant**)
Electrodeless discharge
Method of measuring induced current, C. T. Knipp, J. K. Knipp—948
Electromagnetic theory
Light quanta and the electromagnetic field, J. R. Oppenheimer—725
Problem of rotating magnets, W. B. Pietenpol, E. C. Westerfield—2280
Electrons
Transmission through potential barriers, N. H. Frank, L. A. Young—80, W. Wetzel 1205, W. B. Nottingham—1918(A)
Value of charge from shot effect, B. A. Kingsbury—1458, 1922(A)
Electron distribution in atoms
Of monatomic gases, E. O. Wollan—15
In rare earths in crystals, S. Freed—2122
By scattering of x-rays, G. E. M. Jauncey—1; G. E. M. Jauncey, G. G. Harvey—1071(L)
Stark effect, stereophotographic models, R. W. Wood—346
Electrons in gases
Capture and loss of He ions in He, P. Rudnick—1342
Electrons in metals
Equilibrium distribution outside conductor, A. T. Waterman—1497
Electrons, scattering of (see also **Electrons in gases**)
Probabilities in He, Ne and A, L. C. Van Atta—876
By spherically symmetrical atoms, F. W. Doermann, O. Halpern—193(L)
In thin metal foils, comparison with theory, H. V. Neher—585(A), 1321
Electrons, secondary
Negative ions by bombardment of Pt, J. S. Thompson—1389(L), K.S. Woodcock—1696(L)
From Ni, bombarded by He ions and metastable atoms, M. C. Harrington—1312
From Pt by bombardment with Hg ions, J. E. Henderson, E. Gideon—586(A)
From thin metal foils, H. V. Neher—585(A), 1321
From W, A. J. Ahearn—1858, 1918(A)
Electrons, thermionic
From Co, change with temperature, A. B. Cardwell—2033
Effect of space charge, R. S. Bartlett—1566(L)
Electron and potential distribution outside conductor, A. T. Waterman—1497
Enhanced emission in oxide coated filaments, J. A. Becker, R. W. Sears—2193
Photoelectric and thermionic work function, W. S. Huxford—379
Theory of emission, N. H. Frank—1918(A)
Transmission through potential barrier of thoriated filament, W. B. Nottingham—1918(A)
Electro-optical effects (see also **Photoelectric effect and properties**)
Electro-optical shutter, electric circuit of, H. W. Washburn—584(A)
Electro-optical shutter, theory and technique, F. G. Dunnington—1506
Kerr effect in gases, E. C. Stevenson, J. W. Beams—133
Kerr effect in Rochelle salt, H. Müller—1922(A)
Electrostatics
Potential due to a buried spheroid, J. H. Webb—2056
1,500,000 volt electrostatic generator, R. J. Van de Graaff—1919(A)
e/m
From quantum mechanical calculation, L. D. Huff—501, 589(A)
By refraction of x-rays, J. A. Bearden—835(L), 1919(A)
From Zeeman effect, J. S. Campbell, W. V. Houston—581(A)
Energy states of atoms (see also **Atomic structure, Spectra, atomic**)
Of Gd IV in crystal lattice, S. Freed, F. H. Spedding—670
Levels for equivalent (s, p, d, f) electrons with (jj) coupling, S. D. Bryden, Jr.—1145
Of rare earth ions in crystals, S. Freed—2122

Energy states of molecules (see **Molecular structure and constants, Spectra, molecular**)
Entropy
Of ammonia and methane, D. S. Villars—1552, 1920(A) W. F. Giauque, R. W. Blue, Roy Overstreet—196(L) D. P. MacDougall 2074(L)
Of the universe, R. C. Tolman—797, 1758
Equations of state
General adiabatic equation for gases, T. C. Huang —1385
P-V-T relations of NH_4Cl and NH_4Br, P. W. Bridgman—182
Properties of CO, W. E. Deming, L. E. Shupe—1920(A), 2245
Quantum theory of, J. C. Slater—237
For real gases, H. Margenau—1785(L)
Second virial coefficient, J. G. Kirkwood, F. G. Keyes—576(L), H. Margenau—1785(L)
van der Waals attractions, H. Margenau,—747
Errata
Excitation of high optical energy levels J. E. Mack—2300(L)
A new criterion for predissociation J. Kaplan —1792(L)
Note on the crystal structure of AsI_3 D. Heyworth—1792(L)
Excitation of atoms and molecules
Average life of H^+, L. R. Maxwell—1664
Of high optical energy levels, J. E. Mack—193(L), errata—2300(L)
Low voltage excitation of Na, probability measurements, W. C. Michels—712
Transition probabilities and quenching in Na, N. E. Berry, G. K. Rollefson—1599
Fluorescence
In iodine, effect of argon, L. A. Turner—574(L)
Transition probabilities and quenching, N. E. Berry, G. K. Rollefson—1599
Gamma-rays
Photoelectric absorption, H. Hall, J. R. Oppenheimer, 57, 589(A)
Gases
Properties of CO, W. E. Denning, L. E. Shupe 1920(A), 2245
Gravitation
Absolute determination of gravity, A. C. Longden —1920(A)
Hall effect
In solid mercury, J. T. Serduke, T. F. Fisher—1922(A)
Heat of combustion
Internal molecular potentials, H. A. Stuart—1372
Heat transfer
From solid surfaces to air, R. B. Kennard—1921(A)
High voltage tubes and machines (see also **Ions, high speed**)
Production of high speed ions without the use of high voltages, D. H. Sloan, E. O. Lawrence—2021; E. O. Lawrence, M. S. Livingston—834(L)
500 kilovolt cathode rays, R. E. Vollrath—212
1,500,000 volt electrostatic generator, R. J. Van de Graaff—1919(A)
Hydrodynamics
Stability of a single file of straight vortices, A. T. Jones—2068
Hyperfine structure
Effect on polarization of Cd resonance radiation, A. C. G. Mitchell—473
Of Bi II and Bi III, J. B. Green, J. Wulff—2193
Of heavy elements, theory, G. Breit—463
Of In and Ga, J. S. Campbell, R. F. Bacher—1906(L)
Of Tl II and Tl III, J. B. Green, J. Wulff—2176
Nuclear magnetic moments from hyperfine structure, S. W. Nile—375(L)
Nuclear moment of Re I, W. F. Meggers, A. S. King, R. F. Bacher—1258(L)
Nuclear moment of K, F. W. Loomis, R. W. Wood —854; F. W. Loomis—2153
Intensities in spectra (see also **Spectra, etc.**)
Of Balmer emission lines (stellar) O. Struve, H. F. Schwede—1195
Band spectrum intensities by graphical methods, E. Hutchisson—1921(A)
Of He band, λ600 J. L. Nickerson—1907(L)
Summation rules and perturbation effects in complex spectra, G. R. Harrison, M. H. Johnson, Jr.—757
Of V I and V II, G. R. Harrison—1921(A)
Interference phenomena
In thin metallic films, H. W. Edwards—166
Ionization by impact (see also **Potentials, critical**)
As function of pressure and temperature, A. H. Compton, R. D. Bennett, J. C. Stearns—1565(L)
Of Kr and Xe by positive alkali ions, O. Beeck, J. C. Mouzon—967
Negative ions by bombardment of Pt. J. S. Thompson—1389(L), K. S. Woodcock—1696(L)
Ionization potentials (see **Potentials critical**)
Ionization by radiation (see **Photoionization**)
Ions, high speed (see also **High voltage tubes and machines**)
Hg ions, E. O. Lawrence, D. H. Sloan—586(A)
500 kilovolt cathode rays, R. E. Vollrath—212
Ions in gases
Average life of H^+, L. R. Maxwell—1664
Bombardment of platinum by Hg, J. E. Henderson, E. Gideon—586(A)

Ions in gases (continued)
Mass of gas ions in air, N_2, O_2, and SO_2 from glow discharge, O. Luhr—1730
Mass spectrograph analyses of ions in N_2 and CO, A. L. Vaughan—1687
Negative hydrogen ions from H_2O, D. W. Mueller, H. D. Smyth—1920(A)
Ions, mobility (see also **Ions in gases**)
Absolute values, N. E. Bradbury—1905(L)
Aging of ions in air and N_2, J. Zeleny—969, 2293(L)
Of Na^+ ions in N_2 and H_2 as a function of time, nature of ion, L. B. Loeb—549, 586(A)
Velocity spectrum of ions in air and problem of ionic structure, L. B. Loeb, N. E. Bradbury—1716, J. Zeleny—2293(L)
Isotopes
Atomic species, regularities and continuity of series, W. D. Harkins—1270, 1792(L)
Of Ba, 136 and 137, R. C. Gibbs, P. G. Kruger—1921(A)
Relative abundance of N^{14} and N^{15}, H. C. Urey, G. M. Murphy—575(L)
Relative abundances, H. C. Urey, C. A. Bradley, Jr.—589(A), 718
Search for $O^{18}H$, G. M. Almy, G. D. Rahrer—1816
Liquids (see also **Hydrodynamics**)
General x-radiation and diffraction by liquids, W. C. Pierce—1409
Higher order effects in x-ray diffraction, W. C. Pierce—1413
Magnetic character of liquid crystalline para-azoxyanisol, G. W. Stewart—931
Surface energy of liquids, H. Margenau—365
Magnetic properties
Of An-Fe alloys, J. W. Shih—2051
Anisotropy of XO_3 ions, K. S. Krishnan—833(L)
Of colloidal suspensions, C. G. Montgomery—1782(L)
Of Cu-Ni alloys, E. H. Williams—628
Diamagnetic susceptibility of the rare gas atoms, S. C. Biswas—1784(L)
Effect of internal stress, C. W. Heaps, H. E. Banta—195(L)
Inhomogeneities in the magnetization, F. Bitter—1903(L)
Of liquid crystalline para-azoxyanisol, G. W. Stewart—931
Magneto-caloric effect and mechanism of magnetization, F. Bitter—528, 588(A)
Metamagnetism in Bi crystals, A. Goetz, A. B. Focke—1569(L)
Moment of the Pd atom, A. N. Guthrie, M. J. Copley—360
Moment of S_2, E. J. Shaw, T. E. Phipps—174
Permanent moments of crystals, F. Zwicky—1772
Reversed magnetization in strained wires, I. Langmuir, K. J. Sixtus—2072(L)
Structure sensitiveness of Cu, Ag, Pt, and Bi, F. E. Lowance, F. W. Constant—1547
Transverse Barkhausen effect in Fe, R. M. Bozorth, J. F. Dillinger—192(L)
Thermocouples of longitudinally and transversely magnetized wires of Ni and of Fe, W. H. Ross—179; S. Sears—1254; C. W. Heaps—1391(L)
Mechanics (see **Dynamics**)
Mechanics, quantum—atomic structure and spectra
Dirac electron cloud for H like atom, pictorial representation, H. E. White—513, 589(A)
Evaluation of the matrix components for He, L. P. Smith—1961
Many-electron wave functions, J. H. Bartlett, Jr.—1623
Of two-electron systems, M. H. Johnson, Jr.—1628
Mechanics, quantum—general
Collision problems involving large interactions, O. K. Rice—1943
General solution of Schrödinger's equation and the uncertainty principle, E. L. Hill—2115
Inelastic collisions, C. Zener—277, 588(A)
Inverse-cube central force field, G. Shortley—120
Light quanta and the electromagnetic field, J. R. Oppenheimer—725
Local momentum in wave mechanics, L. A. Young—1612
Motion of a Dirac electron in a magnetic field, value of e/m, L. D. Huff—501, 589(A)
Natural units for atomic problems, A. E. Ruark—2240
One-dimensional problems in quantum mechanics, E. L. Hill—1258(L)
Quadrupole forces in van der Waals attractions, H. Margenau—747
Quantization of large scale events, D. L. Watson—1072(L)
Reflection coefficients and their numerical determination, V. Rojansky, W. Wetzel—1979
Reflection of electrons by a special potential field, E. L. Hill—1072(L)
Schrödinger potential function, R. M. Langer—779
Tables of integrals and functions, N. Rosen—2099
Theory of equation of state, J. C. Slater—237
Transmission of electrons through potential barriers, N. H. Frank, L. A. Young—80, W. Wetzel—1205
Wave mechanics quantization of loaded string, R. B. Lindsay—491
Zero order eigenfunctions, N. M. Gray, L. A. Wills—248

Mechanics, quantum—molecular structure and spectra
Electron pair bond, W. Heitler—243
Energy levels and valence bonds, J. C. Slater—1109
Interaction between atoms with *s*-electrons, N. Rosen—255
Normal state of H_2, N. Rosen—2099
Mechanics, statistical
Types of statistics, models, P. S. Epstein—590(A)
Metals
Colors of thin films, H. W. Edwards—166
Metastable atoms and molecules
Life of Hg and N_2, M. L. Pool—955
Metastable atom emission of electrons from surfaces, C. Kenty—377(L)
Meteorology
Of the earth, temperature effect of O_3 and CO_2, E. O. Hulburt—1876
Heat transfer from solid surfaces to air, R. B. Kennard—1921(A)
Ultraviolet band of ozone, effect of temperature, O. R. Wulf, Eugene H. Melvin—330
Methods and instruments
Absolute determination of gravity, A. C. Longden—1920(A)
Band spectrum intensities by graphical methods, E. Hutchisson—1921(A)
Concentrations from Raman spectra, E. A. Grigler—1387(L)
Double x-ray spectrometer, R. C. Spencer—618
Effect of inductance on damped galvanometer, T. M. Dahm—590(A)
Electrical field giving uniform deflecting force on a molecular beam, E. McMillan—1568(L)
Electron lenses, apertures in charged conductors, C. J. Davisson, C. J. Calbick—585(A)
Electro-optical shutter, theory and technique, F. G. Dunnington—1506
Excitation of high optical energy levels, J. E. Mack—193(L), errata—2300(L)
Heterochromatic photographic photometry, G. R. Harrison, P. A. Leighton—899
High resolution in the infrared, J. D. Hardy—2162
Improved technique for Raman effect, R. W. Wood—2168
Induced currents in glow discharge, C. T. Knipp, J. K. Knipp—948
Infrared spectroscopy, J. Strong—1818
Ionization chamber method of measuring intensities of x-ray lines, S. K. Allison, V. J. Andrew—441
Intercomparison of the high temperature scale, W. E. Forsythe—1247
500 kilovolt cathode rays, R. E. Vollrath—212
1500 kilovolt electrostatic generator, R. J. Van de Graaff—1919(A)
Method of producing negative ions, J. S. Thompson—1389(L)
Na arc, N. E. Berry, G. K. Rollefson—1599
Reflecting power and grating efficiency in the extreme ultraviolet, H. M. O'Bryan—32
Reflection power of metals in thin layers for the infrared, R. B. Barnes, M. Czerny—338
Removal of continuous background from Raman spectra, M. E. High, M. L. Pool—374(L)
Resolving power of double crystal x-ray spectrometer, S. K. Allison—203
Second and third spark spectra in a hollow cathode lamp, C. W. Gartlein, R. C. Gibbs—1907(L)
Supersonic satellites and velocity, W. H. Pielemeier—1236
Three-dimensional vibrograph, J. E. Shrader—1923(A)
Thomas-Fermi equation solution by the differential analyzer, V. Bush, S. H. Caldwell—1898
Mobility of ions (see **Ions, mobility**)
Molecular structure and constants (see also **Spectra, molecular, Raman spectra**)
Energy levels and valence bonds, J. C. Slater—1109
From heats of combustion, for substituent groups in benzene ring, H. A. Stuart—1372
Of the groups XO_3, J. C. Slater—325
Heat capacities and relative amounts of nuclear modifications of methane, D. S. Villars, G. Schultze—998, D. P. MacDougall—2296(L)
Heat of dissociation of Li_2, F. W. Loomis, R. E. Nusbaum—1447
Magnetic moment of S_2, E. J. Shaw, T. E. Phipps—174
Moments of inertia of ethylene, R. M. Badger, J. L. Binder—1442
Of N_2O, E. K. Plyler, E. F. Barker—1827
Raman effect and the carbon-halogen bond, W. D. Harkins, H. E. Bowers—1845
Normal state of H_2, N. Rosen—2099
Valence forces in Li and Be, J. H. Bartlett, Jr., W. H. Furry—1615
Vibrational frequency in the normal state of benzene, C. V. Shapiro, R. C. Gibbs, J. R. Johnson—1170
Vibrations of pentatonic tetrahedral molecules, H. C. Urey, C. A. Bradley, Jr.—1969
Of the water vapor molecules, E. K. Plyler—1784(L)
Multiplets (see also **Spectra, atomic**)
Displacement in isoelectronic sequence, H. T. Gilroy—2217
Zeeman effect in Sn III and Sb I, J. B. Green, R. A. Loring—1289

Neutrons
Cosmic rays, L. M. Mott-Smith, G. L. Locher—1399, L. D. Huff—2292(L)
Range of fast electrons and neutrons, J. F. Carlson, J. R. Oppenheimer—1787(L), W. H. Watson, F. R. Terroux—2291(L)
Nuclear spin (see also **Hyperfine structure**)
Absence of, R. M. Langer—837(L)
Alternating intensities of Na_2 bands, H. C. Urey—1074(L)
Classification of elements, S. D. Bryden, Jr.—1989
Of In and Ga, J. S. Campbell, R. F. Bacher—1906(L)
Of K, F. W. Loomis, R. W. Wood—854; F. W Loomis—2153
Measurement by Stern-Gerlach experiment, G. Breit, I. I. Rabi—2082(L)
Of Re I, W. F. Meggars, A.S. King, R. F. Bacher——1258(L)
Spin of protons in nucleus, H. E. White—2078(L)
Nucleus
Atomic species, regularities and continuity of series, W. D. Harkins—1270, 1792(L)
Structure and moment of momentum, S. D. Bryden, Jr.—1989
Optical constants and properties
Reflection power of metals in thin layers for the infrared, R. B. Barnes, M. Czerny—338
Optical instruments (see **Methods and instruments**)
Paschen-Back effect (see **Zeeman effect**)
Periodic system of atoms
Atomic species, regularities and continuity of series, W. D. Harkins—1270, 1792(L)
Photoelectric effect and properties
In caesium-oxide photocells at room temperatures, E. F. Kingsbury—1918(A)
Of Co, change with temperature, A. B. Cardwell—2033
Effect of adsorbed K^+ ions on threshold of iron, A. K. Brewer—401
Effect of electric fields on the emission from oxide cathodes, W. S. Huxford—379
Efficiencies in the extreme ultraviolet, C. Kenty—2079(L)
Of Hg, thin films, D. Roller—396
Lateral distribution of x-ray photoelectrons, P. Kirkpatrick—1938
Photoelectric and metastable atom emission of electrons from surfaces, C. Kenty—377(L)
Relativistic theory, H. Hall, J. R. Oppenheimer—57, 589(A)
Selective effect from two-component cathodes, A. R. Olpin—1745, 1917(L), W. H. Zachariasen, 2290(L)
Shot effect in photoelectric currents, B. A. Kingsbury—1458, 1922(A)
Of Ta, effect of temperature, A. B. Cardwell—2041
Temperature variation of photoelectric sensitivity, R. H. Fowler—320, L. A. Young and N. H. Frank—838(L)
Theory of photoelectric effect in hydrogen-like atom, angular distribution, J. Frenkel—309; E. L. Hill—1072(L), A. Sommerfeld—1078(L)
Thin films of alkali metal on silver, H. E. Ives, H. B. Briggs—1477, 1917(A)
Of thin unbacked gold films, R. P. Winch—321
Threshold for W by Fowler's method, A. H. Warner—1871
Vectorial effect in thin films of alkali metals, H E. Ives—1209, 1917(A)
Work function of Fe and Ni compared with contact potentials, G. N. Glasoe—1490
Of zinc single crystals, J. H. Dillon—408
Photography
Parallax panoramagrams made with a large diameter concave mirror, H. E. Ives—1922(A)
Photoionization
Of Cs vapor, F. W. Cooke—1351
In high pressure chamber, A. H. Compton, R. D. Bennett, J. C. Stearns—1565(L)
In N_2 at high pressure by cosmic rays, J. W. Broxon—1704
Photometry
Fluorescence and heterochromatic photographic photometry, G. R. Harrison, P. A. Leighton—899
Piezoelectric effect
Oscillation of crystals and x-ray diffraction, B. E. Warren—572(L), R. M. Langer—573(L), C. S. Barrett—832(L), S. Nishikawa, Y. Sakisaka, I. Sumoto—1078(L), G. W. Fox, J. M. Cork—1420, C. S. Barrett, C. E. Howe—2290(L)
Plasmoidal discharges (see **Discharge of electricity in gases**)
Polymerization
In water, J. W. Ellis—693
Potentials, critical
For ions by electron impact in N_2 and CO, A. L. Vaughan—1687
Ionization of C III, I. S. Bowen—128
Of Kr and Xe by positive alkali ions, O. Beeck, J. C. Mouzon—967
Potentials, critical (see also **Ionization potentials**)
Probabilities of energy losses in He, Ne and A, L. C. Van Atta—876
Ultra-ionization potentials of Hg, probability law, C. R. Haupt—282

Potentials, critical (see also **Ionization potentials** (continued)
Ultra-ionization potentials of He, Ne and A, R. L. Womer—454
Ultra-ionization potentials in Hg vapor, A. G. Shenstone—873
Ultra-ionization potentials and spectral data, H. E. White—1786(L), 2016
Predissociation
Enhancement of, by collisions, L. A. Turner—574(L)
In N_2, J. Kaplan—373(L), 1079(L); a correction—1792(L)
A new criterion, J. Kaplan—1079(L); errata—1792(L)
Proceedings of the American Physical Society
Pasadena Meeting, June 15 to 20, 1931—579
Schenectady Meeting, September 10 to 12, 1931—1915
Radiation (see **Thermal radiation**)
Radioactivity
Anomalous scattering of alpha-rays, M. Muskat—23
Conservation of energy and the disintegration of RaE, L. W. McKeehan—2292(L)
Induced by action of x-rays, G. I. Pokrowski—925
Radioactive disintegration, A. Bramley—1567(L)
Raman spectra
From amorphous and crystalline solids and their solutions, A. Hollaender, J. W. Williams—1739
Benzene substitution products by improved technique, R. W. Wood—2168
Carbon-halogen bond, W. D. Harkins, H. E. Bowers—1845
In certain organic compounds, C. S. Morris—141, M. E. High—1837
Concentrations in benzene-toluene mixtures, E. A. Crigler—1387(L)
Effect of solutes on spectra of water, C. C. Hatley, D. Callihan—909
Removal of continuous background from spectrum of CCl_4, M. E. High, M. L. Pool—374(L)
Relativity
Electrostatic analogy to the gravitational red shift, R. J. Kennedy, E. M. Thorndike—591(A)
Model of universe with reversible annihilation of matter, R. C. Tolman—797
Periodic behavior of the universe, R. C. Tolman—1758
Theory of photoelectric effect, H. Hall, J. R. Oppenheimer—57, 589(A)
Reststrahlen
Investigations, 20 to 40μ, J. Strong—583(A)
Scattering of electrons (see **Electrons in gases, Electrons, scattering of**)
Selection rules
Many-electron selection rules, S. Goudsmit, L. Gropper—225
Shot effect
In photoelectric currents, B. A. Kingsbury—1458, 1922(A)
Solutions
Orientation of H_2O rare earth ions, F. H. Spedding, G. C. Nutting—2294(L)
X-ray study of the nature of solid solutions, R. T. Phelps, W. P. Davey—1919(A)
Sound (see **Acoustics**)
Spark discharge
Breakdown potential and electrode material, L. B. Loeb—1891
Fall of potential in the initial states, J. C. Street, J. W. Beams—416
Optical study of the formation stages, F. G. Dunnington—1535
Specific heat
Of methane, D. S. Villars, G. Schultze—998; D. P. MacDougall—2296(L)
Temperature and pressure variation of C_p, CO_2 and He, E. J. Workman—587(A)
Spectra, absorption (see also **Absorption of light**)
Of AgBr and AgI, B. A. Brice—658
Of Br_2, infrared, vibrational analysis. W. G. Brown—1187
Of Br_2, visible, vibrational analysis, W. G. Brown—1179
Of ClO_2, H. C. Urey, H. Johnston—58(A), 2131
Of ethane and ethylene in infrared, R. M. Badger, J. L. Binder—1142
Of Gd^{+++} ion in crystals, F. H. Spedding, G. C. Nutting—2294(L)
Of Gd, S. Freed, F. H. Spedding—670
Of HCN in gas and liquid, F. S. Brackett, U. Liddel—582(A)
Of I_2, W. G. Brown—709
Infrared bands of ammonia, NH_3, methyl bromide, methyl iodide and CO_2, W. W. Sleator—147
Of K_2, nuclear spin, F. W. Loomis, R. W. Wood—854, F. W. Loomis—2153
Line width in Na vapor, S. A. Korff—477
Long wave-length absorption band of CS_2, D. M. Dennison, N. Wright—2077(L)
Magnetic rotation spectrum and heat of dissociation, F. W. Loomis, R. E. Nusbaum—1447
Of N_2O_3, E. H. Melvin, O. R. Wulf—2294(L)
New infrared bands in H_2O, J. W. Ellis—582(A), 693
Of rare earths, S. Freed—2122
Of salts in liquid ammonia, R. W. Wood—1648

Spectra, absorption (see also **Absorption of light** (continued)
Ultraviolet band of ozone, effect of temperature, O. R. Wulf, E. H. Melvin—330
Spectra, atomic
Of alkaline earth metals and inert gases, autoionization, H. E. White—1786(L), 2016.
Of Bi II and Bi III, Paschen-Back effect of hyperfine structure, J. B. Green, J. Wulff—2186
Broadening of the resonance line of He, W. Weizel—642
Of C III and C II, I. S. Bowen—128
Deepest term in Au II, R. A. Sawyer, K. Thomson—2293(L)
Doppler effect in Ne canal rays, W. Romig—1709
Of Element No. 87, H. Yagoda—2298(L)
Energy relations in complex spectra, D. R. Inglis—862
Excitation of high optical energy levels, J. E. Mack—193(L); erratum—2300(L)
Of Hg, Cd and Zn under high frequency excitation, J. Okubo, E. Matuyama—1651
Infrared lines of Ne I and He I, J. D. Hardy—2162
Intensities of Balmer emission lines in stellar, O. Struve, H. F. Schwede—1195
Levels for equivalent (*s*, *p*, *d*, *f*) electrons with (*jj*) coupling, S. D. Bryden, Jr.—1145
Of Li I, isotope separation, D. S. Hughes—857
Low voltage excitation of Na, W. C. Michels—712
Of N I, K. R. More, O. E. Anderson—1995
Of Rb II, O. Laporte, G. R. Miller, R. A. Sawyer—843
Of Sn I, infrared, H. M. Randall, N. Wright—457
Of Tl II and Tl III, Paschen-Back effect of hyperfine structure, J. B. Green, J. Wulff—2176
Of Tu, Yb and Lu under different excitations, A. S. King—583(A)
Of V I isoelectronic sequence, H. T. Gilroy—2217
Spectra, continuous
Emission spectrum of metallic Ag under electron bombardment, F. L. Mohler—1923(A)
Spectra, general
Effect of temperature on band spectrum of Hg, W. M. Nielsen—888
Electrostatic analogy to the gravitational red shift, R. J. Kennedy, E. M. Thorndike—591(A)
High current vacuum arcs, A. S. King—590(A)
Investigations in the far infrared, J. Strong—1818
Light of the night sky and aurora lines, J. Kaplan—1048
Many-electron selection rules, S. Goudsmit, L. Gropper—225
Summation rules and perturbation effects in complex spectra, G. R. Harrison, M. H. Johnson, Jr.—757
Ultra-ionization potentials in Hg vapor, A. G. Shenstone—873
Wave-length standards, C I and Sn in Schumann region, R. V. Zumstein, D. S. Marston—305, of Al, Si and Bi, R. V. Zumstein—2214
Spectra, molecular (see also **Molecular structure and constants**)
Alternating intensities of Na_2 bands, H. C. Urey—1074(L)
Of benzene, vibrational frequency in the normal state, C. V. Shapiro, R. C. Gibbs, J. R. Johnson—1170
Emission spectrum of CO_2, H. D. Smyth—2000
Faint branches in OH bands, G. M. Almy, G. D. Rahrer—1816
Infrared bands of slightly asymmetric molecules, H. H. Nielsen—1432
Intensities by graphical methods, E. Hutchisson—1921(A)
Intensity of λ600 band of He, J. L. Nickerson—1907(L)
Interpretation of the BeF bands, R. S. Mulliken—836(L)
New bands in Hg vapor, J. G. Winans—583(A)
Of N_2O, infrared, E. K. Plyler, E. F. Barker—1827
O_2^+ bands, rotational analysis, D. S. Stevens—1292
Ortho-helium, band spectrum, Zeeman effect, J. S. Millis—1148
Perturbations in He band spectrum, G. H. Dieke—646
Red CN band system, F. A. Jenkins, Y. K. Roots, R. S. Mulliken—1075(L)
Rotational analysis of the first positive (N_2) bands. S. M. Naudé—372(L)
In SO_2, T. C. Chow, H. D. Smyth—838(L)
Λ-type doubling, electron configuration in diatomic molecules, R. S. Mulliken, A. Christy—87
Ultraviolet of CO, electrodeless ring discharge, H. P. Knauss, J. C. Cotton—1190
Vibrations of pentatonic tetrahedral molecules, H. C. Urey, C. A. Bradley, Jr.—1969
Spectra, Raman (see **Raman Spectra**)
Spectroscopy, technique
Band spectrum intensities by graphical method, E. Hutchisson—1921(A)
High current vacuum arcs, A. S. King—590(A)
In the far infrared, J. Strong—1818
Second and third spark spectra in a hollow cathode lamp, C. W. Gartlein, R. C. Gibbs—1907(L)

Stark effect
Stereophotographic models of electron motion, R. W. Wood—346
Sun (see **Astrophysics**)
Surface tension
Surface energy of liquids, H. Margenau—365
Thermal conductivity (see also **Heat transfer**)
Reciprocal relations in irreversible processes: II, L. Onsager—2265
Thermal radiation
Of colored and pure fused quartz, R. W. Wood—487
Intercomparisons of the high temperature scale, W. E. Forsythe—1247
Thermal expansion
Macroscopic and lattice expansion of Bi single crystals, A. Goetz, R. C. Hergenrother—2075(L)
Thermionic emission (see **Electrons, thermionic**)
Thermionic emission of positive ions
From Cu and Ag, H. B. Wahlin—1074(L)
Thermodynamics
Fundamental thermodynamics, G. N. Lewis—376(L)
General adiabatic equation for gases, T. C. Huang—1385
Model of universe with reversible annihilation of matter, R. C. Tolman—797
Reciprocal relations in irreversible processes: II, L. Onsager—2265
Relativistic thermodynamics and behavior of the universe, R. C. Tolman—1758
Ultra-ionization potentials (see **Potentials, critical**)
Valence
Directed valence in molecules, J. C. Slater—1109
Forces in Li and Be, J. H. Bartlett, Jr., W. H. Furry—1516
Quantum theory and electron pair bond, W. Heitler—243
Structure of the groups XO_3, J. C. Slater—325
van der Waal forces
Quadrupole forces, H. Margenau—747; 1785(L)
Virial coefficient
Second virial coefficient, application to He, J. G. Kirkwood, F. G. Keyes—576(L); H. Margenau—1785(L)
Viscosity
And molecular arrangement in octyl alcohols, G. W. Stewart, R. L. Edwards—1575, G. W. Stewart—2082(L)
Vision
An electromagnetic theory, S. R. Cook—587(A)
Relation of wave-length to color sensation, C. A. Rinde—588(A)
Wave mechanics (see **Mechanics, quantum, etc.**)
X-ray absorption
By Hg vapor in *L* region, F. M. Uber—217
In ionization chamber, S. K. Allison, V. J. Andrew—441
K absorption calculated for Sn, L. C. Roess, E. H. Kennard—1263
M-series of Ta, C. A. Whitmer—1164
Photoelectric absorption of ultragamma radiation, H. Hall, J. R. Oppenheimer—57, 589(A)
Soft x-rays in gases, R. G. Spencer—1932
X-rays, diffraction, scattering, reflection and refraction
Atomic scattering power of Cu and O in Cu_2O, G. A. Morton—41
Dependence of Compton line breadth on primary wave-length, J. W. M. DuMond—1094
Diffraction patterns of mixtures, A. W. Kenney, H. Aughey—1388(L)
Dispersion in calcite, L. A. Pardue—1808
Effect of temperature on scattering from rocksalt, W. D. Claus—604
By gases and crystals, G. E. M. Jauncey—1, G. E. M. Jauncey, G. G. Harvey—1071(L)
General radiation and diffraction by liquids, W. C. Pierce—1409
Grating constant of calcite crystals, J. A. Bearden—1389(L), 2089
Higher order effects in liquids, W. C. Pierce—1413
In organic mixtures, A. W. Meyer—1083
Piezoelectric oscillation and the intensity of x-ray reflections, B. E. Warren—572(L), R. M. Langer—573(L); C. S. Barrett—832(L); S. Nishikawa, Y. Sakisaka, I. Sumoto—1078(L); G. W. Fox, J. M. Cork—1420; C. S. Barrett, C. E. Howe—2290(L)
From polyatomic gases, G. E. M. Jauncey—194(L); by quartz, of Cu *K* series, J. A. Bearden—835(L)
Scattering from Al, Cu, and Pb and paraffin, A. W. Coven—1424
From sylvine, G. G. Harvey—593, at low temperature, G. E. M. Jauncey, G. G. Harvey—1925
Temperature and diffuse scattering from crystals, Y. H. Woo—6
X-ray study of the magnetic character of liquid, G. W. Stewart—931
X-rays, emission
Corrected relative intensities of the x-ray lines in the tantalum *L*, V. Hicks—572(L)
New *K*-series line, delta, J. W. M. DuMond, A. Hoyt—839(L)
Relative intensities of lines, S. K. Allison, V. J. Andrew—441
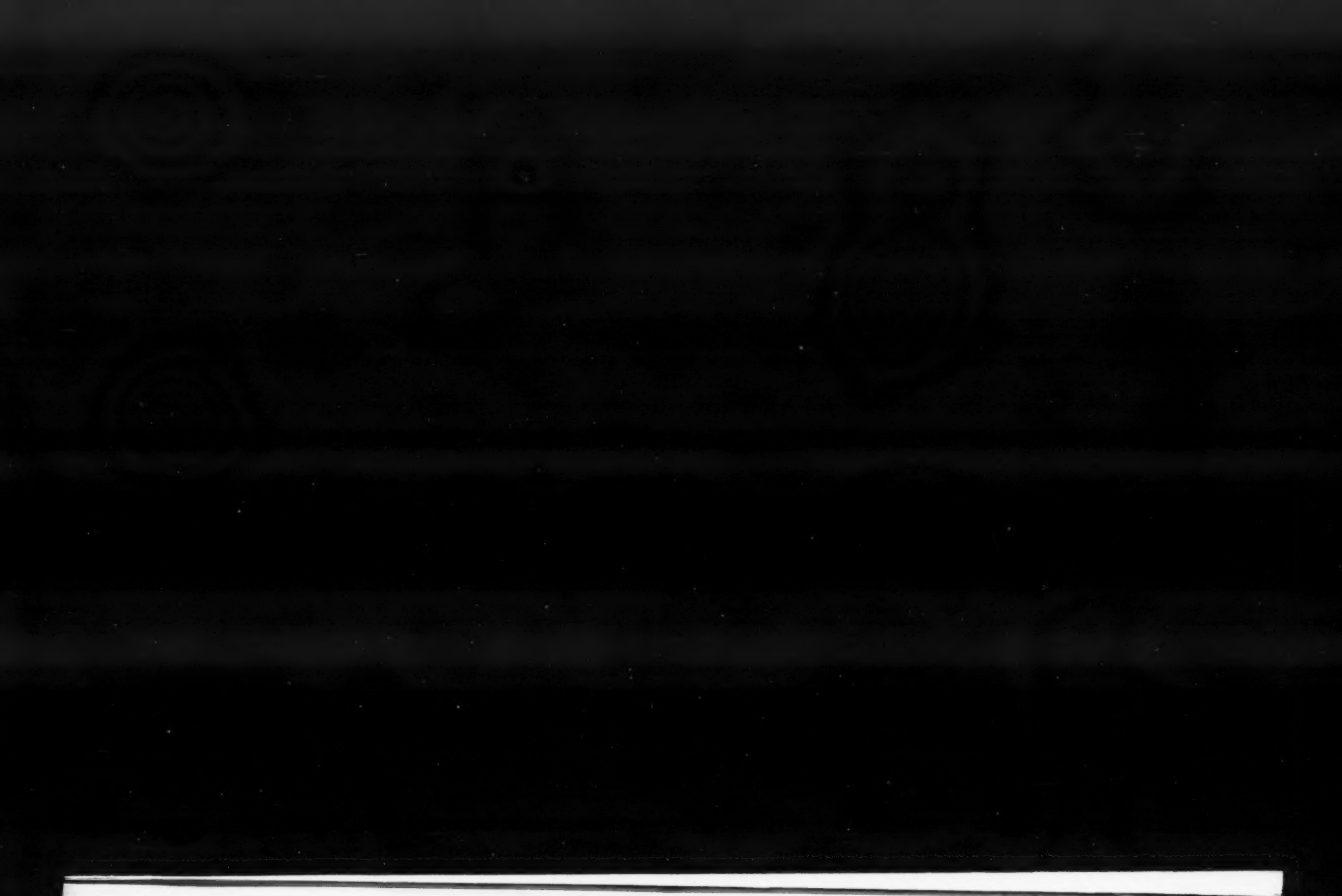
X-rays, emission (continued)
Satellites of $L\beta_2$ for atomic numbers 50 to 60, R. D. Richtmyer—1802
Satellites of M-series, F. R. Hirsh, Jr.—914
Shape of Ag L, Mo K and Cu K lines, R. O. Spencer—630
Structure of soft x-ray lines, W. V. Houston—1797
X-rays, spectroscopy
Double spectrometer, theory of, R. C. Spencer—618
Resolving power of double crystal spectrometer, S. K. Allison—203
Zeeman effect
Hyperfine structure, Paschen-Back effect in Bi II and Bi III, J. B. Green, J. Wulff—2186
Hyperfine structure, Paschen-Back effect in Tl II and Tl III, J. B. Green, J. Wulff—2176
In intermediate coupling, D. R. Inglis, M. H. Johnson, Jr.—1642
Multiplet structure, Sn III and Sb I, J. B. Green R. A. Loring—1289
In ortho-helium band spectrum, J. S. Millis—1148
Patterns at intermediate strengths of field in Ca I W. Bender—588(A)
In solids, F. H. Spedding—2080(L)